



<https://theses.gla.ac.uk/>

Theses Digitisation:

<https://www.gla.ac.uk/myglasgow/research/enlighten/theses/digitisation/>

This is a digitised version of the original print thesis.

Copyright and moral rights for this work are retained by the author

A copy can be downloaded for personal non-commercial research or study,
without prior permission or charge

This work cannot be reproduced or quoted extensively from without first
obtaining permission in writing from the author

The content must not be changed in any way or sold commercially in any
format or medium without the formal permission of the author

When referring to this work, full bibliographic details including the author,
title, awarding institution and date of the thesis must be given

Enlighten: Theses

<https://theses.gla.ac.uk/>
research-enlighten@glasgow.ac.uk

THE PHYSICAL PROPERTIES OF COAL MEASURES ROCKS
AND THEIR BEARING ON THE TECHNIQUE OF ROOF
BOLTING.

A Thesis submitted for the Ph.D. degree (Mining Engineering) of
Glasgow University

by

A.G. Johnston, B.Sc., A.R.T.C.,
Morningside,
Newmains.

December, 1955.



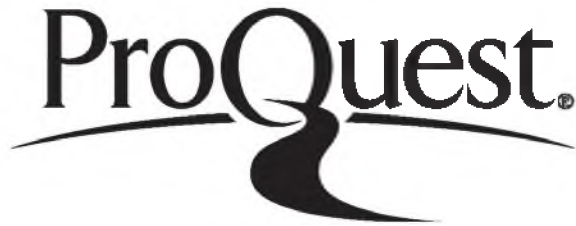
ProQuest Number: 10656335

All rights reserved

INFORMATION TO ALL USERS

The quality of this reproduction is dependent upon the quality of the copy submitted.

In the unlikely event that the author did not send a complete manuscript and there are missing pages, these will be noted. Also, if material had to be removed, a note will indicate the deletion.



ProQuest 10656335

Published by ProQuest LLC (2017). Copyright of the Dissertation is held by the Author.

All rights reserved.

This work is protected against unauthorized copying under Title 17, United States Code
Microform Edition © ProQuest LLC.

ProQuest LLC.
789 East Eisenhower Parkway
P.O. Box 1346
Ann Arbor, MI 48106 – 1346

I N D E X

Page No.

SYNOPSIS

SECTION	A:	PHYSICAL PROPERTIES OF COAL MEASURES ROCK	1
		Apparatus	3
		Collection and Preparation of Rock	
		Specimens	7
		Petrographic Examination of the Rocks	8
		Experimental Procedure and Theoretical	
		Considerations	10
		Experimental Results	20
		Analysis of Results:	28
		Strength of Coal Measures Rock	28
		Determination of Elastic Constants	30
		Time Strain in Coal Measures Rock	33
		Conclusions	35
SECTION	B:	PHOTO-ELASTIC INVESTIGATIONS	37
		Apparatus	40
		Construction of Models	43
		Experimental Procedure	46
		Experimental Results	49
		Analysis of Results:	53
		Suspension Support	53
		Compound Beam Effect	55
		Arched Roadway Support	56
		Conclusions	59
SECTION	C:	UNDERGROUND OBSERVATIONS	61
		Location of Experiments	62
		Types of Bolt and Installation Equipment	62
		Apparatus	64
		Experimental Procedure	72
		Experimental Results	74
		Analysis of Results:	84
		Strain Gauge Apparatus	84
		Torque-Tension Relationship	86
		Variation of Bolt Tension with Time	87
		Anchorage Testing	90
		General Strata Movements	91
		Wooden Bolts	92
		Conclusions	94
SECTION	D:	TESTING OF PLASTER MODELS	97

Page No.

Construction of the Models	98
Loading Arrangements	99
Experimental Results	100
Analysis of Results:	103
Models without Lateral Constraint	103
Models with Lateral Constraint	104
Conclusions	106

BIBLIOGRAPHY

LIST OF ILLUSTRATIONS

APPENDIX

ACKNOWLEDGMENTS

S Y N O P S I S

The investigations here described can be sub-divided into four main sections, viz. (A) The Physical Properties of Coal Measures Rock, (B) Photo-elastic Investigations, (C) Underground Observations and (D) The Testing of Plaster Models. The contents of each section are outlined below.

SECTION A: The various methods employed for the determination of the physical properties of rock are discussed. The use of electrical resistance strain gauges for the measurement of Young's Modulus and Poisson's Ratio of several rock types from the Scottish Coalfields is described. The factors which affect the ultimate strength of stratified rocks are discussed and an attempt is made to predict the total strain which will develop in rock under a given stress after a known time. The results obtained indicate the influence of "time-strain" in computing the stress distribution around an underground excavation. Micro-graphs of the specimens tested are included in an appendix.

SECTION B: Details of the apparatus used and the models constructed for the two-dimensional photo-elastic investigations of any roof bolting systems are given. The functions of roof bolts as a "suspension support" and in the formation of a "compound beam" are analysed. The use of bolting to form a "keystone" in arched shaped roadways is also investigated. The results show the value of bolts in minimising shear stresses at the interfaces of the beds. The

importance of pre-tensioning the bolts by equal amounts is also emphasised by the isochromatic diagrams.

SECTION C: The behaviour of roof bolts installed in an advancing longwall roadway is described. The performance of three types of steel bolts - slot and wedge, expansion shell, wedge and sleeve - and several "wooden bolts" is discussed. Details of the apparatus used for the measurement of bolt tension and strata movements are given. An attempt to measure 'in situ' rock strain by electrical resistance strain gauges is described. The results show a relaxation of bolt tension a few days after installation. The several factors which influence the behaviour of bolts installed in moving strata are discussed. Several illustrations showing the improvements in roadway maintenance where roof bolting is used in conjunction with arched girders are given.

SECTION D: To study the behaviour of bolts after the strata around the excavation have been loaded beyond the "elastic limit", plaster models of the underground roadways were made and tested to destruction in the laboratory. The models were loaded in a vertical compression testing machine. A photographic record of the tests and a detailed analysis of the results are given.

Part of the work here described has been presented in a paper to

The National Association of Colliery Managers and will be published in the "Iron and Coal Trades Review."

An extensive bibliography of the literature consulted is given as an appendix.

SECTION A - PHYSICAL PROPERTIES OF COAL MEASURES ROCK

Before any roof support system can be analysed either by models in the laboratory, or by a full-scale underground investigation, it is necessary to have detailed knowledge of the physical properties of the structural materials subjected to stress and the nature of the forces induced by mining. Consequently, detailed information regarding the physical properties of the rocks surrounding the mine workings is of paramount importance.

In the past, the physical properties of rocks have been determined by many investigators for a variety of purposes including geophysical exploration, oilfield structure, building and roadway construction, etc. In addition many experiments have been performed with mine rocks to determine their crushability, drillability (percussive and rotary), explosive shattering properties, permeability, etc. Obert, Windes and Duvall in their report on the physical properties of mine rock (A1) give an extensive bibliography of rock testing. Furthermore, several investigators (A2 - A8 incl.) have studied the properties of rocks in respect to the strength of mine structures - pillar sizes, gallery design, rock bursts, etc. However, in many of the published reports on the physical properties of rocks, there are only brief descriptions of the composition of the rock which render correlation of the results almost impossible.

In view of the lack of specific information regarding the physical constants of the Carboniferous rocks, a series of tests was carried out on several rock types commonly found associated with the seams in

Scottish mines. For each rock type studied an attempt was made to relate the elastic properties to the mineral composition, grain size and cementing material.

In addition to the determination of the elastic constants an investigation of the "time-straining" or "pseudo plastic flow" of several of the rock types was carried out. The majority of the tests were based on similar ones carried out by D.W. Phillips (A9, A10, A11) using electrical methods for the strain measurement instead of "mechanical-optical" devices.

APPARATUS

(a) Strain Measurement

The strains which occur in rocks under stress are of a very low order and consequently the strain measuring apparatus must have a high sensitivity. Many methods, such as levered mechanical gauges (A12) or optical gauges - Martens-type extensometer fitted with an auto-collimation telescope, the Spingometer, or the Phillips-Davies apparatus (A9) - have been used for the determination of rock strain. Mechanical and optical gauges do not lend themselves to automatic recording of strain at several points in quick succession and they are quite unsuitable for field investigations (especially underground). To overcome these difficulties various types of electrical devices have been used for accurate strain measurement both in the laboratory and in the field (A13 - A16 incl.). The electrical resistance strain gauge (A17 and A18) has been developed in civil and aeronautical engineering investigations with marked success. It was decided to investigate the suitability of such gauges for laboratory tests on rock specimens and possibly adapt the method for the measurement of the strain developed in rocks 'in situ' around mining excavations (see later).

The strain gauges found to be the most suitable for the laboratory tests were the De Havilland Bakelite HNR/2400/1 type, and the Phillips PR/9210/03 type.

Initially a De Havilland steady stress bridge (D.C.) was used for recording the strains but later a Phillips bridge (A.C.) with a

higher sensitivity was used.

De Havilland Bridge (Type 8/A.12): A schematic circuit diagram illustrating the basic principles (Wheatstone Bridge) involved in this D.C. instrument is shown in Fig. 1A. The instrument uses the "null-point balancing" method, with a graduated potentiometer reading the percentage change of resistance directly. An external spot galvanometer can be incorporated to increase the sensitivity of the instrument. Input power is provided by 12-volt batteries or from a laboratory "eliminac" power pack. Twelve channels are incorporated in the bridge to permit twelve gauges to be read in succession. In this instrument a compensating gauge is required for each active gauge used. Plate 1A shows the instrument set up for use in a bending test.

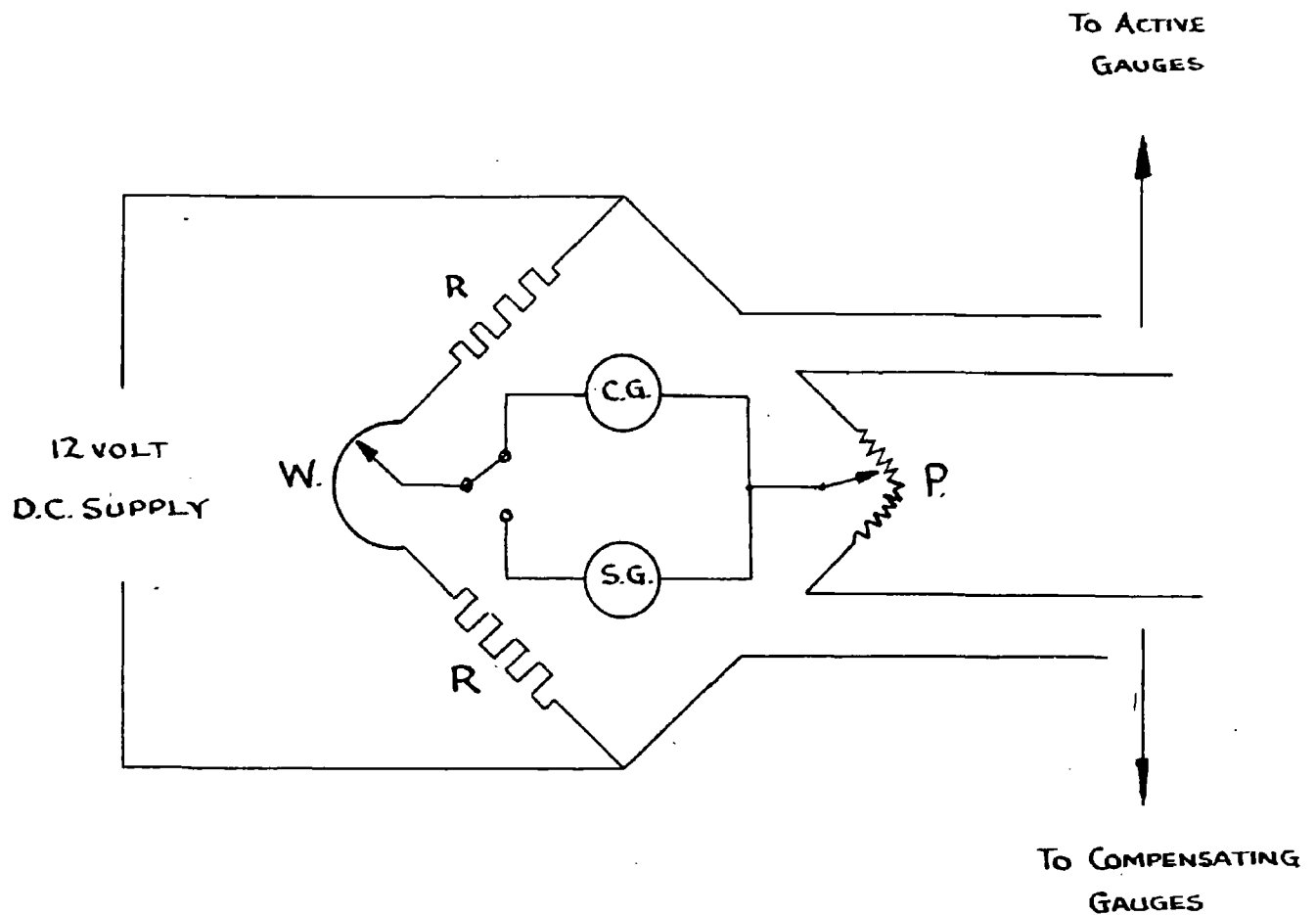
Phillips Direct Reading Bridge (Type GM.5536/01): This instrument is also based on a Wheatstone Bridge arrangement; the bridge being fed with a carrier wave of 4,000 cycles per second from an oscillator unit. Balance of the bridge for amplitude and phase is obtained by variable condensers C_1 and C_2 (see schematic diagram Fig. 2A). The diagonal voltage arising during measurement is amplified by a highly stable and sensitive four-stage amplifier. A phase-sensitive ring demodulator determines the "polarity" of the signal which is then recorded by a D.C. micro-ammeter. Input power to the instrument is from the A.C. mains, a variable transformer being incorporated to permit a wide choice of mains voltage. In addition a switching unit (type GM.5545), which permits strain

measurement at ten points, can be connected to the measuring bridge. The switching unit incorporates balancing condensers and resistors for each gauge circuit, and control resistors for checking the calibration of the meter. Individual compensating gauges can be used if the temperature variations between measuring points are large, but, if required, one compensating gauge can be used for two or more active gauges. The apparatus can also be used for the measurement of dynamic strains when coupled to an oscillograph or pen recorder. This unit was used for all the underground measurements (see later) as well as the laboratory tests. The measuring bridge and switching unit are shown in Plate II A.

(b) Loading Machines

Compression Testing: All the compression tests on the rock specimens were carried out on a ten-ton Avery Universal machine. This is an electrically operated hydraulic machine, the loads being measured directly on a dial indicator reading to ten tons in increments of 0.05 tons. Fibre-board pads were placed between the machine platens and the specimen in all the tests.

Tensile Testing: The tension tests on the rock specimens were carried out on a Avery Single Lever testing machine. The loads were applied by gravity using an efficient screw mechanism. Loads up to 5,000 lb. could be applied in increments of 10 lb.; measurement being made by means of a steelyard.



R : *FIXED RATIO ARMS*

P : *INITIAL BALANCE POTENTIOMETER*

W : *CALIBRATED SLIDE WIRE*

C.G. : *COARSE GALVANOMETER*

S.G. : *SPOT GALVANOMETER*

FIG. 1.A. SCHEMATIC CIRCUIT DIAGRAM OF
DE HAVILLAND BRIDGE

BRIDGE BALANCING

CARRIER WAVE

MODULATION

CAPACTORS

SOCKETS

SOCKETS

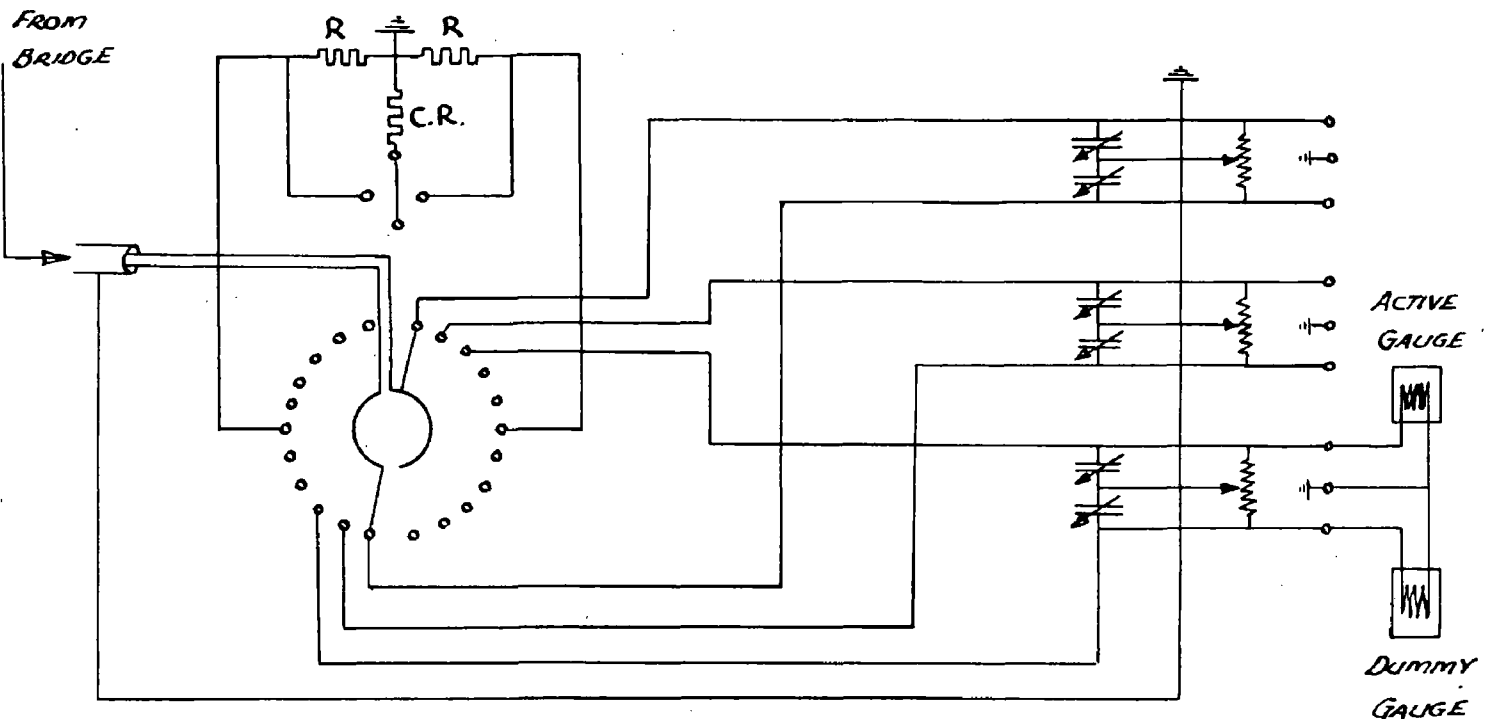
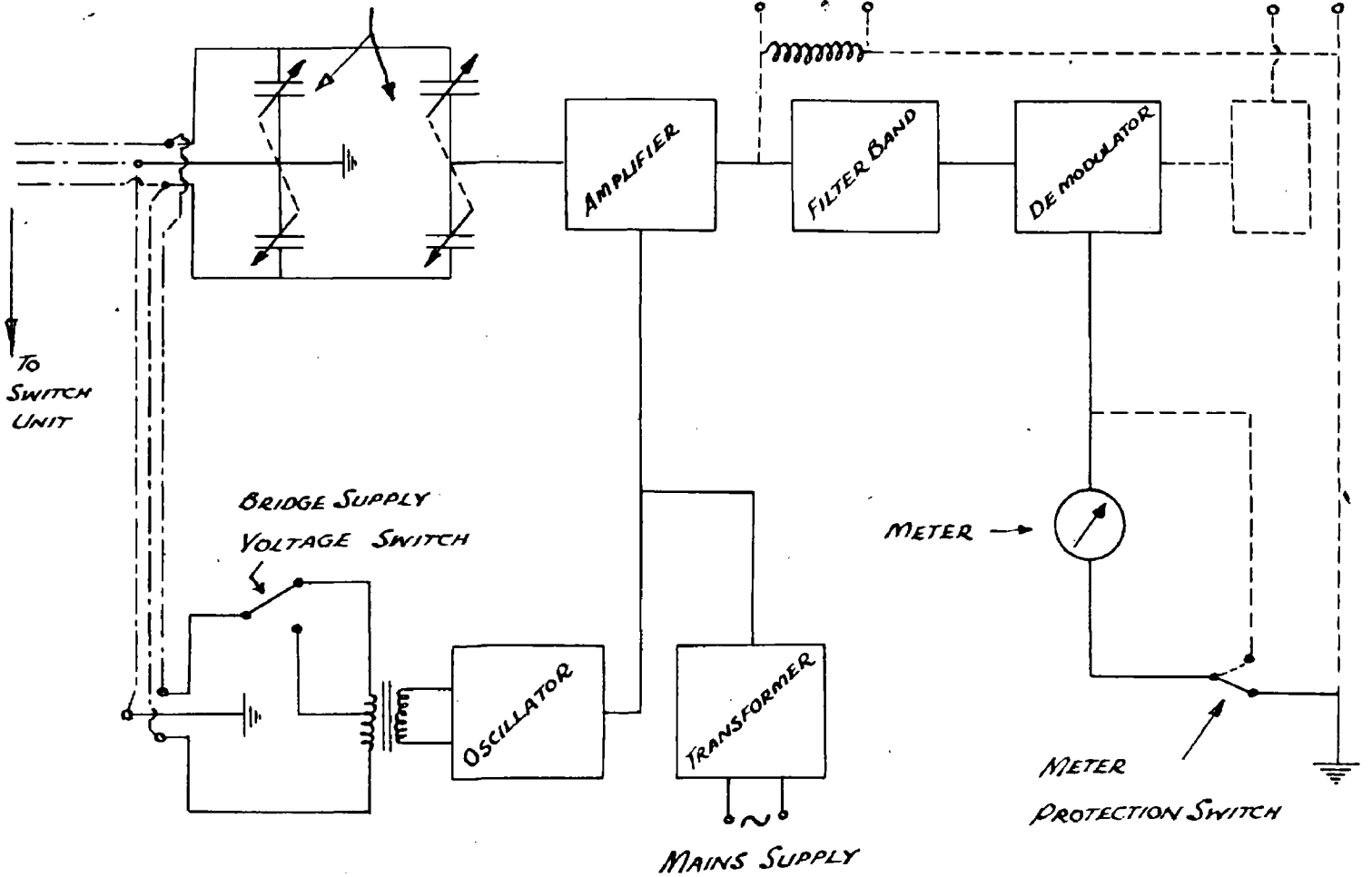


FIG 2.A. SCHEMATIC CIRCUIT DIAGRAM PHILIPS BRIDGE

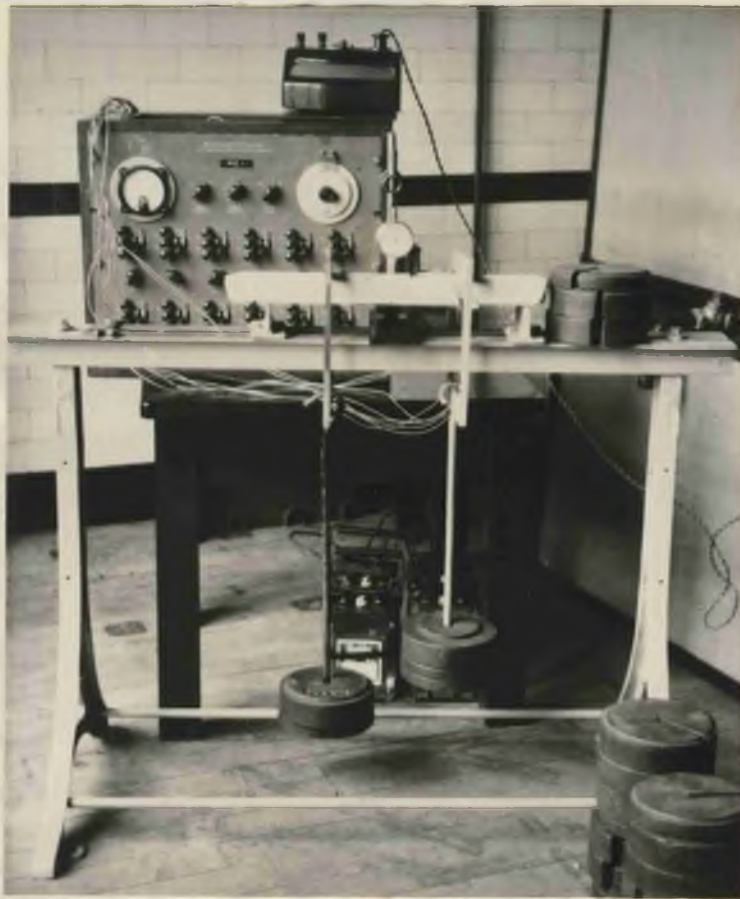


PLATE I A

De Havilland D.C. Strain Measuring Bridge

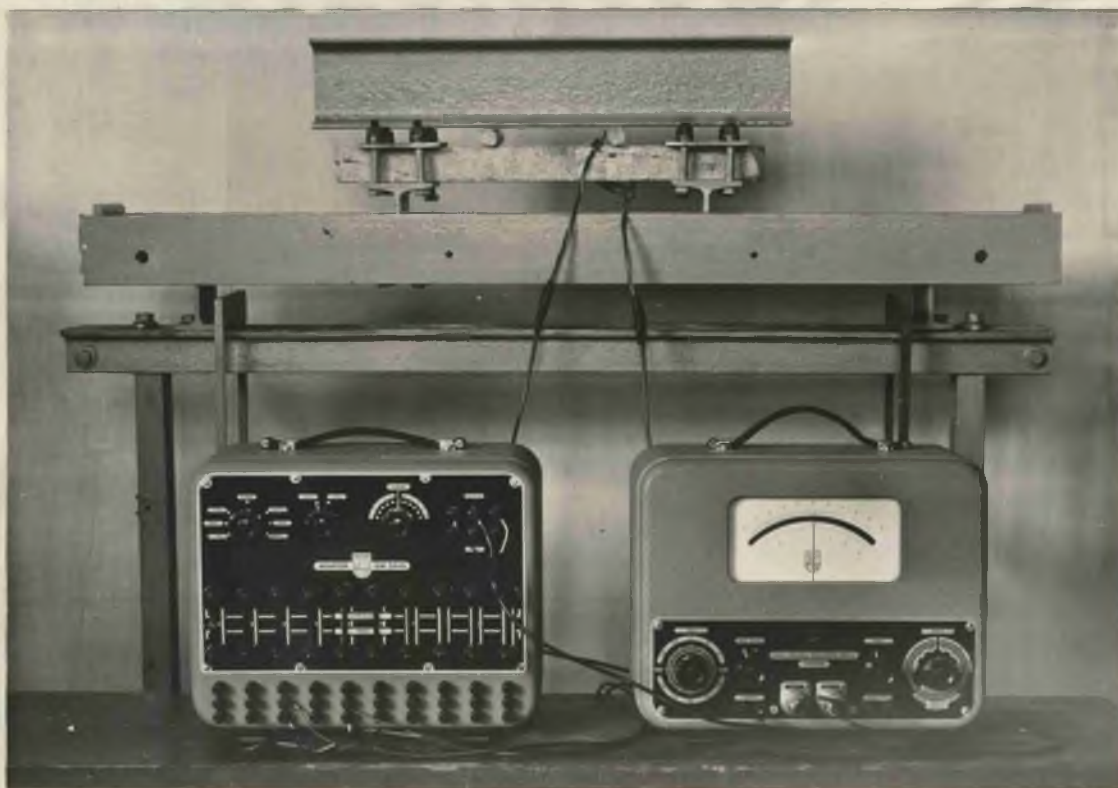


PLATE IIA

Phillips A.C. Direct Reading Strain Bridge

Considerable difficulty was encountered in fitting the specimen in standard tensile testing clamps. Special clamps had to be designed which would apply pure tension to the specimen without causing failure of the rock by compression in the clamps. The clamps adopted are shown in Plate III A. The spherically seated joint (in the clamp) was placed as close to the end of the specimen as possible, and in line with the axis of the specimen to permit self-alignment of the specimen in the machine.

Bending Tests: The loading frame used in all the bending tests is shown in Plate I A where a simply supported rock beam is being tested in pure bending, i.e. equal loads at the quarter points. A channel girder fitted with clamps for "fixed end conditions" could be mounted on top of the frame when required. A "fixed beam" specimen is being tested in this way in Plate II A. All loading of the specimens in the bending tests was by riders and dead weights.

(c) Rock Dressing Equipment

The apparatus used for dressing the rock specimens is shown in Plate IV A. The specimen is held in the spring loaded clamp which is aligned perpendicular to the rotary table, to enable the end faces of the specimens to be ground parallel. The carborundum powder on the table is kept moist by a fine water spray. A D.C. motor with resistance speed control provides the drive to the grinding table. Final smoothing of the rock surface (for the application of strain gauges) is by hand, using fine grinding powder and the glass polishing plate shown.

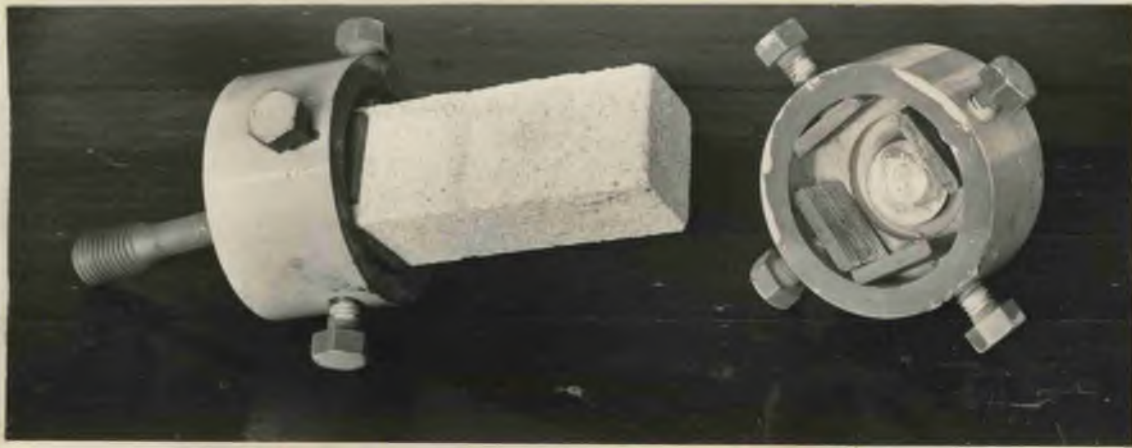


PLATE IIIA

Tensile Testing Clamps



PLATE VA

Representative Group of Rock Specimens

PLATE IVA



Rock Dressing Equipment

Collection and Preparation of Rock Specimens

The rock samples were collected from several collieries in the Central and Ayrshire coalfields. Slabs of rock, macroscopically homogeneous and free from fractures, joints, slips, etc., weighing about 1 cwt. were carefully selected underground. The slabs were cut from face areas unaffected by blasting or from stone drifts in the vicinity of coal seams. The sampling positions, relative to the seams, were noted.

The blocks of rock were taken from the mine as soon as possible after cutting and were transported to a local firm of masons where they were cut, by diamond saw, into the specimen sizes listed below. Due to the large quantity of cooling water used when cutting, several of the rock slabs selected disintegrated while being cut. This applied particularly to clay rocks and fakes. The specimen sizes were:-

2" x 2" x 3"	compression tests,
2" x 2" x 6"	tensile tests,
2" x 1½" x (18" to 24")	bending tests.

A representative group of specimens is shown in Plate V A.

The cut specimens were ground by various grades of carborundum on the rock dressing apparatus to ensure that the loading faces of the compression specimens were parallel, and to prepare the rock surface for the application of the gauges. It was not possible to grind the bending specimens with the apparatus; consequently it was necessary to resort to hand grinding.

Petrographic Examination of the Rocks

A study of previous investigations of the physical properties of rocks reveals considerable difficulty in correlating the results obtained by different experimenters, because of the variation in the nomenclature of similar rock types found in different localities. Consequently some classification, other than the local rock names, is necessary. The most satisfactory method for the classification of sedimentary rocks is based upon the dominant grain size; the shape of the grains, nature of the cementing material, and the mineralogical composition have also to be considered. The classification adopted is similar to that suggested by Milner (A19) and used by Hudspeth and Phillips (A20) since it was found to be more applicable to the rock types studied, than the classification by Harley (A21).

CLASSIFICATION

<u>Grade</u>	<u>Dominant Grain Size</u>	<u>Rock Type</u>
Scree, shingle or gravel	2.0 mm. or over	Conglomerate
Very coarse Sand	2.0 mm. to 1.0 mm.	Very coarse grained sandstone
Coarse Sand	1.0 mm. to 0.5 mm.	Medium sandstone
Fine Sand	0.1 mm. to 0.05 mm.	Fine grained sandstone
Silt	0.05 mm. to 0.01 mm.	Siltstone
Mud or Clay	Less than 0.01 mm.	Mudstone, shale, clay, etc.

Thin sections were made of all the rock types, the mineralogical examinations and particle size determination being made in a Vickers Projection Microscope fitted with a graticule.

In order to facilitate reference the rocks tested have been given code numbers:- DH1 to DH7 and CM1 to CM5. A description of each rock type and micro-photographs of typical sections are given in the Appendix.

EXPERIMENTAL PROCEDURE AND THEORETICAL CONSIDERATIONS

The experimental work can be sub-divided into three main parts, viz. -

- (a) The determination of the ultimate strength of Coal Measures Rock in compression and tension, and the correlation of the strength values obtained with the composition of the rock.
- (b) The plotting of "stress-strain" diagrams for rocks in compression, tension and bending, and the calculation of the elastic constants under different conditions.
- (c) An investigation of the time-straining of rocks and the possibility of predicting the "time v strain" relationship for certain rock types in specified loading conditions.

Considering each part and any theoretical considerations involved:-

(a) Strengths of Coal Measure Rocks

It has been suggested by several investigators that the strength of sedimentary rock is governed by the following factors:

Dominant grain size - theoretical considerations would appear to indicate that the smaller the grain size the greater will be the strength of the rock, since the interstitial space is at a minimum with small grains.

The shape of the grains - this factor was not considered in the investigation since in the majority of the rock types tested the rock grains were rounded.

The nature of the cementing medium - this seems to be the most

important factor in determining the ultimate strength of a given rock. A range of sandstone specimens, of similar grain size, and various cements was examined in an attempt to establish their relative strengths.

Mineralogical composition - wide variation of the composition of any rock type will obviously affect the strength, so only sandstones with similar compositions were considered in the tests to determine the influence of grain size and cementing medium.

Phillips (A10) outlined the theory by which the most effective shear planes could be determined for any rock under a given stress, provided the "internal friction factor" (Navier's Theory) for the rock type was known. In several of the specimens tested in compression the inclinations of the fracture planes were measured and the friction factor calculated from the relationship:

$$\tan 2 \theta = \frac{P_1 - P_3 - 2KQ}{K(P_1 - P_3) - 2Q}$$

where:

P_1 and P_3 are applied forces (principal stresses)

Q is the rotational shear stress

θ is the inclination of the most effective shear plane
with respect to the principal stress plane

K is the "internal friction factor"

Considering an unconstrained compression test -

$$Q = 0 \text{ and } P_3 = 0$$

$$\therefore \tan 2\theta = \frac{P_1}{KP_1} = \frac{1}{K}$$

$$\text{i.e. } \tan 2 \text{ (angle of shear plane)} = \frac{1}{\text{Friction Factor}}$$

or Friction Factor = cotangent 2 (angle of shear plane)

Experimental Procedure: Several specimens of each rock type were accurately ground to ensure that the loading faces were truly parallel. The specimens were then subjected to uniform direct pressure on two faces, the other surfaces being free from constraint.

In the tension tests several specimens of each rock type were tested to destruction. The specimens had to be carefully fixed in the loading clamps to ensure that pure tension, and no bending, was applied to the specimens otherwise erroneous results would have been obtained.

(b) Determination of Elastic Constants

The variations of the elastic constants with stress, of the rock types previously classified, were studied in compression, tension and bending. In all the tests strain was measured by resistance strain gauges.

Application of the Strain Gauges: The accuracy of the resistance strain gauge is largely dependent upon the security of the bond between the gauge and the surface of the test specimen. The desirable properties of an adhesive for fixing gauges are:-

- (1) Good adhesion to both surfaces under high strain.
- (2) It should not set so hard as to crack under load.
- (3) It must have a low moisture sensitivity.
- (4) It should be a very good electrical insulator.
- (5) It should be suitable for application and setting in
the cold state (especially for field investigations).

A series of tests was carried out with different types of cements; Araldite Cold Setting Filler proved to be the most suitable cement for bonding the gauges to the rock surface. The Araldite Filler (100 parts) was mixed with the Hardener (8 parts) and the mixture allowed to stand for 15 minutes before use to permit evaporation of any excess Hardener. It was found that better bonding and insulation of the gauge was obtained if the surface was pre-coated with cement, covered with a thin sheet of capacitor tissue, and then the gauge applied in the usual manner (A22). Although Araldite is termed "cold setting" it was necessary to cure the specimen for approximately 20 hours at 40° C to ensure that the cement matrix was fully polymerised. The curing was carried out in an aluminium chamber fitted with infra-red heating elements. Plate VI A shows three compression specimens, and a rock beam fitted with gauges.

Compression Tests: The stress-strain curves were obtained by taking readings of longitudinal and lateral strain as quickly as possible after applying the load, to offset any tendency for "time-straining" of the specimen. Loading was applied up to a maximum of 75% of the ultimate

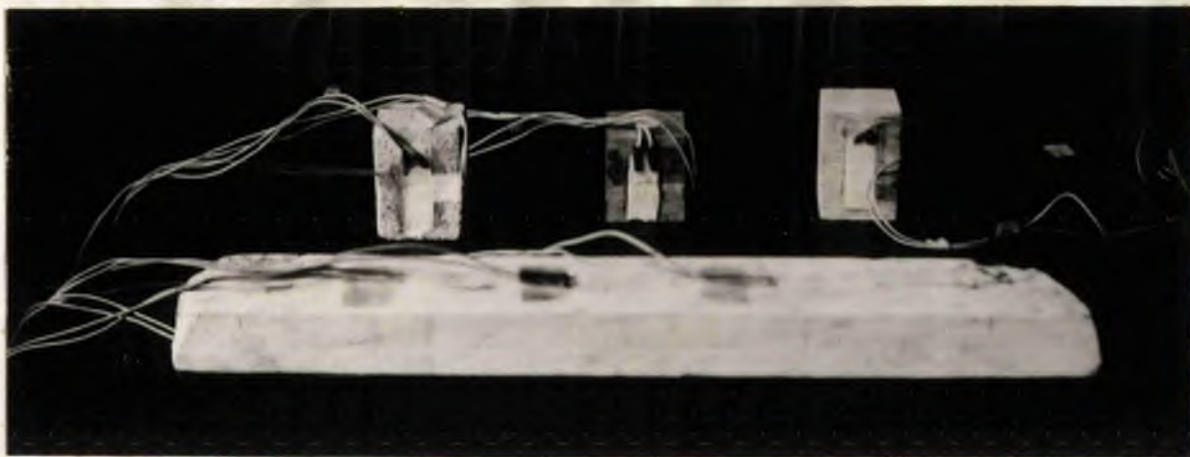


PLATE VIA

Specimens fitted with Strain Gauges



PLATE VIIA

Specimens after Testing

strength of the material. Strain values were also noted as the load was reduced. The procedure was repeated for the second and third cycles of loading.

Values of Young's Modulus (E) and Poisson's Ratio (σ) were calculated from the stress-strain curves. The variations of E and σ with applied stress were plotted.

Another property of rocks which is very important in the study of their behaviour around underground excavations, is their capacity for storing strain energy (A_8, A_{10}). The strain energy per unit volume developed in some of the rocks under compression was plotted against the applied stress.

Tension Tests: The procedure adopted for the tension tests was similar to that followed in the compression tests. The variations of Young's Modulus and Poisson's Ratio with stress were plotted for each of the rock types tested.

Bending Tests: Several tests were carried out on rock beams with both free and fixed end conditions. The strains recorded at various points on the upper and lower surface of the beam were plotted against the applied load.

It is known that for ductile materials strained within the elastic limit, the "neutral axis" (i.e. the unstrained fibre when the material is subjected to pure bending) lies along the middle of the beam. However with materials such as rock, which are not purely elastic in

their behaviour, the position of the neutral axis is not necessarily in the middle of the beam. The position of the neutral axis depends on the relative values of Young's Modulus in tension and compression - a proof of this phenomenon has been derived by Phillips (A10).

(c) Time Strain in Coal Measures Rock

All solids when subjected to great pressures show a continuous deformation or "flow" with time. This flowing or inelastic behaviour of solid materials is known as "plasticity." Rock and concrete which are usually considered as brittle materials also exhibit "flowing" under certain loading conditions (A10, A23, A24). The flowing of strata into underground excavations has been noted for many years and indeed several Continental engineers consider the "flowing property" of rocks to be the most vital one in determining the pressure distributions around mine workings. Holland (A8) refers to the importance of plasticity of coal and associated rocks in the phenonema of rock bursts. Phillips (A10) concludes from his laboratory tests on rocks, that the total strain produced by a given load consists of two parts, viz. immediate strain and time-strain, the latter being sub-divided into "elastic" and "plastic" time-strain. Consequently, it is the total strain developed in a rock under stress which is more important than the strain developed immediately after the load is applied. Hence, experimental values of the elastic constants of rocks are of little value if the effect of time cannot be considered in the prediction of

strain (or deformation) under certain loading conditions.

Similar time-straining effects have been noted for other materials, including steel (A25) and plastics. Pao and Marin (A26) in their studies of the prediction of creep curves from stress-strain data used experimental results obtained from plexiglass in tension. It is realised that there is a vast difference in the structure of the homogeneous plastic and the relatively heterogeneous rocks used in the tests here described but since the observed "time v strain" relationship of both materials is quite similar, a method based on the one derived by Pao and Marin was used in an attempt to predict the total strain developed in the rock as a function of time.

The "strain-time" curve for a given value of applied stress is derived thus:-

A family of stress-strain curves for different strain rates (such as shown in Fig. 3A) are obtained for the material under test. The higher the strain rate the greater is the slope of the stress-strain curve and so with instantaneous loading the strain rate (U) is assumed to be infinite - i.e. with an infinite strain rate the material does not have time to creep under any one load, and consequently the stress strain relationship is linear.

However for strain rate U_1 (Fig. 3A) the material does have time to creep and the total strain is OQ at stress S_1 . The strain OQ is made up of $OP + PQ$ where $PQ = AB$ and represents the time-strain or creep

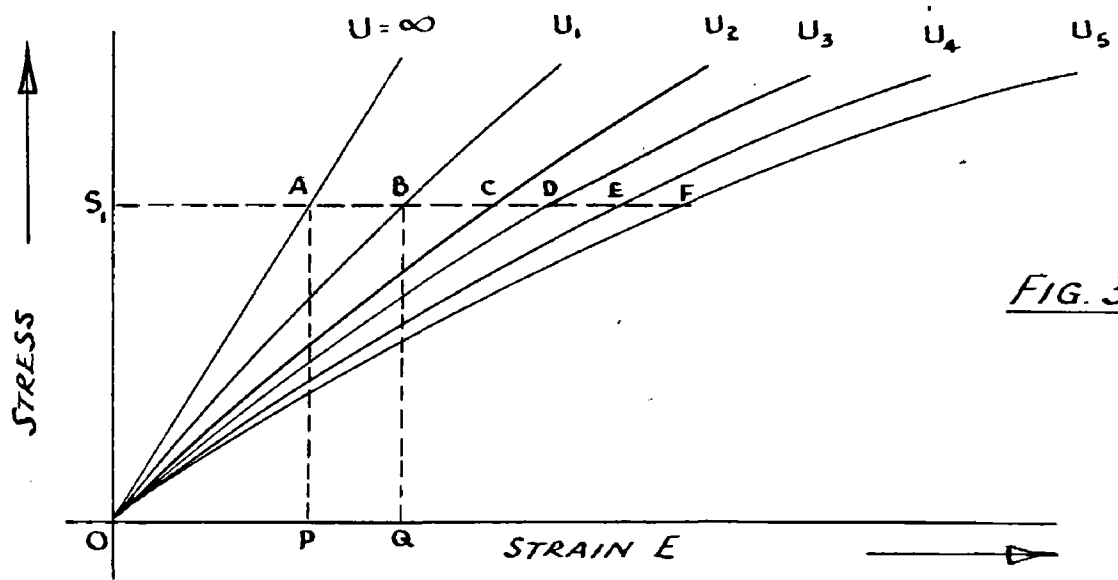


FIG. 3.A.

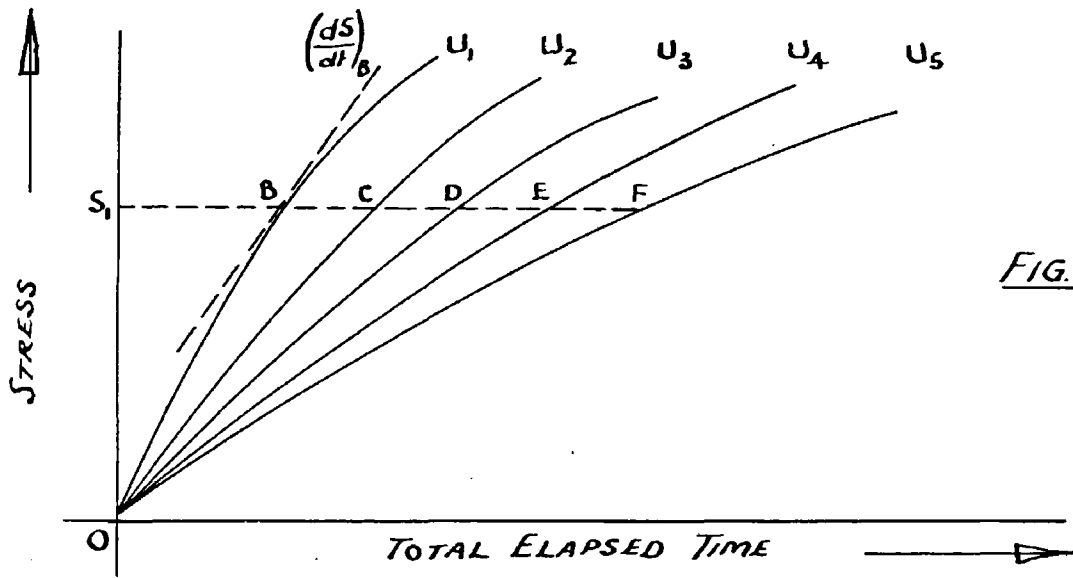


FIG. 4.A.

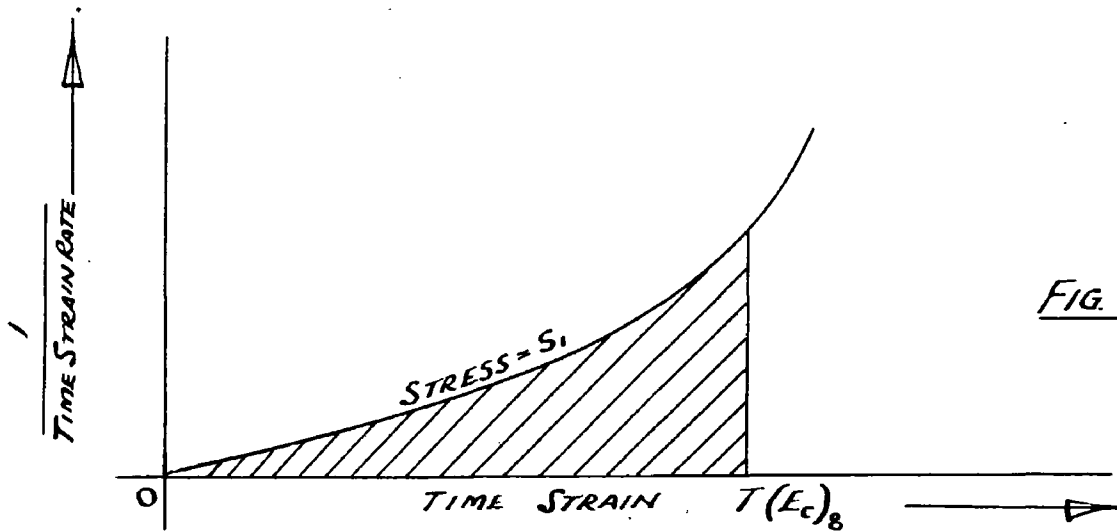


FIG. 5.A.

that took place under a varying stress and in the time necessary to load the specimen from a stress value $S = 0$ to $S = S_1$.

At any time t , the total strain E_t is the sum of the immediate strain (considered as wholly elastic) and the time strain (considered as partly elastic and partly plastic). Or, in symbols,

$$E_t = E_e + E_c \dots\dots\dots(i)$$

where E_e and E_c are the immediate and time strains respectively.

Differentiating (i) with respect to time t ,

$$\frac{dE_t}{dt} = \frac{dE_e}{dt} + \frac{dE_c}{dt} \dots\dots\dots(ii)$$

By Hooke's Law,

$$E_e = \frac{S}{M}$$

where $S =$ stress and $M =$ Modulus of Elasticity.

Also, $\frac{dE_t}{dt} = U =$ total strain rate.

Therefore, by substitution, equation (ii) becomes

$$U = \frac{1}{M} \cdot \frac{dS}{dt} + \frac{dE_c}{dt} \dots\dots\dots(iii)$$

To evaluate $\frac{dE_c}{dt}$ from equation (iii) $\frac{dS}{dt}$ must be known. $\frac{dS}{dt}$ can be found by plotting stress against total elapsed time, and finding the gradient at the required point, say point B on the U_1 curve of Fig. 4A.

Hence from equation (iii)

$$\frac{dE_c}{dt} = U_1 - \frac{1}{M} \left(\frac{dS}{dt} \right)_B \dots\dots\dots(iv)$$

Therefore, the strain rate, and time strain can be evaluated for any

required stress value at any of the strain rates $U_1, U_2, \text{etc.}$

Also, if the reciprocals of the time strain rate values are calculated, and plotted against the corresponding time strain for each selected stress value, curves of the form shown in Fig. 5A will be obtained. If the time strain $(E_c)_B$ is represented by OT then the time required for the material to creep at constant stress S_1 to a time strain $(E_c)_B$ (i.e. equal to AB in Fig. 3A) will be represented by the area under the $\frac{1}{dE_c/dt} \text{ v } E_c$ curve, since

$$\text{time} = t = \int dt = \int \frac{dE_c}{(dE_c/dt)}$$

$$\text{i.e. } t = \int_0^{E_c} \frac{1}{(dE_c/dt)} dE_c \dots\dots\dots(v)$$

Therefore, for a series of values of the time strain the corresponding time values can be determined and the "creep v time" curve can be plotted for any selected value of applied stress.

Experimental Procedure

Bending Tests: A simply supported beam was fitted with gauges. Suitable increments of load were applied and the corresponding strains noted for instantaneous loading and incremental loading with measured time intervals between the application of the loads. A few days were allowed between each test to permit recovery of any elastic time strain in the beam. From the observed results "time-strain v time" curves were deduced by the theory outlined above and compared with

similar curves obtained by experiment.

Tension Tests: A series of tension specimens were prepared from the same rock sample, and subjected to a series of time strain tests similar to those outlined for the bending specimens, but in this case a separate specimen was used for each "strain rate". From the observed results, "time-strain v time" curves were deduced and compared with experimental curves.

In addition to the tests from which the final "strain v time" curves were calculated several experiments were carried out on the other rock types in bending and tension. In all the experiments carried out the familiar stepped curve was obtained.

EXPERIMENTAL RESULTS

(a) Strength of Coal Measures Rock

As many tests to destruction as possible were made with each of the classified rock types. Tests were made in tension and compression, both parallel and perpendicular to the bedding planes if suitable specimens were available. Table No.1A below summarises the results obtained; each stress value quoted is the mean of at least three experimental results.

TABLE No.1A

Code No.	Rock type	Ult. Tensile Strength (lb./in. ²)		Ult. Compressive Stress (lb./in. ²)	
		Perp. to Bedding	Parl. to Bedding	Perp. to Bedding	Parl. to Bedding
DH1	F.G. Sandstone	-	-	16,450	10,600 V
DH2	N.G. Sandstone	236	-	6,500	-
DH3	Siltstone	-	-	11,230	10,000 V
DH4	Siltstone	246	565	7,120	-
DH5	F.G. Sandstone	-	-	9,870	5,380
DH6	C.G. Sandstone	82	-	1,450	-
DH7	Clay Siltstone	195	-	14,500	-
CM1	M.G. Sandstone	220	-	5,500	-
CM2	F.G. Ironstone	620	-	10,900	-
CM3	M.G. Sandstone	270	-	7,550	-
CM4	M.G. Sandstone	-	-	10,000	-
CM5	M.G. Sandstone	175	-	4,200	-

Legend -

F.G. - fine grained

M.G. - medium grained

C.G. - coarse grained

V. - failed with violence

Considering the range of sandstones tested, the following results can be abstracted, to illustrate the influence of particle size and cementing medium on the ultimate strength of the rock in tension and compression. In the analysis only the ultimate stresses applied perpendicular to the bedding planes (if any) are considered.

TABIE No.2A
Effect of Particle Size

Code No.	Average Grain Size (mm.)	Compressive Stress (lb./in. ²)	Tensile Stress (lb./in. ²)
DH6	0.620	1,450	80
CM1	0.450	5,500	220
CM5	0.193	5,600	175 (W)
HD2	0.136	6,500	236
HD1	0.094	16,450	-

Note: All above specimens have siliceous cementing medium.

TABLE No.3AEffect of Cementing Medium

Code No.	Av. Grain Size (mm.)	Comp. Stress (lb./in. ²)	Tensile Stress (lb./in. ²)	Cement Type
CM3	0.13 - 0.37	7,550	270 (A)	Calcareous
HD2	0.136	6,500	236	Siliceous
GM4	0.12	10,000	-	Ferruginous
HD5	0.039	9,870	-	Calcareous
HD1	0.094	16,450	-	Siliceous
CM2	0.077	10,900	620 (IS)	Ferruginous

Legend - W - specimen very wet (*CMS.*)
 A - angular shaped grains
 IS.- ironstone rather than sandstone

After testing the specimens were carefully removed from the testing machine and the positions of the fracture planes noted. Plate VII A shows several specimens after testing. The inclinations of the shear planes in the compressive specimens were noted and values of the "internal friction factor" (Navier's Theory) were calculated. Table No.4A shows the average values of 'K' obtained for three of the rock types tested.

TABLE No. 4AInternal Friction Factors

Code No.	Average Inclination of Shear Planes	Friction Factor K
CM5	34°	0.4
CM1	30°	0.58
DH2	22°	1.03

(b) Determination of Elastic Constants

Compression: Stress-strain diagrams were plotted for each of the rock specimens tested. Typical of the diagrams obtained is that for specimen CM1 shown in Fig. 6A. The relationship between stress and strain is non-linear; consequently Hooke's Law is not valid and a true "elastic modulus" for the rock does not exist. The second, third and subsequent loading cycles give "hysteresis loops" which are almost exactly superimposed: the values of Young's (or Elastic) Modulus and Poisson's Ratio are calculated from such "loops".

There are two methods by which Young's Modulus can be determined from a non-linear stress-strain relationship, viz. -

$$(1) \quad \text{Young's Modulus} = \frac{\text{Total Stress}}{\text{Total Strain}}$$

for a given stress value, i.e. the secant modulus, and

$$(2) \quad \text{Young's Modulus} = \frac{\text{Incremental Stress}}{\text{Incremental Strain}}$$

for a given stress value, i.e. the tangent modulus.

The variations of the modulus (calculated by both methods) with applied stress for specimen CM1 are shown in Fig. 7A.

Poisson's Ratio can also be determined using either the "tangent" or the "secant" method for a given stress value. The variations of Poisson's Ratio with stress for both methods of calculation are shown in Fig. 8A. Also shown is the variation of the "secant ratio" with stress calculated from the initial loading curve.

The strain energy per unit volume developed in the specimen when under compression is shown in Fig. 9A. The variation of the curves obtained using the different values of elastic modulus is clearly shown.

Another typical stress-strain diagram (Specimen CM5) for rock in compression is shown in Fig. 10A. Similar forms of curves were obtained for the remaining specimens tested in compression. From the stress-strain curves the variations of Elastic Modulus and Poisson's Ratio with stress were determined. The "tangent values" of E and G for the range of rock types tested are shown in Figs. 11A to 14A inclusive.

The strain energy per unit volume developed in the rocks tested is illustrated in Fig. 15A.

COMPRESSION SPECIMEN C.M.I.
LATERAL & LONGITUDINAL STRESS-STRAIN CURVES

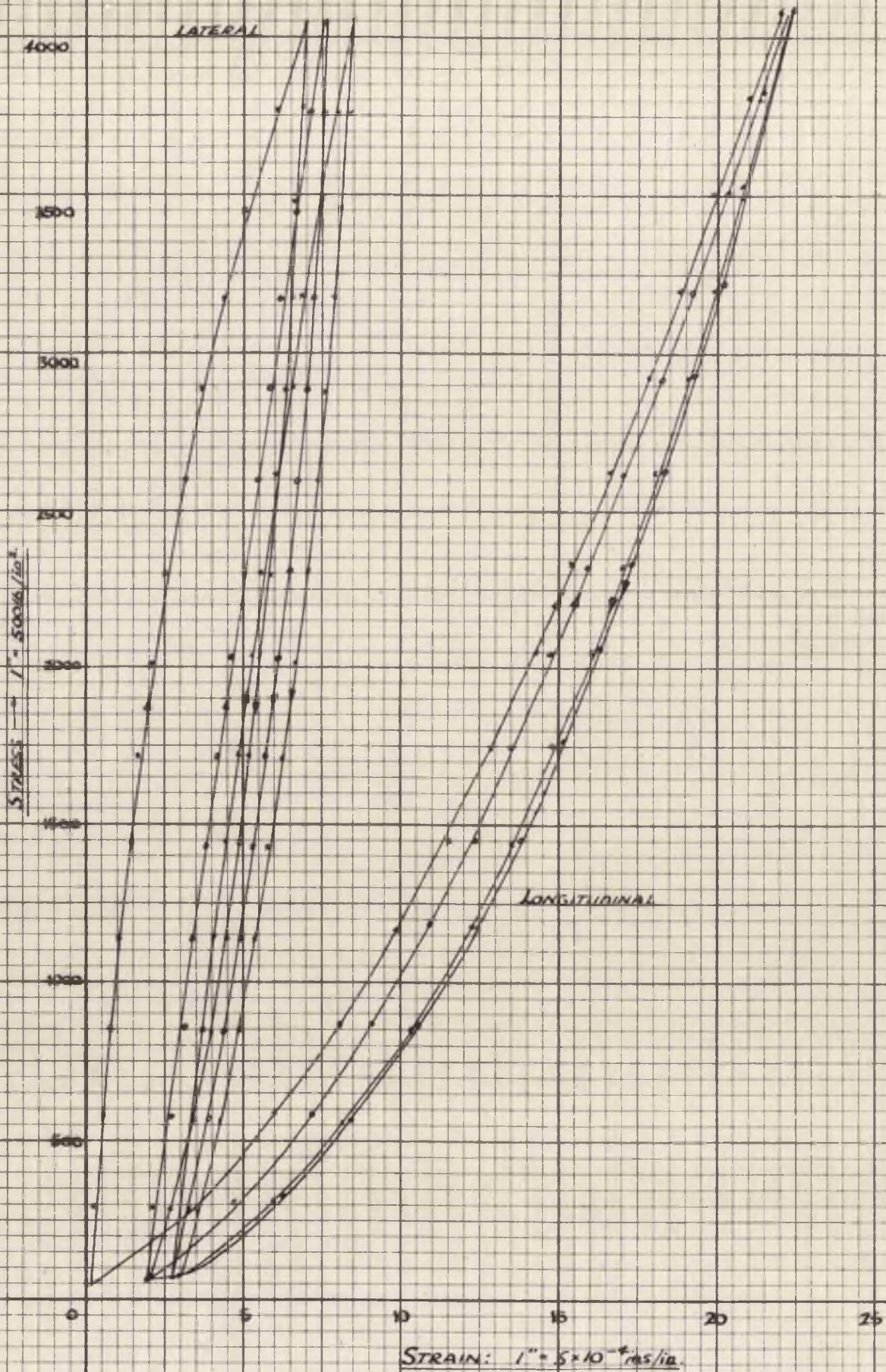


FIG. 6A

VARIATION OF ELASTIC MODULUS C.M.I.
(THIRD LOADING CYCLE)

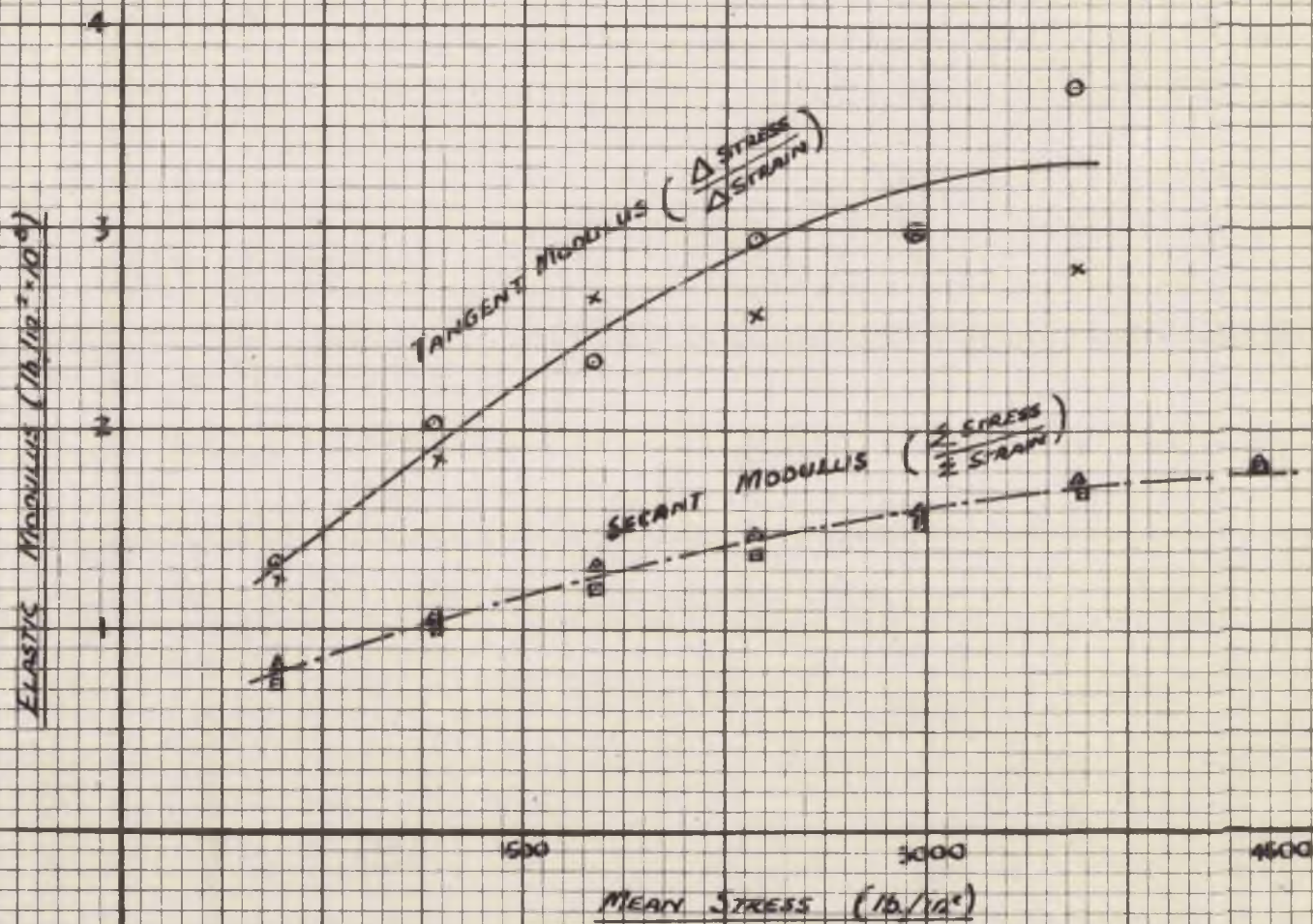


FIG. 7A.

Key to
symbols

VARIATION OF POISSON'S RATIO C.M.I.

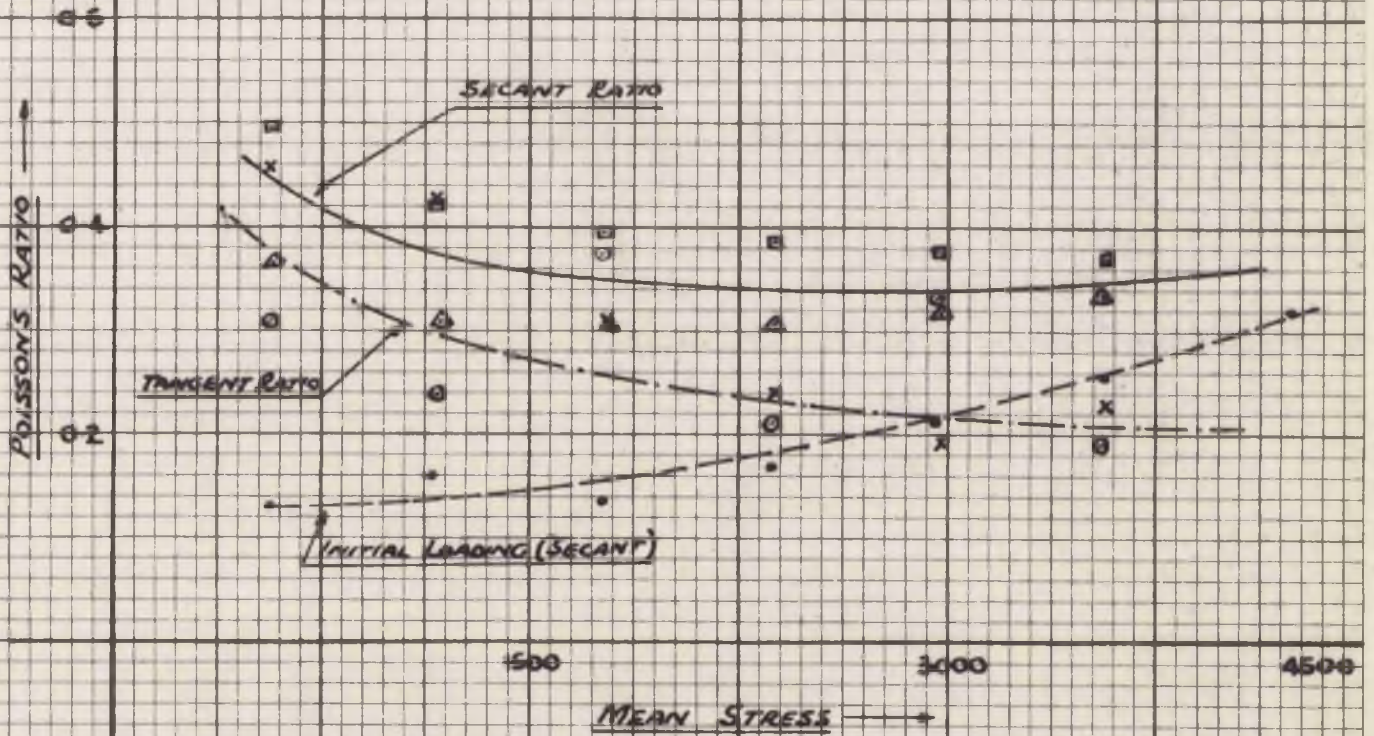


FIG 8.A.

Key to symbols

STRAIN ENERGY / UNIT VOLUME C.M.I.

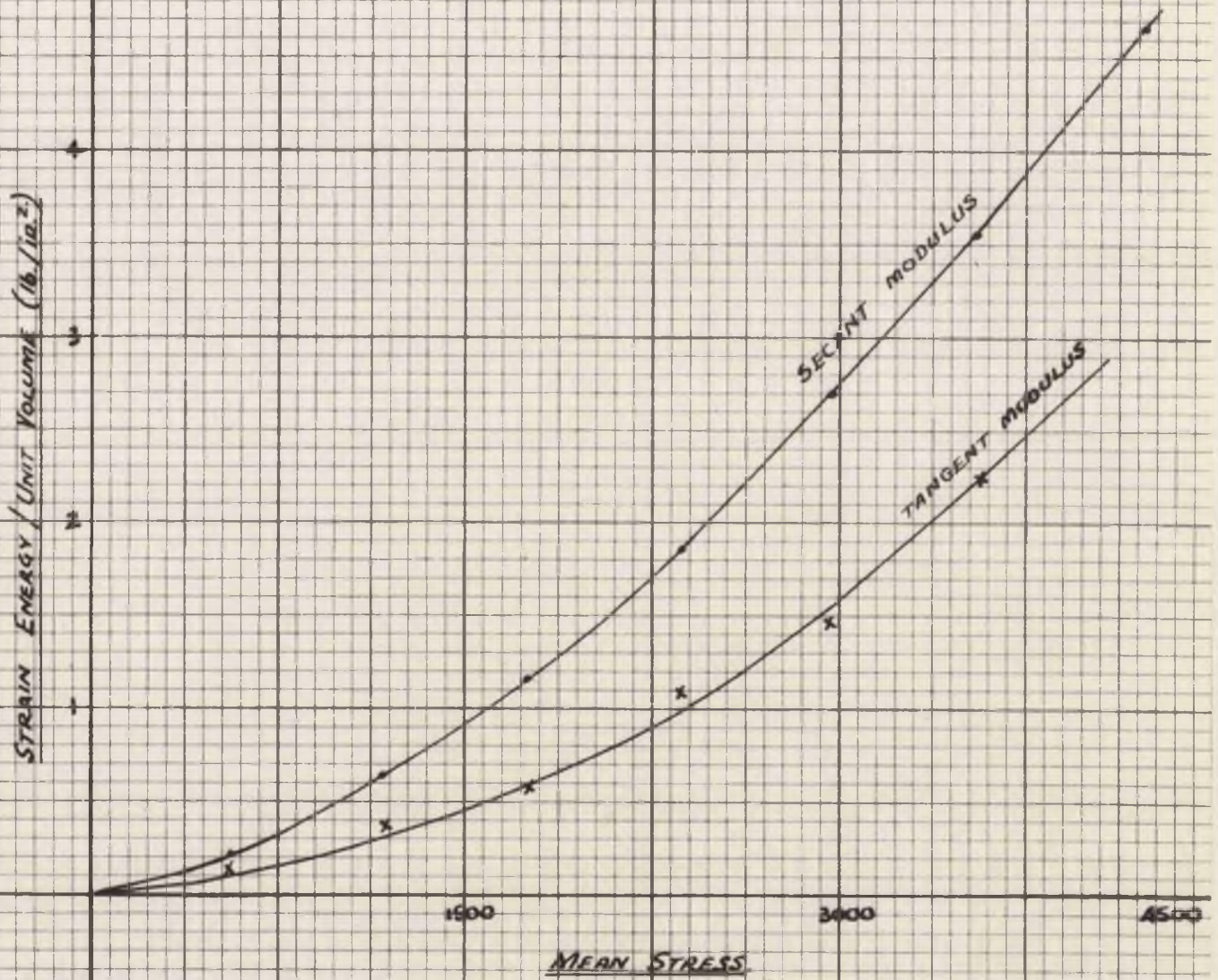


FIG. 9.A.

COMPRESSION - SPECIMEN C.M.5
LATERAL & LONGITUDINAL STRESS STRAIN CURVES

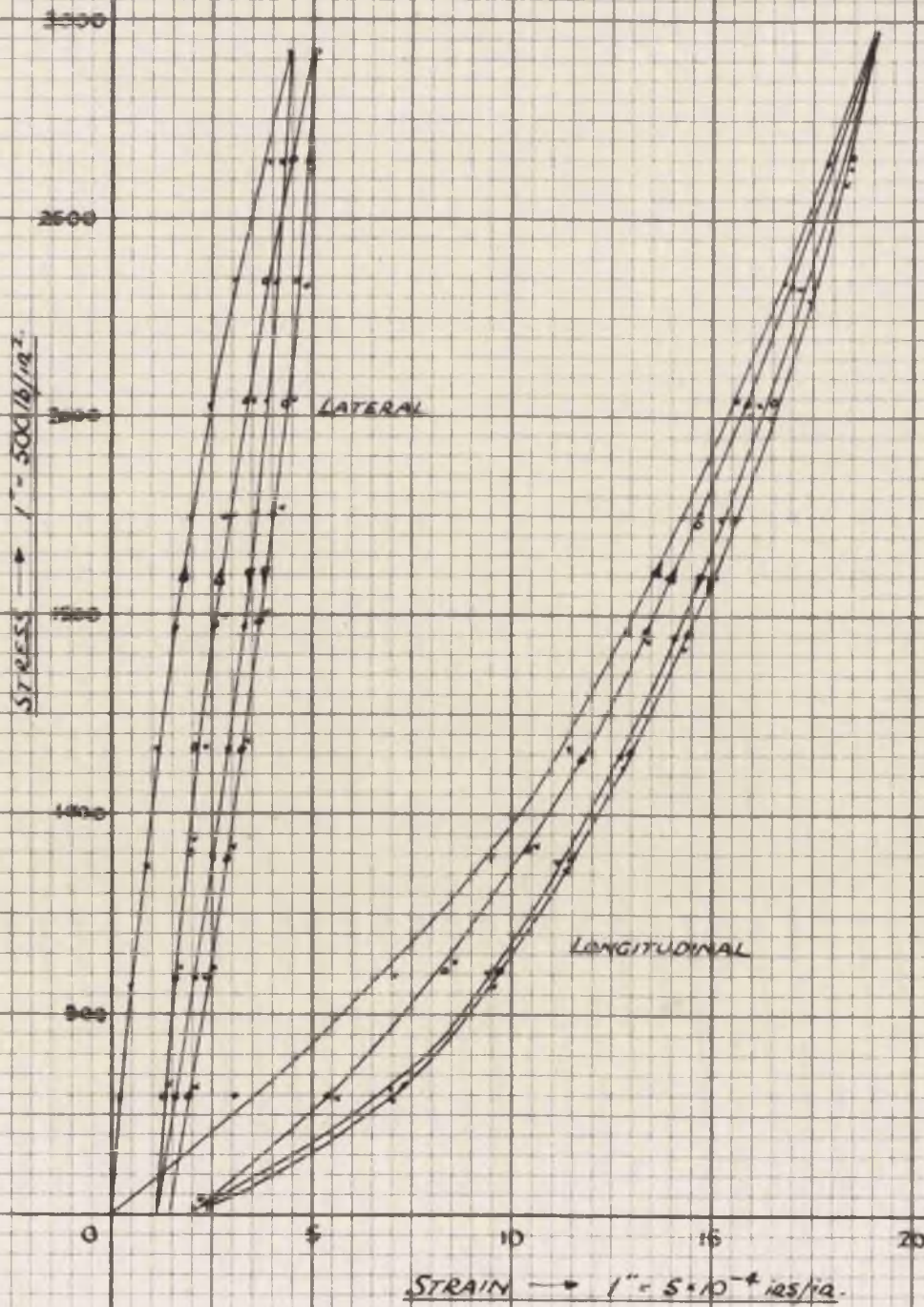


FIG. 10A.

ELASTIC MODULUS V STRESS (COMPRESSION)

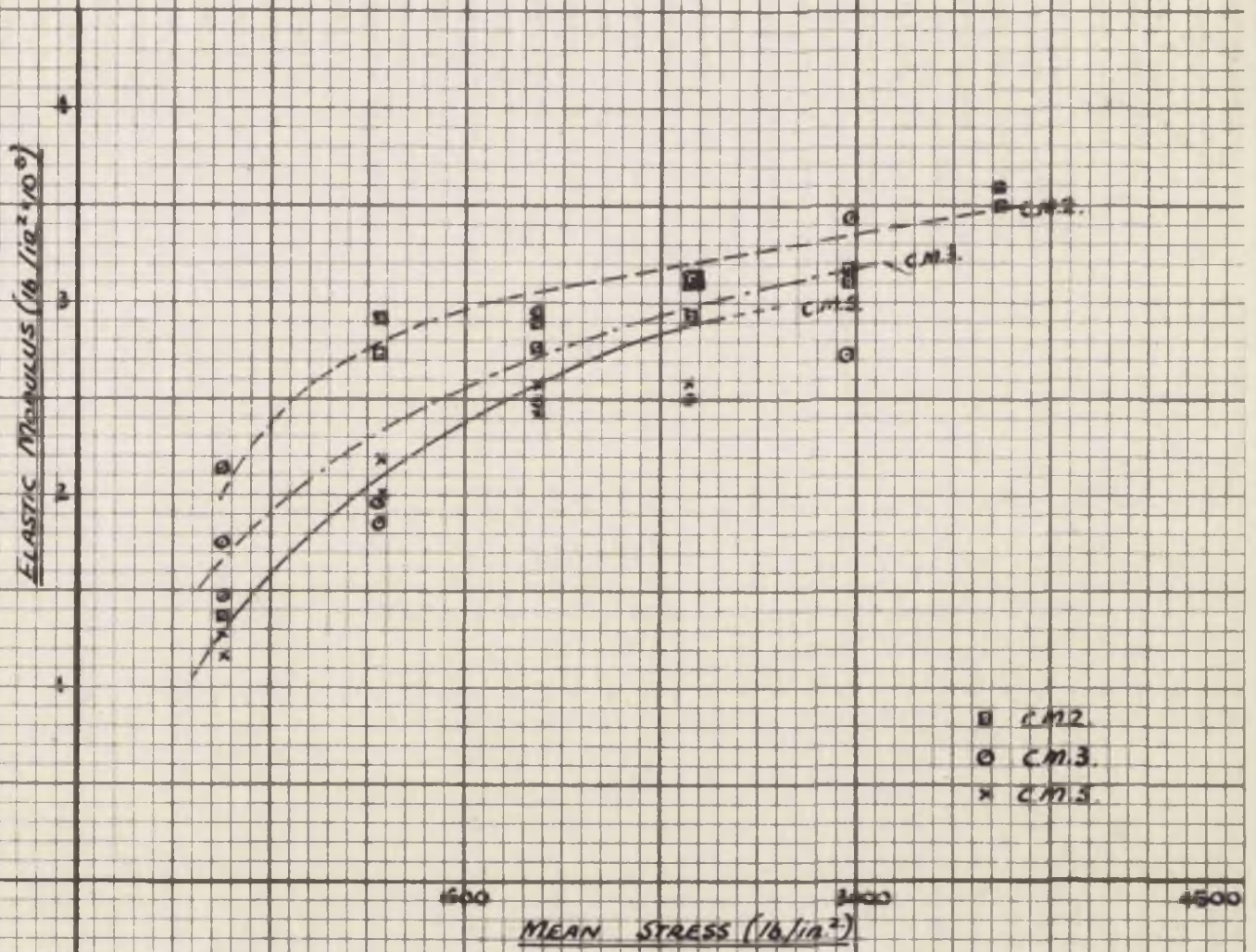


FIG. II.A.

ELASTIC MODULUS V. STRESS (COMPRESSION)

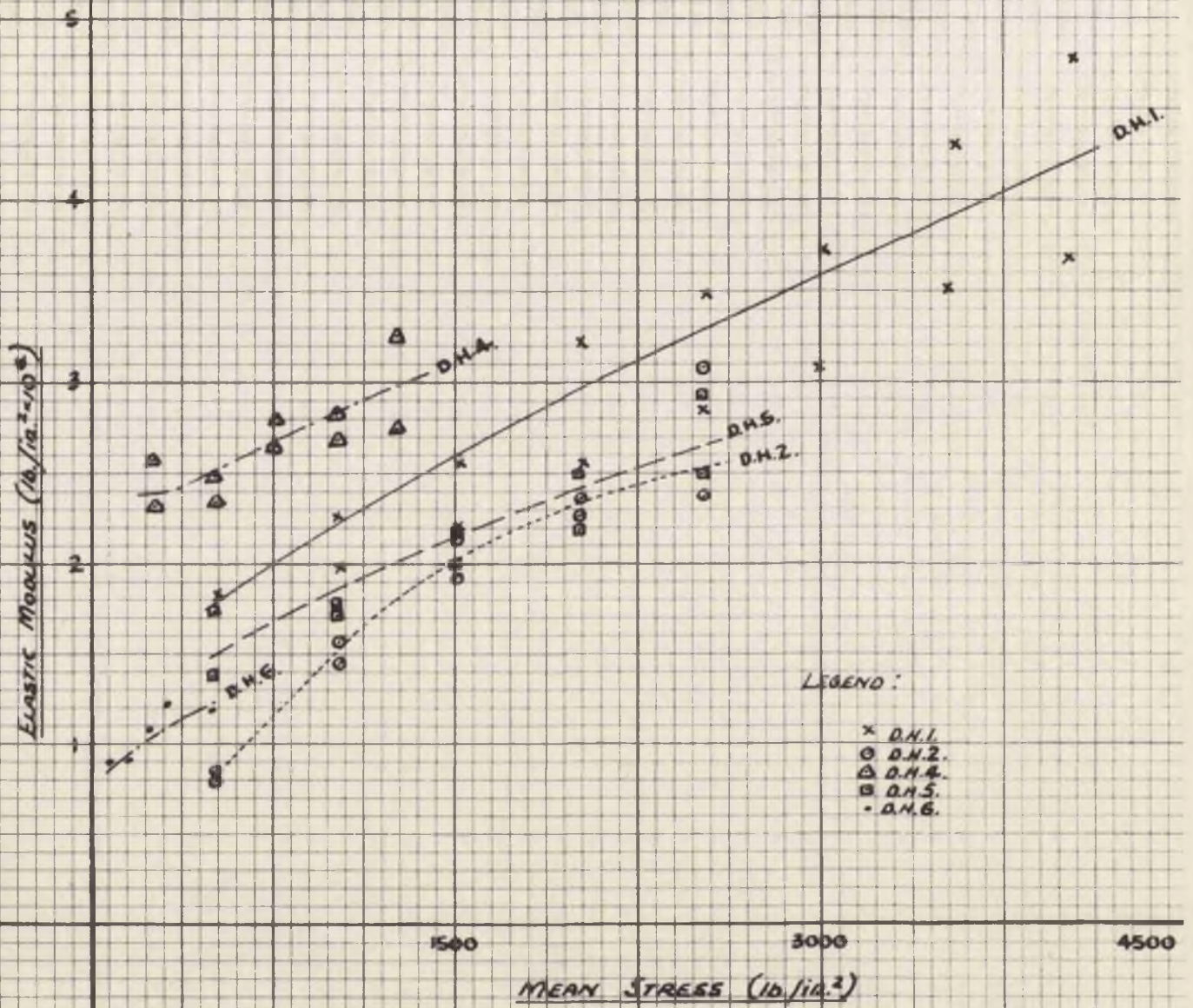


FIG. 12.A.

ELASTIC MODULUS V. STRESS (COMPRESSION)

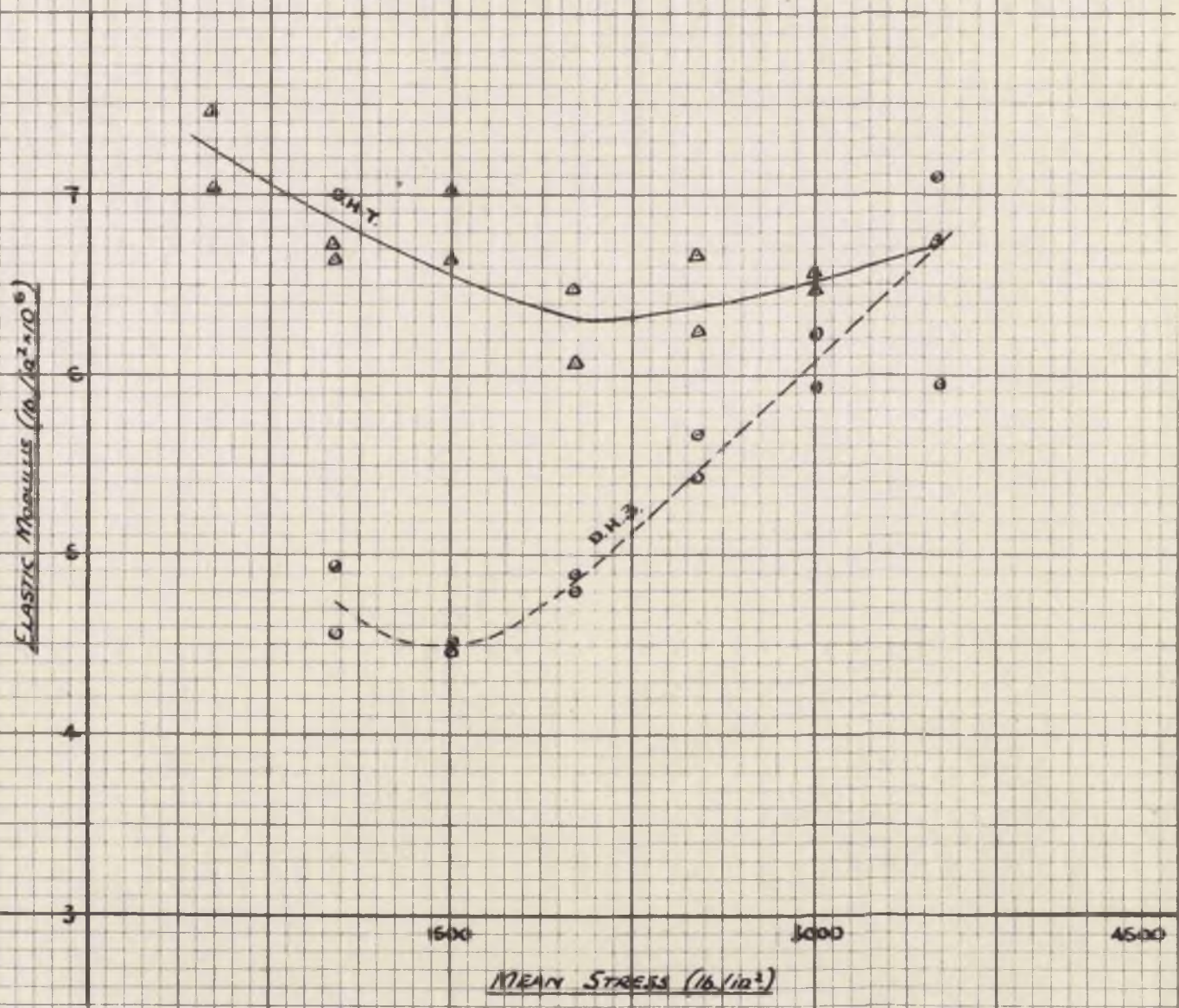


FIG. 13.A

POISSON'S RATIO V. STRESS (COMPRESSION)

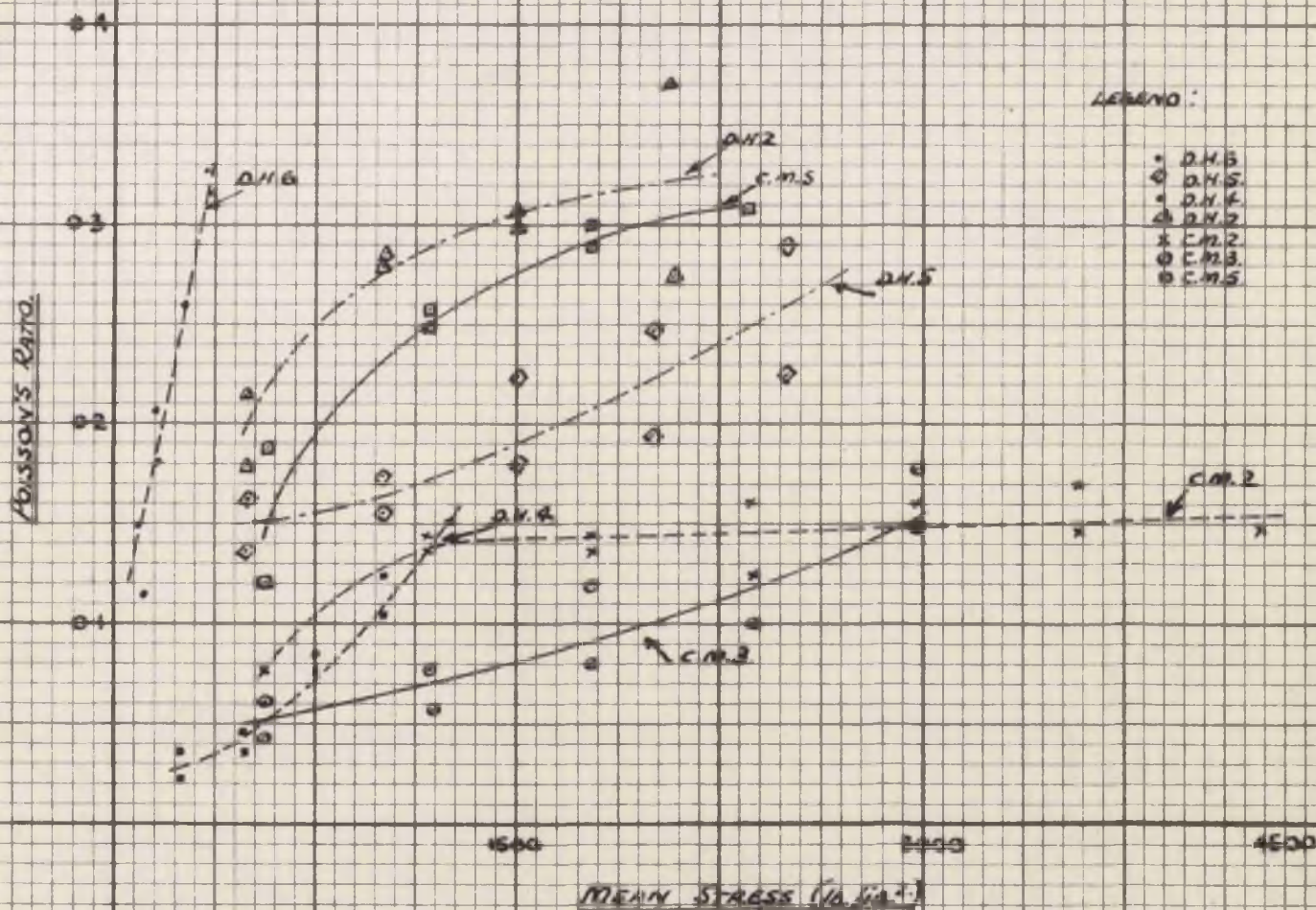


FIG. 14-A

STRAIN ENERGY/UNIT VOLUME (COMPRESSION)

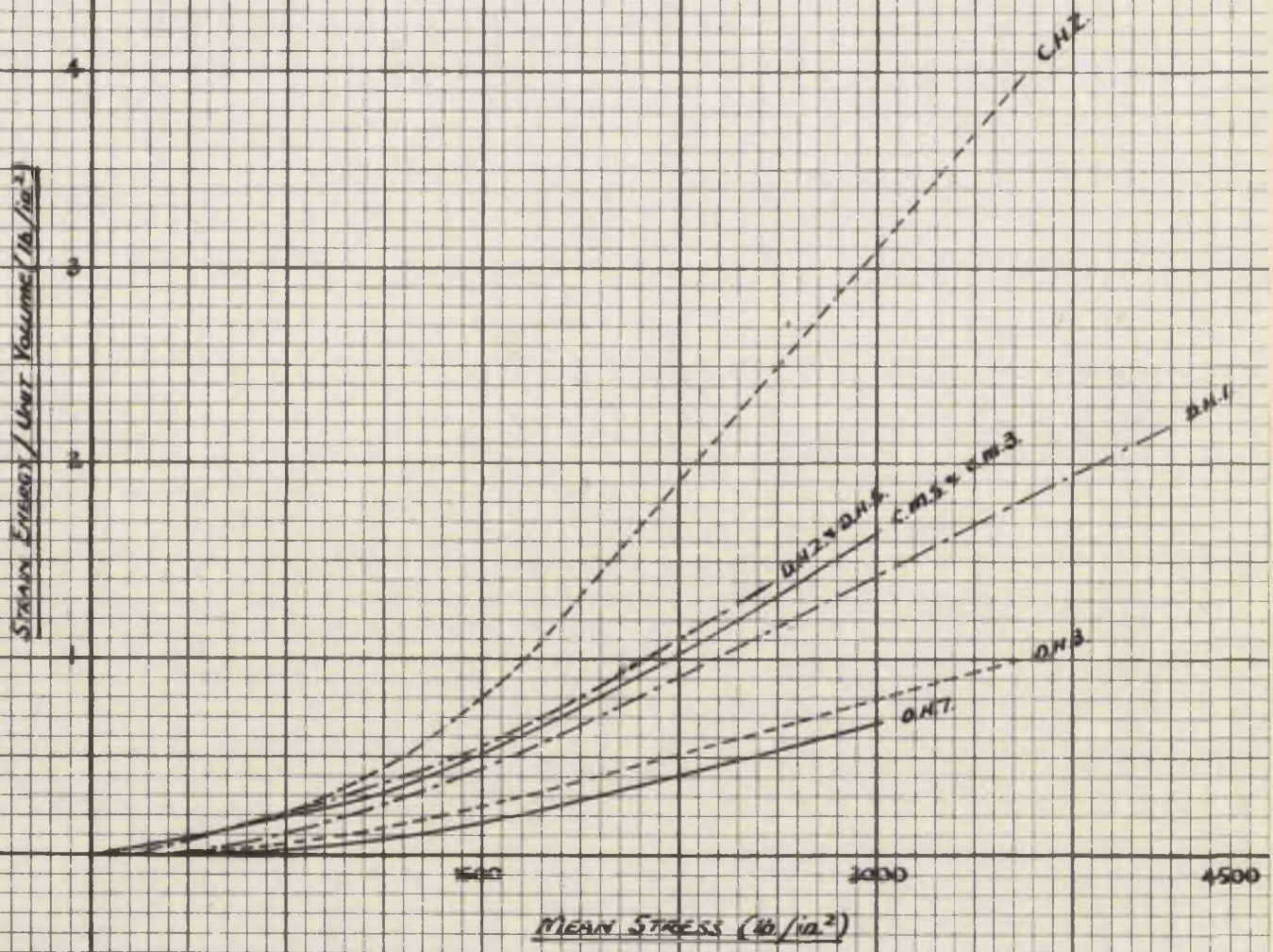


FIG. 15.A.

Tension: Due to the difficulties involved in preparing tensile specimens, the range of rock types covered was smaller than for the corresponding compression tests. A typical tension stress-strain diagram, for specimen DE2, is shown in Fig. 16A.

The variations of the Elastic Modulus (both "tangent" and "secant" values) with stress for specimen DE2 are shown in Fig. 17A. The lateral strains measured in the tensile tests were so small that variations in Poisson's Ratio over the stress range covered could not be determined with accuracy.

The relationships between the "secant" value of the Elastic Modulus and applied stress for the other rock types tested in tension are shown in Fig. 18A.

TENSION SPECIMEN D.H.2.
LATERAL & LONGITUDINAL STRESS-STRAIN CURVES

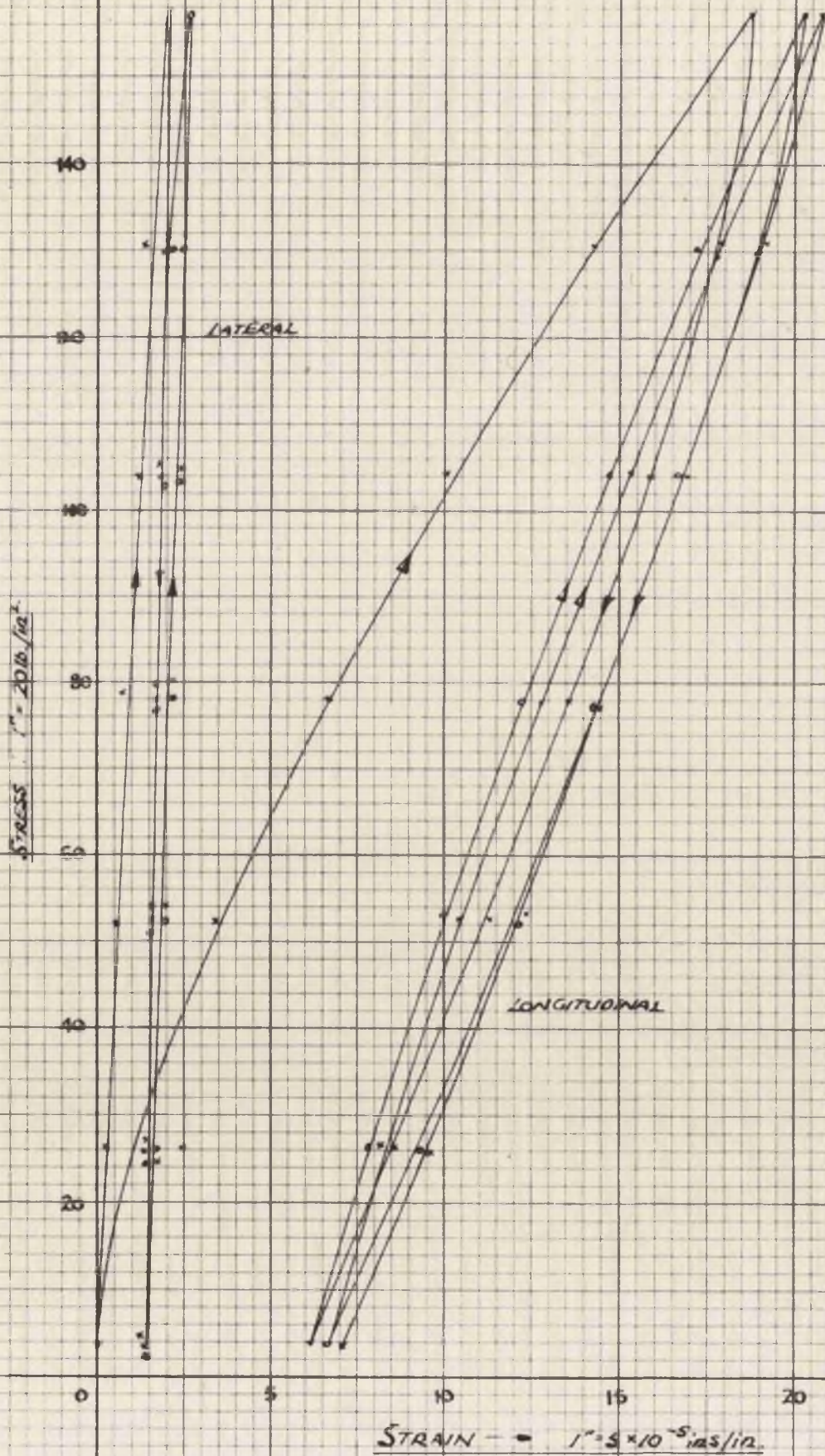


FIG. 16.A

VARIATION OF ELASTIC MODULUS D.H.Z.

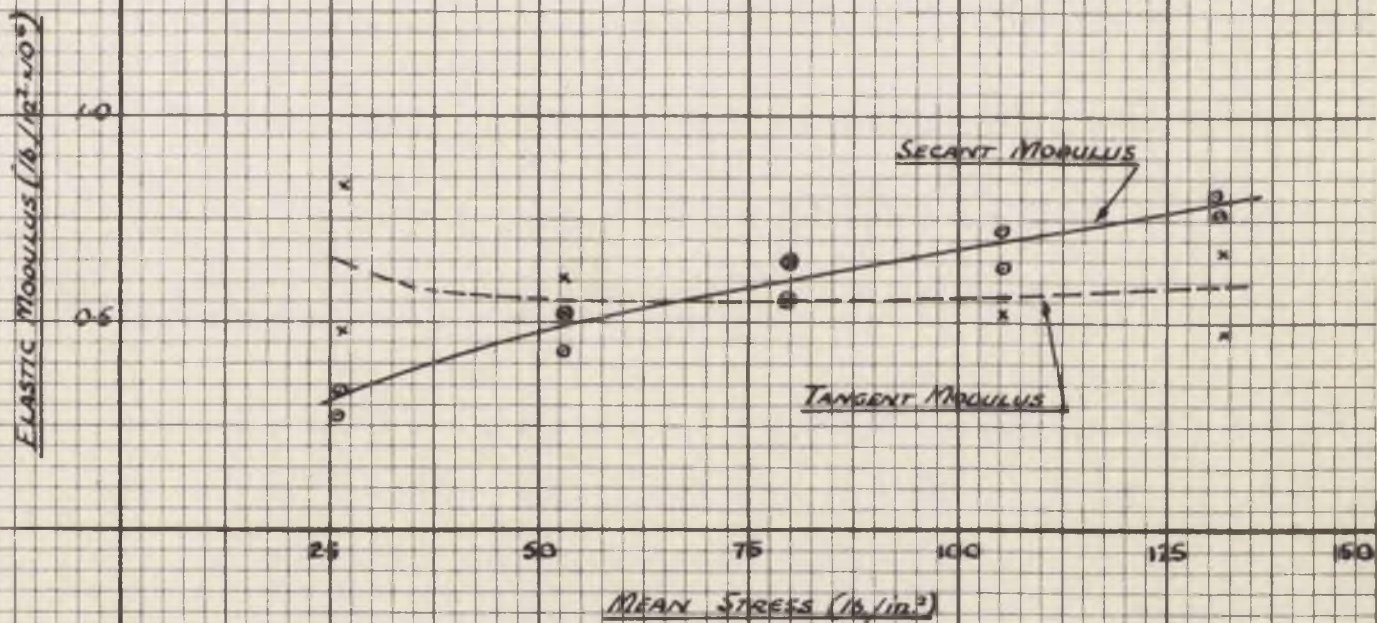


FIG. 17A.

ELASTIC MODULUS V. STRESS (TENSION).

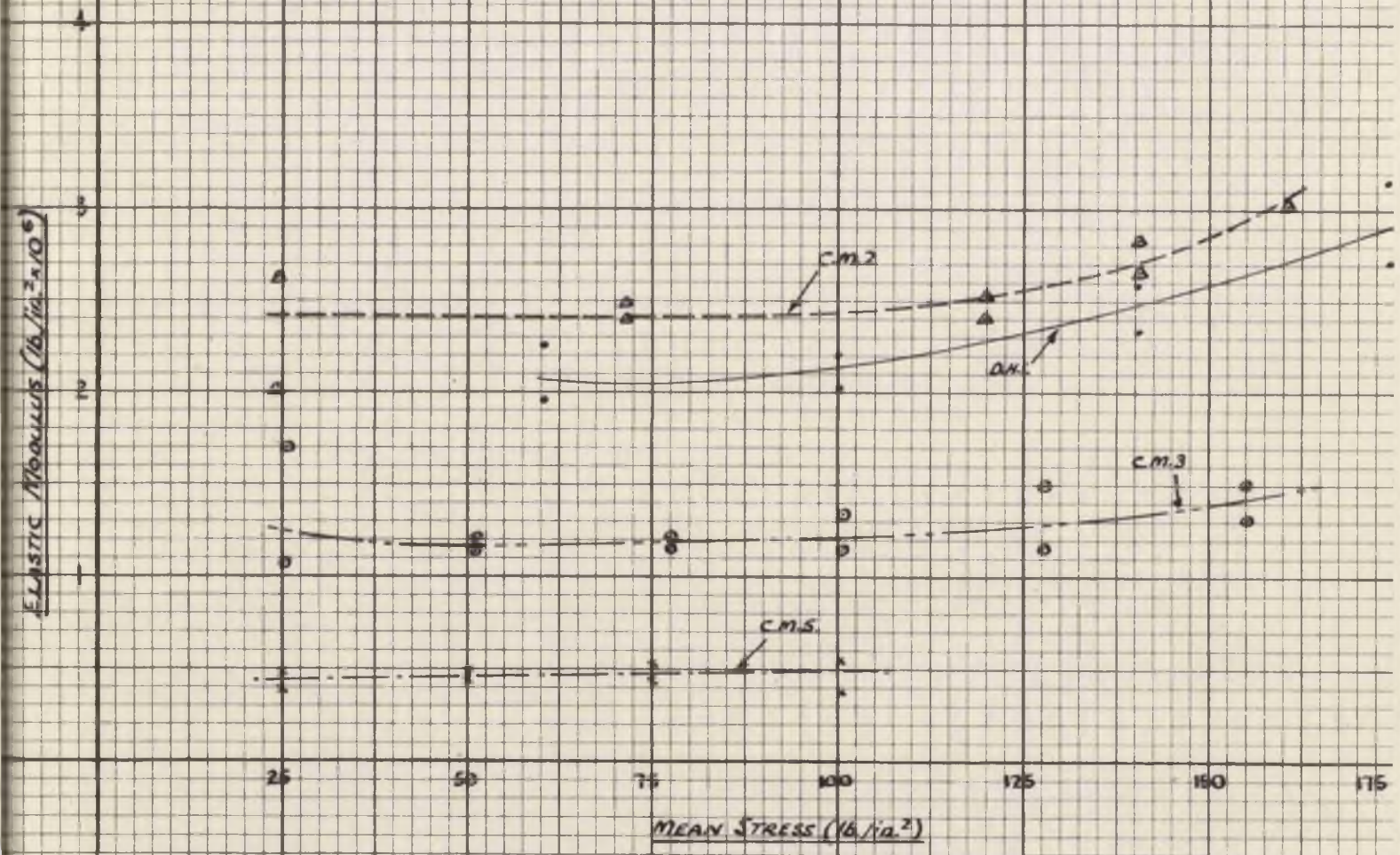


FIG. 18.A.

Bending: Beams were tested with both "fixed" and "free" (simply-supported) end conditions. Typical of the load-strain diagrams obtained are those for specimens DH2 and CMI which are shown in Figs. 19A - 21A.

In addition to plotting load-strain diagrams for varying conditions several rock beams were tested to destruction. The development of the fractures induced by bending was noted. The positions of the fractures in specimen DH2 tested in bending are shown in Plate VII A (vide ante).

SIMPLY SUPPORTED BEAM D.H. 2.
TOP AND BOTTOM FIBRE STRESS-STRAIN CURVES.

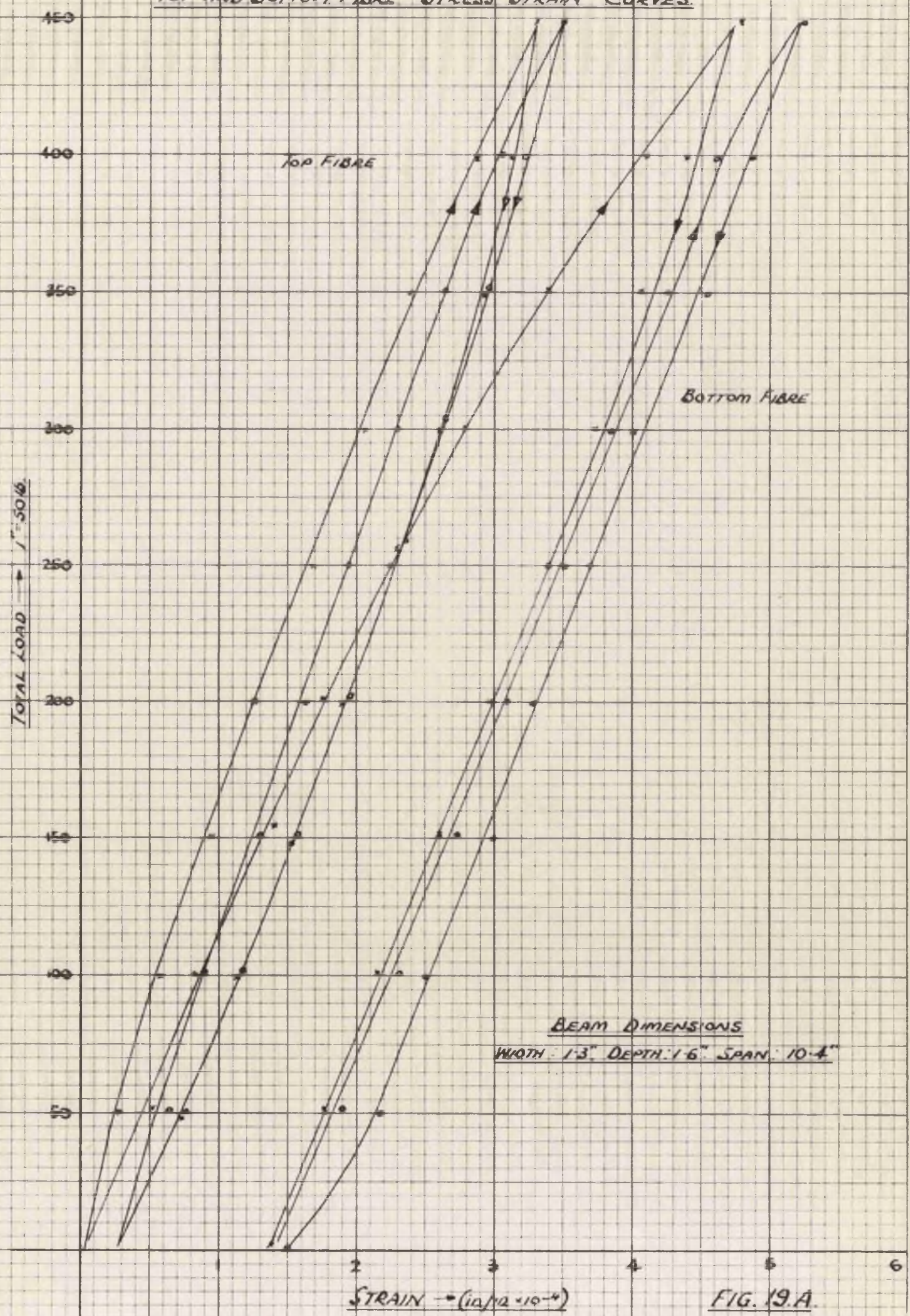


FIG. 19.A

FIXED BEAM D.H.2.
TOP AND BOTTOM FIBRE STRESS-STRAIN CURVES

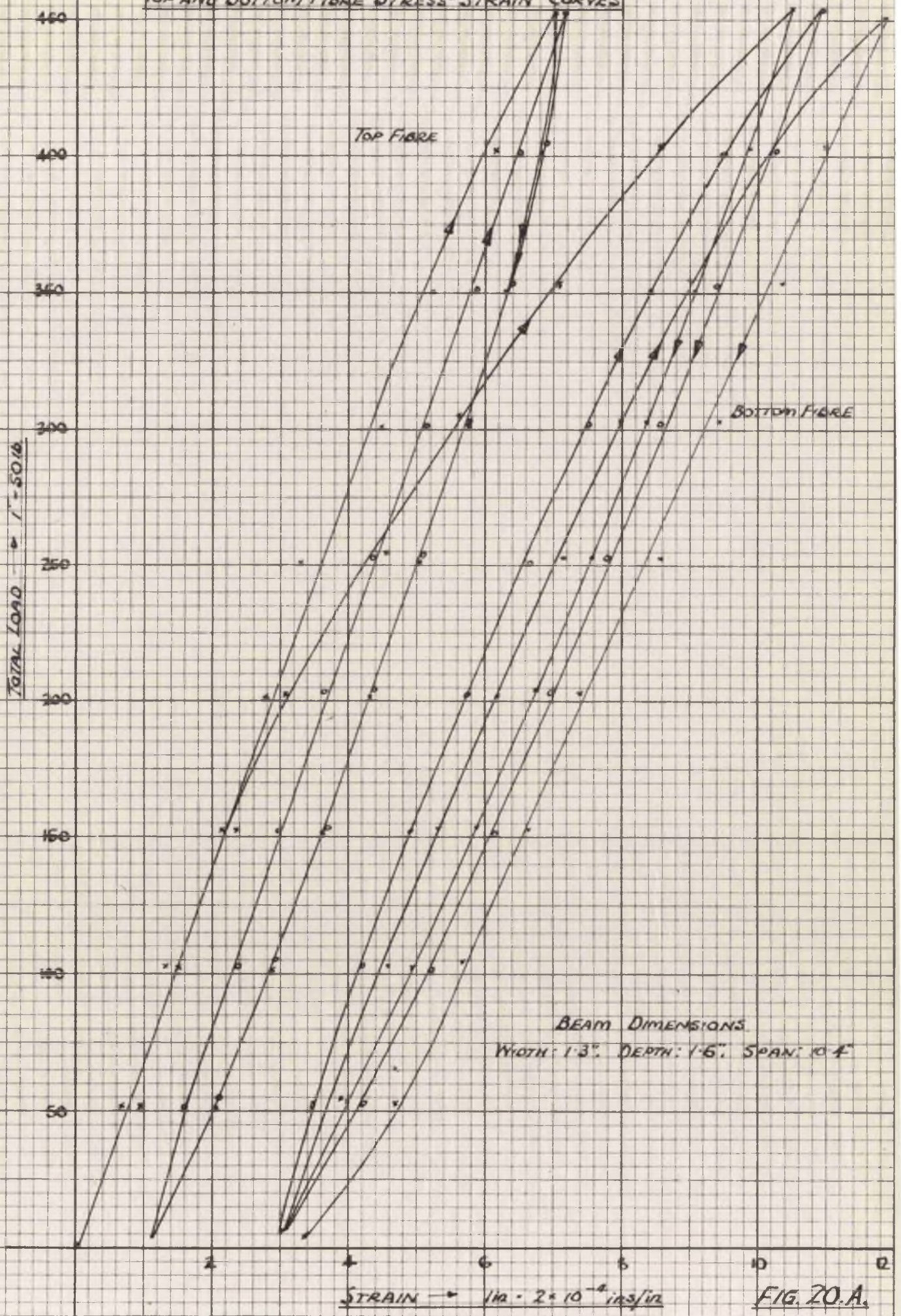


FIG. 20.A.

COMPARATIVE STRESS-STRAIN CURVES

BENDING TEST - SPECIMEN C.M.1

(FIRST LOADING CYCLE)

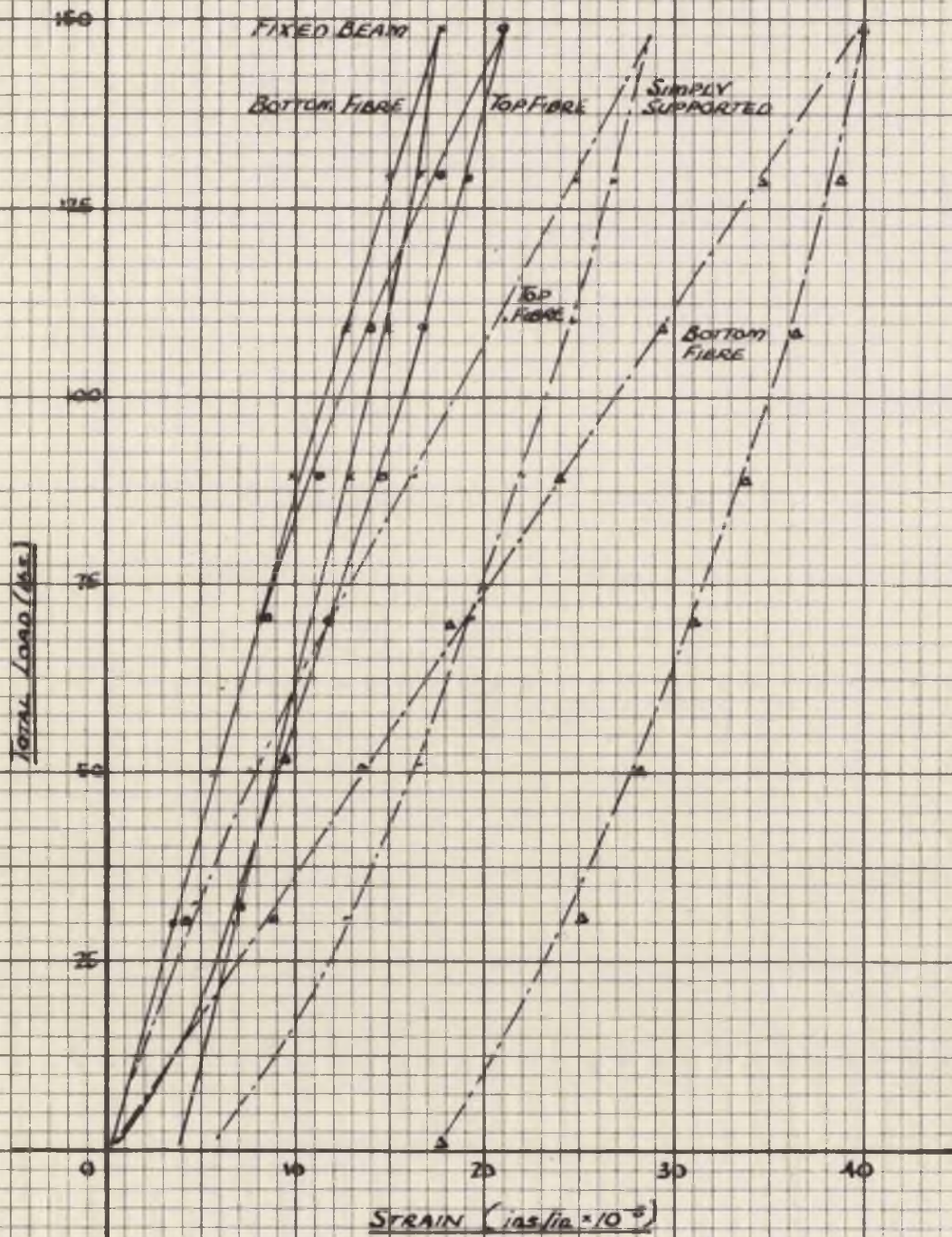


FIG. 21.A.

(c) Time Strain in Coal Measures Rock

Several time-strain investigations were carried out with specimens in tension and bending. The familiar form of "stepped" curve obtained with prolonged incremental loading is shown for both tension and bending tests in Fig. 22A and 23A respectively.

In addition to the above time-strain investigations some experiments were performed with a view to predicting the "strain v time" relationship for a given rock type under specified loading conditions. Fig. 24A shows the family of stress-strain curves, obtained with different strain rates for specimen CMI in bending. From these curves the relationships shown in Fig. 27A were derived. Fig. 25A and 26A formed the intermediate steps in the prediction of the "strain v time" curves plotted in Fig. 27A.

The experimental results and predicted "strain v time" curves for specimen CM5 in tension are also shown in Fig. 28A and 29A respectively. The intermediate curves have been omitted.

TIME-STRAIN TEST: TENSION D.H.2.

(15 MINUTE INTERVALS)

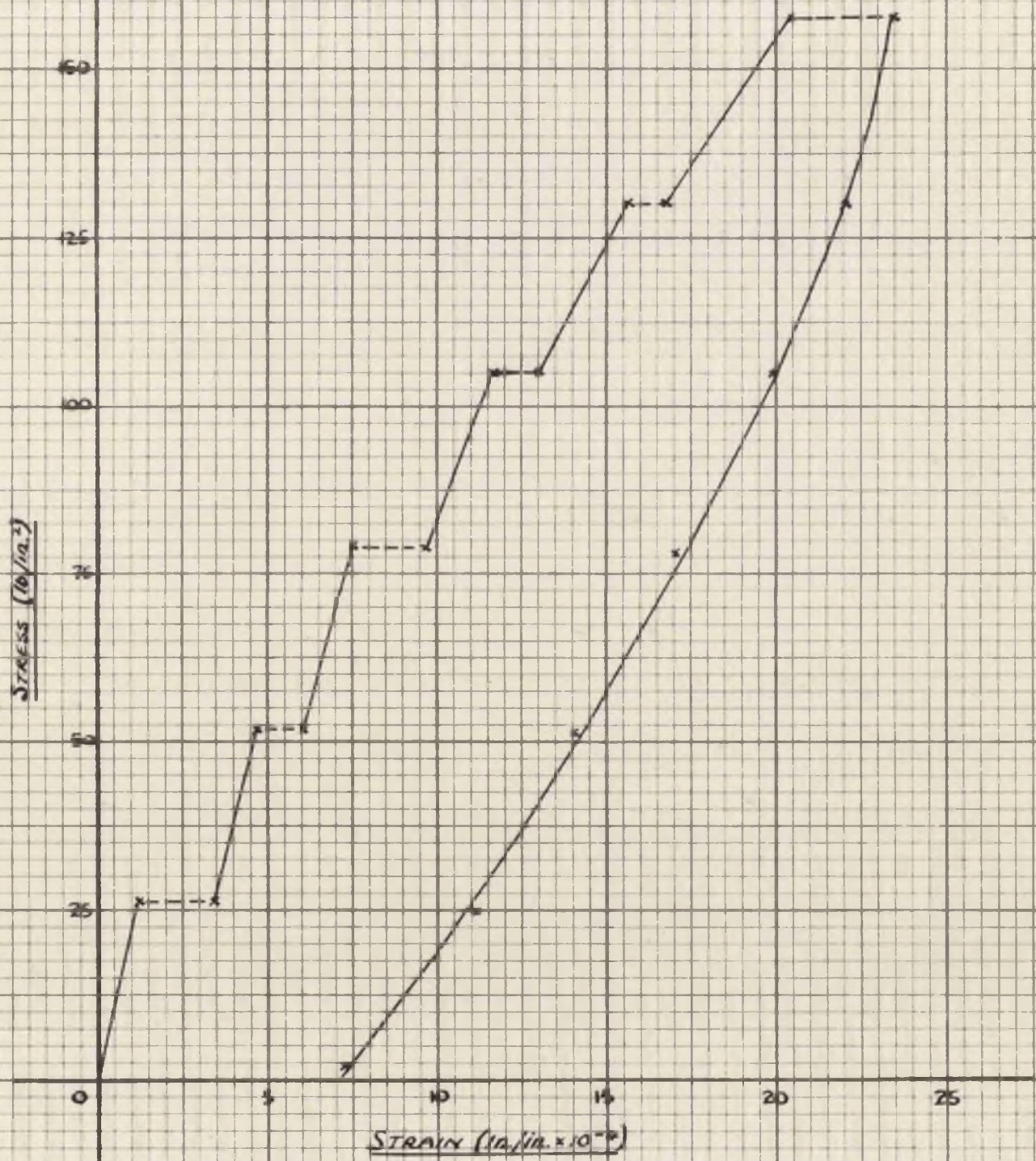


FIG. 22.A.

TIME STRAIN TEST: SIMPLY SUPPORTED BEAM D.H.2.
(30 MINUTE INTERVALS)

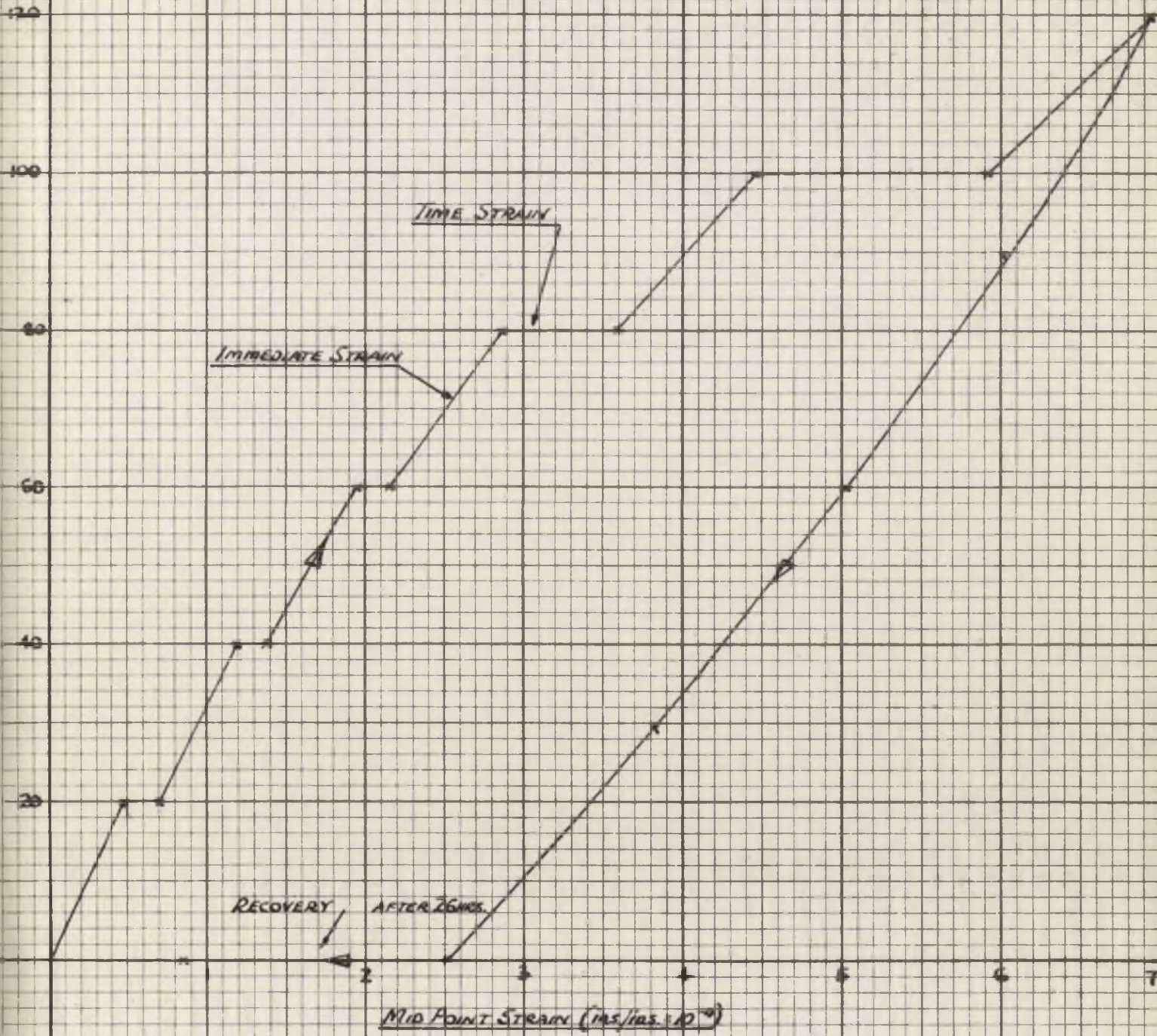


FIG. 73 A

TIME-STRAIN TEST: BENDING C.M.I.

STRESS-STRAIN CURVES FOR VARIOUS STRAIN RATES

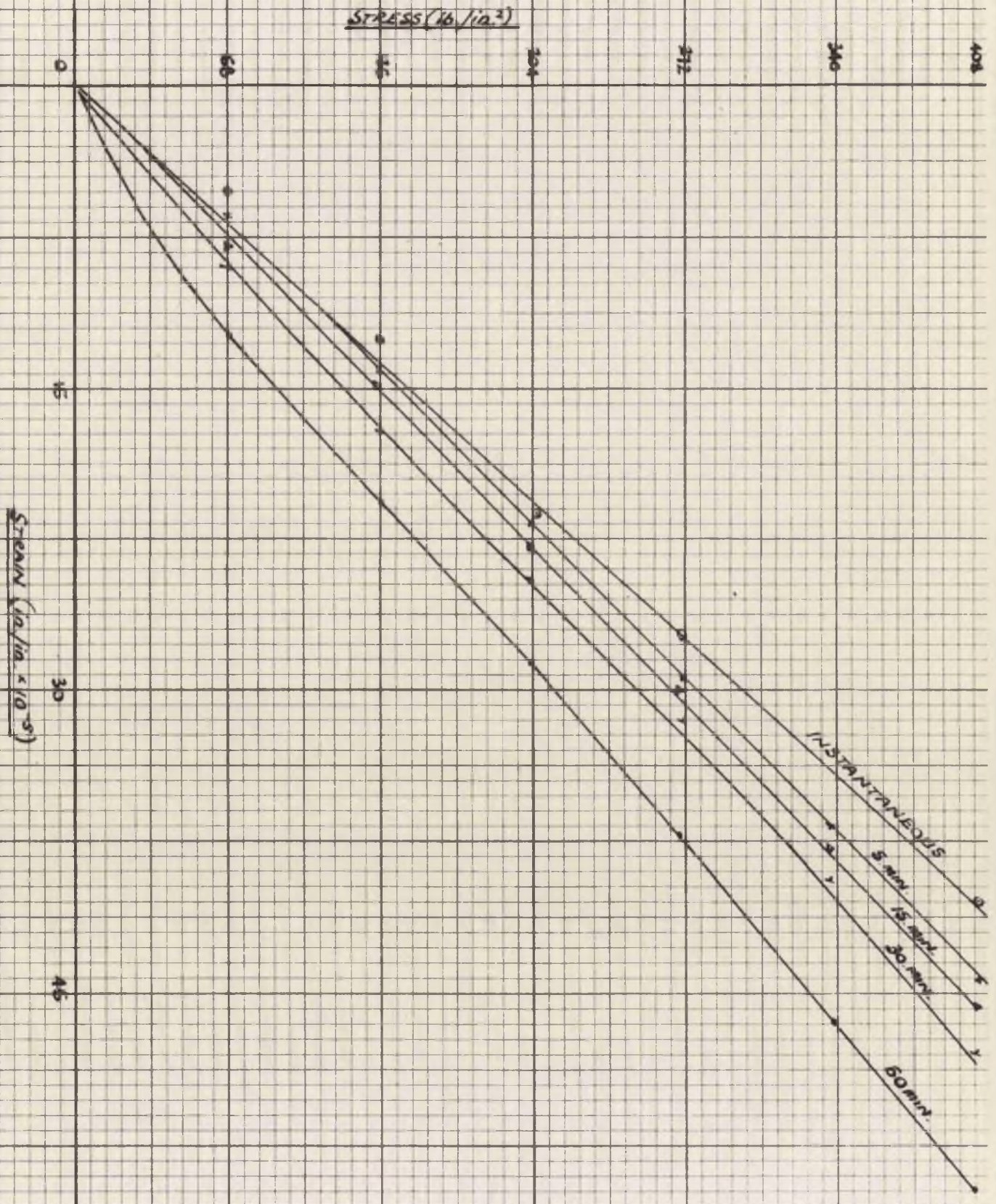


FIG. 24.A.

TIME-STRAIN TEST: BENDING C.M.I.
STRESS & TOTAL TIME FOR VARIOUS STRAIN RATES.

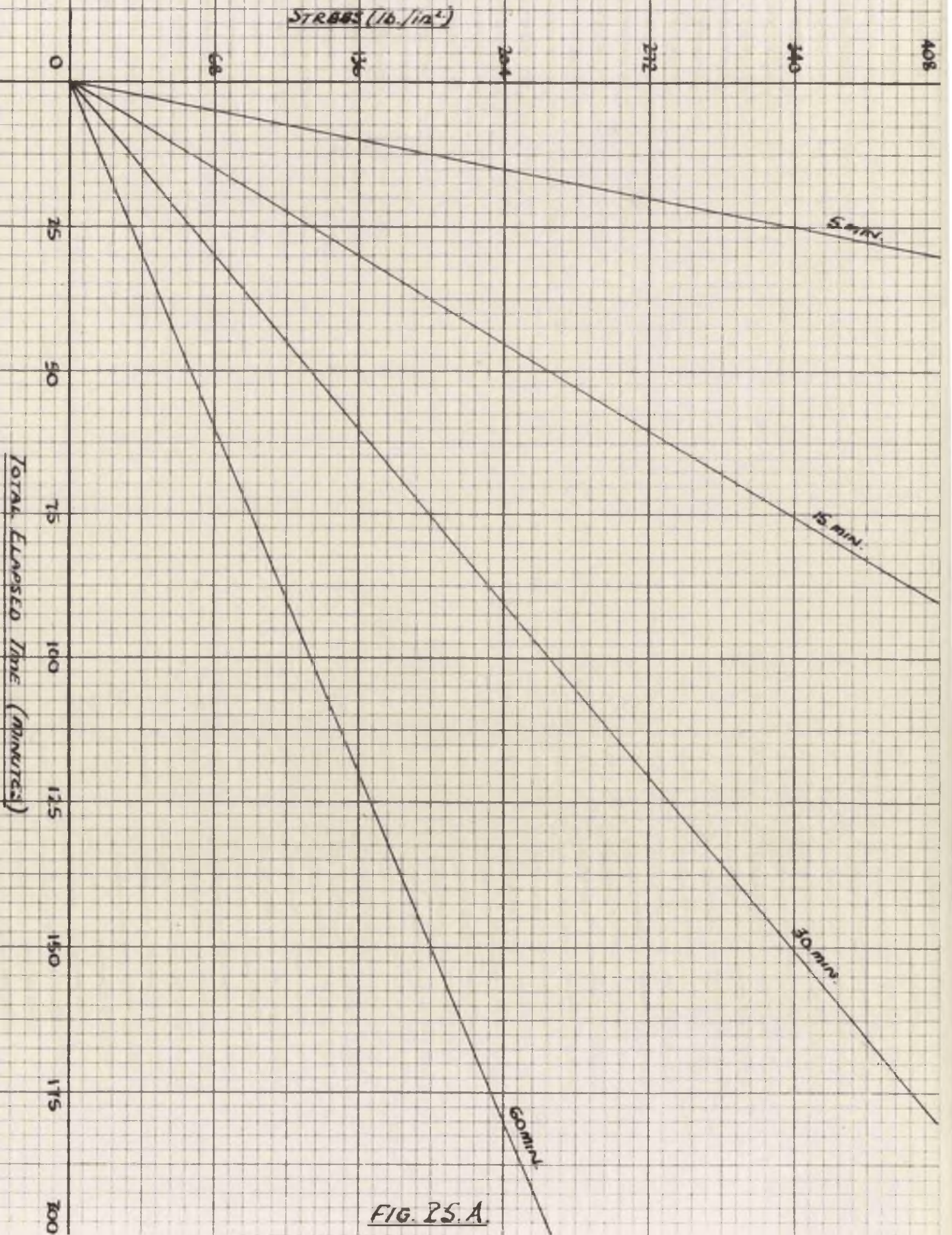


FIG. 25.A.

TIME - STRAIN TEST: BENDING C.M.V

TIME - STRAIN RATE RECIPROCAL V TIME STRAIN

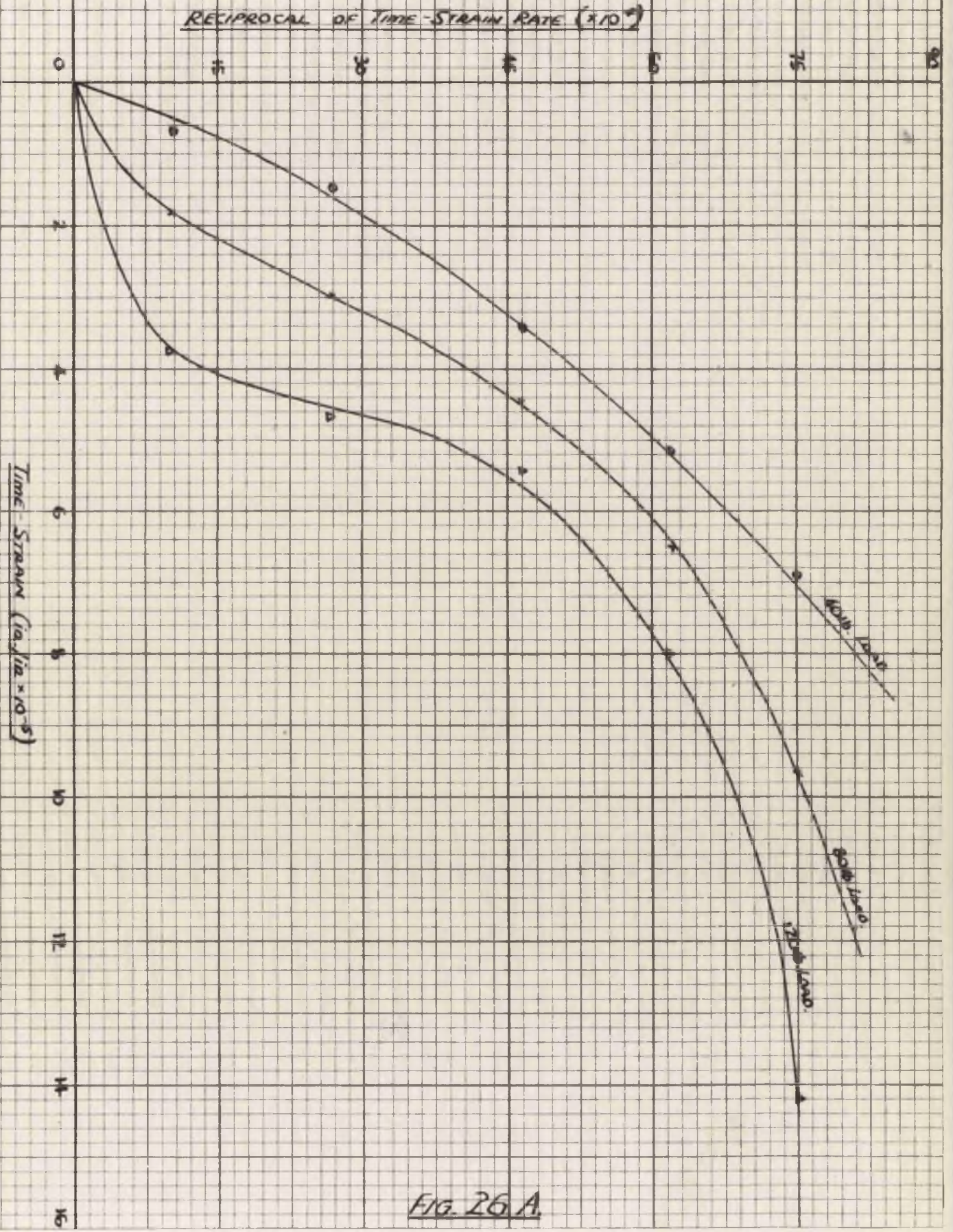


FIG. 26.A

TIME-STRAIN TEST: BENDING C.M.I.

CALCULATED & EXPERIMENTAL TIME-STRAIN & TIME CURVES.

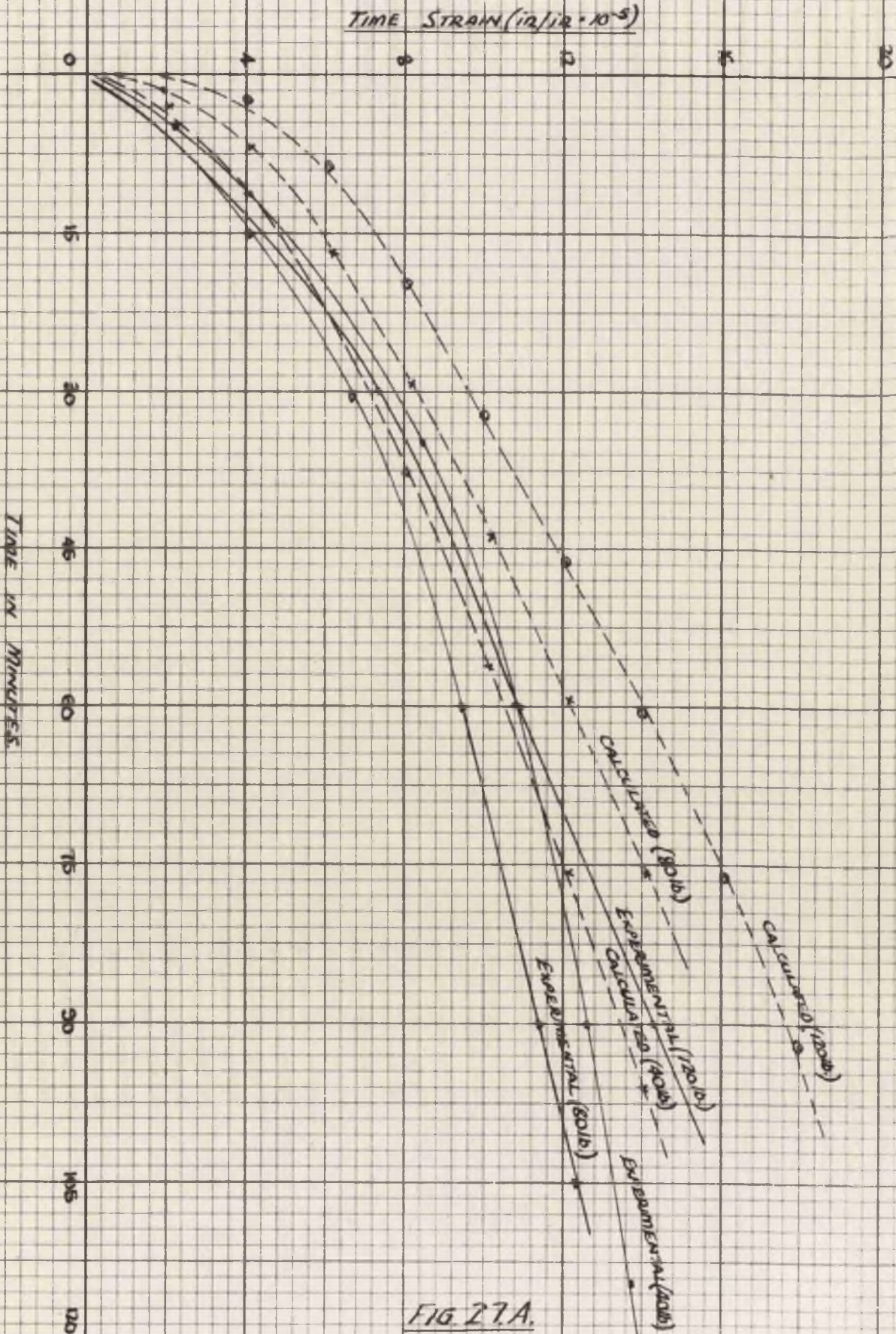


FIG. 27A.

TIME-STRAIN TEST: TENSION C.M.S.

STRESS STRAIN CURVES FOR VARIOUS STRAIN RATES

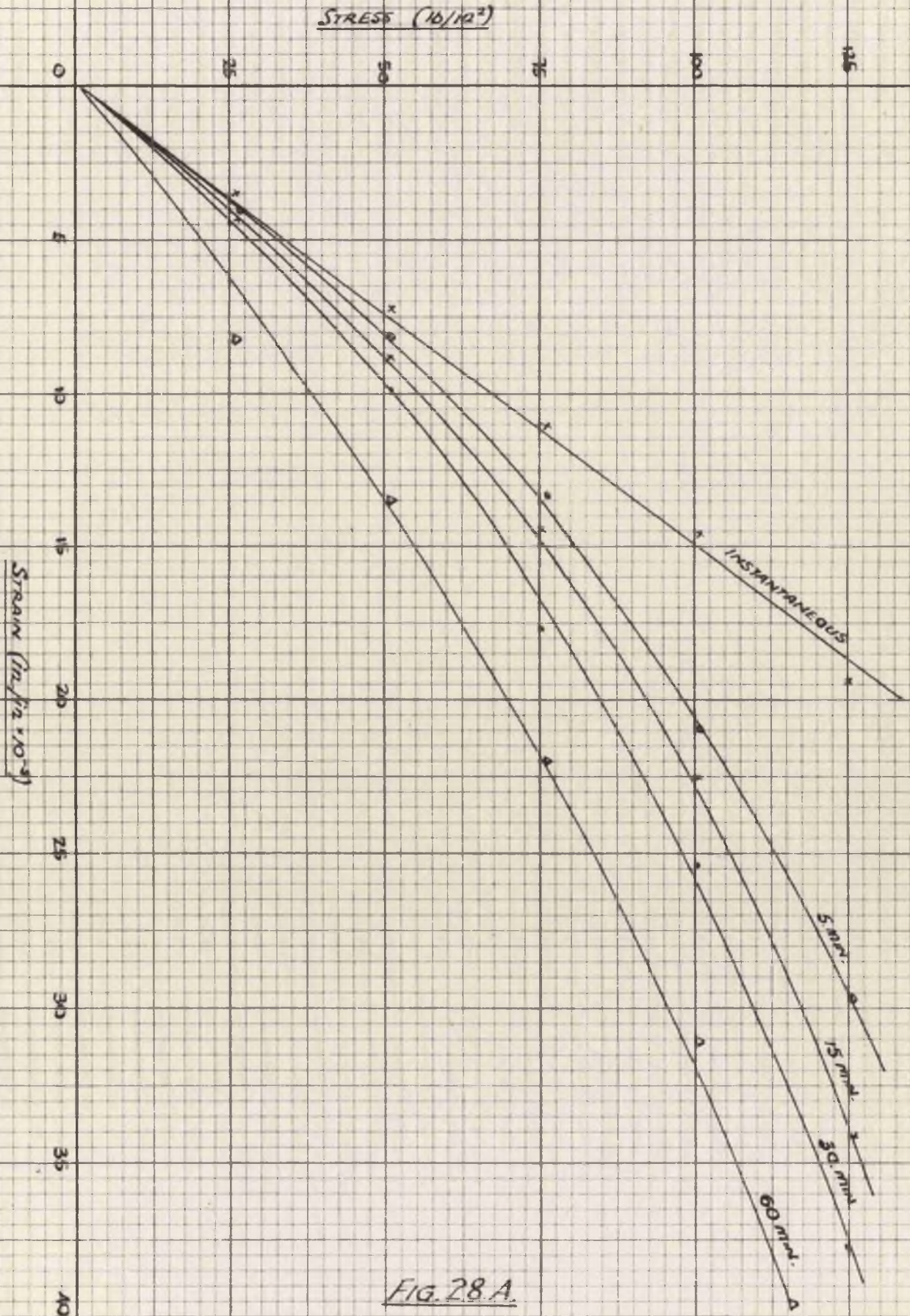


FIG. 28 A.

TIME - STRAIN TEST: TENSION C.M.S

CALCULATED & EXPERIMENTAL TIME - STRAIN & TIME CURVES

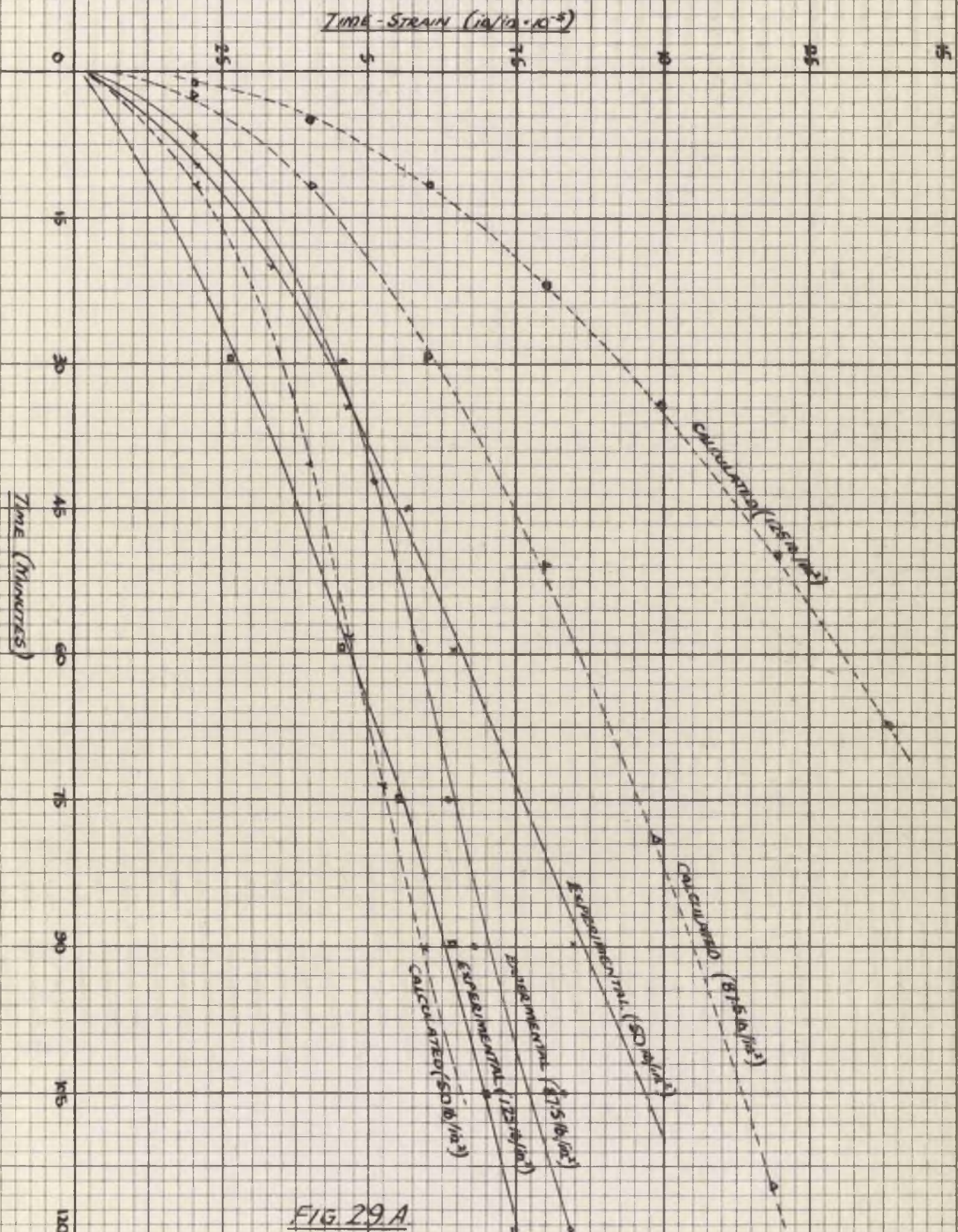


FIG. 29.A

ANALYSIS OF RESULTS

General

(i) The resistance wire strain gauge proved to be suitable for the measurement of rock strain in laboratory tests provided the gauge is securely bonded to the rock surface. A suitable cementing medium for this purpose is Araldite Cold Setting Filler and Hardener 951.

(ii) The determination of the instantaneous loading stress-strain relationship for rocks in compression tension or bending is more accurate with the Phillips Bridge since it gives the strain reading directly with no lag between each increment of load to permit time straining of the specimen being tested.

(iii) The methods adopted for the preparation of the rock specimens are suitable for the stronger rock types (e.g. sandstones, siltstones, etc.) but modifications are required to enable specimens of shales and other weaker rocks to be prepared.

Strengths of Coal Measures Rocks

(i) For the limited range of rock types studied the relative strengths were found to be:- sandstones, siltstones, mudstones and shales (i.e. strongest to weakest). However such groupings are of little value because wide variations in the strength of different rock types were recorded. Furthermore, the presence of natural weaknesses (slip planes etc.) cannot be considered in laboratory tests.

(ii) Considering the range of sandstones listed in Table No.2A

it is seen that for any given cementing medium (in this case siliceous) the larger the particle size the weaker is the rock. (N.B. - Further ranges of specimens with other cements are required to ensure the validity of this analysis.)

(iii) The effects of various types of cementing medium on the ultimate strengths of sandstones are shown in Table No.3A. It appears that for sandstones with similar particle sizes the order of strength is ferruginous, siliceous and calcareous. (Clay cement is weakest of all but no suitable specimens could be prepared for testing.) Specimen CM3 seems to be an exception to the above statement but a study of thin sections of the rock reveals the presence of many angular shaped grains which will give added strength to the rock. The compressive strength of specimen CM2 is lower than expected but the tensile strength is high - it is thought that this specimen may be considered as a weak ironstone rather than a ferruginous sandstone since it is composed of approximately equal amounts of iron and silica particles.

(iv) There does not appear to be any fixed relationship between the ultimate tensile and compressive strengths of the rock types studied. However, it is shown that the tensile strength of specimen DH4 is much higher (approximately twice) when the tension is applied parallel to the bedding planes rather than perpendicular to them.

(v) The overall mineral composition also affects the strength of the rock - it can be considered as a measure of the heterogeneity.

It appears that the presence of large amounts of mica weakens the rock. This may be due to the foliated structure of the mineral inducing slip planes when the specimen is loaded.

(vi) Summarising, the factors which affect both the tensile and compressive strengths of Coal Measures Rocks are:- cementing medium, particle size, shape of the grains and overall mineral composition. However, the ultimate strength of a rock 'in situ' is greatly affected by natural weaknesses in the rock (slip planes, fossils, carbonaceous matter, etc.)

(vii) The strength values determined for each of the rock types are only relative and not absolute since the strength of a small cube of any rock (in the laboratory) is different from the strength developed by the same material 'in situ' (AS etc.).

Determination of Elastic Constants

(i) The stress-strain diagrams obtained in the compression tests of all the rock types are of similar form to those obtained by Phillips (A10) using mechanical-strain gauges. A wide hysteresis loop is obtained for the first loading cycle but the second, third and subsequent loadings give much narrower loops which are almost superimposed (see Fig. 6A).

(ii) Similar stress-strain curves were obtained for the rocks in tension, except that the second and third loading cycles did not give superimposed hysteresis loops. This is probably due to a slower rate

of recovery of tensile time-strain (elastic portion) than compressive time-strain. The difference in the nature of the tension and compression stress-strain curves is clearly illustrated in Fig. 20A, which shows both the upper and lower fibre strain-load curves for a bending test on specimen D12.

(iii) Since the stress-strain relationships (both in compression and tension) are non-linear, Hooke's Law is invalid and true "elastic constants" for the rocks do not exist. However, values of Young's Modulus (E) and Poisson's Ratio (ν) can be calculated for any given value of applied stress using either the "tangent" or the "secant" method of calculation. Considering the results plotted in Fig. 7A (i.e. E and ν for G1) it is seen that the tangent modulus is higher than the secant modulus and that both increase with stress. The values used in both calculations are from the third loading cycle. The "scatter" of the results is higher in the case of the tangent modulus since only a small part of the stress-strain curve is considered for each calculation, whereas for the secant modulus the whole curve (up to a given stress value) is used and consequently the percentage difference between consecutive points is much smaller in the latter case. The difference between the "loading" and "unloading" values of the tangent modulus for a stress of 3,540 lb./in.² should be noted - the difference is due to the changeover from the "loading" to the "unloading" curve and not to any particular property of the material. (N.B. - This difference in the tangent values obtained for E and for the highest applied stress is seen for all the curves plotted.)

(iv) Similar reasoning applies to the determination of Poisson's Ratio for rocks; the secant ratio being higher than the tangent ratio (Fig. 8A). If the third loading cycle is considered the value of ϵ for specimen CMI decreases slightly with increase of stress and thereafter remains fairly constant but if the initial loading curves are used in the calculations, ϵ appears to increase steadily with increase in stress. Thus before using any value of ϵ for a given rock the previous "straining history" of the rock should be known.

(v) The variation of Strain Energy per Unit Volume with applied stress (CMI) shown in Fig. 9A clearly illustrates the difference in the results obtained with the tangent and the secant moduli.

(vi) It is thought that the tangent modulus is more suited to the study of rock stresses in mining since initially the rocks are pre-stressed and the forces induced by mining constitute the second loading cycle. Furthermore the tangent modulus gives a close approximation to the immediate (elastic) strain developed and the total strain for any particular stress can be computed by use of "time-strain data" (see later).

(vii) The relationship between the Elastic Modulus and applied stress for the other rocks tested is shown in Fig. 11A, 12A and 13A. For all the specimens except DH3 and DH7, the elastic modulus increases with stress (most of the values are between 3 and 4×10^6 lb./in.²). In the case of the siltstones (DH3 and 7) the modulus shows a slight decrease followed by a gradual increase, with increasing values of

stress. Muller (A3) shows that the values of E for most rocks increase with stress with the exception of slate and Holland (A8 and A27) obtains similar results to those here described for his tests on rocks associated with coal seams.

(viii) Fig. 14A shows the relationship between Poisson's Ratio and stress for the remainder of the rock types tested; the ratio shows a slight increase for increasing values of stress. This is in agreement with the results obtained by Phillips (A10).

(ix) For the tension tests the average value of Young's Modulus for the rocks was found to be lower (between 1 and 3×10^6 lb./in.²) than in compression. The tension modulus also increases with applied stress but the rate of increase is lower than the compression modulus (see Fig. 18A). There appears to be little or no variation of Poisson's Ratio with increase of tensile stress.

(x) The results of the bending tests (Fig. 19A - 21A) give similar stress strain diagrams to those obtained in the compression and bending tests. The strain values recorded for the bottom fibre are considerably higher than for the upper fibre at corresponding loads. Phillips (A10) has demonstrated that the position of the neutral axis in bending depends on the relative values of elastic modulus in tension and compression - hence the difference in extreme fibre strains. On testing a beam of sandstone (HD2) to destruction the fracture plane developed (see Plate VII A) corresponds to the theoretical line of most effective shear with the hade of the fracture changing direction at the

neutral axis which is considerably nearer to the upper surface of the beam.

Time-Strain in Coal Measures Rock

(i) The familiar "stepped" stress-strain curve obtained when each increment of load was left for 15 minutes during a tension test on specimen DH2 is shown in Fig. 22A. Phillips obtained similar results for compression and bending tests on shales and sandstones (A10). Corten (A25) in his tests with gravity loading of steel beams also obtained comparable results. In both the tension and bending tests (Fig. 22A and 23A) it is seen that the immediate (or elastic) strain parts of the diagram have different gradients. Hence the assumption that instantaneous loading gives an elastic stress-strain relationship is not correct (see later "prediction of time-strain").

(ii) In the experiments to predict the "time-straining" of rocks under a given applied stress the calculated and experimental curves show fairly good agreement both for the bending and tension tests (Fig. 27A and 29A respectively). In both cases the discrepancy between the calculated and experimental curves increases with increase of stress. For all stress values chosen, except one, the calculated strains after a given time are higher than the strains recorded experimentally.

(iii) Although the method used for the prediction of time strain gives reasonably accurate results it should be used with caution because

several assumptions are made in applying the theory (outlined earlier) to rock straining, viz. -

- (a) The strain rates for the family of stress-strain curves shown in Fig. 24A are average values determined after the curves were plotted but the theory assumes the strain rates to be pre-determined constants for any particular test.
- (b) Theoretically the stress-strain curves should be obtained by allowing the material to strain continuously at a given strain rate. This was not possible with the apparatus used and the method of obtaining the stress-strain curves was to allow the time-strain to develop at fixed load values and from the resulting "stepped curve" a smooth curve was plotted.
- (c) The theory assumes that the strain developed immediately after application of the load is completely elastic but actually the strain developed in rocks always consists of an elastic part and a plastic part. (N.B. - The variations of the slopes of the "elastic" parts of a typical stress-strain curve are shown in Fig. 22A).
- (iv) The similarity of the experimental and predicted strain-time curves indicates that some form of "equation of state" (A23) exists for rock but since graphical procedures are used in the analysis the actual form of the "equation" need not be known.
- (v) Although the assumptions made in applying the theory are fairly "sweeping" the method seems to indicate a field for further investigation.

C O N C L U S I O N S

(1) The electrical resistance strain gauge with an A.C. measuring bridge is suitable for the measurement of rock strain in laboratory tests. The accuracy of the method depends upon the bonding of the gauge to the rock surface and the linear response of the gauges at low strain values. Due to the inherent "time-strain" property of rocks a direct reading bridge is more accurate than a "null-point" bridge for the determination of stress-strain diagrams.

(2) The relative strengths of the Coal Measures Rocks tested were found to be:- sandstones, siltstones, mudstones and shales. However the presence of natural weaknesses greatly influences the ultimate strength of rocks 'in situ' and this factor cannot be allowed for in laboratory tests.

(3) For the range of sandstones studied it was found:- (a) the larger the particle size, the weaker is the rock for any given cementing medium, (b) for a given particle size the strength of the rock is governed by the cementing mediums which have the following relative strengths:- ferruginous, siliceous, calcareous and clay, (c) the shape of the grains and overall mineral composition also affect the ultimate strength of the rock.

(4) There does not appear to be any fixed ratio between the compressive and tensile strength of any rock type.

(5) On subjecting a rock to stress, either in compression tension or

bending, a hysteresis effect is obtained. There are no true elastic "constants" for rocks and generally the Elastic Modulus and Poisson's Ratio increase with applied stress. However some exceptions to this general rule were found particularly in the siltstones where an initial decrease followed by an increase in the values of E and ν with increase of stress were noted. Values of E and ν for any rock type should always be related to the applied stress, and previous straining history of the material. The method adopted for the calculation of the "constants" should also be stated.

(6) The values of E in tension is less than in compression for any given rock. The direction of application of stress with respect to the laminations greatly affects the tensile strength of the rock.

(7) The total strain developed in rock under a given load is a function of time. Phillips analysed the rates of development of time strain. The method here described for the prediction of "time-strain" gives reasonably accurate results and also indicates the existence of an "equation of state" for rocks. However it should be noted that several assumptions are made in applying the theory to rock strains which limit its general application.

SECTION B - PHOTO-ELASTIC INVESTIGATIONS

The design of suitable support systems to control the strata movements around underground excavations requires knowledge of the redistribution of the rock stresses induced by mining together with the physical properties of the materials subjected to stress. There have been many theories suggested to explain the pressure distribution around mine working (B1); most of the theories are based on visual underground research and generally are limited to a particular mining field. In recent years there has been an increasing use of sensitive instruments to record the effects of different forms of support, methods of working etc., but most of the measurements have been concerned with the manifestations of rock pressure rather than the pressure itself. Another approach to the problem has been made by the study of models in the laboratory (see Section D). Use has also been made of the photo-elastic method of stress analysis to determine the stresses around underground excavations.

Photo-elasticity has been widely used in the other branches of engineering; details of the development of the method, the theory involved and the interpretation of the results are given in the extensive publications of Coker and Filon (B2), Frocht (B3), Hetenyi (B4) and others. In the study of rock pressures photo-elasticity has been used by Bucky and Sinclair (B5), Mindlin (B6) and Duvall (B7, B8) in America, by Tincelin (B9), Guinard (B10), Pirard (B11) and others on the Continent. In Britain the method was first used by Hudspeth

and Phillips (B12) and more recently by Potts and his associates who have developed the technique and applied it to a wide range of problems (B13 to B19 incl.).

Due to the heterogeneity of rocks, the effects of pre-mining disturbances, the irregularities in the shape of mine excavations etc., several simplifying assumptions are made in applying the method - the strata are assumed to be an infinite medium, the boundaries of the excavations regular, etc. These assumptions are justified in the study of large scale problems such as shaft disturbances (B14), partial extraction (B7, B8, B18, B19), gallery shapes (B10, B17 etc.) etc., but when the problem is more particular caution must be observed in applying the results of photo-elastic analysis since Coal Measures Rocks are not truly elastic in their behaviour under stress (Section A). Hence the model results cannot be applied directly to the prototype but an overall impression of the stress distribution can be obtained. Furthermore, since most rocks fail in shear the isochromatic diagrams obtained from the photo-elastic experiments illustrate the critical zones of shear stress concentration without further analysis.

In the past few years increased use has been made of roof bolting as a mean of support in gate-roads and headings. In some cases the bolts have formed the entire support system and in others they have been used in conjunction with conventional forms of support. Generally the

bolting patterns adopted have been designed by some form of "trial and error" method. In the present work models were constructed to study the effects of various bolting patterns, bolt tensions, etc., with a view to designing suitable bolting patterns for use underground without having to carry out extensive underground trials.

APPARATUS(a) Polariscope

The polariscope used in the investigation is shown in Plate I B. A chain drive system couples the polariser and analyser to a graduated control handle at the screen end of the bench to facilitate the plotting of isoclinic lines. Quarter-wave plates can be inserted to give "circularly polarised light" when isochromatic diagrams are being investigated. Details of the various components are:-

Light Source: Two lamps are provided in the lamphouse - a 250W projection lamp for white light and a 250W high pressure mercury vapour lamp for mono-chromatic light. Wratten filters No.77 and No.58 used with the mercury vapour lamp give the mercury green line (wavelength 5461 A.U.). The lamp house can be rotated about its vertical axis to facilitate interchange of the light source.

Condensers: The condensers are 6 inch diameter plano-convex lenses used to give a parallel beam of light through the model being studied.

Polarisers: "Polaroid" sheets $5\frac{1}{2}$ inches in diameter, fitted between glass plates, are used for both the polariser and the analyser.

Projection Lens: A 3 inch diameter compound lens is used for projecting a magnified image on the screen for the analysis of isoclinics etc. When it is required to photograph stress fringes the

projection lens is replaced by a half-plate Sanderson camera. Kodak 0.250 plates were used for recording the stress fringe photographs.

(b) Loading Arrangements

The models are loaded by a system of levers designed to allow both horizontal and vertical movement of the model with the straining frame. This is useful when models larger than the polarisers are being studied. For the study of roof bolting systems the loading arrangements were as shown in Fig. 1B. From the point load at X (Fig. 1B) an approximately uniformly distributed load is obtained by the device shown. The "box" construction of the loading gear allows the "anchor bar" to remain unloaded when the C.R.39 beam is under load. Clearance holes for the bolts are drilled in the base of the box, and a thin rubber sheet is interposed between the loading surface and the beam to minimise local contact stresses. In addition to the vertical loading over the unsupported span of the model, horizontal constraint and additional "abutment" loading can be provided by the loading screws shown. The intensity of the "additional" loads is measured by strain gauge load cells positioned as illustrated. The metal plates which support the beam models can be removed to enable larger models (arched roadway sections etc.) to be investigated.

(c) Ancillary Equipment

Compensator: A Soleil-Babinet type compensator was used for the determination of fractional orders of interference. It was

used mainly for the measurement of edge stresses when the fringe pattern was approximately parallel to the boundary of the model.

Extensometer: A "Hounsfield" extensometer was used for the measurement of bolt tension. The instrument consists of a clamping frame which fixes two gauge points (2 inch gauge length) to the specimen; a micrometer screw arrangement is used to measure the deflections of a ball-crank lever linked to the moveable gauge point. Platinum contacts fitted to the micrometer "make" a circuit for a small electric bulb - so eliminating the effects of the "personal equation" which is usually involved in the reading of a micrometer. The use of the instrument for the measurement of bolt tension is described under "Procedure".

CONSTRUCTION OF MODELS

In the study of roof bolting techniques the range of models investigated consisted of three main groups, viz. (a) suspension support, (b) compound beam effect, and (c) arched roadway support. The materials used for the construction of the models were Columbia Resin (C.R.39), Bakelite (BT/61/893), Catalin and Perspex, the latter being used only for the determination of isoclinic lines. The bolts were made from 0.065 inch diameter wire screwed to take No. 10 B.A. nuts. The bolt plates and roof bars were made from copper sheet.

(a) Suspension Support

In the investigation of the use of roof bolts to "suspend" a weak stratum from a much stronger one above beams of C.R.39 8 inches by 1 inch by $\frac{1}{4}$ inch simulated the lower bed while a steel bar represented the "anchoring bed". Clearance holes for the bolts were drilled through the beam using a No.52 drill and reaming them with a No.50 drill (.0700"). The cutting edges of the drills were modified as suggested by Jenkins (B20) to minimise the machining stresses induced in the material by drilling. The reduction in the induced stresses is shown by comparing Plates IIB and IIIB. The models were cut from polished sheets of plastic using a 5" x 1/16" medium speed circular saw mounted between centres in a lathe. The cut edge obtained was free from chipping but the finished edges of the model were prepared

by filing to minimise the edge stresses. To ensure equal bolt tension, the load was applied through brass sleeves (see Fig. 1B) and the strain developed in the sleeves measured with an extensometer.

(b) Compound Beam

Another application of roof bolting in coal mines is the clamping together of several thin strata to form a compound beam. To study this use of bolting, models, consisting of two beams of C.R.39, 8" x $\frac{1}{2}$ " x $\frac{1}{4}$ ", which could be bolted together, were made. The holes for the bolts were drilled as before, the bolt heads being countersunk in the upper stratum to permit uniform loading of the beam over the entire span.

(c) Arched Roadway Support

In the models of a longwall gate road the arched section was cut from $\frac{1}{4}$ inch thick C.R.39 sheet. The "anchorage bed" was also made from C.R.39 - the interface being accurately machined to minimise local stress concentrations. A strip of polythene was placed between the beds to allow free lateral movement. The roof bolt holes were drilled in the manner previously described; the holes in the upper bed were tapped to take the screwed end of the roof bolts. An attempt was made to anchor the bolts with the "slot and wedge" principle but it was not possible to obtain sufficient anchorage - consequently all the bolts were anchored simply by screwing them into tapped holes. The road-side "packs" were made from stiff rubber sheet which allowed considerable yield before its maximum resistance was developed - comparable to

underground conditions. The floor of the roadway was also made from Columbia Resin. Many models of this type were made with beds of different thicknesses; several models fractured along the line of the bolt holes when under load. One model was constructed with several strata made up of different materials (C.R.39, Bakelite and Catalin), the roadside packs again being made from rubber sheeting.

Details of the models are shown in the fringe photographs and several models can be seen in the foreground of Plate IB.

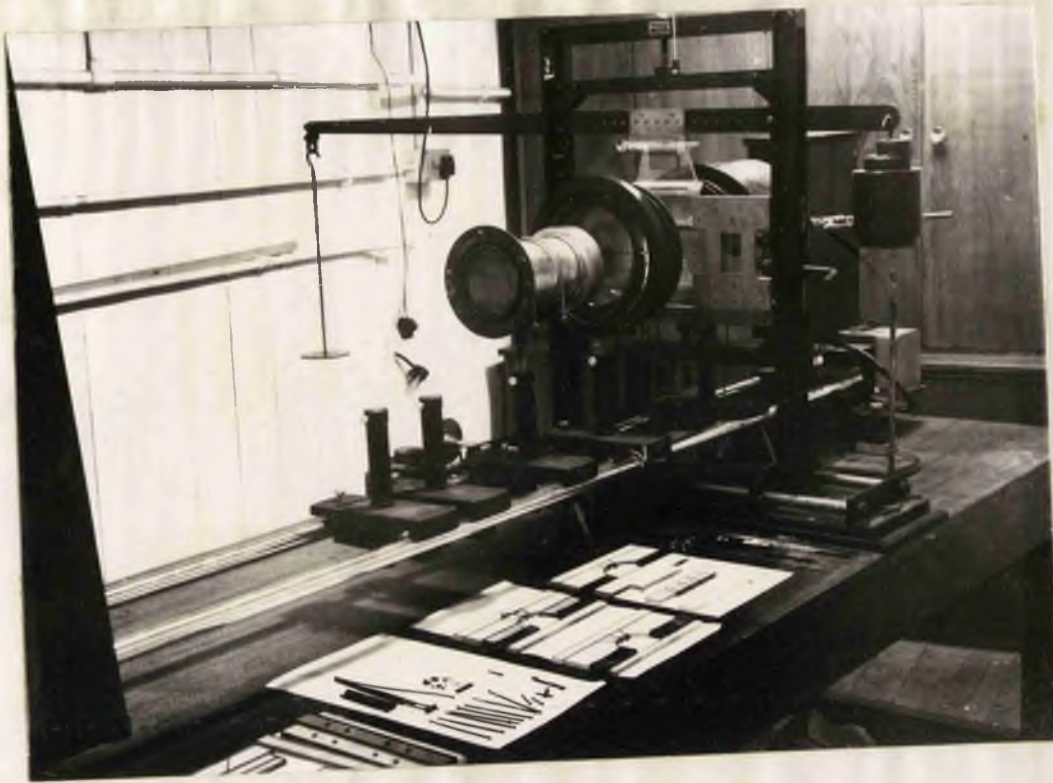


PLATE IB:

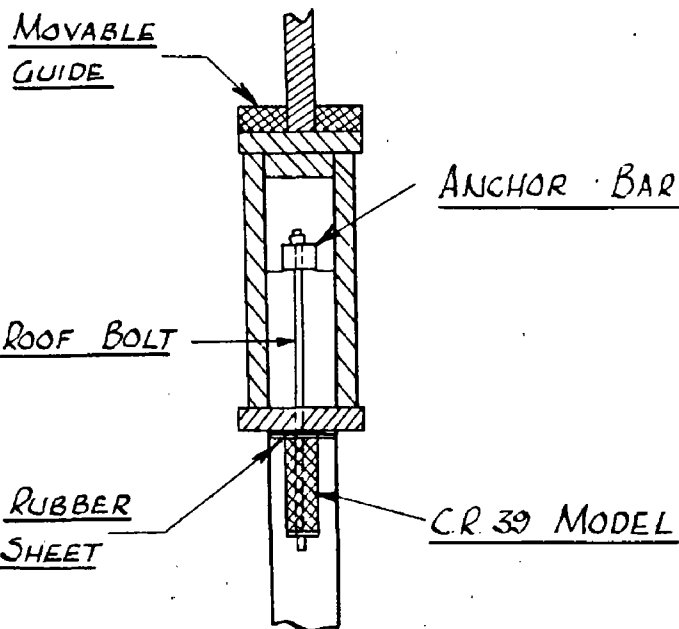
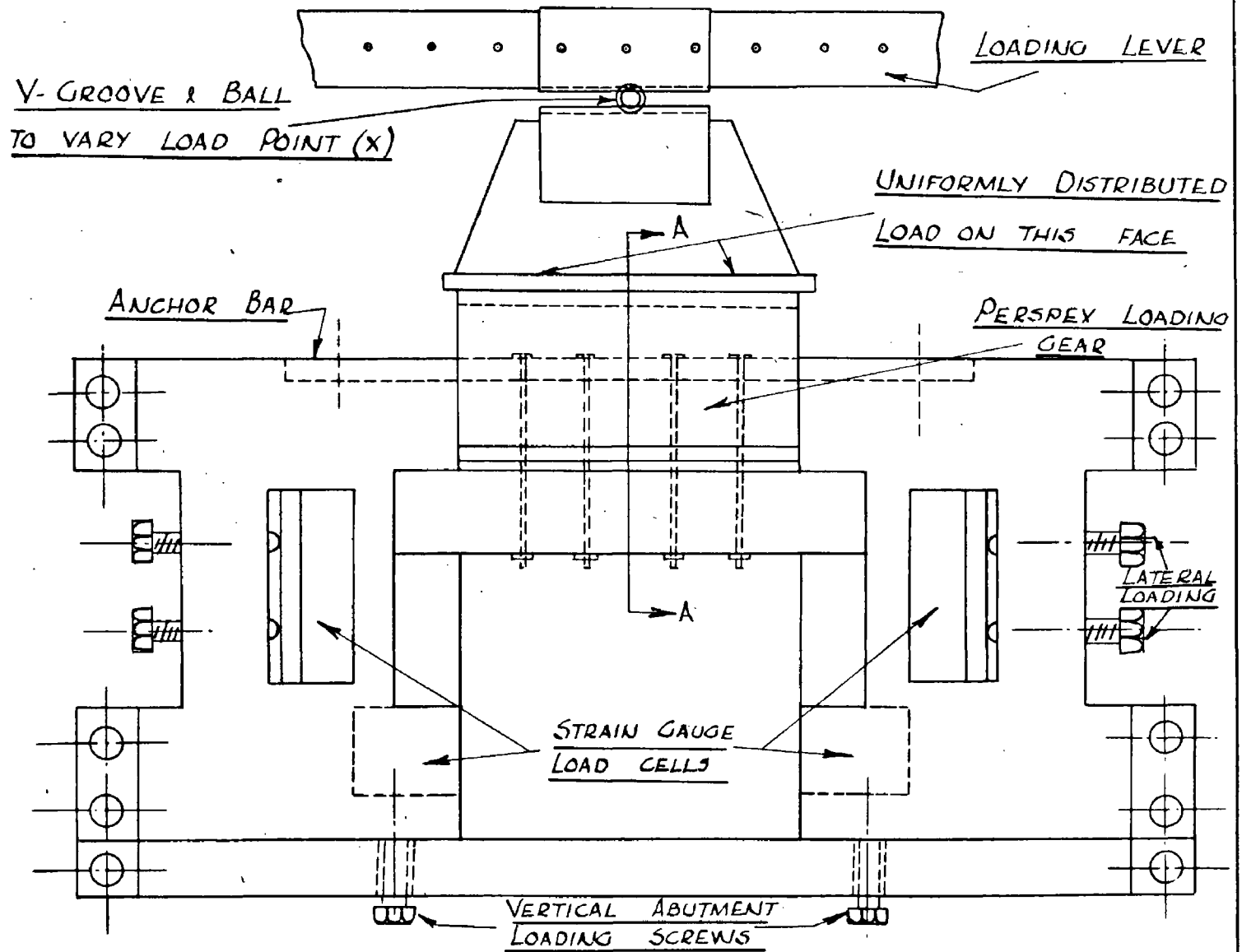
Photo-elastic Bench and Models



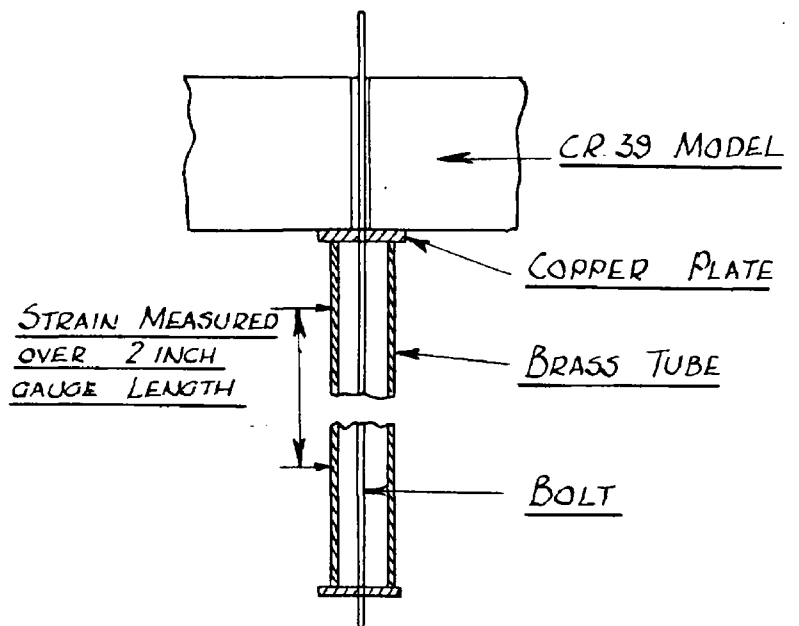
PLATE IIB: Machining Stresses
around Drill Hole in C.R.39



PLATE IIIB: Elimination of
machining stresses with Modified
Technique



SECTION A-A



MEASUREMENT OF BOLT TENSION

FIG 1B MODEL LOADING ARRANGEMENTS

EXPERIMENTAL PROCEDURE

In addition to the many underground experiments carried out to determine the effects of different roof bolting systems several investigators have studied the re-distribution of stresses caused by bolting of beams, etc. in the laboratory. Different techniques have been used including centrifugal testing (B21) and the testing of model bolts installed in concrete beams (B22). By these "destructive" methods, the critically stressed zones are revealed but an overall impression of the re-distribution of stresses throughout the model cannot be obtained. The procedure adopted for the photo-elastic tests although similar in principle to that used by Bucky (B21) and Wuerker (B22) gives a more general picture of the stresses around bolted excavations. Beyer and Solakian (B23) used a comparable method to that here described in their photo-elastic analysis of stresses in composite materials. In their tests the reinforcing bars were cast in the models and not inserted into drilled holes.

The procedure adopted in the tests can be sub-divided as follows:-

(a) Properties of the Model Materials

The "fringe constants" for the photo-elastic materials used in the investigation were determined by the testing of a beam in pure bending. The isochromatic diagram and calculations for the calibration of of the C.R.39 specimen are given in the "Results".

Tests were carried out on the material used for the model bolts

to determine the ultimate tensile stress and the elastic modulus. The brass sleeves used for the measurement of bolt tension were calibrated in a separate test to enable the bolts to be set to a pre-determined tension directly.

(b) Isoclinic Lines

The isoclinic lines were obtained by projection and direct tracing - no photographs of individual isoclinic lines were made. Perspex models were used for the determination of the isoclinic patterns.

(c) Isochromatic Patterns

Isochromatic diagrams for each stage of the investigations were recorded photographically. The effects of "pinning" the strata together by simply inserting the bolts without tension were studied - this test was intended to simulate the action of wooden "bolts". The variations of stress distribution with non-uniform bolt tension, square roof plates, roof bars, etc. were also investigated. A test was made to illustrate the effect of placing a rubber pad between the plate and the roof in a similar manner to the prop soles suggested by Jenkins (B24) in his study of floor penetration.

(d) Measurement of Bolt Tension

In the preliminary tests considerable difficulty was experienced in applying equal tensions to the bolts. Consequently it was necessary to measure the bolt tension in a separate operation. The following methods of measuring the bolt tension were investigated:-

Applied Torque: A simple torque-meter was constructed to allow

the application of a known torque to the bolts. However, since the tension required in each bolt was relatively small the influence of friction forces etc. on the nuts and bearing plates was such that the method was very inaccurate.

Optical Method: A small block of C.R.39 was interposed between the nut and the bearing plate. When the bolt was tensioned the C.R.39 was under compression causing interference fringes in the material. Due to the low forces being applied and the influencing of machining and edge stresses in the blocks of C.R.39, the accuracy of the method was low.

Extensometer: The length of the bolts was increased and a brass tube was placed between the nut and the bearing plate as shown in Fig. 1B. The strain developed in the tubes was measured by a Hounsfield Extensometer and from a previous calibration the tension in the bolts could be determined directly. However it was not found possible to fit the extensometer to the bolts while the model was under load in the straining frame and so only the initial tension in the bolts was recorded and not the tension developed under load. Reasonable accuracy could be obtained with this method and it was adopted for all the experiments.

EXPERIMENTAL RESULTS(a) Properties of the Model Materials

Stress Optical Coefficient: The isochromatic pattern for the centre portion of a beam of C.R.39 is shown in Fig. 2B. The total change in interference order from the top to the bottom of the beam is found by extrapolation.

For a beam in pure bending:-

$$\text{Extreme fibre stress} = \frac{M \times \frac{d}{2}}{I}$$

and for a rectangular section,

$$I = \frac{1}{12} bd^3$$

where

M = Bending moment on section (in lb.)

d = Depth of beam (inches)

I = Moment of Inertia of section (in.)⁴

b = Thickness of beam (in.)

$$\begin{aligned} \therefore \text{Total change in stress between extreme fibres} &= 2 \times \frac{M \times \frac{d}{2}}{\frac{bd^3}{12}} \\ &= \frac{12M}{bd^2} \dots\dots\dots(1) \end{aligned}$$

By definition, Stress Optical Coefficient (C) is given by,

$$C = \frac{(p - q) \times b}{n} \dots\dots\dots(2)$$

where (p - q) = Difference between principal stress (lb./in.²)

n = Order of the interference fringe

The units of the coefficient are lb./in.²/order/in. - stress difference.

In a beam in pure bending, the principal stress normal to the edge of the beam is zero, i.e. $q = 0$. Therefore the total stress across the section can be substituted for $(p - q)$ in equation (2), thus:-

$$C = \frac{12M}{bd^2} \times \frac{b}{n} \quad (\text{lb./in./order})$$

$$\therefore C = \frac{12M}{nd^2}$$

For the C.R.39 specimen tested:

$$M = 84.7 \text{ in.lb.}$$

$$d = 1.00 \text{ in.}$$

$$n = 10.4 \text{ orders}$$

$$\therefore C = \frac{12 \times 84.7}{1^2 \times 10.4}$$

i.e. Stress Optical Coefficient (C.R.39) = 97.7 lb./in. x order.

The coefficients for the other materials were obtained in the same way.

Roof Bolts: From a series of tensile tests (some to destruction) on the material used for the bolts the following results were obtained:-

$$\text{Young's Modulus} = 26.7 \times 10^6 \text{ lb./in.}^2$$

$$\text{Ultimate Load} = 735 \text{ lb.}$$

$$\text{Average Diameter} = 0.065 \text{ in.}$$

Brass Loading Tubes: The results of the calibration test on a specimen of the tube used for the measurement of bolt tension are shown in Fig. 3B.

(b) Isoclinic Lines

The isoclinics for each model were obtained by direct tracing. Typical of the diagrams obtained are those for a beam with and without bolts (the bolting pattern being the 4-bolt suspension support), shown in Fig. 4B and 5B. The corresponding diagrams of stress trajectories are shown with the isoclinic diagrams.

The stress trajectories obtained for the unbolted arch section were similar to those obtained by Potts (B17) and Guinard (B10) for arched shaped galleries in a continuous medium.

(c) Isochromatic Patterns

The isochromatic patterns for various loading conditions of each group of models were obtained using monochromatic light with the dark field arrangement of the polariscope. Plates IVB and XVIB show the fringe patterns obtained with the specified loading conditions. Considering each group of models separately:-

Suspension Support - Plates IVB, VB and VIB show the shear stress distribution over the span with and without bolts under different applied loads. The distribution of stress induced by equal tension in the bolts (zero applied load) is shown in Plate VIIB. Plates VIIIB and IXB illustrate the effects of unequal bolt tension and the use of a roof bar in place of "patch" plates.

Compound Beam - The redistribution of stress caused by bolting two independent beams together is illustrated in Plates XB and XIB. The reduction in stress concentration at the edge of the patch plates when a yielding pad (rubber) is interposed between the plate and the roof is shown in Plate XIIB.

Arched Roadway Support - Representative of the isochromatic patterns obtained for the models of an arched roadway are those shown in Plates XIIIIB and XIVB. The model used in this particular experiment was made entirely of C.R.39 with hard rubber to simulate the roadside packs. The bolting pattern was based on the results obtained from previous experiments. Plate XIIIIB shows the stress distribution across the section without bolts and the effects of simply inserting the bolts without applying tension are seen in Plate XIVB. This latter condition is comparable to using wooden bolts or pins (see Section C). The stress distribution when all three bolts are tensioned equally is shown in Plate XVB while the effect of tensioning the centre bolt alone is illustrated in Plate XVIIB.

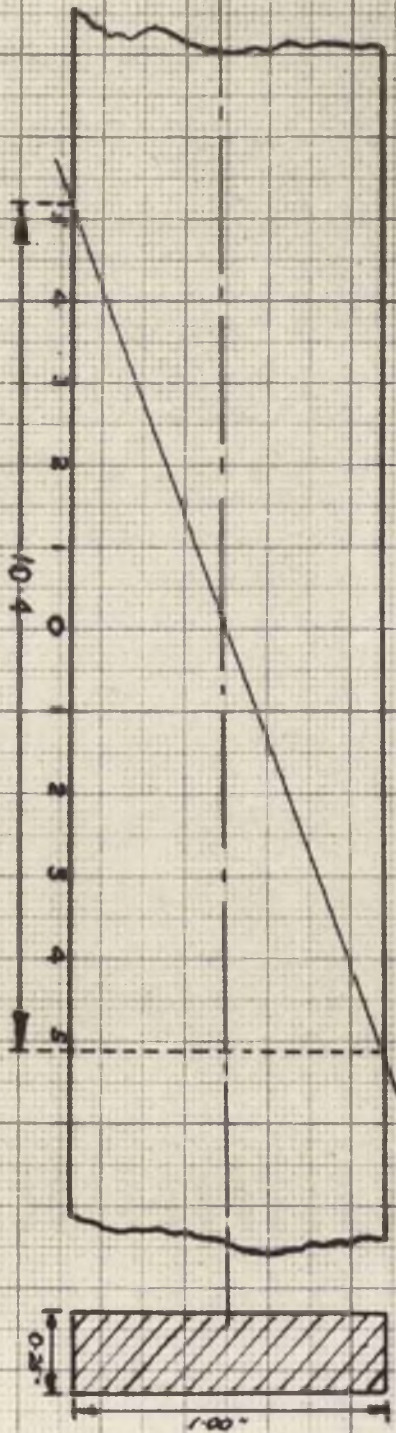
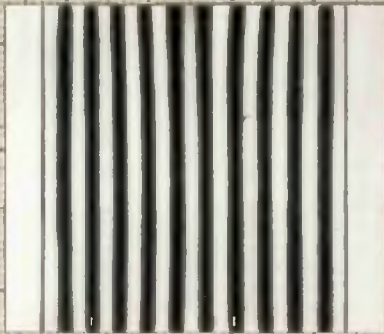


FIG 2B.

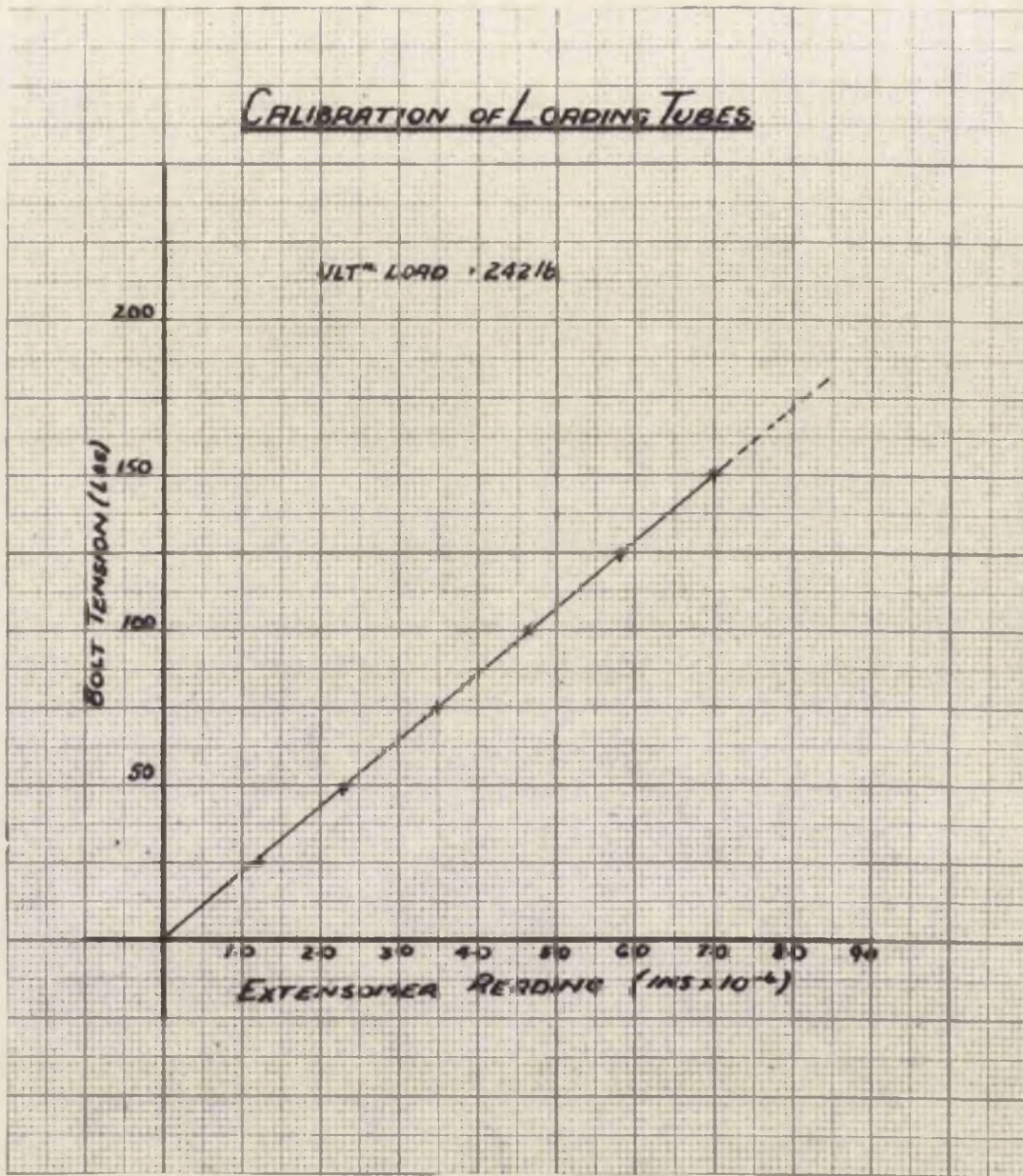


FIG. 3B.

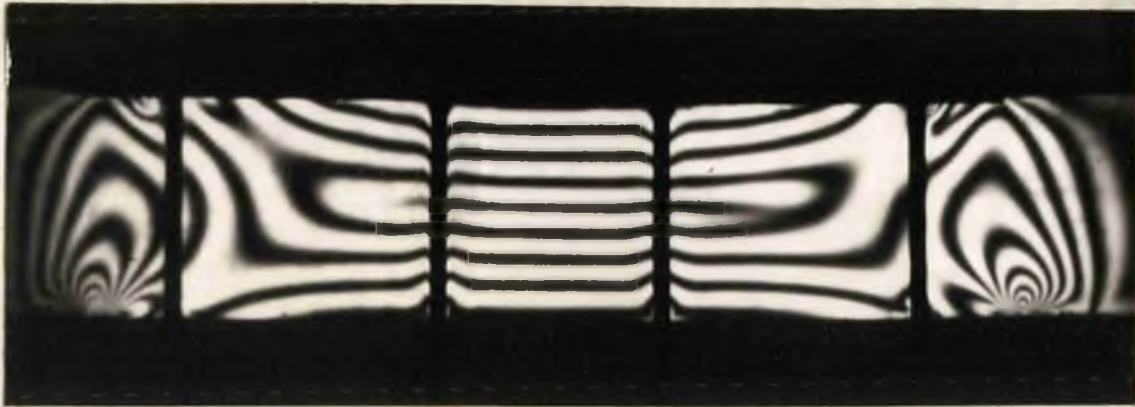


PLATE IVB

Suspension Support. Applied Load 328 lb./in.²
Bolt tension zero.

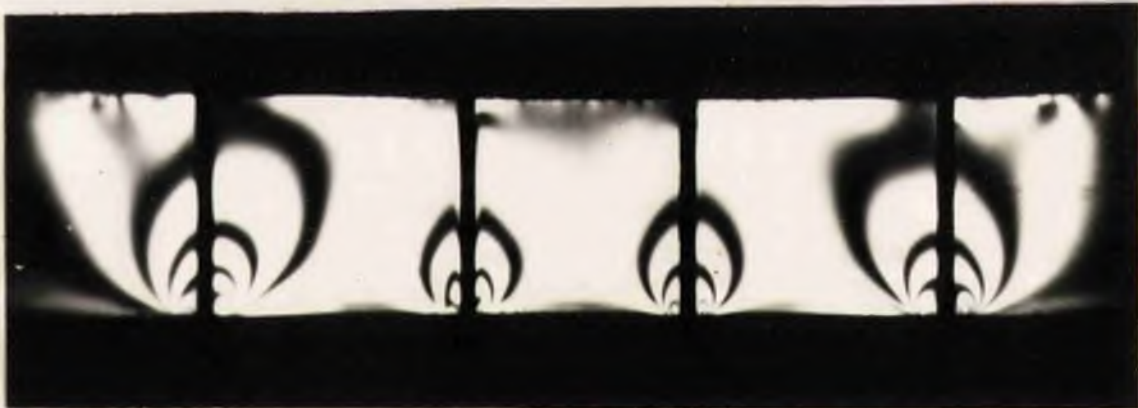


PLATE VB

Suspension Support. Applied Load 227 lb./in.²
Equal bolt tension (3 units strain)



PLATE VI B

Suspension Support. Applied Load 328 lb./in.²
Equal bolt tension (3 units)

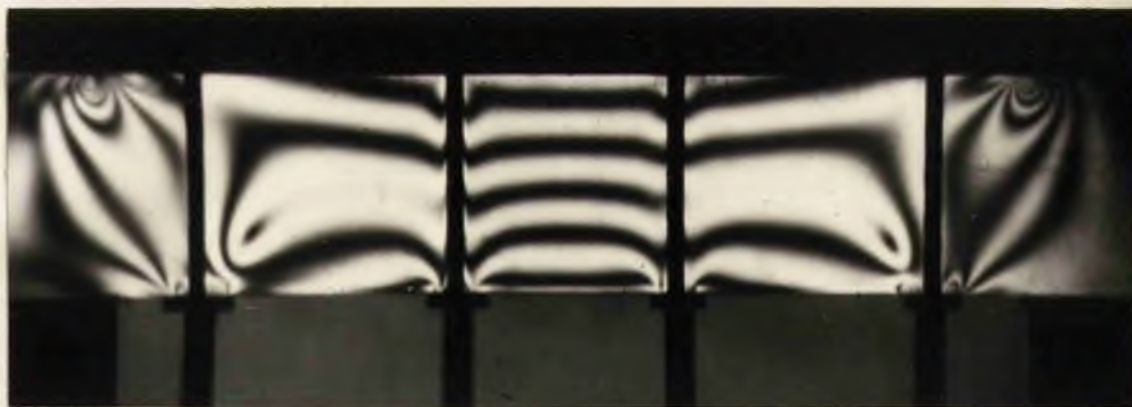


PLATE VII B

Suspension Support. Applied Load zero.
Equal bolt tension (3 units)

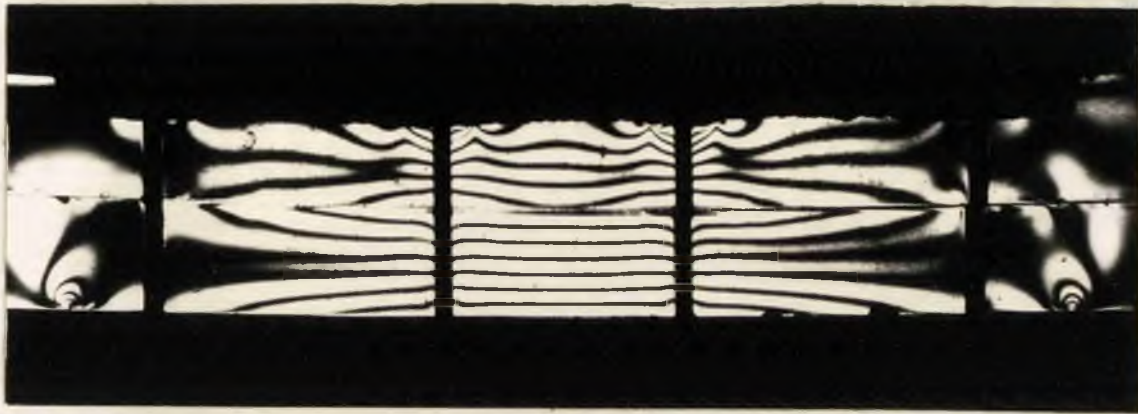


PLATE XB Compound Beam. Applied Load 70 lb./in.²
Without bolts.

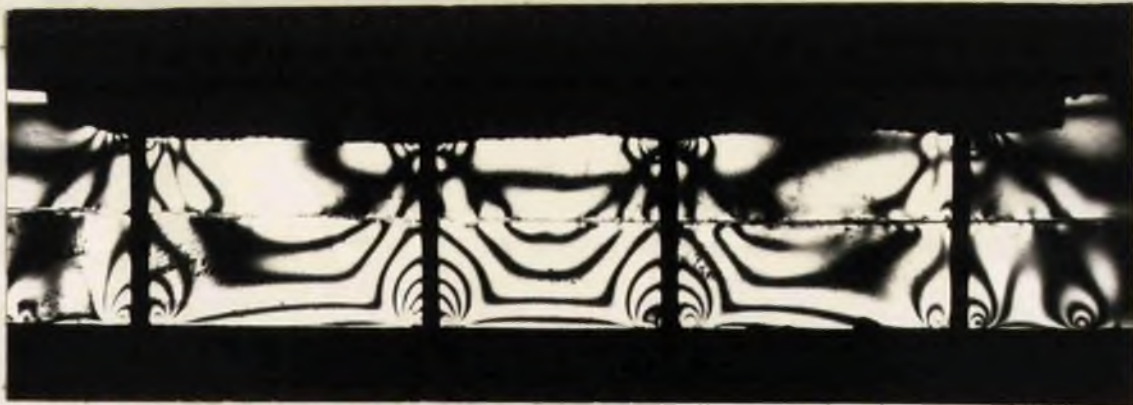


PLATE XI B Compound Beam. Applied Load 70 lb./in.²
4-bolts equal tensions.

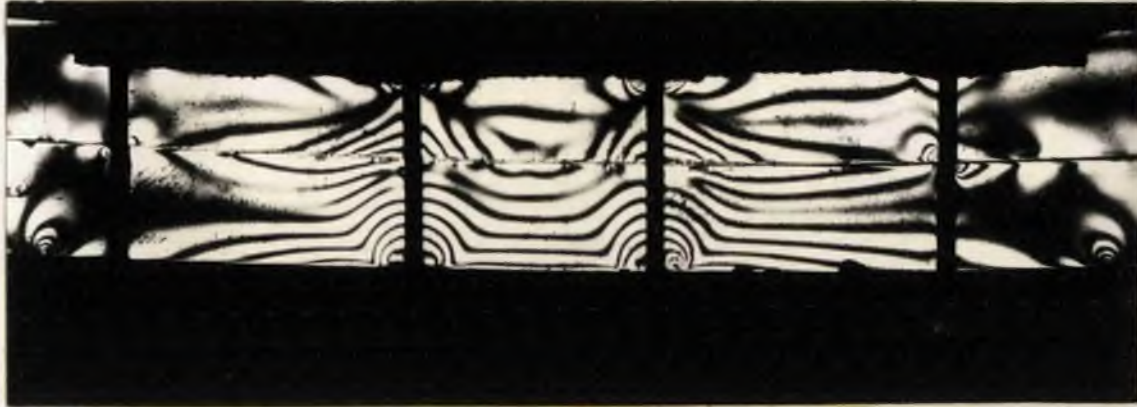


PLATE XIIB

Compound Beam. Applied Load 70 lb./in.^2
2-bolts equal tensions. Rubber pad in
position (left hand bolt).

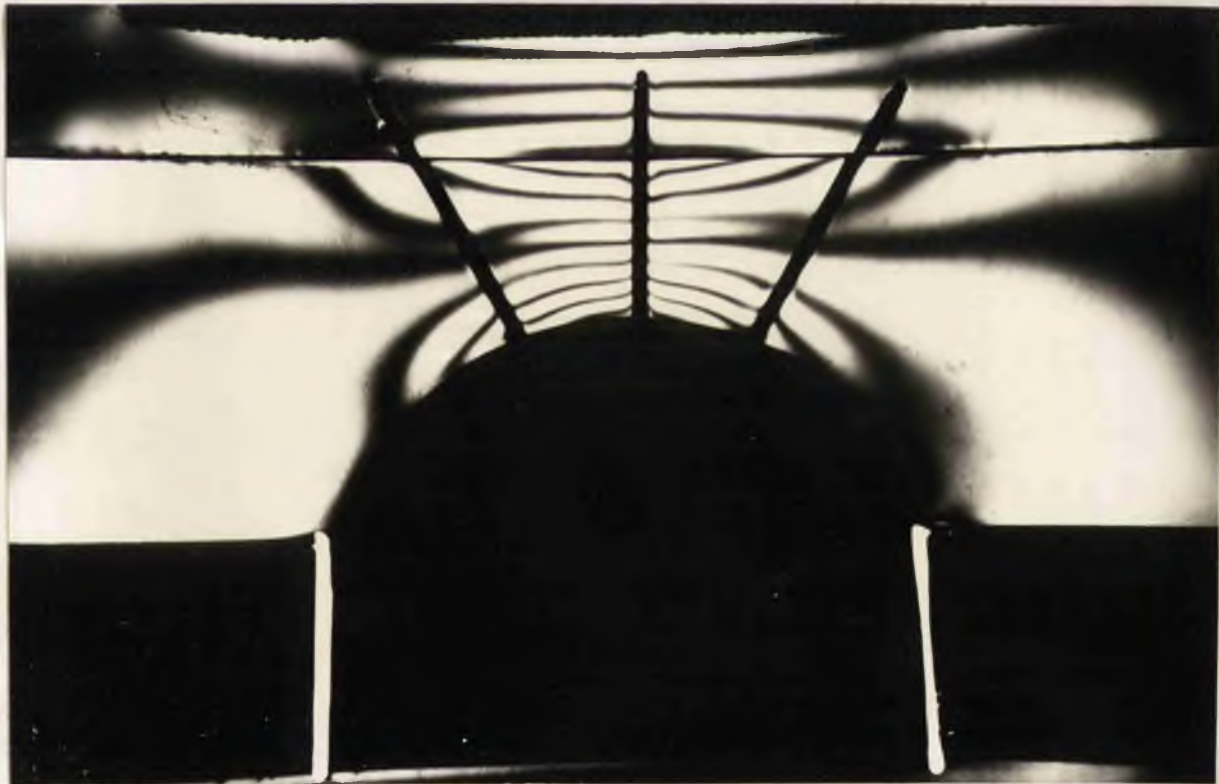


PLATE XIIIIB

Applied Load 80 lb./in.^2 without bolts.



PLATE XIVB

Applied Load 80 lb./in.² Bolts installed
tension zero.

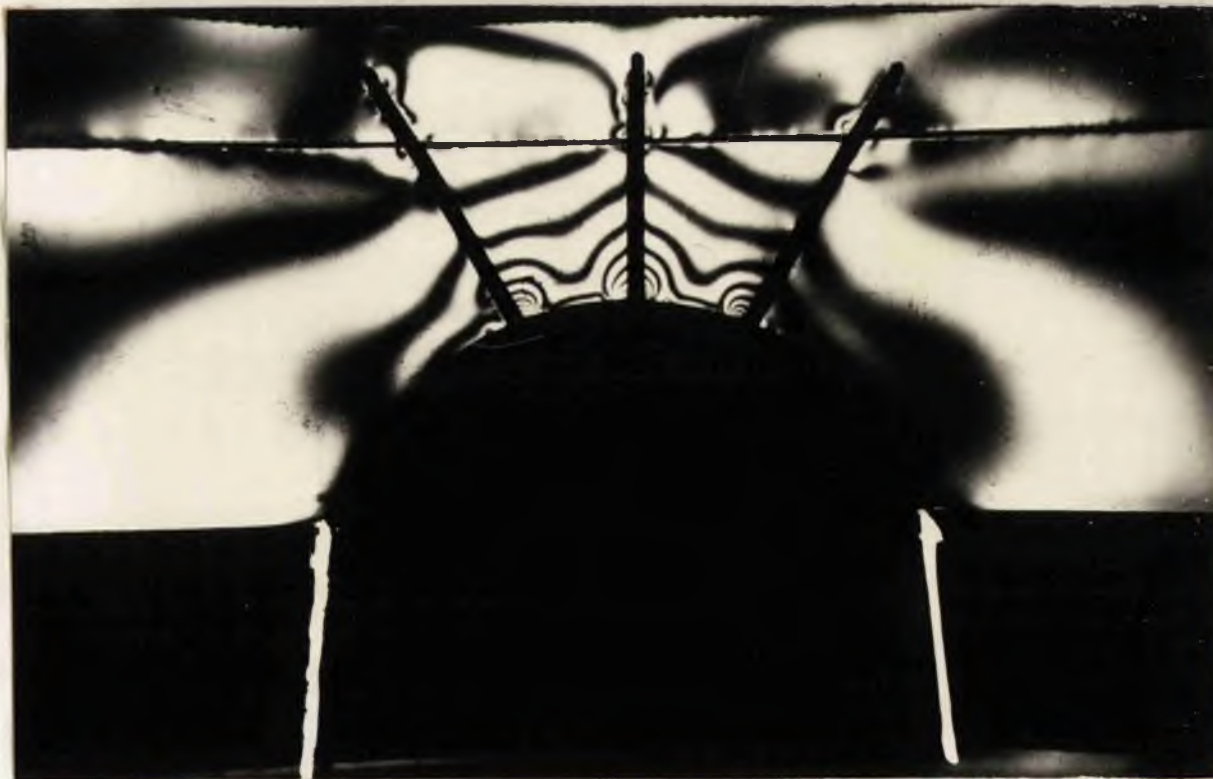


PLATE XVb

Applied Load 80 lb./in.² Bolts installed
with equal tension.

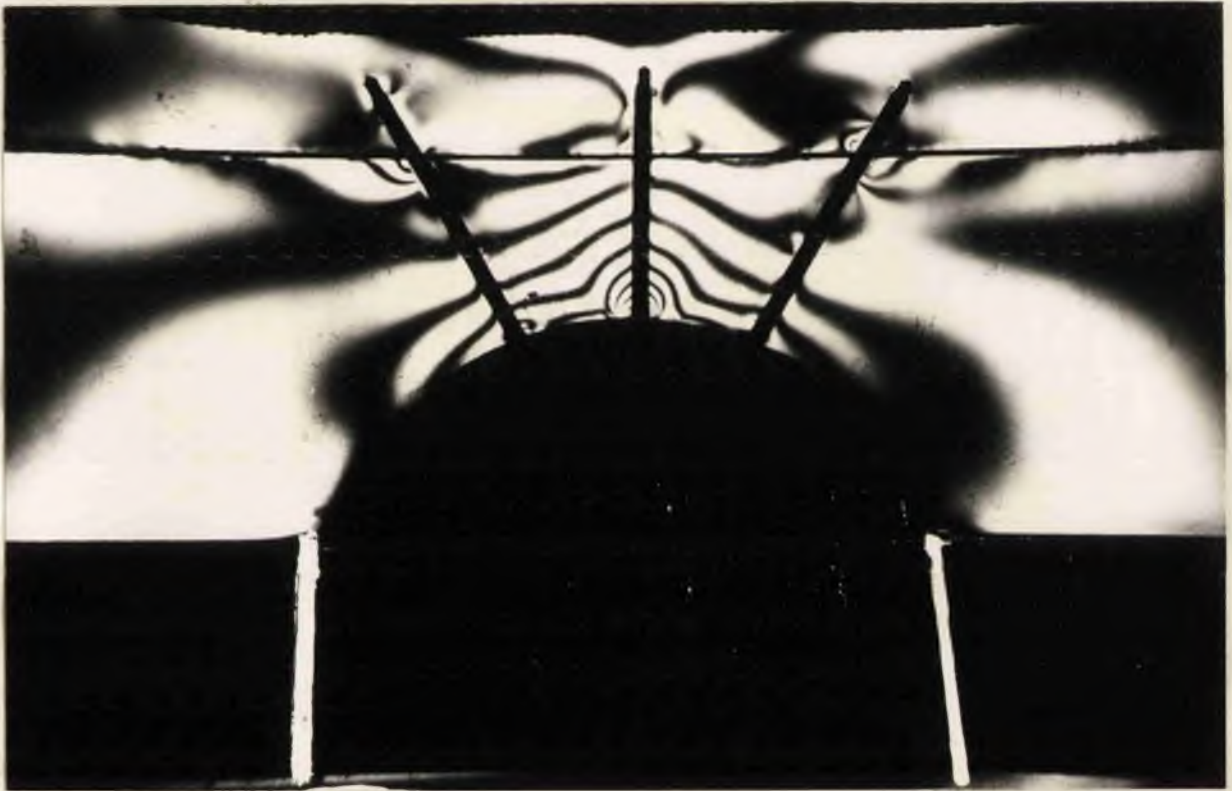


PLATE XVIB

Applied Load 80 lb./in.² 3 bolts installed.
Centre bolt only tensioned.

UNBOLTED SPAN - ISOCLINICS & STRESS TRAJECTORIES

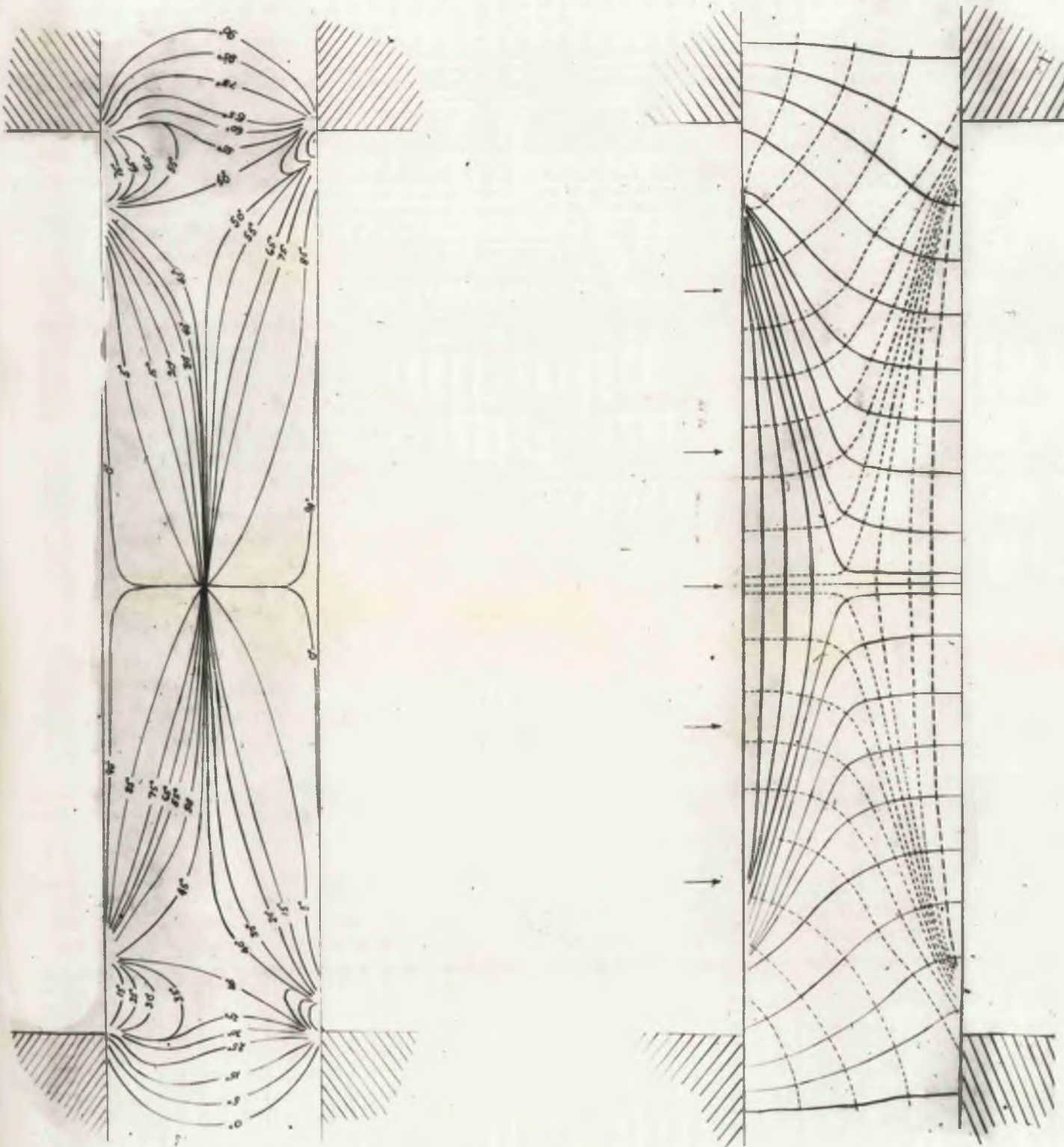


Fig. 4.B.

BOLTED SPAN - ISOCLINICS & STRESS TRAJECTORIES.

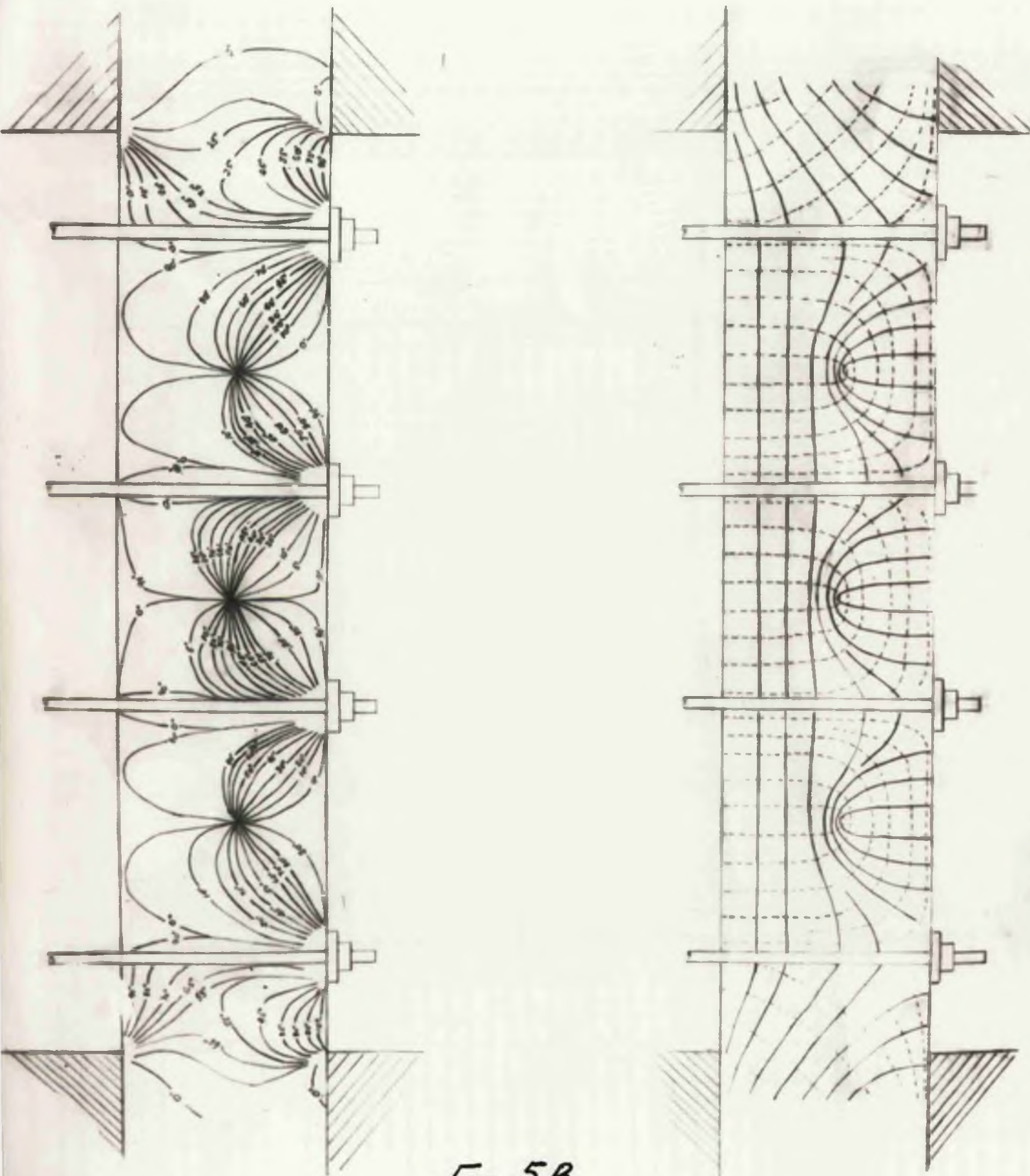


FIG. 5B.

ANALYSIS OF RESULTS

1. It is known that Coal Measures Rocks do not behave strictly as elastic bodies when under stress (Section A), consequently the analysis of the results obtained in the photo-elastic investigations must be qualitative rather than quantitative. Potts, in his analysis of several mining problems (B16, B17 etc.) has used the "unit" method of analysis, i.e. the stress distribution is given in terms of the total applied stress, but the nature of the investigations here described does not permit such a method of analysis.
2. In the construction of the models the roof bolts are placed within the photo-elastic material, hence the optical effects recorded in the vicinity of the bolts cannot be analysed correctly with normal two-dimensional photo-elastic methods.
3. In the initial experiments several failures of the bolts occurred due to shearing of the threads and to overcome this weakness it was necessary to use steel wire for the bolts. The use of steel (for the bolts) resulted in the ratio $\frac{E \text{ model bolts}}{E \text{ C.R.39}}$ being much higher than the ratio $\frac{E \text{ bolts}}{E \text{ rock}}$, so that the conditions of similarity between the model and the prototype are not accurate.

Suspension Support:

- (1) The re-orientation of the principal stresses throughout a "suspended" roof bed due to bolting is shown by comparing Fig. 4B and 5B. Similar diagrams were obtained with "two" and "three" bolting patterns.

(ii) In the unbolted span (Plate IVB) the shear stress concentrations over the rib sides are very high and there is considerable tensile stress on the lower fibre over most of the span. Thus failure will take place either in tension (at mid-span) or in shear (over the rib sides) depending upon the physical properties of the rock bed. The effects of introducing 4-bolts (with sufficient initial tension) are shown in Plates VB and VIB. In the former case when the applied load is 227 lb. per square inch the introduction of the bolts has almost neutralised the tensile stress on the lower fibre of the bed. When the applied load is increased tensile stress again develops in the lower fibres of the bed (Plate VIB). The distribution of tensile stress (in fringe orders) along the lower fibre of the roof bed for each of the above conditions is shown in Fig. 6B.

(iii) The concentration of shear stress is higher around the bolts nearest the rib sides and the introduction of bolts reduces the shear stress concentration immediately over the rib sides.

(iv) The initial tension applied to each of the bolts must be uniform otherwise the bolts merely distort the stress distribution over the span and may actually promote fracturing of the roof bed by acting as "stress raisers". This is especially important if the roof bed is weak in shear (Plate VIII B).

(v) It is seen that there is always a concentration of shear stress around the patch plates which may in some cases cause failure

of the support system due to crumbling of the immediate roof bed around the plate. Plate IXB illustrates the shear stress distribution when a roof bar extending across the entire span is used in place of the plates. The use of the bar appears to have eliminated the high stress concentrations around the bolts but it should be remembered that if a section along the axis of the roadway was considered then the stress distribution would resemble that shown in Plate VB.

Compound Beam Effect:

(i) Plate XB shows the shear stress distribution when two strata, subjected to bending, are acting independently. It is seen that the fringe order on the lowest fibre of the bottom stratum at mid-span is 3.8, corresponding to a tensile stress tangential to the roof of approximately 1490 lb. per square inch for an applied load of 70 lb. per square inch.

(ii) When four bolts, equally tensioned, are installed in the beams before subjecting them to the same load, the fringe order at mid-span is 2.4 - giving a tensile stress of 940 lb. per square inch.

(iii) The clamping together of the beds almost eliminates the shear stress along the underface between the two beds.

(iv) Thus provided sufficient tension is applied to the bolts it may be possible to bind several thin strata together into a compound beam which could withstand the applied load without failure at mid-span.

(v) Jenkins (B24) in his photo-elastic experiments of floor

penetration by props illustrated that the shear stress concentration at the edge of the prop bases could be reduced by the introduction of a rubber pad between the base of the prop and the floor. Failures of roof bolts also occur because of the high shear stresses induced around the patch plates. A similar pad to that suggested by Jenkins is shown between the plate and the roof bed (C.R.39) for the left bolt in Plate XIIIB. Comparison of this bolt with the right one reveals a marked reduction of shear stress. The value of this pad, in practice, will depend mainly upon the physical properties of the roof bed (plastic flowing etc.).

Arched Roadway Support:

(i) Many investigations of the stress distribution around roadways of various shapes have revealed that failure is most likely to occur in the tension zone over the roof of the excavation. Guinard (B10) deduces from his photo-elastic and mathematical studies that even at the greatest depths worked in iron mines the galleries fail in tension at the keystone before the ultimate compressive stress is developed at the abutments of the arch. Plate XIIIB illustrates the shear-stress distribution around an arched shaped roadway in stratified material. Examination of the isochromatics reveals a tensile stress at the base of the keystone of 1560 lb. per square inch for an applied load of 80 lb. per square inch.

(ii) By inserting bolts, in the pattern shown, into the roof of the roadway and anchoring them in the stratum above (without apply-

ing tension) the tensile stress at the keystone is reduced to 1490 lb. per square inch and furthermore there is a reduction of the shear stress developed on the lower fibres of the anchorage stratum. The effects of simply "pinning" the beds of the keystone together was extended by using "wooden bolts" in the underground investigations, (see Section C).

(iii) By applying equal tensions to the three bolts (all installed within the tension zone) the tensile stress at the keystone is reduced to 1100 lb. per square inch and the shear stress along the interface is almost eliminated (Plate XVB).

(iv) When all three bolts are in position, but only the centre one is tensioned, there is still a reduction of the tensile stress at the keystone - illustrating that the centre bolt is the most vital one in reducing the intensity of the tensile stress over the roadway.

(v) The reduction of the tensile stress at the keystone (under the specified conditions) is shown diagrammatically in Fig. 7B. The stress values used in plotting the results are merely relative and cannot be applied directly to the prototype because of the dissimilarity (previously discussed) of the model and actual underground conditions.

(vi) In the models the bolts have a 100% anchorage - a factor which is never achieved in practice (see Section C). With this pattern the bolt anchorages are within the "tension zone" (for certain loading conditions) which may cause "creep" of the bolt anchorages

underground, but provided systematic re-tightening of the bolts is adopted this disadvantage may be overcome.

(vii) In addition to the model (arched roadway) here described several compound models composed of strata of different materials (Bakelite, Catalin, etc.) were made. The results obtained were similar but it is thought that the variation in Poisson's Ratio of the materials, influence of surface friction etc., induce stresses at the interfaces which further complicate the analysis of the results and their application to working conditions underground.

FRINGE ORDERS.

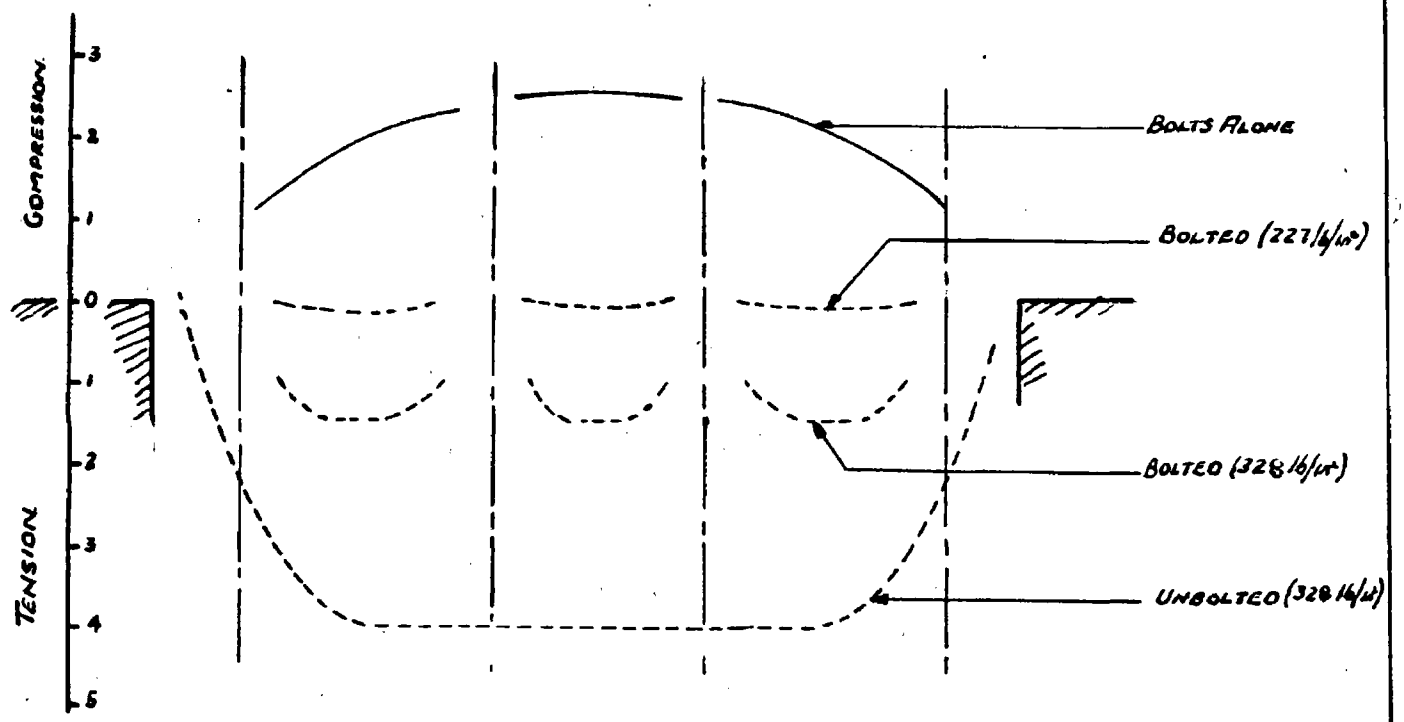


FIG. 6 B. SUSPENSION SUPPORT.

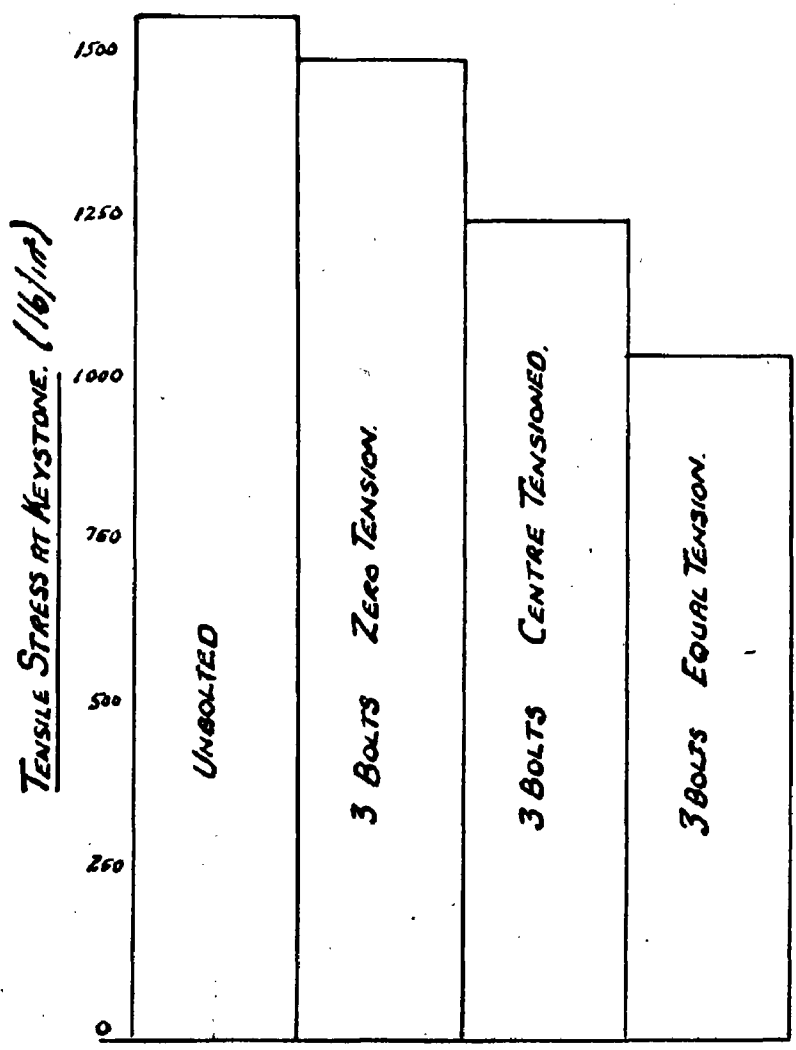


FIG. 7 B
ARCHED ROADWAY
SUPPORT

C O N C L U S I O N S

1. Since Coal Measures Rocks are not truly elastic in their behaviour under stress, and because of the difficulties in simulating underground conditions by models, the results obtained from photo-elastic investigations are qualitative rather than quantitative.
2. The applications of two-dimensional photo-elasticity are limited because it is not always possible to construct models which truly represent the conditions existing across any particular section of an underground excavation.
3. There are three principal applications of roof bolting in coal mines viz. suspension support, formation of a compound beam and arched roadway support. In each case the use of bolts reduces the tensile stress developed on the lower fibres of the immediate roof bed.
4. The initial tension applied to each of the bolts must be uniform otherwise local concentrations of stress are developed which may induce premature failure of the roof.
5. The use of yielding pads (rubber) between the patch plates and the roof reduces the concentration of shear stress at the edges of the plates.
6. In the support of longwall gate roads, a 3-bolt pattern installed within the tension zone materially reduces the tensile stress developed at the "keystone" which is normally the weakest part of the excavation. This use of bolts was further investigated underground (Section C) and by stratified plaster models (Section D) - all

three investigations revealed the saving in roadway maintenance which can be achieved when the "keystone" is reinforced.

7. It is suggested that future investigations of roof bolting systems by photo-elasticity should be carried out with three-dimensional models made up of strata of different materials. The influence of induced surface stresses (at the interfaces of the beds) should be studied and the materials used for the models should have similar "constant ratios" (e.e. $\frac{E \text{ bolts}}{E \text{ rock}}$) to those of the prototype. The method of loading the models should also receive consideration, to permit closer correlation of the model results with those obtained underground.

SECTION C - UNDERGROUND OBSERVATIONS

To extend the laboratory investigations of roof bolting as a support in stratified deposits, and to determine the applications and limitations of the electrical resistance strain gauge and ancillary equipment for use underground, a full-scale bolting programme was commenced at Northfield Colliery, Shotts, during September, 1954. All the experiments were carried out in the main gate of an advancing longwall face; the bolting being used in conjunction with the normal arch-girder supports. Three types of steel bolt - slot and wedge, expansion shell, wedge and sleeve - were investigated as well as some wooden "bolts" or pins. No observations were made in stoop and room workings because most of the available literature on bolting techniques (C1 to C7 inclusive) is concerned with 'solid' working while comparatively few trials have been recorded in longwall workings.

Location of Experiments

Northfield Colliery, Shotts, is a small unit with an output of 500 tons per day. The shafts are sunk to the Productive Coal Measures; sections of the strata to the East and West of No.1 South District are shown in Fig. 16. It is a non-gassy mine which allowed freedom in the use of electrical apparatus.

The site chosen for the tests was the main gate of No.1 South Section shown in Fig. 1C. This roadway in the Main Coal is 470 feet from the surface, and has proved very difficult to maintain - three or four re-rippings being necessary in some parts.

Types of Bolts and Installation Equipment

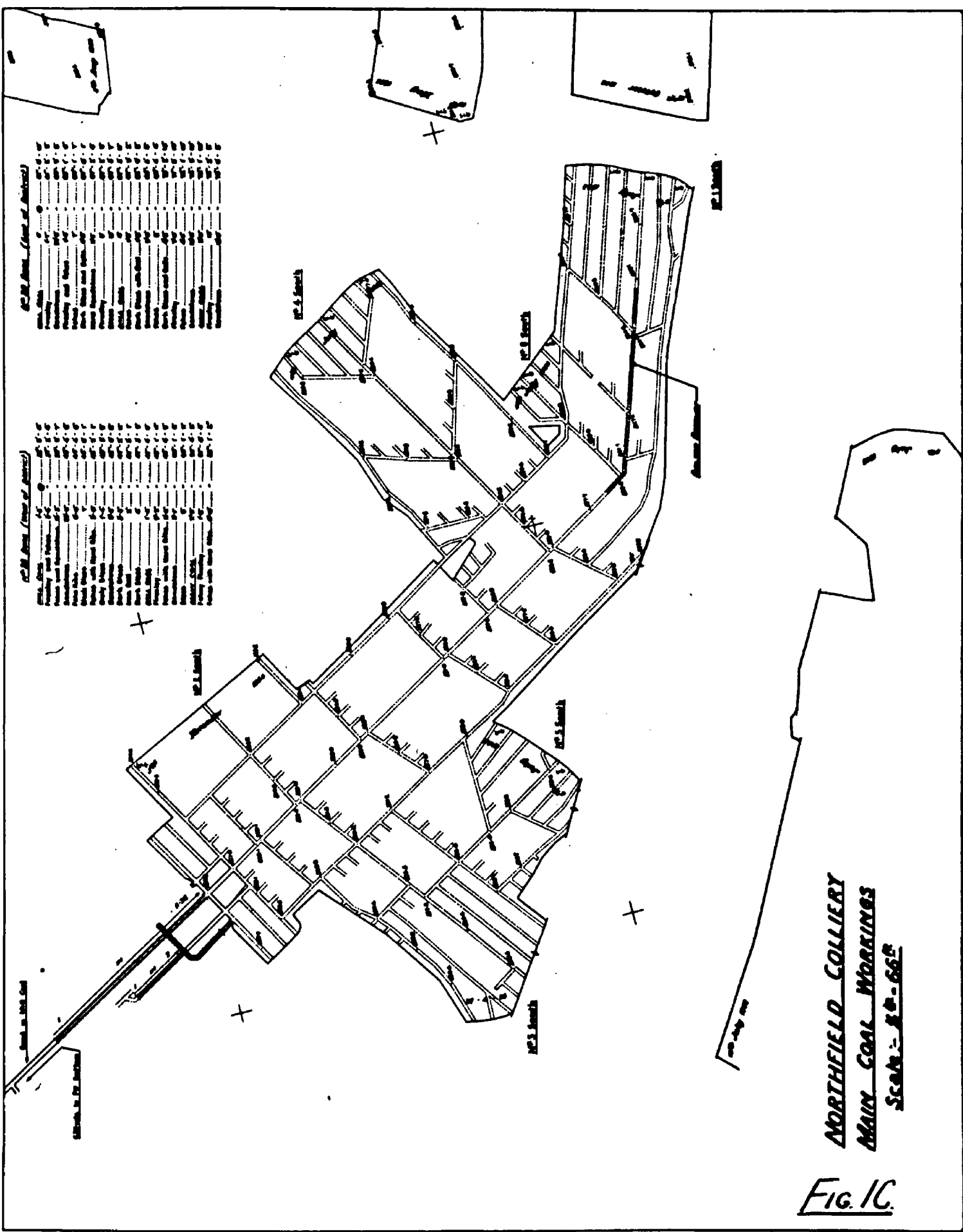
Many types of roof bolt have been devised recently; details of the various forms of 'anchoring' devices can be found in the publications of Wright and McDonald (C4), Hodkin and Lawrence (C9), Panek, Barry and McCormick (C10), Rabcewicz (C11) and others.

Three types of steel bolt were selected for the tests - each one representative of a particular form of anchor design. Details of the bolts used are given in Table No.1C below.

TABLE No.1C

Types of Bolt

	<u>Slot and Wedge</u>	<u>Shell</u>	<u>Wedge and Sleeve</u>
Type	Burned Slot	"Shotts" type	Bayliss, Jones & Bayliss
Length	5 ft.6 in.	5 ft.6 in.	3 ft.6 in.
Diameter	1 in.	$\frac{3}{4}$ in.	59/64 in.



PC 1.1 Seam (Cont. of Previous)

PC 1.1.1	PC 1.1.2	PC 1.1.3	PC 1.1.4	PC 1.1.5	PC 1.1.6	PC 1.1.7	PC 1.1.8	PC 1.1.9	PC 1.1.10	PC 1.1.11	PC 1.1.12	PC 1.1.13	PC 1.1.14	PC 1.1.15	PC 1.1.16	PC 1.1.17	PC 1.1.18	PC 1.1.19	PC 1.1.20	PC 1.1.21	PC 1.1.22	PC 1.1.23	PC 1.1.24	PC 1.1.25	PC 1.1.26	PC 1.1.27	PC 1.1.28	PC 1.1.29	PC 1.1.30	PC 1.1.31	PC 1.1.32	PC 1.1.33	PC 1.1.34	PC 1.1.35	PC 1.1.36	PC 1.1.37	PC 1.1.38	PC 1.1.39	PC 1.1.40	PC 1.1.41	PC 1.1.42	PC 1.1.43	PC 1.1.44	PC 1.1.45	PC 1.1.46	PC 1.1.47	PC 1.1.48	PC 1.1.49	PC 1.1.50	PC 1.1.51	PC 1.1.52	PC 1.1.53	PC 1.1.54	PC 1.1.55	PC 1.1.56	PC 1.1.57	PC 1.1.58	PC 1.1.59	PC 1.1.60	PC 1.1.61	PC 1.1.62	PC 1.1.63	PC 1.1.64	PC 1.1.65	PC 1.1.66	PC 1.1.67	PC 1.1.68	PC 1.1.69	PC 1.1.70	PC 1.1.71	PC 1.1.72	PC 1.1.73	PC 1.1.74	PC 1.1.75	PC 1.1.76	PC 1.1.77	PC 1.1.78	PC 1.1.79	PC 1.1.80	PC 1.1.81	PC 1.1.82	PC 1.1.83	PC 1.1.84	PC 1.1.85	PC 1.1.86	PC 1.1.87	PC 1.1.88	PC 1.1.89	PC 1.1.90	PC 1.1.91	PC 1.1.92	PC 1.1.93	PC 1.1.94	PC 1.1.95	PC 1.1.96	PC 1.1.97	PC 1.1.98	PC 1.1.99	PC 1.1.100
----------	----------	----------	----------	----------	----------	----------	----------	----------	-----------	-----------	-----------	-----------	-----------	-----------	-----------	-----------	-----------	-----------	-----------	-----------	-----------	-----------	-----------	-----------	-----------	-----------	-----------	-----------	-----------	-----------	-----------	-----------	-----------	-----------	-----------	-----------	-----------	-----------	-----------	-----------	-----------	-----------	-----------	-----------	-----------	-----------	-----------	-----------	-----------	-----------	-----------	-----------	-----------	-----------	-----------	-----------	-----------	-----------	-----------	-----------	-----------	-----------	-----------	-----------	-----------	-----------	-----------	-----------	-----------	-----------	-----------	-----------	-----------	-----------	-----------	-----------	-----------	-----------	-----------	-----------	-----------	-----------	-----------	-----------	-----------	-----------	-----------	-----------	-----------	-----------	-----------	-----------	-----------	-----------	-----------	-----------	-----------	-----------	------------

PC 1.2 Seam (Cont. of Previous)

PC 1.2.1	PC 1.2.2	PC 1.2.3	PC 1.2.4	PC 1.2.5	PC 1.2.6	PC 1.2.7	PC 1.2.8	PC 1.2.9	PC 1.2.10	PC 1.2.11	PC 1.2.12	PC 1.2.13	PC 1.2.14	PC 1.2.15	PC 1.2.16	PC 1.2.17	PC 1.2.18	PC 1.2.19	PC 1.2.20	PC 1.2.21	PC 1.2.22	PC 1.2.23	PC 1.2.24	PC 1.2.25	PC 1.2.26	PC 1.2.27	PC 1.2.28	PC 1.2.29	PC 1.2.30	PC 1.2.31	PC 1.2.32	PC 1.2.33	PC 1.2.34	PC 1.2.35	PC 1.2.36	PC 1.2.37	PC 1.2.38	PC 1.2.39	PC 1.2.40	PC 1.2.41	PC 1.2.42	PC 1.2.43	PC 1.2.44	PC 1.2.45	PC 1.2.46	PC 1.2.47	PC 1.2.48	PC 1.2.49	PC 1.2.50	PC 1.2.51	PC 1.2.52	PC 1.2.53	PC 1.2.54	PC 1.2.55	PC 1.2.56	PC 1.2.57	PC 1.2.58	PC 1.2.59	PC 1.2.60	PC 1.2.61	PC 1.2.62	PC 1.2.63	PC 1.2.64	PC 1.2.65	PC 1.2.66	PC 1.2.67	PC 1.2.68	PC 1.2.69	PC 1.2.70	PC 1.2.71	PC 1.2.72	PC 1.2.73	PC 1.2.74	PC 1.2.75	PC 1.2.76	PC 1.2.77	PC 1.2.78	PC 1.2.79	PC 1.2.80	PC 1.2.81	PC 1.2.82	PC 1.2.83	PC 1.2.84	PC 1.2.85	PC 1.2.86	PC 1.2.87	PC 1.2.88	PC 1.2.89	PC 1.2.90	PC 1.2.91	PC 1.2.92	PC 1.2.93	PC 1.2.94	PC 1.2.95	PC 1.2.96	PC 1.2.97	PC 1.2.98	PC 1.2.99	PC 1.2.100
----------	----------	----------	----------	----------	----------	----------	----------	----------	-----------	-----------	-----------	-----------	-----------	-----------	-----------	-----------	-----------	-----------	-----------	-----------	-----------	-----------	-----------	-----------	-----------	-----------	-----------	-----------	-----------	-----------	-----------	-----------	-----------	-----------	-----------	-----------	-----------	-----------	-----------	-----------	-----------	-----------	-----------	-----------	-----------	-----------	-----------	-----------	-----------	-----------	-----------	-----------	-----------	-----------	-----------	-----------	-----------	-----------	-----------	-----------	-----------	-----------	-----------	-----------	-----------	-----------	-----------	-----------	-----------	-----------	-----------	-----------	-----------	-----------	-----------	-----------	-----------	-----------	-----------	-----------	-----------	-----------	-----------	-----------	-----------	-----------	-----------	-----------	-----------	-----------	-----------	-----------	-----------	-----------	-----------	-----------	-----------	-----------	------------

NORTHFIELD COLLIERY
MAIN COAL WORKINGS
 Scale: 1/4" = 10'

FIG. 1C.

	<u>Slot and Wedge</u>	<u>Shell</u>	<u>Wedge and Sleeve</u>
Thread	Cut	Cut	Rolled
Young's Modulus	30.7 x 10 ⁶ lb./in. ²	30.3 x 10 ⁶ lb./in. ²	-
Yield Strength	40,100 lb./in. ²	44,400 lb./in. ²	44,700 lb./in. ²
Ult. Tensile Strength	64,300 lb./in. ²	69,400 lb./in. ²	74,400 lb./in. ²
Length of Slot	12 in.	-	-
Wedge	1 1/4" x 1" x 1" to 1" x 1/16"	-	-
Shell	-	Cast Phosphor Bronze	Mild Steel

In addition to the three types of steel bolts some wooden 'bolts' or pins were used. There have been several experiments carried out with wooden bolts in tunnels and narrow work (C12, C13, C14) but no records of similar tests in longwall work could be traced. Details of the construction of the wooden bolts are given in Fig. 20.

Initially the 'plate' was fixed by driving a second wedge into the head of the bolt, but this method did not prove effective, and the method finally adopted was to drive hardwood wedges between the roof and the plate (see Plate XVII C later).

The types of plates or washers employed were a 4" x 4" x 3/8" flat plate, and a 9" x 9" x 3/8" dished plate, with and without wooden pads between the plates and the roof. The design of the dished plates was based on that used by McKensy (C15) in his experiments in Australia.

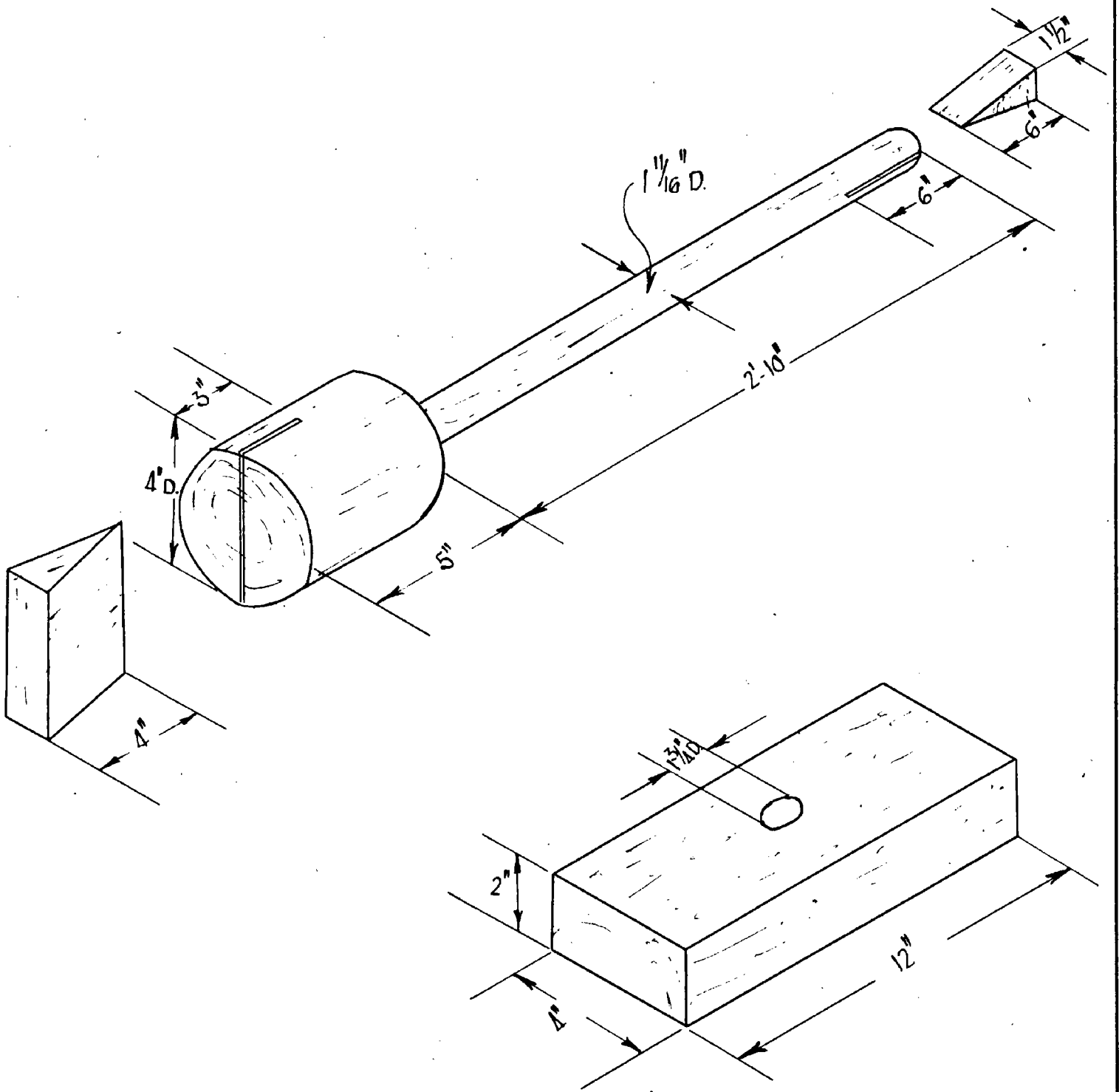


FIG. 2C.

DETAIL OF WOODEN BOLTS.

The equipment used in the pit for the installation of the bolts was:-

Drilling: Initially all hole boring was executed using a Consolidated Pneumatic compressed air rotary drilling machine (type 327S) but due to the increasing thickness of an ironstone band about 3 feet above roof level, the rotary machine had to be replaced by an Atlas percussive machine, mounted on a stopper leg.

Bolt Installation: When the rotary drill was in use the wedge bolts were driven using a modified C.P. concrete breaker (type 11S). The use of the percussive machine eliminated the need for the breaker as the bolts could be driven with the drilling machine fitted with a suitable 'dolly'. A compressed air impact wrench was used for installing the shell bolts. The wedge and sleeve bolts were set using the patent hydraulic setting device supplied by Bayliss, Jones and Bayliss.

Tensioning of Bolts: The initial and subsequent tightenings of all bolts were done by means of a C.P. impact wrench (type 36S).

APPARATUS USED IN THE TESTS

(a) Measurement of Bolt Tension

The variation of bolt tension as the face advanced was recorded using electrical resistance strain gauges. Several workers including Middendorf (C16), Verdet (C17) and Tincelin (C18) have used pressure cells - either hydraulic or strain gauge - placed between the roof and

the bearing plate to measure variation in bolt load. This method, although attractive from an economics viewpoint (the cells can be re-used), has the disadvantage that the reaction of the bolts fitted with cells may be appreciably different from normal bolts without cells (compare with measurement of prop load (C19)). To eliminate this variable, the method chosen was to fit strain gauges directly on several standard bolts and calibrate them in tension in the laboratory before installing them underground.

The bolts were thoroughly cleaned and the gauges fixed as specified by the suppliers in their manual (C21). Exceptional care was taken during the curing of the gauges with infra-red lamps to ensure good adhesion and eliminate the effects of "zero-shift" after calibration.

American investigators (C20) have used strain gauges for bolt load measurement with a "double bridge" circuit, i.e. a bridge formed with gauges on the strained material as well as the measuring bridge. This arrangement claims to offset the variation of contact resistance in the gauge leads and any bending effects on the bolt. However, a "control bolt", i.e. a bolt fitted with gauges in the normal way and left underground for some time, showed that the effect of variation in contact resistance was so small that it was considered unnecessary to use a "double bridge" circuit, provided care was taken to clean the connections and bridge terminals. The method of fixing the gauges is shown in Figs. 3C and 4C.

In order to measure the effect of drift or "zero shift" of the gauges a bolt, fitted with gauges, was tensioned up in a pipe, and placed underground in the same conditions as the measuring bolts. Readings of the bolt tension taken at regular intervals remained constant, indicating that the curing and protection of the gauges was adequate for underground conditions. The arrangement is shown in Plate I C.

Due to the humid atmosphere underground, and the possibility of encountering acid mine water, great care had to be taken in the protection of the gauges. Furthermore the likelihood of mechanical damage due to the rough handling inevitable underground had to be allowed for in the gauge protection. The methods used were:-

(i) Slot and Wedge Bolts - Several coats of micro-crystalline wax were applied over the gauges and the bolt within the notches. The wax was applied when the bolt was warm - using infra-red lamps - to permit the wax and bolt to cool together and so reduce the tendency for the wax to flake off. A rubber sleeve was then drawn over the waxed area and sealed to the bolt with Bostik 252 compound. The sleeve was coated with latex rubber solution to seal any pinholes. Finally, a polythene sleeve was drawn over the entire gauge assembly to protect it from acid water (if present).

(ii) Expansion Shell Bolts - Since the bolts were only $\frac{3}{4}$ inch diameter it was impracticable to place the compensating gauges around

ACTIVE GAUGES

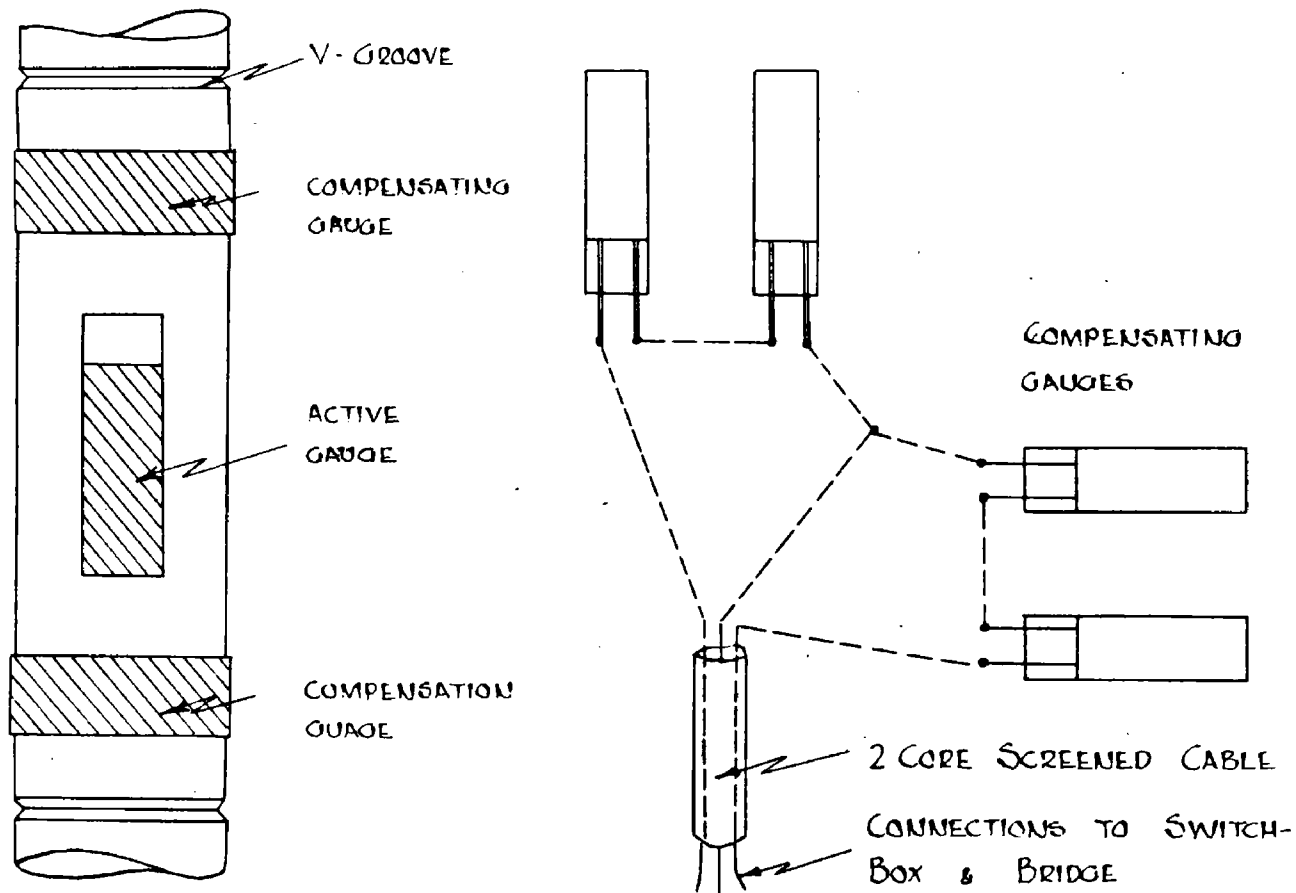


FIG 3C WEDGE BOLTS

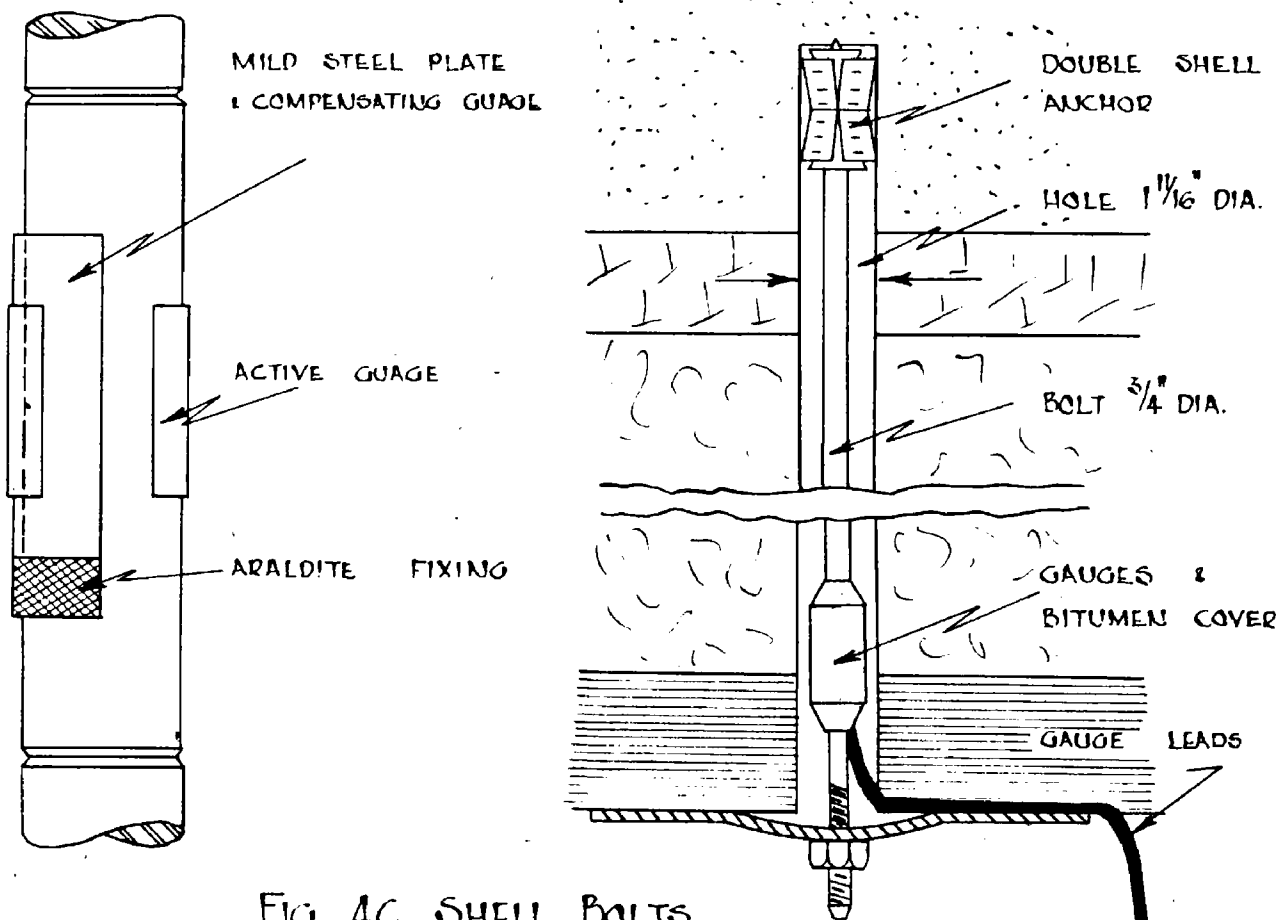


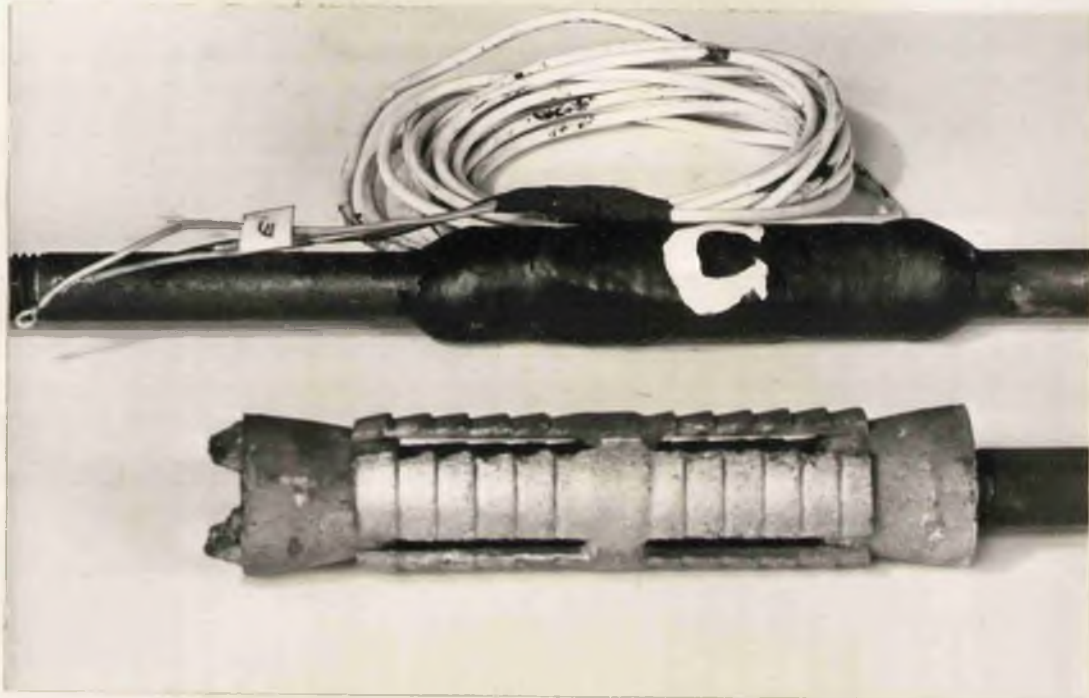
FIG. 4C SHELL BOLTS

PLATE IX



Control Bolt to Check Drift of Gauges

PLATE IIC



Shows the protective covering for the gauges fitted to a roof bolt and the "Shotts" type double-cone expansion shell.

the periphery of the bolt (as for the slot and wedge type). A mild steel plate with the same physical properties as the bolt steel, on which the compensating gauge was mounted longitudinally, was fitted to the bolt as shown in Fig. 4C. Since the plate is in contact with the bolt, temperature variations are transmitted to the gauge, but as it is fixed (by Araldite) to the bolt at one point only, no strain is imposed on the plate when the bolt is loaded. To accommodate the expansion shells a 1.11/16 inch diameter hole was required but since the bolt steel is only $\frac{3}{4}$ inch diameter there was considerable "play" of the bolt in the hole during installation. It appeared therefore, if the gauges were protected in the same way as for the wedge bolts there would be a danger of damage to the gauge elements by impact against the sides of the hole. Consequently, after waxing as before, the bolt was bound with varnished tape to "fill out" the protection. Finally a $\frac{1}{4}$ inch thick coat of bitumen was applied over the tape to withstand any knocks during installation. The arrangement is shown in Fig. 4C and Plate II C.

(b) Strain Bridge

Phillips direct reading bridge (GM5536) and ten-channel switching unit (GM5545) was used for all strain measurements underground. The electrical supply to No.1 South District is direct current and so a small motor-generator lighting unit was utilised to give an A.C. supply

of 110 volts for feeding the measuring bridge. A 5-core T.R.S. drill cable supplied the power from the lighting unit to the bridge. Plate III C shows the instruments connected up ready for use underground.

(c) Torque Meters

Two types of torque meter were used. One meter measured the maximum torque applied to the nut at any instant, and the other meter was of the spring-loaded type which when set to a pre-determined value would slip and so no further torque could be applied to the nut.

(d) Anchorage Testing Equipment

Pulling tests were made using a Gullick hydraulic device (borrowed from Scottish Division, National Coal Board). It consists of a hydraulic unit $3\frac{1}{2}$ inches diameter and $9\frac{1}{2}$ inches long, through which a $1\frac{1}{2}$ inch diameter hole is bored to take the "strain bar" which is tapped at one end to screw on to the bolt under test. The other end of the strain bar is the same diameter as the main unit, to take the thrust from the eight separate rams, each $\frac{3}{8}$ inch diameter, contained in the outer rim of the main unit. Hydraulic pressure is supplied by a hand-operated pump, capable of exerting a thrust of 16 tons on the bolt. Strain bars are available for use with 1 inch or $\frac{3}{4}$ inch diameter bolts. The apparatus is similar to that used by Wright (C22) and the American investigators.

The movement of the bolt under tension was measured using either a spring-loaded dial gauge fitted on a rod set between the end of the

strain bar and the floor, or by a telescopic tube fixed in a tripod stand, and bearing against the bottom of the strain bar. The latter device was used when the bolt "draw" was expected to be quite considerable. Barry, and others (C23) proved that direct measurement methods (as above) are preferable to the measurement of piston displacement.

(e) Measurement of Bed Separation

To enable accurate records of roof convergence and bed separation to be obtained several recorders (Pitt Safety Appliances Co. design) were used. The design of the instruments is similar to that described by Winstanley (C24). The recorders were set up in the same manner as described by Cowan and Sharpe (C25) for the measurement of bed separation; the instruments are shown set up in Plate IV C.

Bed separation was also measured by an optical "stratascope" similar to the one described by Wright and McDonald (C4). This instrument permitted visual examination of the strata being bolted. The design is based on the "Introscope" (C26) used for detecting breaks in shotholes. Details of the construction are shown in Fig. 5C. The instrument consists basically of a 1 inch diameter tube with a front-surfaced mirror, illuminated from behind by a small bulb at the objective end, and a telescope with diagonal eyepiece at the lower end. The eyepiece can be replaced by a modified box camera to permit the photography of bed separation etc. The instrument, fitted with a tripod, is shown in Plate V C, and a photograph taken with the instrument of a crack in a specimen of sandstone is shown in Plate Va C.

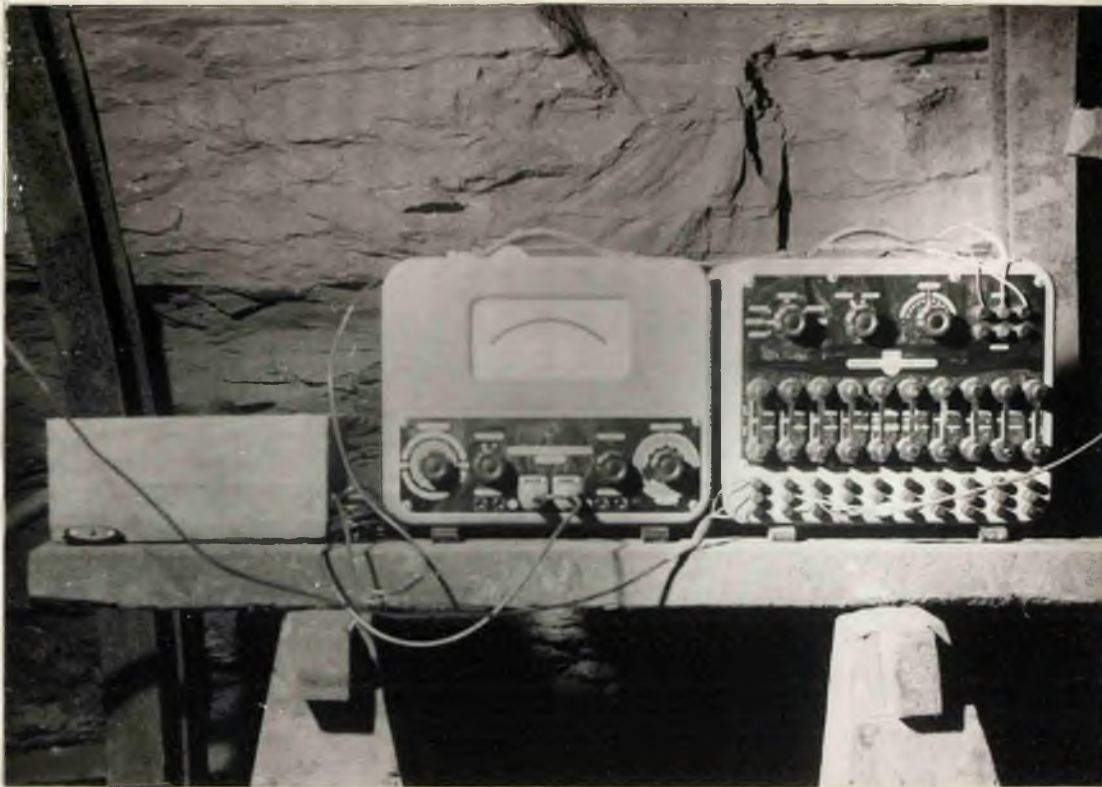


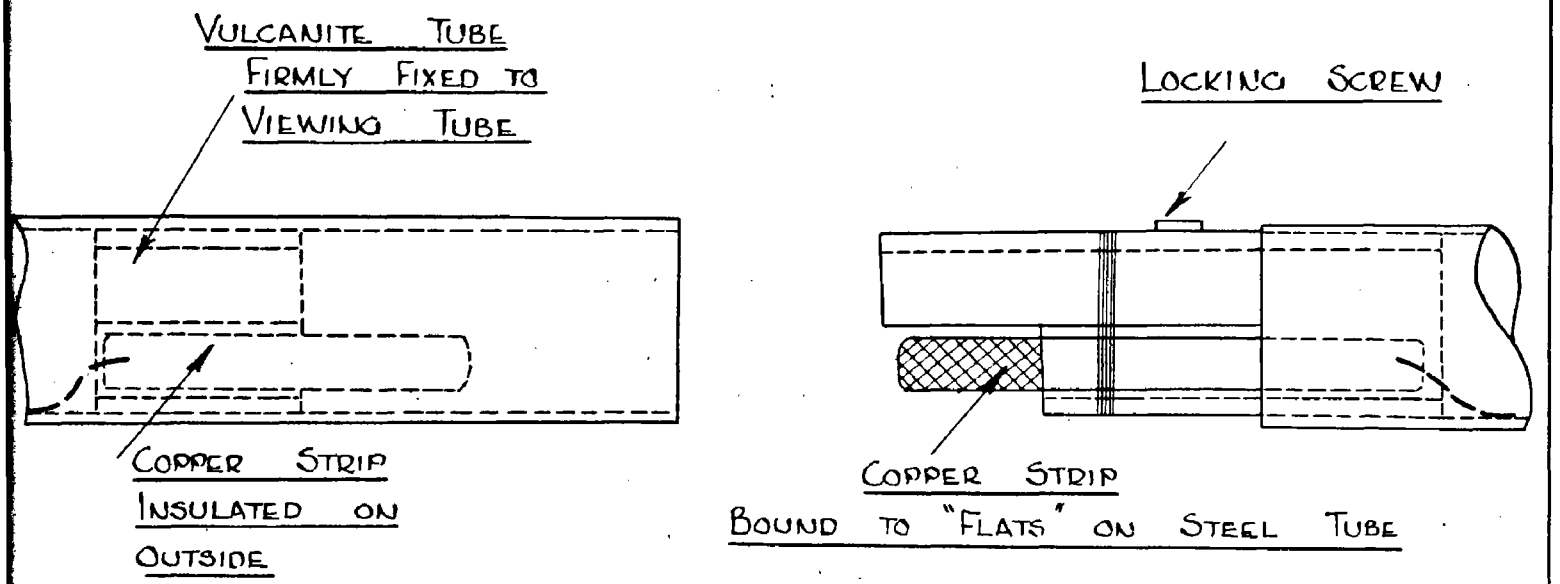
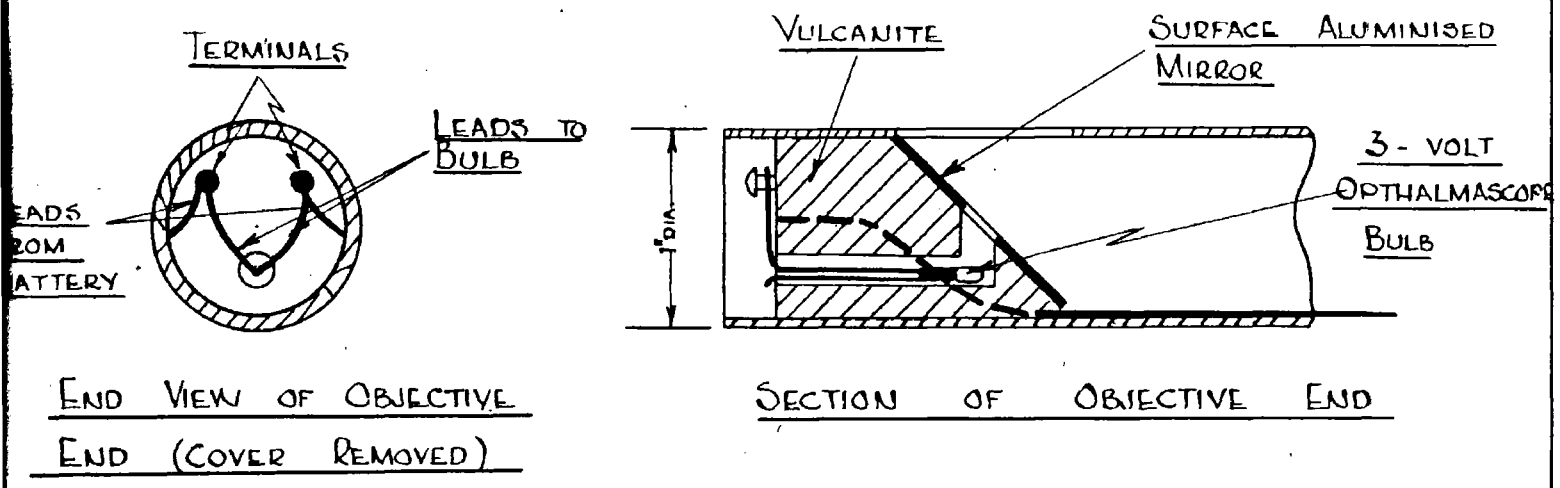
PLATE III C

Strain Bridge in use Underground



PLATE IV C

Convergence Recorders measuring Bed Separation



DETAILS OF ELECTRICAL FITTINGS AT TUBE JOINT (DESIGNED TO MINIMISE BLOCKING OF VIEWING TUBE)

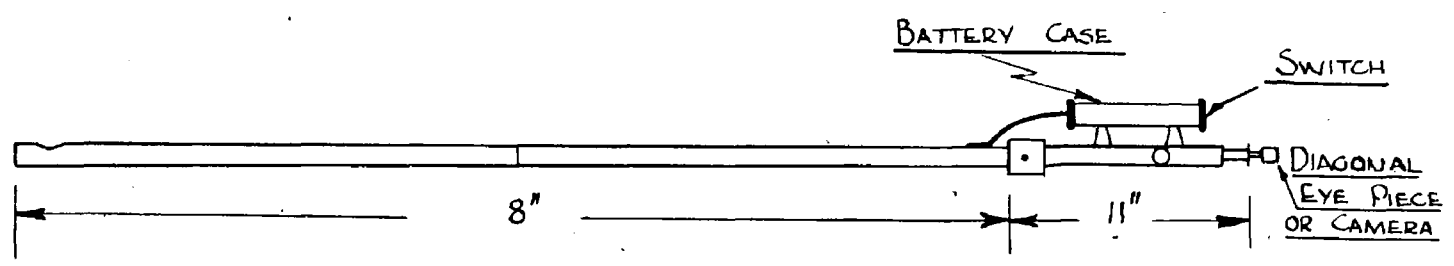


FIG 5C. DESIGN OF STRATASCOPE



PLATE VC

Stratascope



PLATE VaC

Crack in Sandstone Specimen

(f) General Strata Movements

As well as the convergence records and visual examination with the stratascope measuring stations were set up in the roadway. These stations consisted of plugs set in the roof, floor and sides as shown in Fig. 6C. The plugs eliminated erroneous results due to flaking of the sides and provided suitable points for fixing the measuring rod in position.

To permit detailed study of changes in the condition of the roadway, photographs of given sections were taken at regular intervals (027).

(g) Measurement of Rock Strain

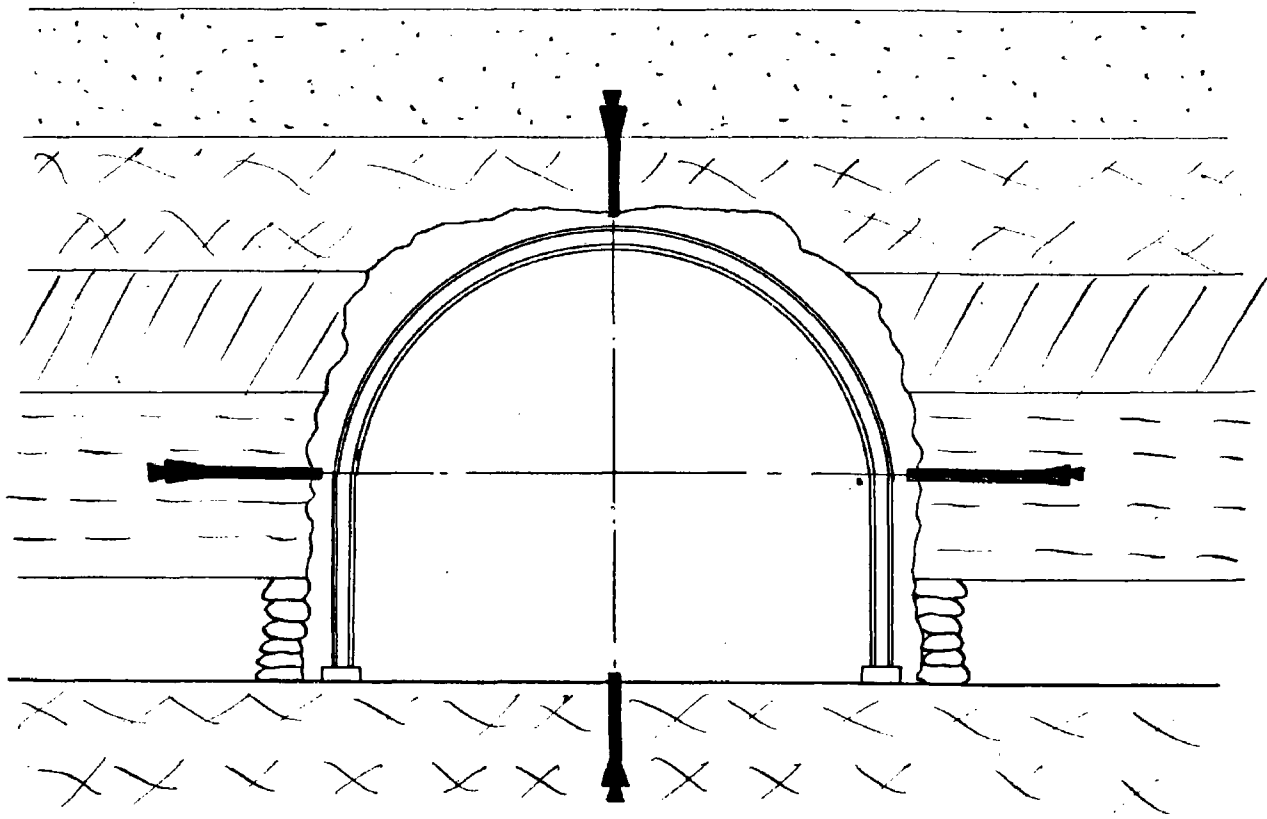
Following the use of electrical resistance strain gauges for the direct measurement of the physical properties of rocks, discussed previously, an attempt was made to measure 'in situ' strains using a similar technique. The method adopted for fixing and protecting the gauges was as follows:-

The selected place was dressed by hand chisel and smoothed with a compressed air rotary grinder. Any surface moisture present was driven off by setting up an infra-red lamp near the zone for 3 to 4 hours. The gauge was then fixed in position using Araldite and left under pressure for 2 hours. The cement was cured by leaving the lamp in position for a further 24 - 30 hours. When the cement matrix was set, a felt pad was placed over the gauge and a rubber cap, fitted with lead wires (vulcanised seal), was placed over the gauge, and sealed to the rock surface with Bostik compound. A small bag of silica gel was sealed under the rubber

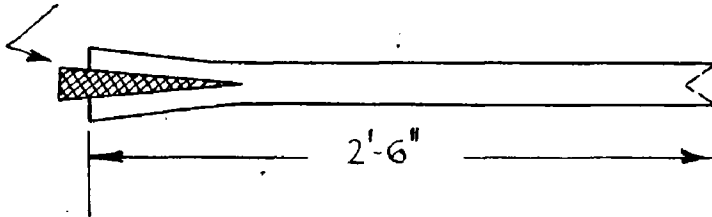
cap to absorb any moisture which may have been trapped. A 60-watt electric bulb was left burning beside the gauges, for the duration of the tests, to minimise the condensation of moisture on the caps and leads. Compensating gauges were similarly mounted on a detached slab of the same rock and placed in the vicinity of the active gauges. The arrangement of the drying lamps and gauges fixed in position are shown in Plates VI C and VII C.

FIG. 6C.

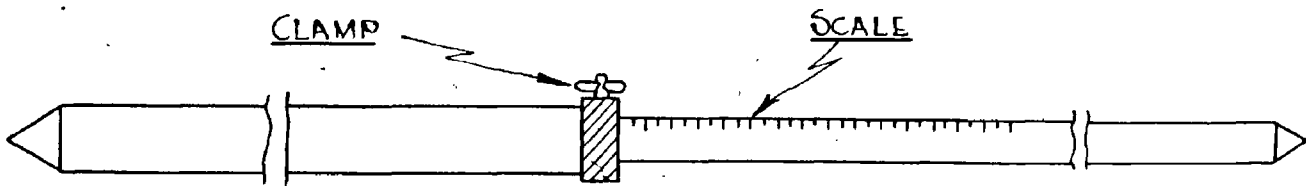
MEASURING STATION



ANCHORING WEDGE



DETAIL OF PLUG.



MEASURING ROD



PLATE VIC

Infra-red Drying Lamp



PLATE VIIC

Strain Gauges on Roof of Roadway

EXPERIMENTAL PROCEDURE

To enable the workmen to become familiar with the drilling equipment and technique of installing the bolts, a short length of roadway was bolted after the erection of the conventional supports. The pattern adopted for the test length was the "3-bolt one" investigated in the photo-elastic experiments (vide ante). Initially all three bolts were installed between the last girder and the ripping lip but it was found that the trimming shots of the following cut usually dislodged some rock in the vicinity of the side bolts so the pattern was modified thus:- the centre bolt was installed as close to the face as possible and the side bolts were installed the following day. It is thought that this method ensures that the roof is bolted effectively as soon as it is exposed.

All bolts were numbered and the supervisor filled in a sketch plan (specimen shown in Fig. 7C) recording the date of installation, setting torque, re-tightenings and any other relevant information.

Since only a limited number of bolts could be fitted with gauges and calibrated in the laboratory, an investigation of the relationship between "applied torque" and "bolt tension" was carried out for all the measuring bolts installed. The method adopted was based on a similar investigation in America (C20) so that a direct comparison of results would be possible.

Values of tension on the measuring bolts were obtained regularly

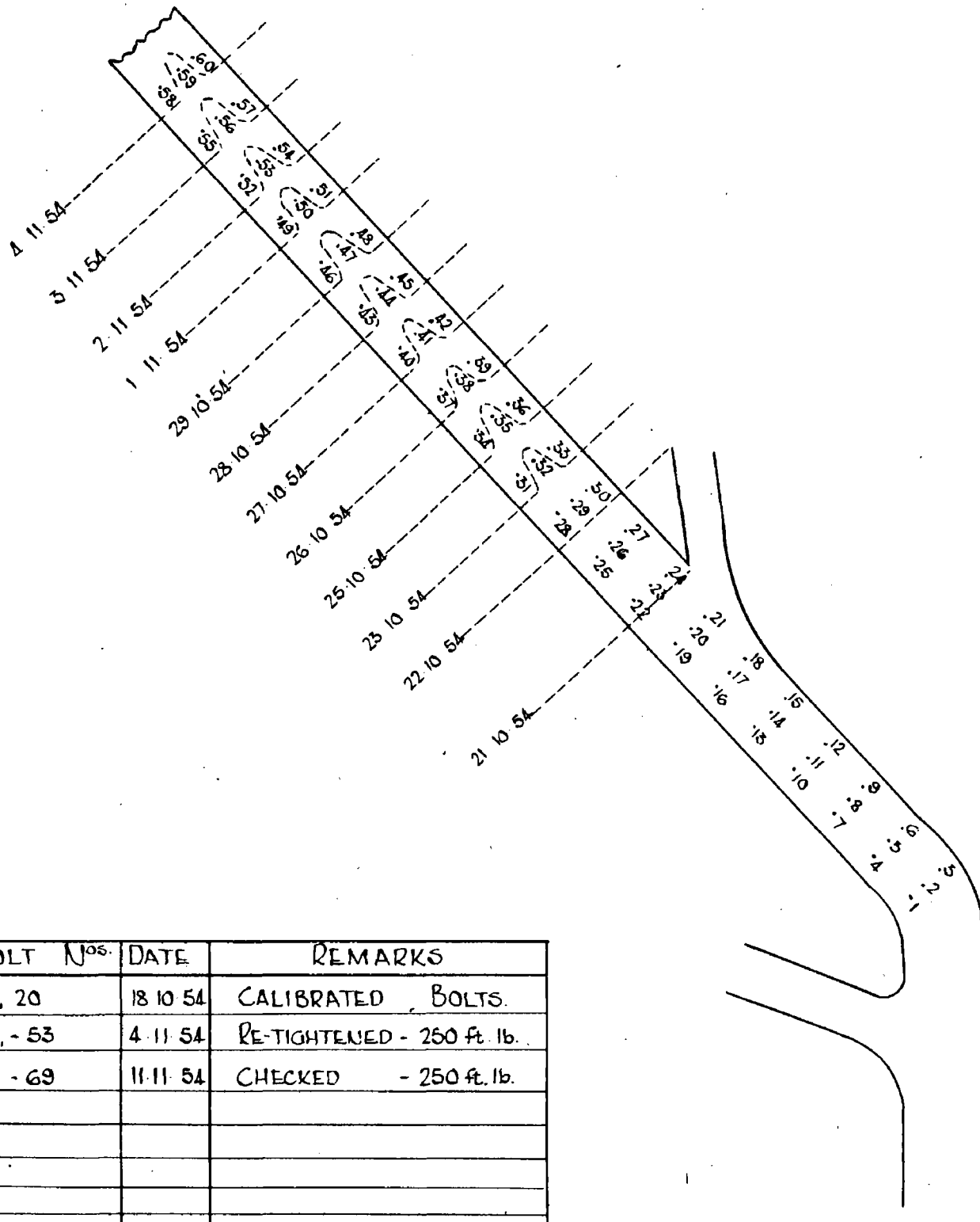
throughout the duration of the tests as well as torque readings on all the bolts installed.

Pull tests to ensure the effectiveness of the bolt anchorages were carried out systematically by means of the hydraulic pulling device. The "draw" of the bolts under tension was also recorded.

Convergence records were obtained for the immediate roof of the seam by setting recorders in the face track and leaving them in the packs. Bed separation between the immediate roof of the roadway and bolt anchorage horizon was also obtained. Horizontal and vertical movements of the strata were found at the measuring stations set up in each test length of the roadway.

Some information regarding the straining of the immediate roof bed between the bolts was obtained from the strain gauges fixed thereto, and changes in the conditions of the bolted and unbolted test lengths were recorded photographically at regular intervals.

FIG.- 7C SUPERVISOR'S RECORD CHART



EXPERIMENTAL RESULTS

Torque-Tension Tests

Slot and Wedge Bolts: The selected bolts fitted with gauges were set up in a hydraulic tensile testing machine in the laboratory. Simultaneous values of the applied load and instrument reading were obtained for loads within the elastic limit of the bolt steel. In this way calibration curves for the measuring bolts were obtained. Specimen calibration charts are shown in Figs. 8C and 9C. This direct method of calibration was preferred to the calculation of bolt load from strain measurements, since it eliminated errors in assuming:-

- (a) the steel for all bolts had exactly similar elastic constants.
- (b) the gauge factor of the strain gauges was fully developed (i.e. perfect adhesion between bolt and gauge).
- (c) zero strain on the compensating gauges.
- (d) the gauges were axially aligned.

The bolts were stored underground at least 48 hours to permit equalisation of the temperature of the bolts and the mine atmosphere. All the calibrated bolts were installed in the normal manner at different parts of the roadway for subsequent use in the 'tension-time' tests. During the initial and any subsequent tensioning of the bolts the applied torque and bolt tension were recorded simultaneously.

The results obtained for five bolts are presented graphically in

in Fig. 10C. Seven bolts were prepared but two were damaged during installation and no reliable results were obtained from them.

Also plotted on Fig. 10C are the linear torque load relationships, found by the method of least squares, for the Northfield tests and similar tests carried out in America (C20).

The empirical relationships derived are:-

(i) Sandstone (U.S.A.)

$$T = 37 + 0.0253P$$

(ii) Shale (U.S.A.)

$$T = 12 + 0.0236P$$

(iii) Combination of (i) and (ii)

$$T = 24 + 0.0255P$$

(iv) Northfield

$$T = 14.24 + 0.0263P$$

where

T = applied torque in ft.lb.

P = bolt tension in lb.

The equation for Northfield can be transposed thus:-

Tension (tons) = $-0.2415 + 0.0169 \times \text{Torque (ft. lb.)}$ which is more suitable for the direct determination of bolt tensions.

Due to the variable strata conditions at Northfield subdivision of the results according to "rock type" was not warranted.

WEDGE BOLT N^o 3 (107)

LOAD	DEF ^{ns}	LOAD	DEF ^{ns}
0.0	-	5.5	6.85
0.5	0.6	6.0	7.5
1.5	1.9	6.5	8.1
2.0	2.45	7.0	8.7
2.5	3.1	7.5	9.3
3.0	3.7	8.0	9.9
3.5	4.35	8.5	10.5
4.0	5.0	9.0	11.1
4.5	5.6		
5.0	6.2		

INSTRUMENT CON.: BLUE
 RED
 GREEN
 DEFLECTION : RIGHT

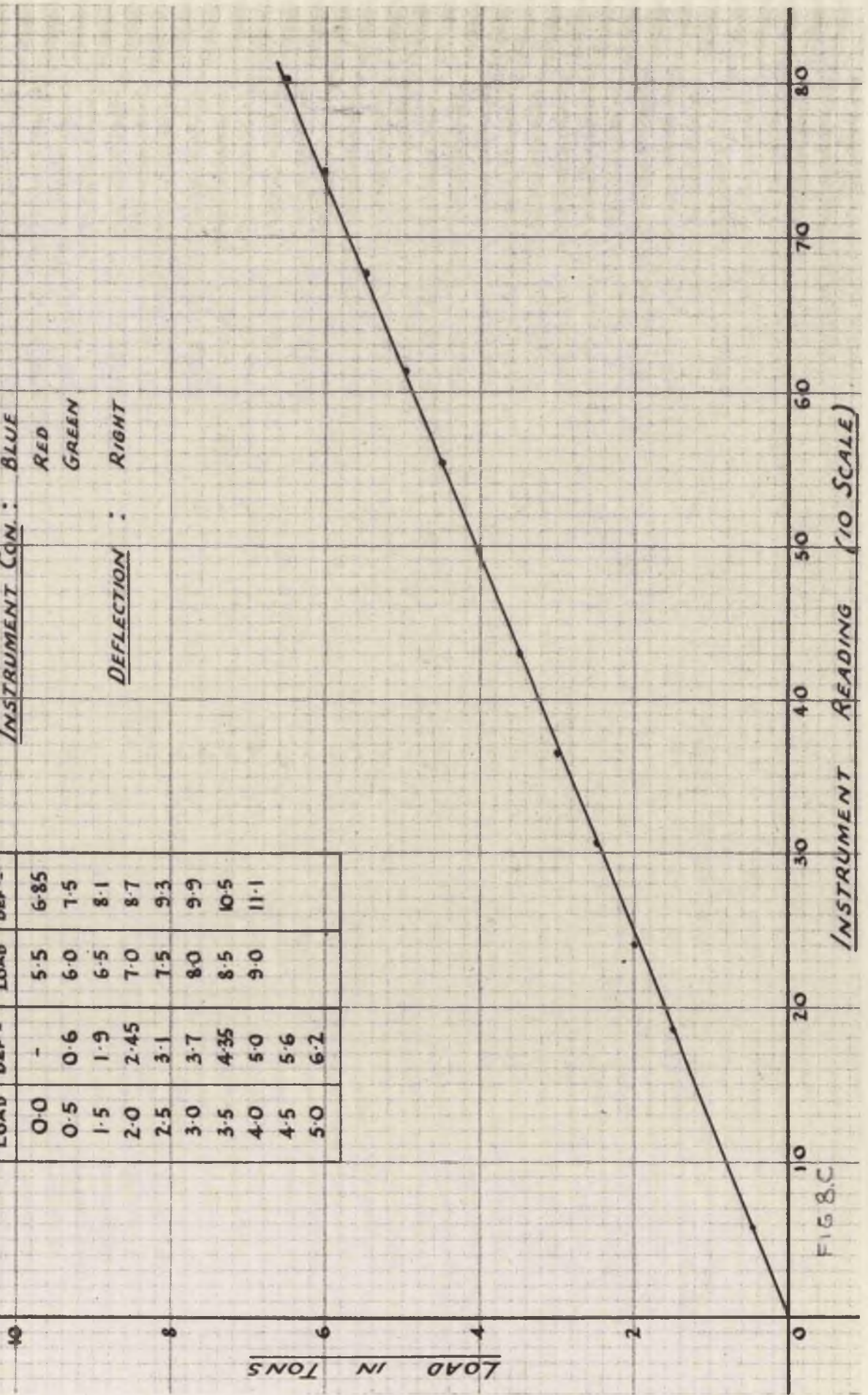


FIG. 8.C

WEDGE BOLT No 6 (89)

INSTRUMENT CON. : BLUE

RED

GREEN

DEFLECTION : LEFT

LOAD	DEFUN.	LOAD	DEFUN.
0.0	-	5.0	5.5
0.5	0.6	5.5	6.1
1.0	1.1	6.0	6.7
1.5	1.7	6.5	7.3
2.0	2.2	7.0	7.8
2.5	2.7	7.5	8.45
3.0	3.3	8.0	9.0
3.5	3.9	8.5	9.7
4.0	4.4		
4.5	4.95		

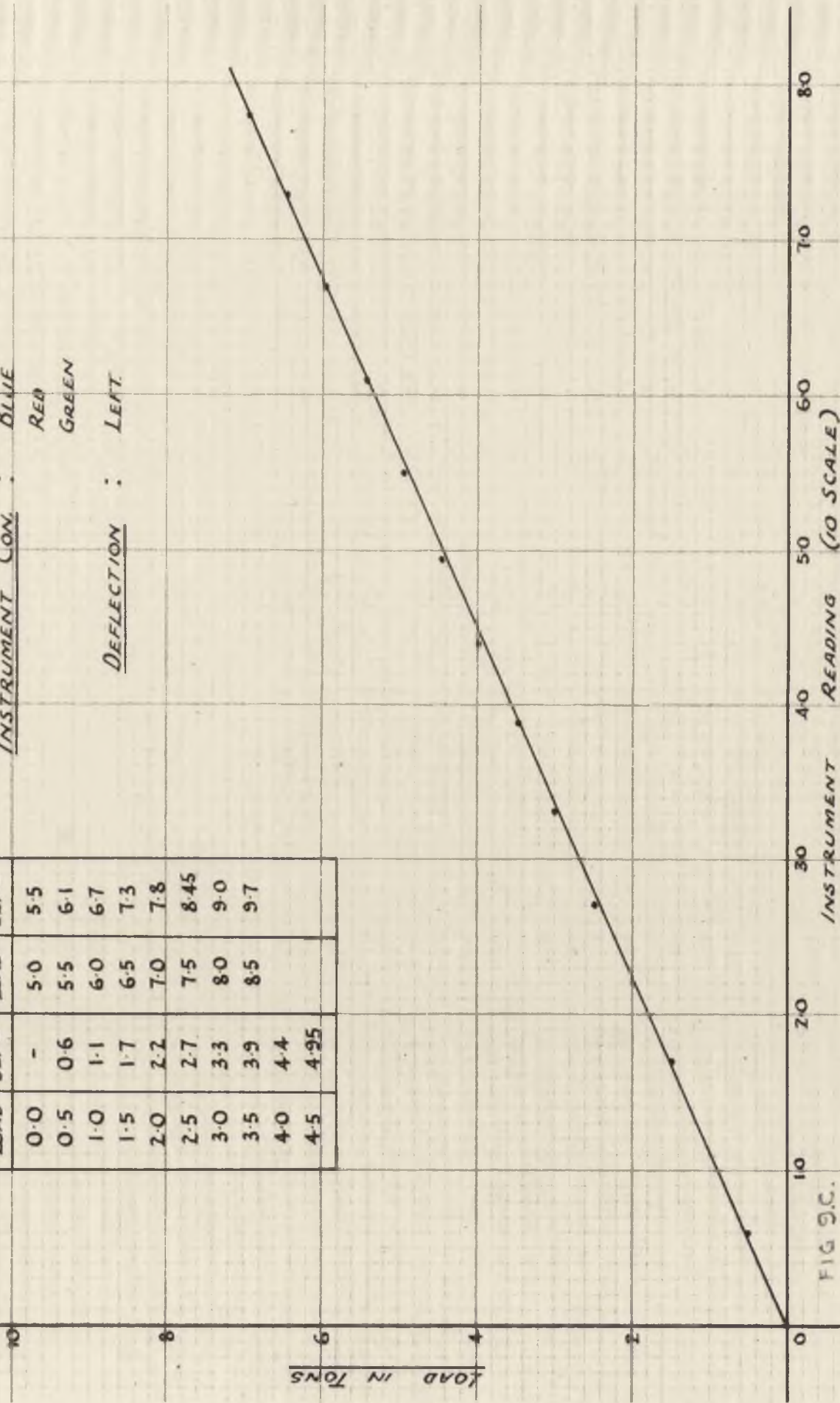


FIG 9C.

TORQUE - LOAD RELATIONSHIP

SLOT & WEDGE BOLTS

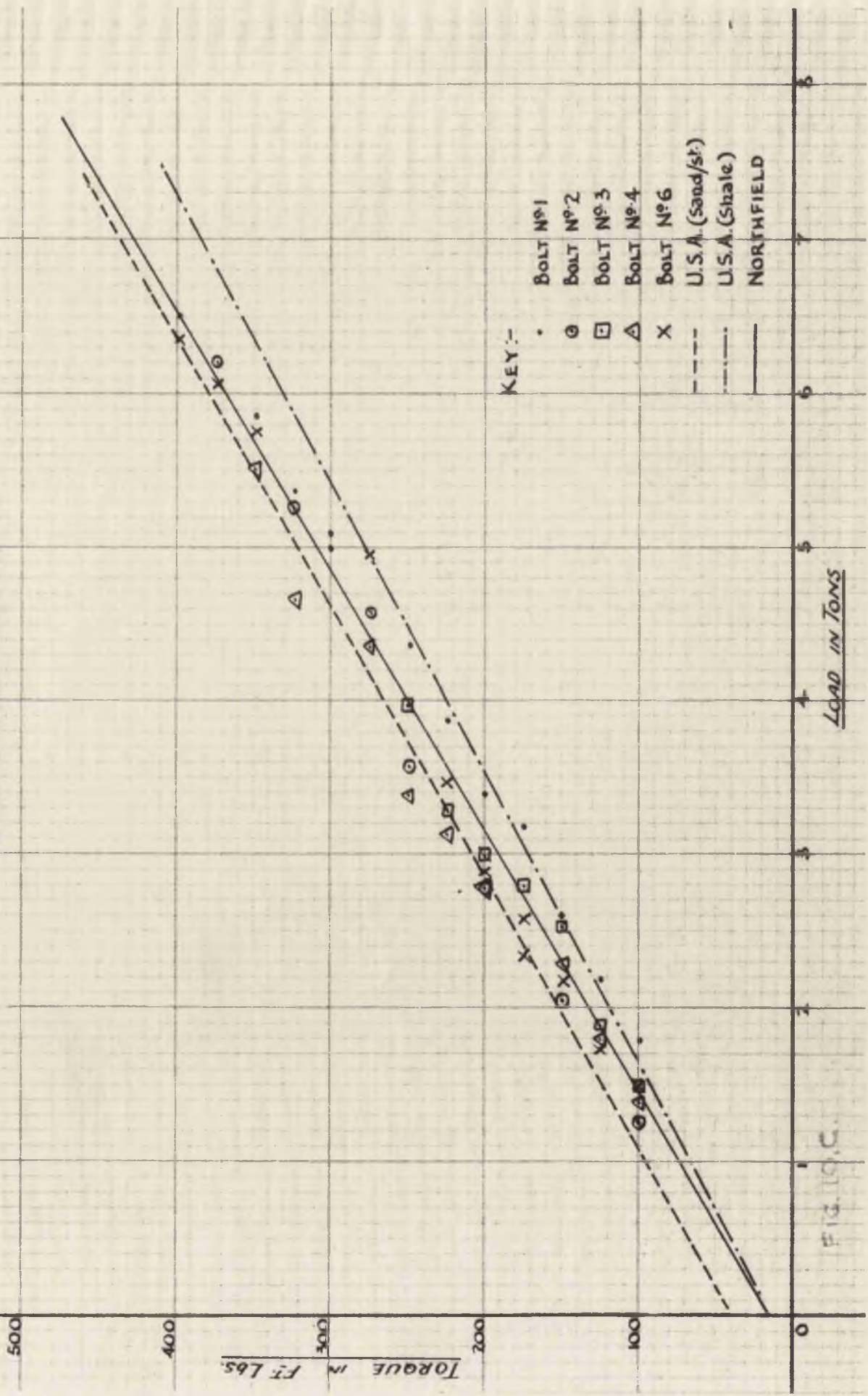


FIG. 10C.

Shell Bolts: No experiments were carried out on the 'torque-tension' relationship for the $\frac{3}{4}$ inch diameter shell bolts.

Barry, Panek and McCormick (C10) have experimented with a wide variety of shell-bolt designs installed both in sandstone and shale. They found that the scatter of the results was wide and consequently many tests were necessary to establish an empirical relationship which would be generally applicable. In view of the findings of the Americans and the fact that the "Shotts type" shell bolt has a limited application, no attempt was made to establish a 'torque-tension' relationship, and consequently only laboratory calibrated bolts fitted with gauges could be used in the 'tension-time' tests (see later).

The relationship: Bolt Load (lb.) = 39.8 x Torque (ft. lb.) for shell bolts established by the Americans could not be employed in the Northfield tests because the formula is only applicable to bolts with forged heads, where the tension in the bolt is modified by the torsional stresses set up when setting the bolt. All shell bolts tested at Northfield had separate nuts and plates.

Variation of Bolt Tension with Time

Slot and Wedge Bolts: When the calibrated bolts were installed underground the variation of bolt tension was recorded regularly as the face advanced. The results are shown graphically in Figs. 11C and 12C where bolt tension v. time is plotted, and since the face advance was regular at 4 feet 6 inches per day the approximate distance between any particular bolt and the face, at any given time, can be computed if required.

It was found that all the bolts installed "relaxed", i.e. lost tension after a few days. In order to investigate the effects of this relaxation some of the bolts were re-tightened to their original tension and others were left without any further torque being applied.

To study the effect of the location of the bolts within the pattern, on the "load-time" relationship, the positions of the bolts were varied, viz. -

Bolt No.19 (cal No.2) - side bolt

Bolt No.20 (cal No.4) - centre bolt

Bolts Nos. 89, 101 &
110 - centre bolts

Due to damage of the lead wire by blasting it was not possible to obtain tension measurements for Bolt No.20 after 24th November, 1954, but regular torque measurements were made and the bolt tension computed from the relationship found earlier.

Shell Bolts: The variation of bolt tension with time was

recorded as for the wedge bolts. The bolts were calibrated in the laboratory in a hydraulic testing machine. Typical calibration curves are shown in Figs. 13C and 14C. Five tons was the maximum load applied during the calibration to preclude the possibility of overstraining the bolts.

All the measuring bolts were 5 feet 6 inches in length except bolt B which was 3 feet. The setting torque applied to all shell bolts was 150 ft. lb. Two bolts were re-tensioned after the initial relaxation and two were left without further tensioning.

Six bolts were calibrated but only the results of bolts A, B, D and F are discussed: bolt C was damaged in transit underground and the lead wires of bolt E were cut by the screw-threads during installation.

The results obtained are shown graphically in Figs. 15C and 16C.

Anchorage Testing

The security of various forms of roof bolt anchoring devices has been studied by many investigators both in America and Europe (C11, C16, C22, C23, C28). Many experiments have been performed to determine the most suitable type of anchor for any particular rock, the optimum initial tension to be applied to each class of bolt, the relationship of torque and anchorage, etc.

However, the tension tests here recorded were mainly to

determine the efficacy of the bolt anchorages used. A few results typical of those obtained are shown in Table No. 2C below. The tension value quoted is the applied tension just prior to the anchor "slipping".

TABLE No.2C

<u>Bolt No.</u>	<u>Type</u>	<u>Applied Tension</u> (tons)	<u>Remarks</u>
49	Slot & wedge	10.7	
72	do.	7.95	
83	do.	11.0	
179	Shell	4.8	Strata very wet - water dripping from roof
192	do.	6.6	
197	do.	8.4	
285	Bayliss, Jones & Bayliss Wedge and sleeve	11.4	
289	do.	12.2	

Note: In many cases much higher tensions than those tabulated above were obtained when the bolt anchor had taken a second grip in the hole.

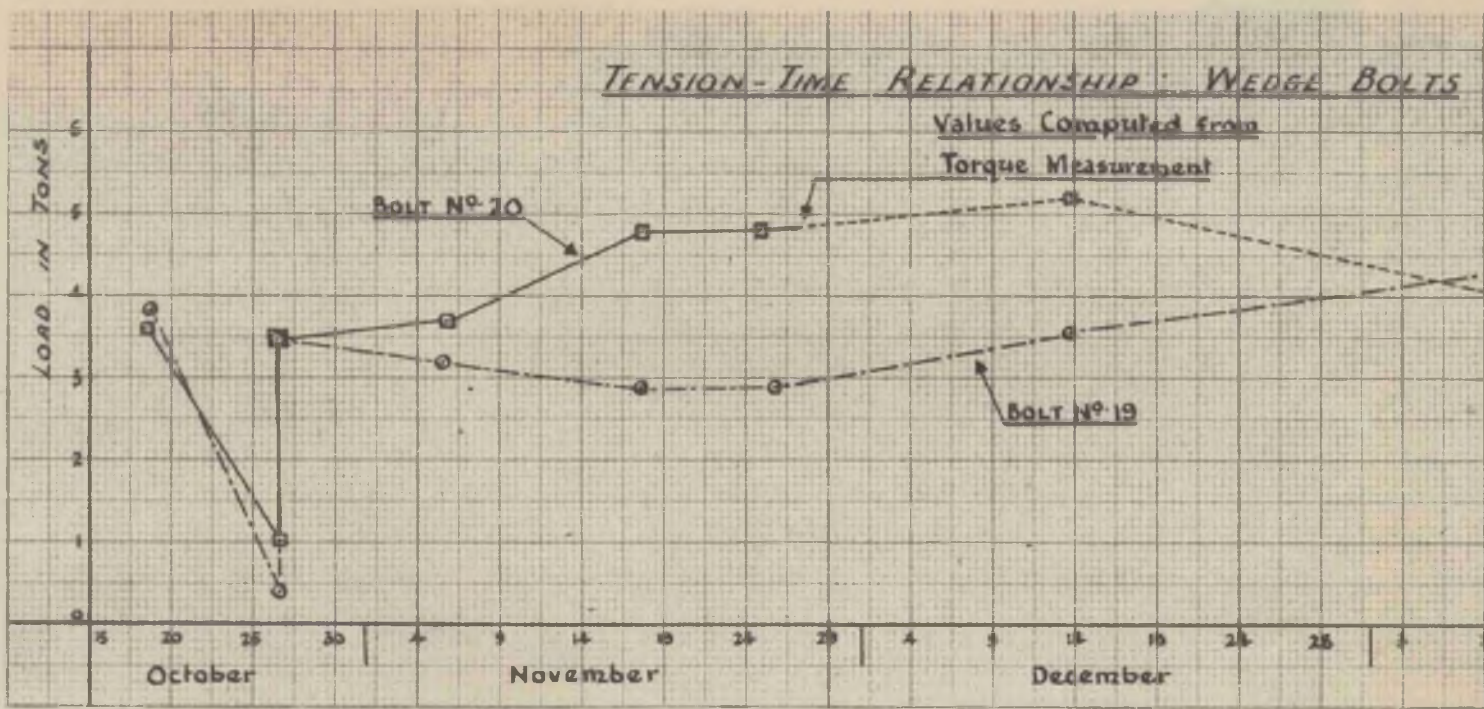


FIG. 11C

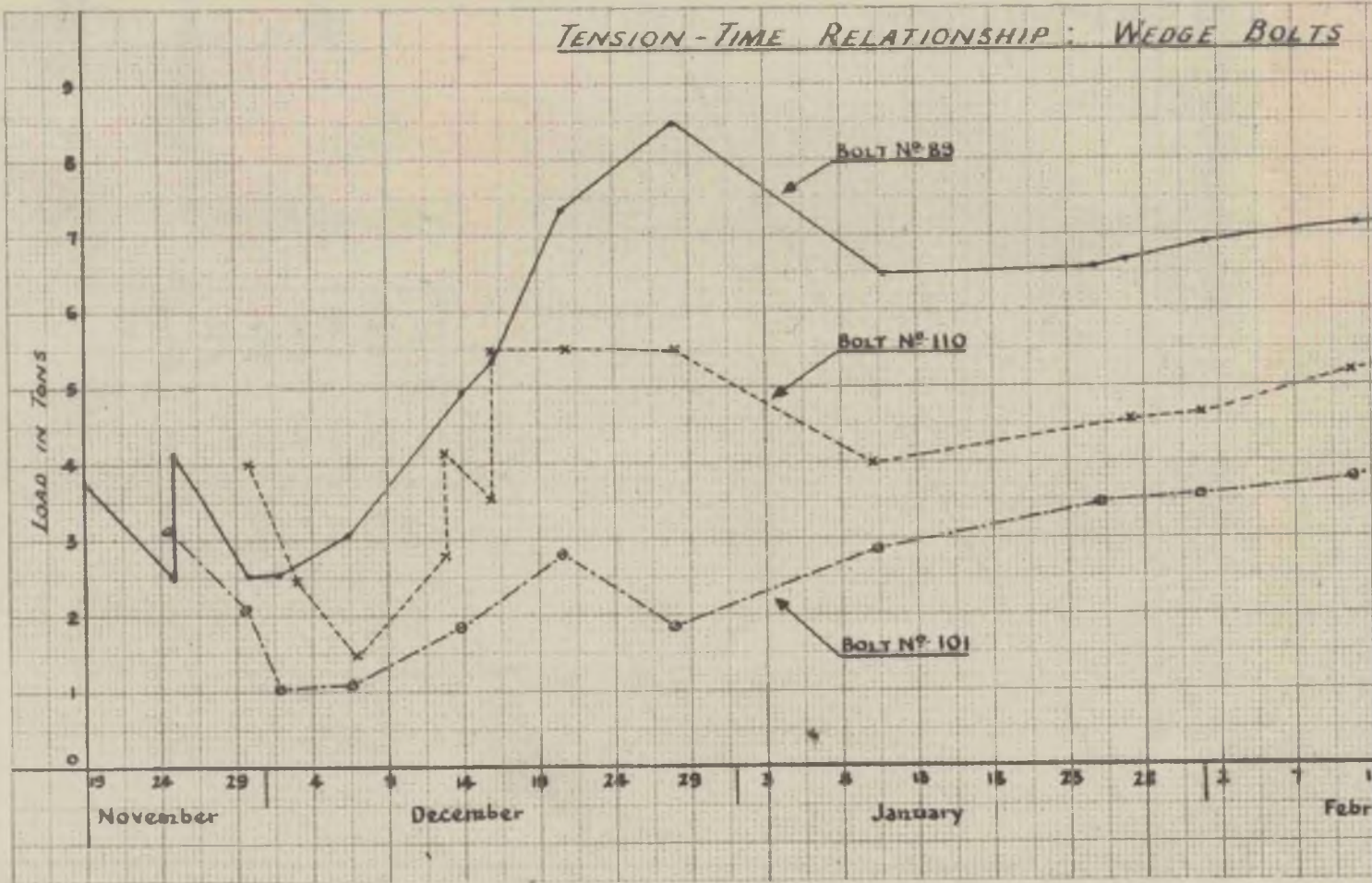


FIG. 12C

SHELL BOLT A

INSTRUMENT CON. : BLACK

BLUE

GREY

DEFLECTION : LEFT

LOAD	DEF ^{IN.}	LOAD	DEF ^{IN.}
0.0	-	3.0	5.0
0.5	0.85	3.5	5.9
1.0	1.7	4.0	6.75
1.5	2.5	4.5	7.55
2.0	3.5	5.0	8.4
2.5	4.2		

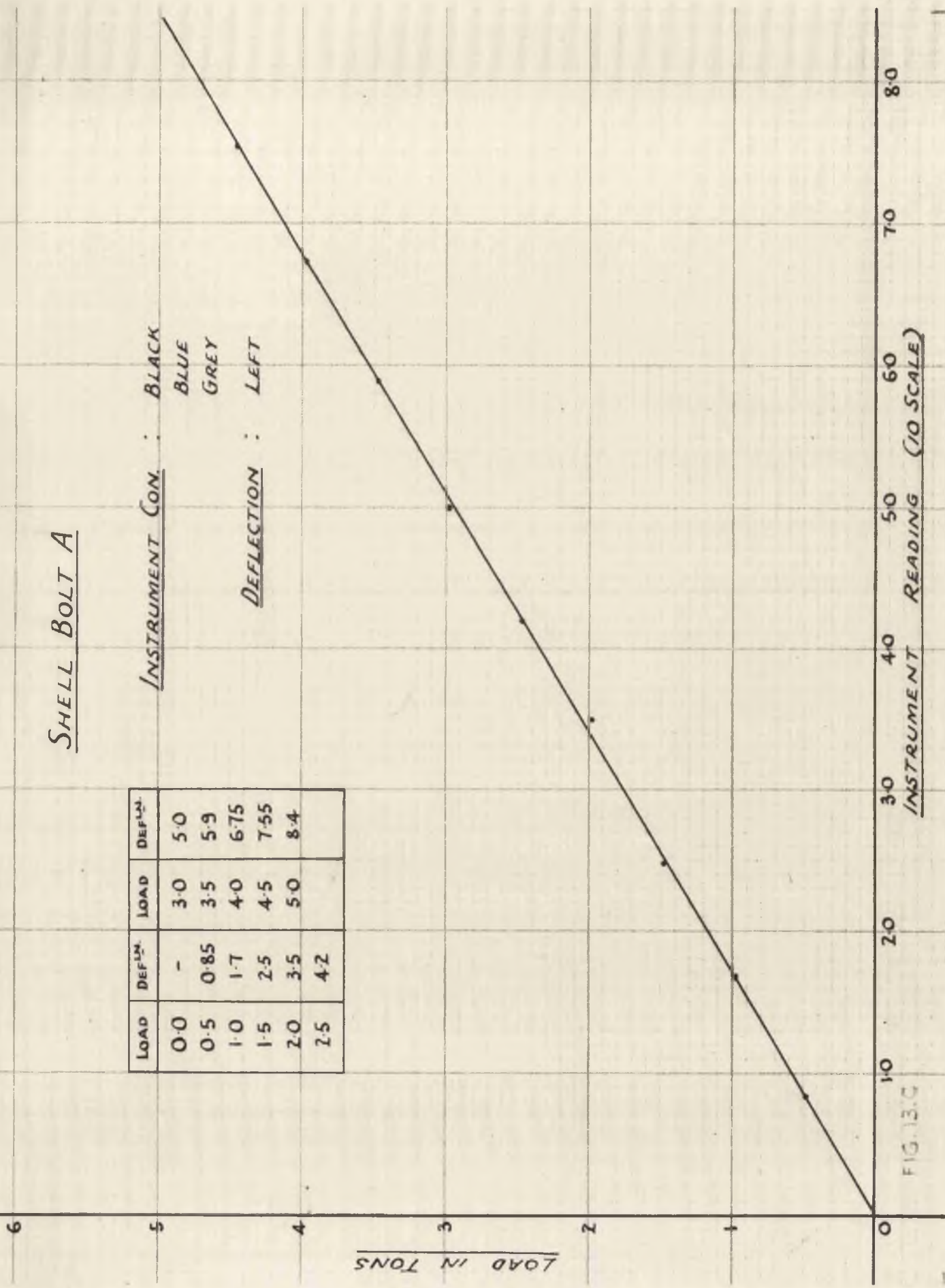


FIG. 13.C

SHELL BOLT E

INSTRUMENT CON. : BLACK

GREEN

GREY

DEFLECTION : RIGHT

LOAD	DEFIN.	LOAD	DEFIN.
0.0	-	3.0	5.6
0.5	0.9	3.5	6.5
1.0	1.85	4.0	7.45
1.5	2.8	4.5	8.35
2.0	3.7	5.0	9.2
2.5	4.65		

LOAD IN TONS

80

70

60

50

40

30

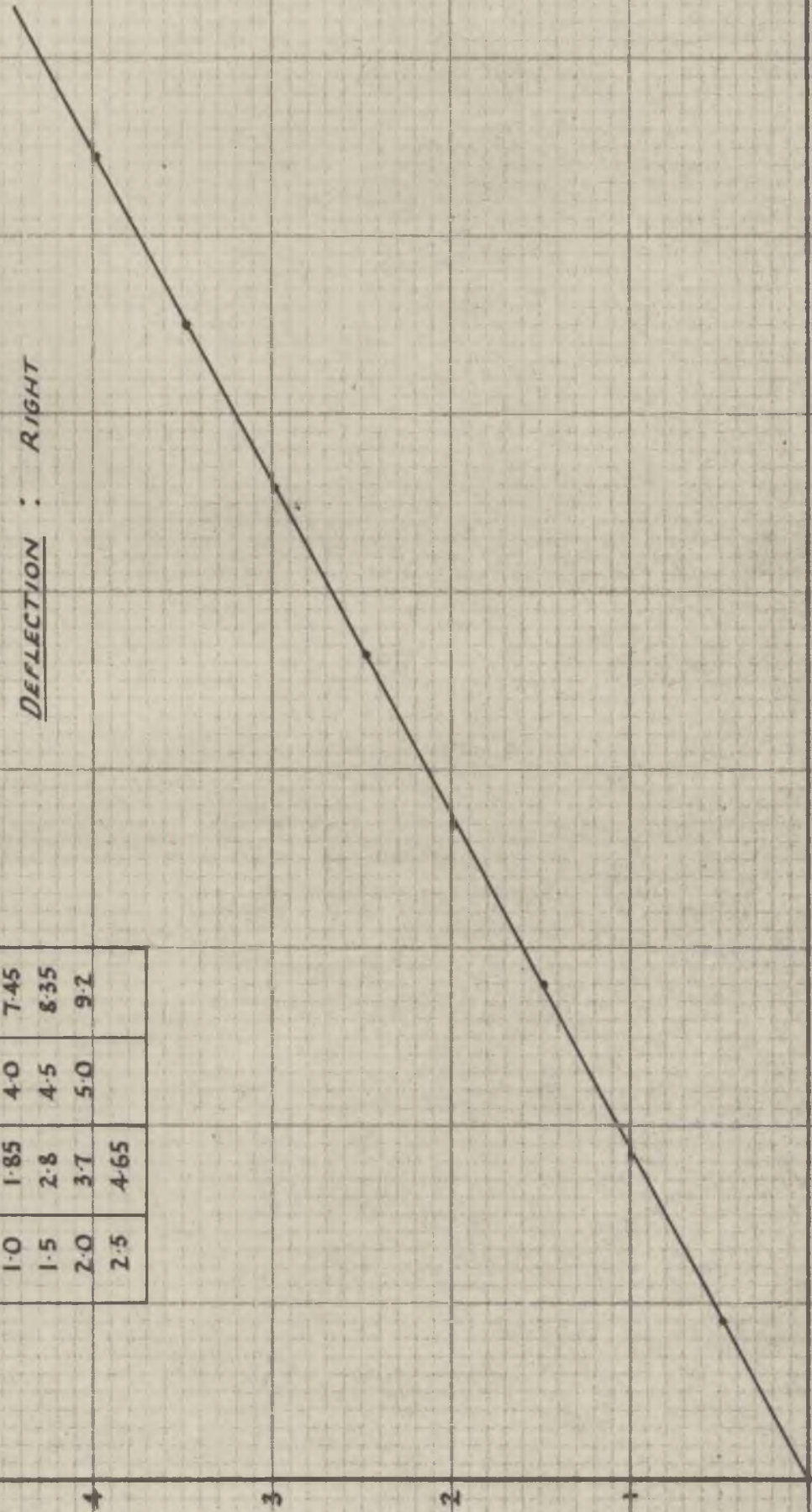
20

10

0

INSTRUMENT READING (10 SCALE)

FIG. 14.C.



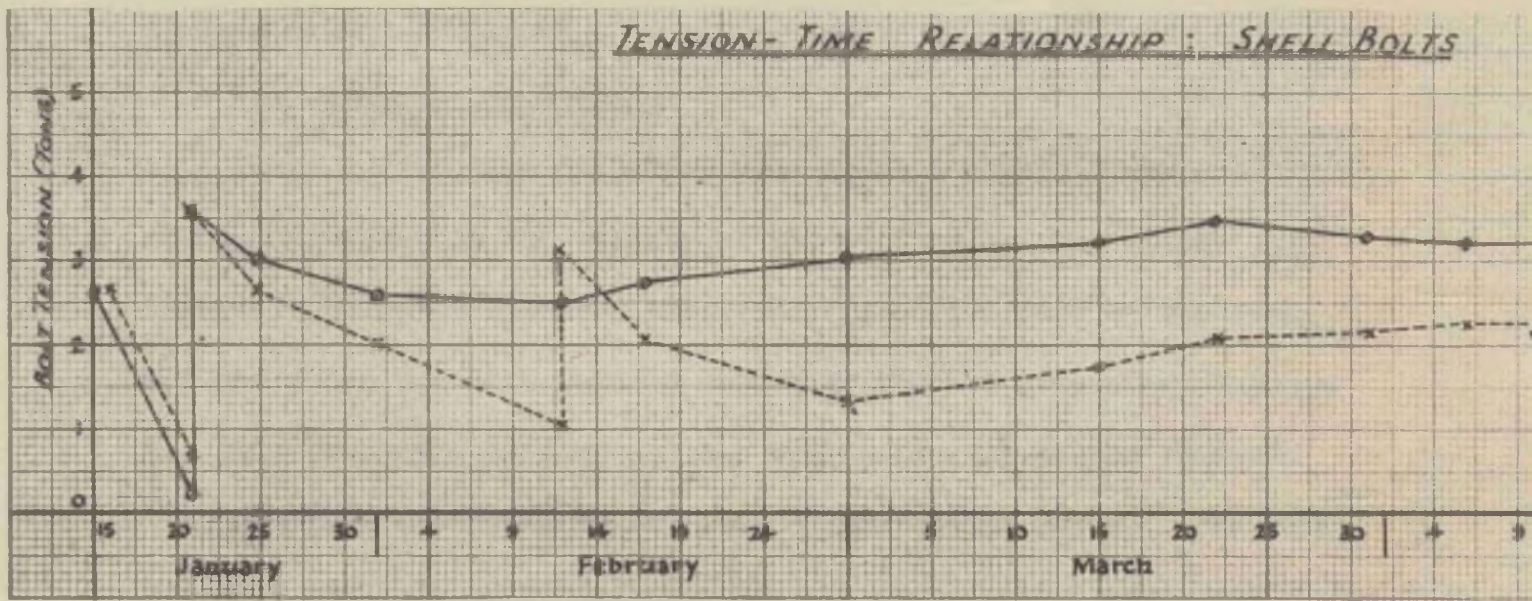


Fig. 15C.

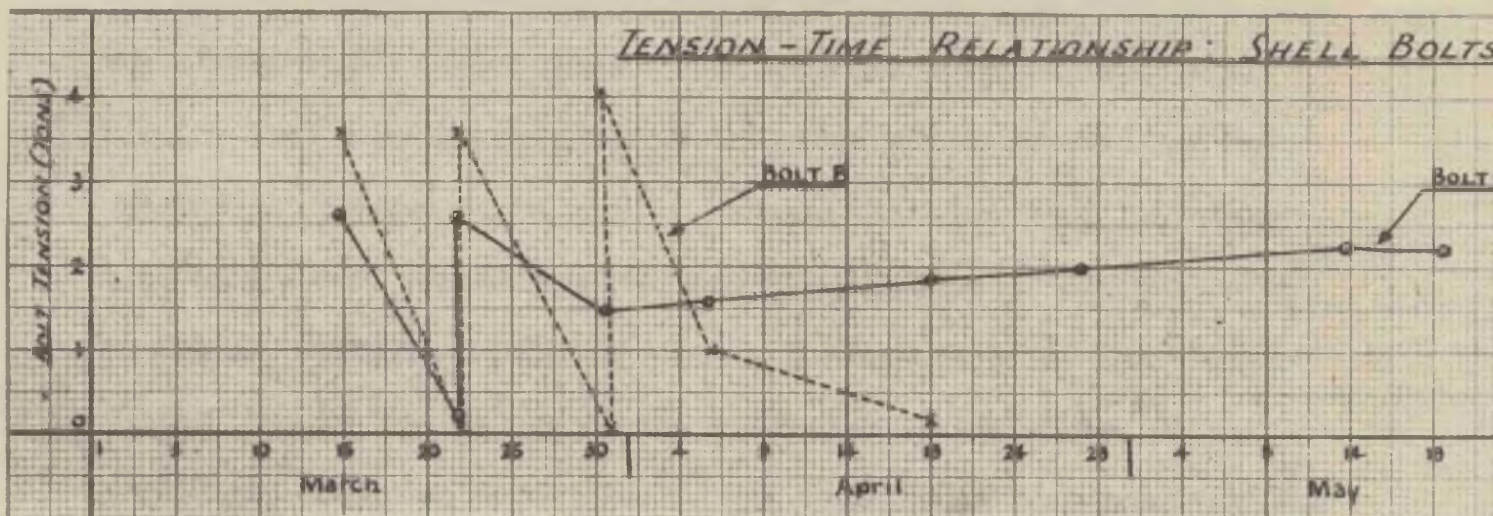


Fig. 16C.

General Strata Movements

(a) Convergence Records

Three convergence recorders were used to obtain records of strata movements in the vicinity of the roadhead. One of the recorders measured the movement of the immediate roof of the seam, and the other two were used to determine the bed separation between the bolt anchorage horizon and the immediate roof of the roadway.

Records were obtained for each of the bolted zones. The total movement and rate of convergence for the steel bolted zones was similar. The roof in the wooden bolted zone lowered slightly more than in the other test lengths. The results obtained in the wedge bolted area are shown in Figs. 17C and 18C.

To supplement the results obtained from the convergence recorders regular visual examinations of the roof bolt holes were made with the stratascope. Separation of the beds was noted close to the ripping lip. In the majority of the examinations carried out bed separation appeared to be greater between the lower roof beds than between the beds remote from the excavation, i.e. the deflection of the strata diminished with increasing distance from the immediate roof. Due to the coating of the inside of the bore-holes with drillings, considerable difficulty was experienced in determining bed separation with the stratascope and consequently no accurate measurements could be made. No clear photographs of separation were obtained using the stratascope underground.

CONVERGENCE RECORDS - WEDGE BOLTED ZONE

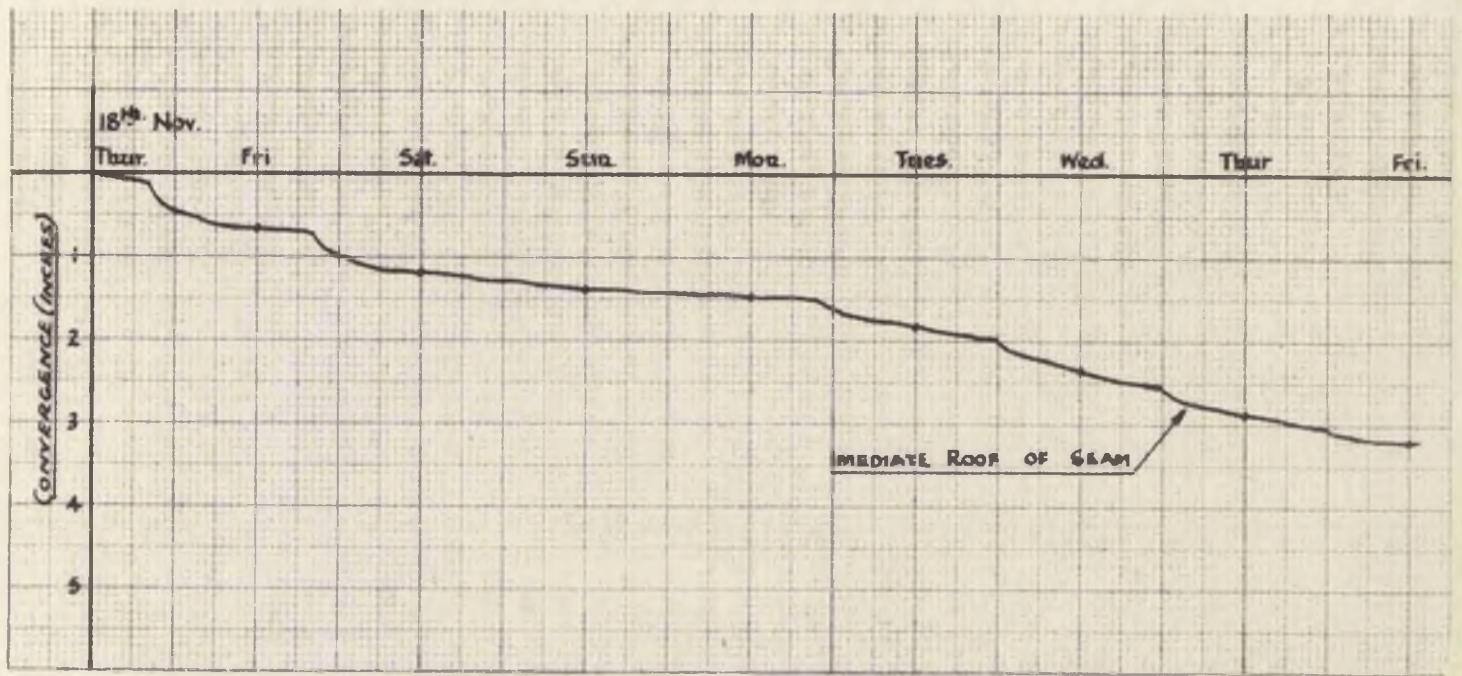


Fig. 17C.

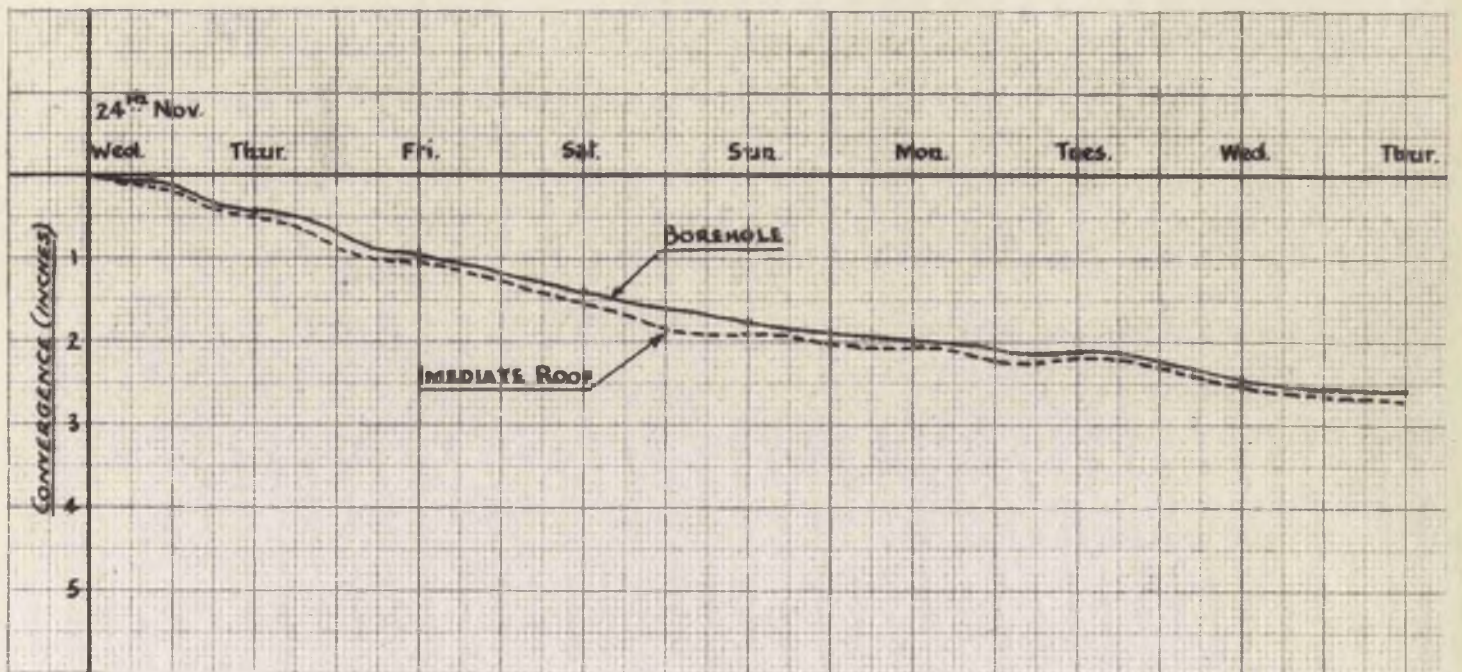


Fig. 18C.

(b) Measuring Stations

A more general impression of the strata movements in the bolted roadway, than provided by the convergence recorders, is obtained from the observations made at the measuring stations. The positions of the stations are shown in the sketch plan (Fig. 19C).

- (i) No.1 Station - in the wedge bolted zone. The results are shown graphically in Fig. 20C.
- (ii) No.2 Station - in the shell bolted zone. The results are shown graphically in Fig. 21C.
- (iii) No.3 Station - in the short length of roadway supported with wooden bolts. The results are shown in Fig. 22C.

To provide a further comparison of the bolted section with a similar length of roadway lined with conventional supports (c.a. girders) only, bolting was stopped on 8th April, 1955. It was intended to establish a further measuring station in the unbolted roadway, but the strata conditions changed completely and no reliable comparative figures could be obtained. The changed strata conditions are clearly illustrated in Plate VIII C, which shows the ripping lip (supports removed) made up entirely of sandstone with some current bedding. The massive sandstone extended several feet above the level of the roadway.

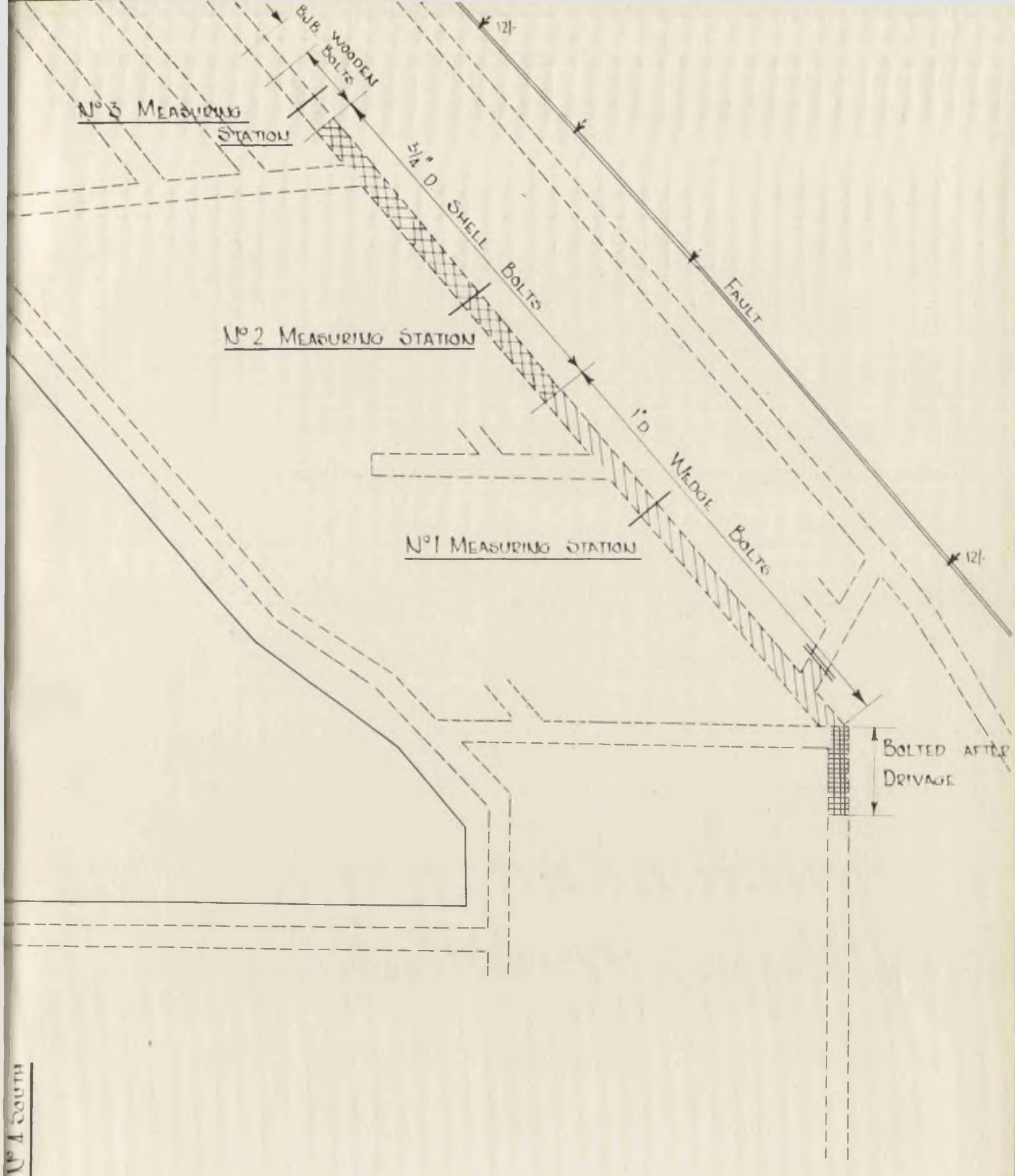


FIG 19C POSITIONS OF MEASURING STATIONS

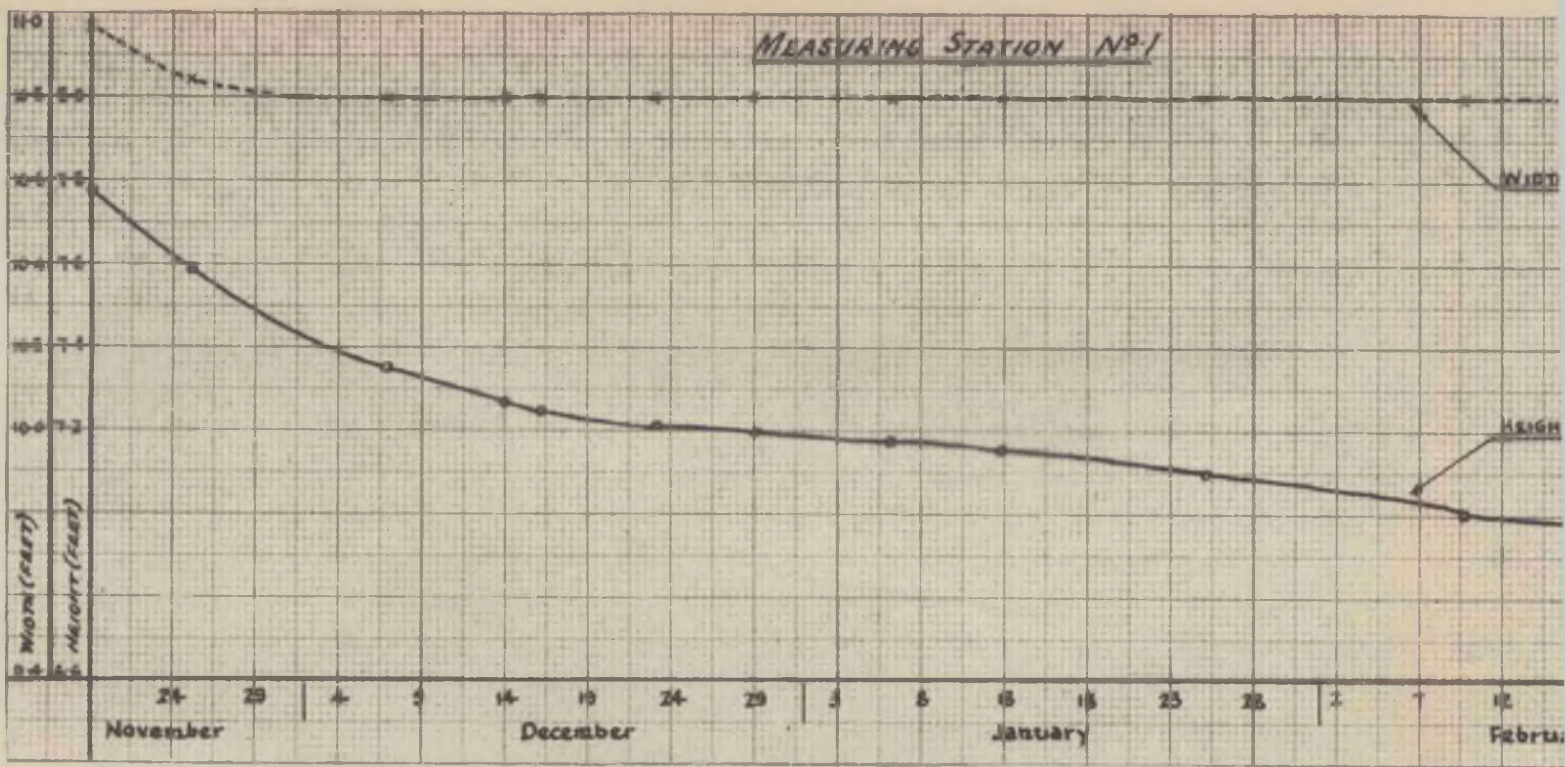


FIG. 20C.

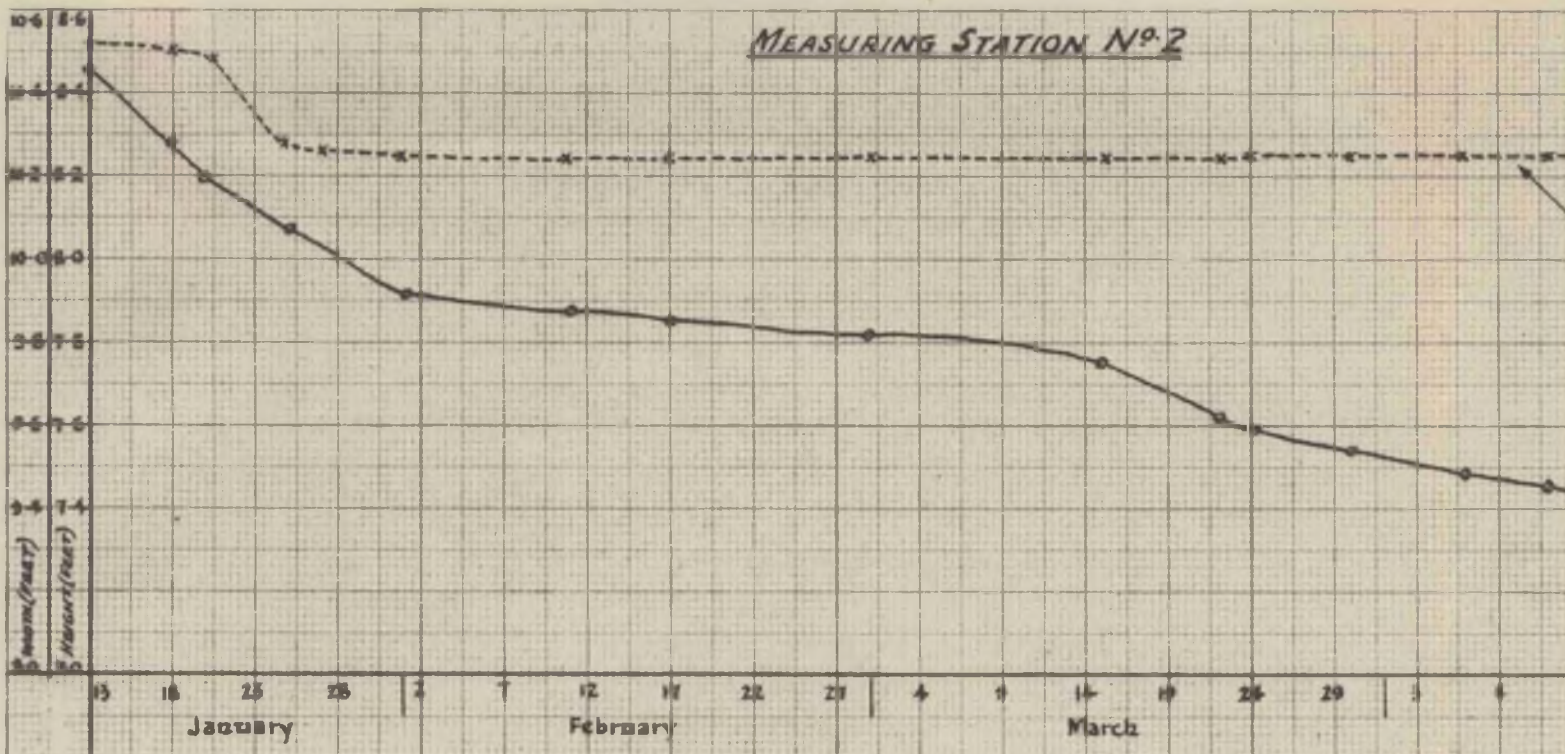


FIG. 21C.

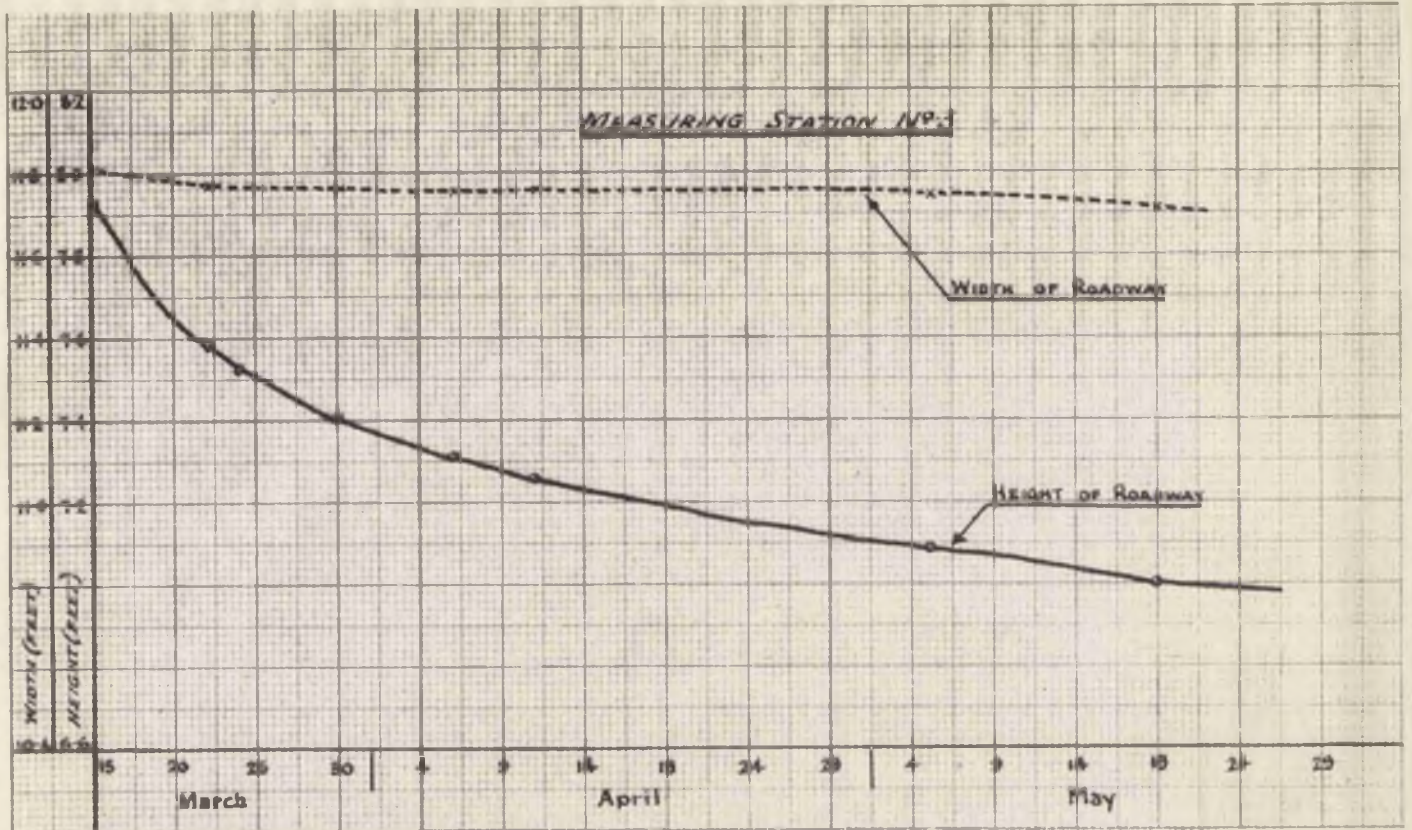


FIG. 22C.

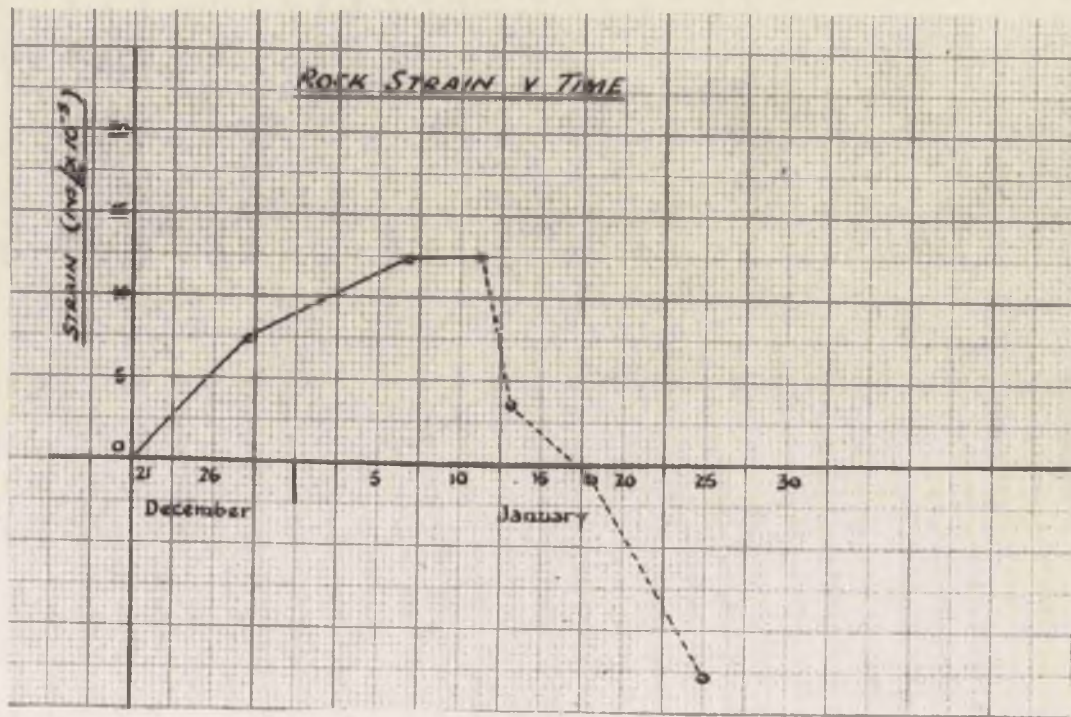
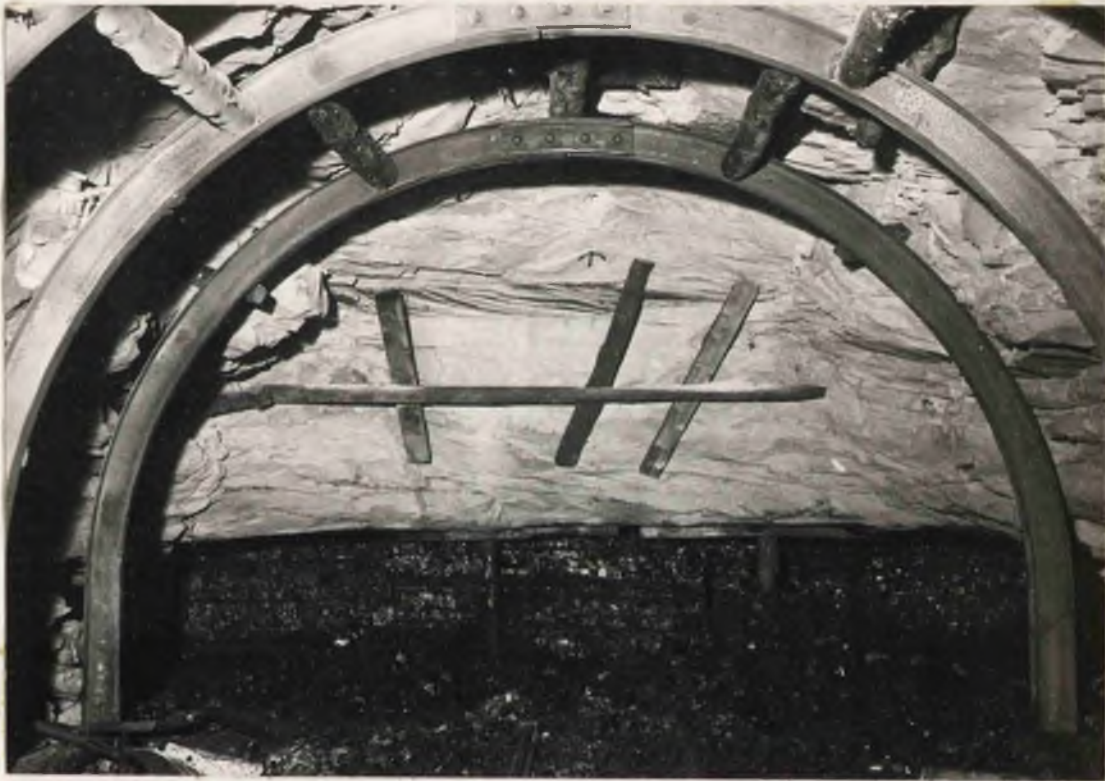


FIG. 23C.

PLATE VIIIIC



Ripping Lip (supports removed) showing marked change in strata conditions. Note the current bedding in the massive sandstone.

(c) Photographic Records

The improvement of roof conditions by the introduction of bolting is clearly shown by comparing the photographs taken in the unbolted length of roadway with those taken in the bolted section after (approximately) the same time had elapsed. The strata conditions were similar in both lengths of roadway.

UNBOLTED SECTION

PLATE IX C



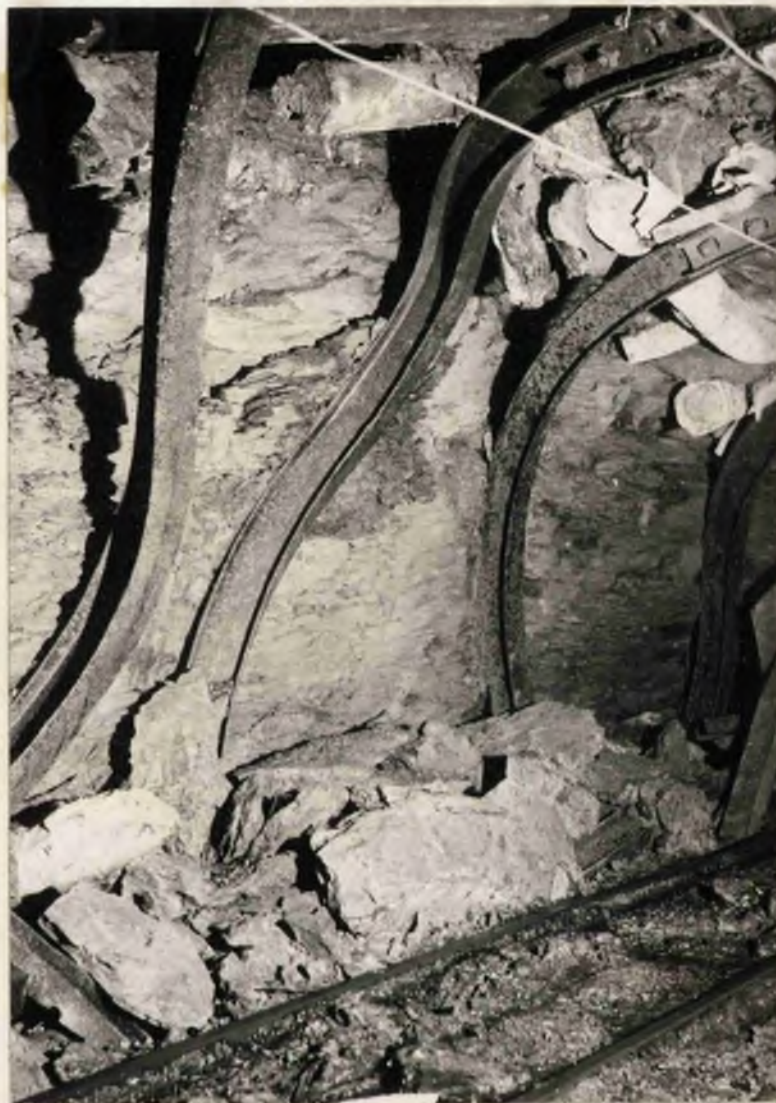
16th March, 1955. This plate shows the conditions in the unbolted roadway. The failure of the immediate roof bed is clearly seen; resulting in large amounts of fallen debris which has to be cleared to the roadsides. Part of the roadway which has been re-ripped can be seen in the background.

PLATE X C.



16th March. 1955. Looking inbye from the re-ripped length towards the unbolted roadway. The excessive roof lowering is clearly seen and also the complete failure of immediate roof over the centre of the excavation - resulting in movement of the sides into the roadway. (Compare this plate with the results obtained in the laboratory plaster model tests later.)

PLATE XI C



14th January, 1955. This plate taken 110 feet inbye from the junction with No.4 South main gate in the unbolted roadway shows the severe distortion of the girders and the amount of loose rock which has fallen from the roof.

BOLTED SECTION

PLATE XII C



14th May, 1955. Looking outbye towards the wedge-bolted section. The girders are not distorted to any extent, and the immediate roof bed has remained intact. Note particularly the absence of fallen rock at the roadsides and the small amount of timber used with the girders.

PLATE XIII C



14th May, 1955. Looking outbye from the shell-bolted section.

PLATE XIV C



23rd December, 1954. Showing wedge bolts with small plates
(installed 11th November, 1954.)

PLATE XV C



14th May, 1954. The immediate roof bed shows no sign of failure and there is no distortion of the girders after five months. The roof has lowered, as the wood block between the girder and the roof is severely crushed.

WOODEN BOLTS

It was not possible to obtain records of the variation of load on the wooden bolts (vide ante), but the following photographs illustrate their behaviour during the three months after installation.

PLATE XVI C



25th February, 1955. Showing three of the wooden bolts about one week after installation.

PLATE XVII C



14th May. 1955. There is no marked breaking-up of the roof between the bolts. The wedges between the plates and the roof show sign of weighting.

Measurement of Rock Strain

Electrical resistance strain gauges were fitted to the immediate roof bed in an attempt to measure the strain developed in the rock with and without roof bolting. (The method used for fixing and protecting the gauges is described under "apparatus"). The active gauges, on the roof, were balanced against similar compensating gauges fixed to a detached slab of rock. The results obtained from gauge No.1 are shown graphically in Fig. 23C.

Gauge No.1 was fixed in position on 21st December, 1954, but the roof in that part of the roadway was first exposed on 4th November, 1954, and consequently the rock would be strained quite considerably before the gauge was located.

Similar results were obtained from gauge No.2. No reliable results were obtained from the third gauge due to a failure in the electrical circuit.

ANALYSIS OF RESULTS

The purpose of the underground investigation was twofold: firstly to find the applications and limitations of the electrical resistance strain gauge equipment for underground work, and secondly to extend the laboratory investigations of roof bolting. From the tests described the following analysis ensues:-

Strain Gauge Apparatus

(i) The Phillips portable strain bridge and switch unit proved to be suitable for use in non-gassy mines but several modifications are required before the instruments can be used in inflammable atmospheres (i.e. Class B mines). The provision of shock-proof cases would facilitate the transport of the instruments inbye.

(ii) The gauges used were capable of recording variations in tension of the roof bolts with sufficient accuracy for the duration of the tests.

(iii) The use of the single bridge circuit for the strain gauges on the bolts was adequate; no effects of variation in contact resistance were recorded.

(iv) The protective coatings applied to the gauges fitted to the bolts and to the rock roof were found to be suitable for the conditions encountered underground.

(v) The results obtained from the gauges fitted on the roof (vide Fig. 23C) show a slight increase in tensile strain of the rock during the three weeks after installation of the gauges. This increase

in strain may have been due to an increase in the load applied to the rock beam or simply the "time-strain" of the rock under the same applied load. At this stage fine hair cracks developed around the gauges (Plate VII C) and successive readings of the gauges showed a continuous decrease in tensile strain which continued below the original zero, indicating that the rock was considerably strained before the gauges were fixed in position.

(vi) Due to the short gauge length (c. 1 inch) of the gauges used for measuring the 'in situ' rock strains any irregularity in the composition of the rock (slip planes, inclusions of carbonaceous matter, above-average particle size, etc.) would materially affect the value of the strain measured. Consequently, for any future investigations the following modifications to the technique are suggested:-

(a) Strain gauges of three or four inch gauge length (i.e. similar to the gauges used in concrete investigations) should be employed to measure average values of the strain in the required direction.

(b) Alternatively, the gauges could be mounted on thin metal bars which can be located on the surface by pins fitting into plugs embedded in the rock face. This method would obviate the failure of the gauges due to flaking of the rock surface and would be useful for averaging the strain over longer gauge lengths.

(c) If possible the gauges should be fitted in position

as soon as the roof is exposed - preferably ahead of the face - to measure the total strain developed in the rock due to the forces induced by mining.

ROOF BOLTING IN LONGWALL ROADWAYS

Torque-Tension Relationship

(i) The calibration curves for wedge bolts Nos. 3 and 6 (Figs. 8C and 9C) are both linear with very little scatter of the experimental results. However the gradient of the line for bolt No.6 is greater than that for bolt No.3, indicating an apparent difference in the modulus of the bolt steel. Thus, it is clear that the method of direct calibration used for all the measuring bolts is preferable to calculation of bolt tension from strain measurements.

(ii) The empirical relationship between "applied torque" and "bolt tension" for the tests carried out was found to be

$$\text{Bolt Tension (tons)} = -0.2415 + 0.0169 \times \text{Torque (lb. ft.)}$$

(iii) From Fig. 10C it is seen that the equation obtained for the Northfield tests is similar to the one derived by the American investigators. There is, however, a slight difference in the gradient of the lines. This difference may be due to differences in the bearing surfaces of the dished plate and nuts, the varying nature of the strata, etc., but it is thought that the difference in the types of threads on the bolts studied, may be the most important factor; in the American experiments sixteen rolled- and three cut-threaded bolts were used, whereas at Northfield only cut-threaded bolts were tested.

Variation of Bolt Tension with Time

Slot and Wedge Bolts (Figs. 11C and 12C)

(i) The setting tension applied to the bolts installed fell to approximately zero a few days after the bolts were set. This "relaxation" was noted in all bolts irrespective of their position in the bolting pattern.

(ii) Measuring bolts Nos. 19, 20 and 89 were re-tightened to the original tension after the initial "relaxation". Thereafter the tension in the bolts gradually built up - in most cases the tension did not increase uniformly with time but rather increased in stages, with an occasional relaxation for some three months after the installation. Thereafter the tension in the bolts remained fairly constant (between 4 and 6 tons).

(iii) Bolts Nos. 101 and 110 were not re-tightened after the initial "relaxation", but in both cases the load on the bolts gradually increased. This "natural re-tightening" of roof bolts has been observed by several workers both in Britain and the Continent (C16, C9).

(iv) Tests carried out to determine the rate of this relaxation of bolt tension (see contribution to discussion of Hodkin and Lawrence's Paper (C9)) revealed that the loss of tension was greatest soon after the bolt was installed. Consequently, if bolting is to provide adequate support for the immediate roof, systematic re-tightening of

the bolts should commence in the same shift.

(v) Similar trends in the variation of bolt tension with time, in longwall workings, have been recorded by other investigators. Figs. 24C, 25C and 26C show the results of three such investigations, one in the French Iron Ore Mines (C29), one in the Ruhr (C16) and the third in a colliery in Britain (C30). It is interesting to note that the bolts installed in the headings in the iron ore mines showed a considerable reduction in tension for a few days after the installation of the bolt.

(vi) From the observations at Northfield and analysis of other similar experiments it is thought that the relaxation of bolt tension takes place in two separate phases - anchor creep and variation of the amount of bed separation. Considering each phase:-

(a) Anchor Creep: From the photo-elasticity experiments discussed previously, it is seen that there are localised concentrations of stress around the bolt anchorages - even where the stress is distributed along a considerable length of the borehole (as in the photo-elastic models where the bolt anchorage was provided by simply tapping the drill-holes). Thus, in practice, where the load is concentrated over a much smaller length of the bore hole, much higher stress concentrations must result around the "anchor". Consequently anchor slip will ensue due to the failure of the sides of the bore-hole, and also because the rock around the anchorage, which is highly stressed,

will "creep" due to the "time-strain" characteristic of Coal Measures Rock (vide ante). Furthermore, where bolts are installed in very "tough" rock with a small "time-strain" tendency, yield of the anchorage can be expected due to overstraining of the bolt steel around the anchorage device, e.g. the "toes" of the split rod or the expansion shell.

(b) Variation in Amount of Bed Separation: It is generally accepted by most investigators that bed separation takes place ahead of a longwall face so that even when roof bolts are installed close to the ripping lip there is some separation between the strata. Hence, initially, the bolts act as a suspension support rather than form a compound beam. However, as the face advances the main roof lowers towards the nether roof (the latter being supported by the road-side packs) causing a reduction in the amount of bed separation and consequent relaxation of bolt tension.

In the experiments carried out by Middendorf and Jacobi in Germany, where the bolts were installed in a heading driven in advance of the face (see Fig. 25C) the setting tension was maintained in the bolts until the face line advanced ahead of the bolts, when the bolt tension "relaxed", followed by a gradual increase. The results of these tests, and those at Cossall Colliery (Fig. 26C), seem to support the theory outlined above. No further comparisons between the German results and those obtained at Northfield are warranted, because the German tests were carried out in a tailgate with a solid rib-side.

BOLT TENSION v. TIME (AFTER TINCELIN)

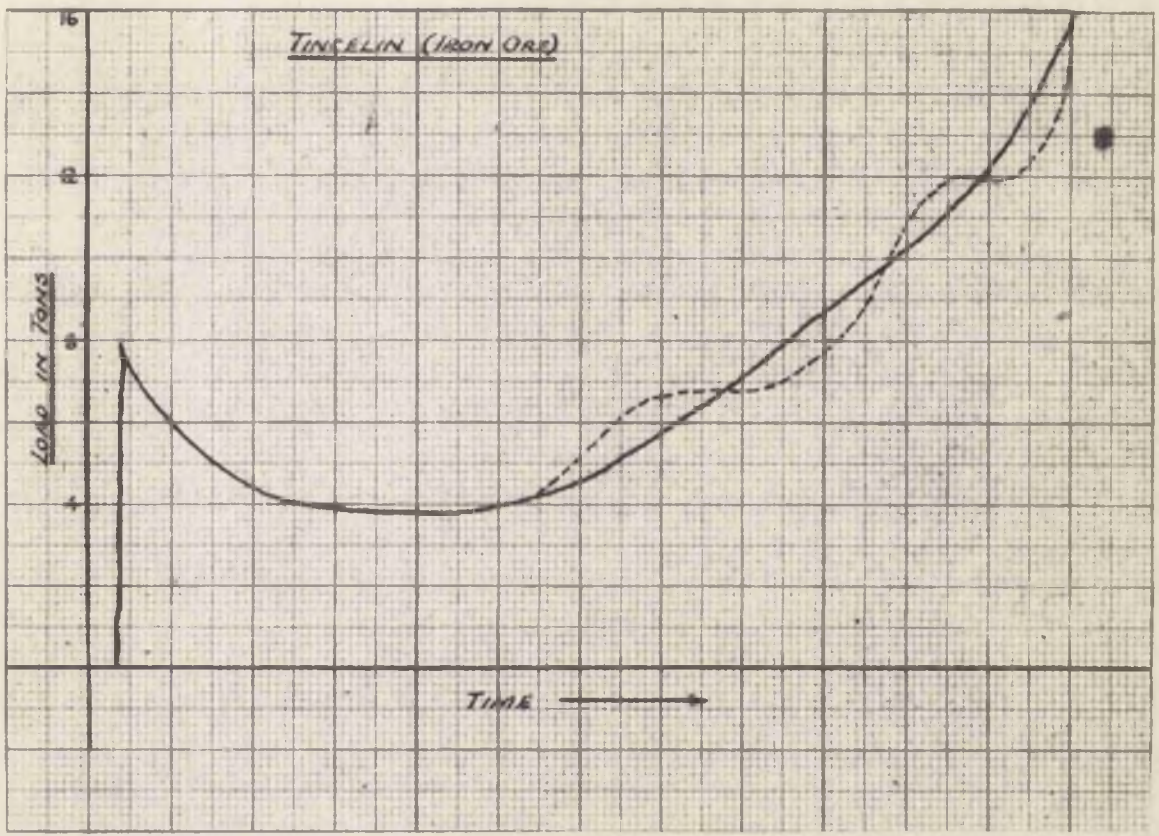


FIG. 24C.

BOLT TENSION TIME (AFTER MIDDENDORF & JACOBI)

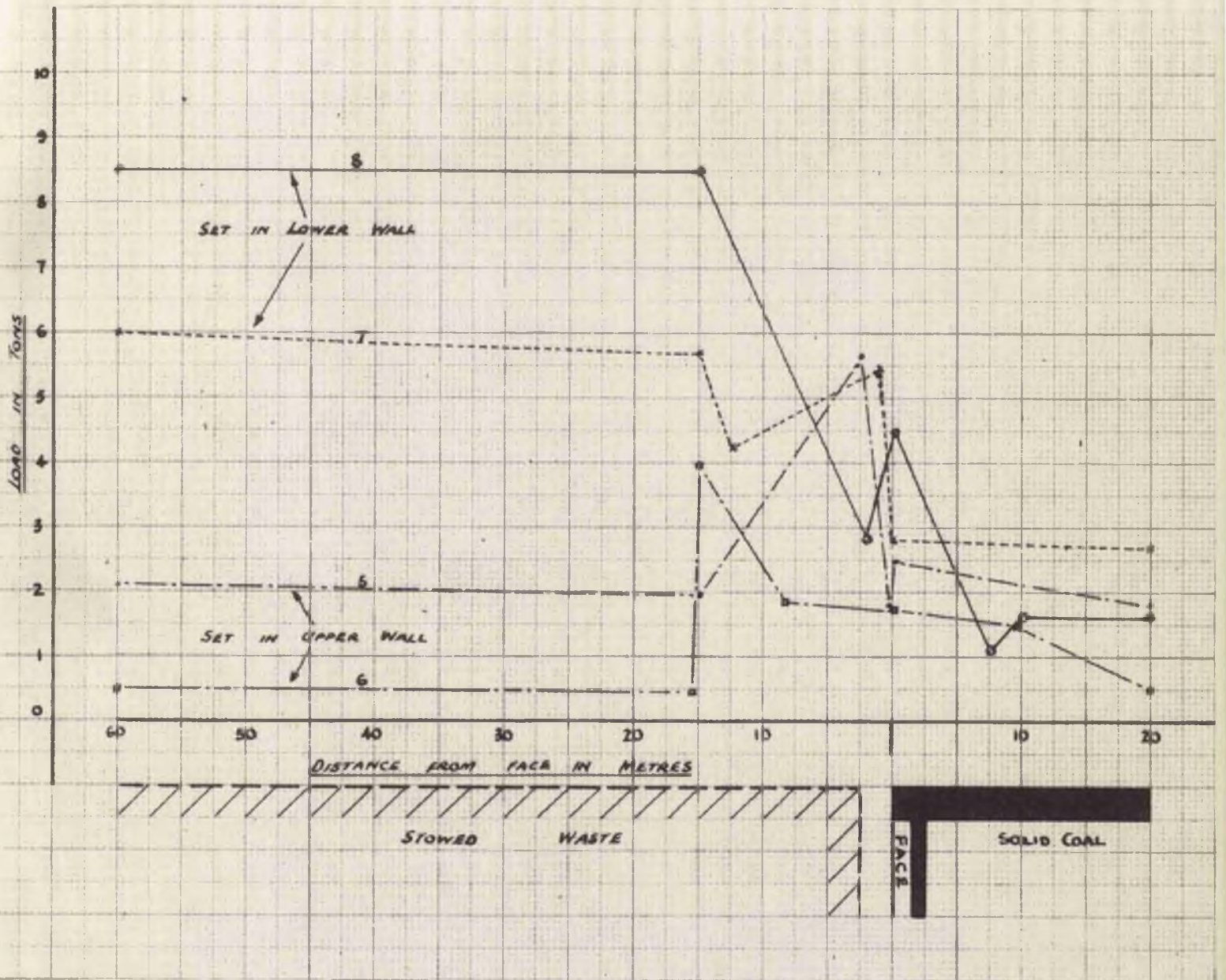


FIG. 25C.

BOLT TORQUE v TIME

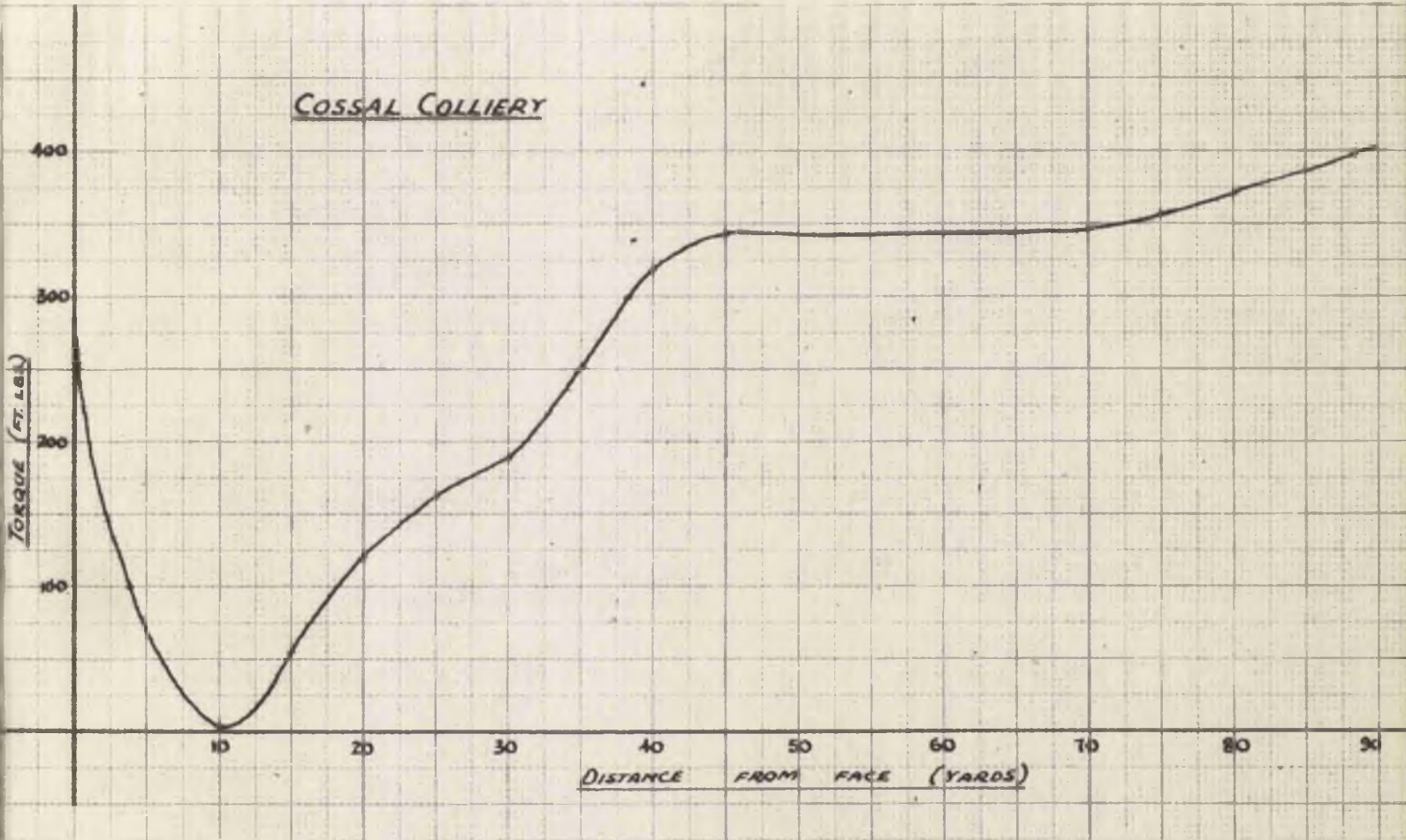


FIG. 26C.

(vii) The position of the bolt within the pattern does not influence the shape of the "tension-time curve".

Expansion Shell Bolts (Figs. 15C and 16C)

(i) All the shell bolts illustrated the same "relaxation" phenomena as discussed for the wedge bolts.

(ii) The maximum tension developed in the shell bolts was lower than in the corresponding wedge bolts.

(iii) Shell bolt B, which was only 3 feet in length, was installed in a bed of very weak shale. After a few days the tension in the bolt had relaxed to zero and the bolt was re-tightened. A similar relaxation took place again, and the bolt never showed any tendency towards "natural re-tightening". It is thought that the anchorage bed, in this case, was too weak to withstand the high stresses imposed by expansion of the shell, thus causing repeated relaxation of bolt tension.

Anchorage Testing

(i) From the traction tests carried out, the Bayliss, Jones & Bayliss wedge and sleeve bolt proved to be the most suitable type for the conditions. The slot and wedge and shell bolts also developed an anchorage resistance above that of the maximum tension measured in the bolts.

(ii) The shell bolt anchorage slipped at loads below the other types tested.

(iii) Routine anchorage testing proved to be necessary for ensuring that the bolts were installed correctly and that they were performing

their designed duty and not giving a false sense of security.

General Strata Movements

(i) From Figs. 17C and 18C it is seen that the cumulative bed separation between the anchorage horizon and the immediate roof of the roadway is oscillatory. This supports the theory that the relaxation of bolt tension is partly due to variation in the amount of bed separation.

(ii) Bed separation is greatest between the lower strata and decreases with increasing distance above the roadway. Hence roof bolts should be installed as soon as the roof is exposed to minimise the separation between the lower strata and so maintain the strength of the natural "rock beam".

(iii) The stratascope proved to be very useful for studying variations in bed separation etc., but several modifications are required to make the instrument suitable for underground conditions - viz. a high powered light source, a lens system with a much higher resolving power and a racking device to facilitate scanning of the sides of the borehole.

(iv) The function of the bolts in forming a "keystone" over the roadway, and so preventing excessive roof lowering and lateral movement of the sides is illustrated by comparing the photographs taken in the bolted and unbolted test lengths. The small amount of side movement is seen in the results obtained at the measuring stations (Figs. 20, 21 and 22C).

(v) The rate of roof subsidence was least in the wedge bolted zone and greatest where the wooden pins were used. However in all the test lengths (bolted) the strata movements recorded were smaller than those observed in the unbolted length of roadway.

(vi) The use of roof bolts greatly minimised the distortion of the arch girders (compare Plates XI C and XII C). Thus, if bolts are used in conjunction with conventional supports (c.a. girders) in longwall gate-roads, roadway maintenance costs will be considerably reduced.

Trials with Wooden Bolts

(i) The wooden bolts used were effective in forming the desired "keystone" above the excavation. However, since wooden bolts depend primarily upon skin friction for the formation of the keystone it is suggested that longer and larger diameter bolts should be used in future trials.

(ii) No direct measurement of the variation of tension in the wooden bolts was possible, but the crushing of the tensioning wedges shown in Plate XVII C illustrates some increase of the load on the bolt.

(iii) Driving of wedges between the "plates" and the roof proved to be a more effective way of tightening the plates initially than insertion of wedges into the head of the bolt.

(iv) From the results obtained at the measuring stations it is seen that roof subsidence is greater where wooden bolts are used than

with steel bolts. This excessive roof movement will cause distortion of the girders, or if the immediate roof bed is friable the girders will penetrate the roof and induce flaking of the rock between the girders. (N.B.- The latter is seen commencing in Plate XVII C.) Therefore, where wooden bolts are being used together with c.a. girders long stilts should be provided on the girders to permit the higher roof convergence without distortion of the girders.

C O N C L U S I O N S

(1) The electrical resistance strain gauge and ancillary equipment proved satisfactory for the underground investigations. The accuracy of the method used for the measurement of bolt tension was adequate for the tests carried out.

(2) Considerable development of the technique adopted for the measurement of 'in situ' rock strain is necessary before the method can be generally applied.

(3) The use of roof bolts in conjunction with normal arch girder supports greatly improved the conditions of the main gate in an advancing longwall district.

(4) The empirical relationship between "applied torque" (measured by torque meter) and "bolt tension" for the slot and wedge bolts was found to be -

$$\text{Bolt tension (tons)} = -0.2415 + 0.0169 \times \text{Torque (lb. ft.)}$$

(5) All the bolts installed (with the exception of the wooden pins) showed a "relaxation" of tension within a few days of being set.

This relaxation is thought to take place in two phases - one due to creep of the bolt anchorage device, and the other due to variation in the amount of bed separation behind a longwall face.

(6) After the initial "relaxation" the bolts which were left slack gradually tensioned up due to "natural re-tightening" (caused by deflection of the lower roof beds). If the initial stressing of the

bolt is too high then this natural re-tightening may result in failure of the bolt unit, by stripping of the threads, etc. This failure can be prevented by the use of dished plates, or spring washers, designed to yield at loads below the "ultimate tensile strength" of the bolt steel.

(7) The stratascope designed for the measurement of bed separation was useful but several modifications are required before it can be used to full advantage.

(8) Bed separation above the bolted roadway was minimised by the introduction of roof bolts (in the pattern discussed in the photo-elastic experiments - vide ante). The bolts formed a "keystone" above the roadway and reduced strata movements around the roadway considerably. (The formation of the "keystone" is illustrated by the plaster model tests).

(9) Roof subsidence was greatest in the test length supported by wooden bolts and girders, but it was still considerably smaller than the subsidence in the unbolted roadway.

(10) The results obtained with wooden bolts used in conjunction with arch girders were encouraging and warrant an increase in trials of this form of support to find its applications and limitations in longwall mining.

(11) Of the four bolt types studied in this investigation the Bayliss-Jones-Bayliss wedge and sleeve bolt was the most satisfactory. The

design of this bolt combines the advantages of the expansion shell type with the simplicity of the slot and wedge design. The additional time required to instal the bolt is offset by the fact that the setting device provides a measure of the anchorage capacity of each bolt installed. Consequently, regular pull tests on selected bolts are not required to ensure that the bolts are being properly installed.

SECTION D - TESTING OF PLASTER MODELS

The results of the photo-elastic analysis are limited to the study of stress distributions around the excavations when the rocks are not stressed beyond their elastic limit. Furthermore it is known that Coal Measures Rock is not truly elastic and may show plastic flow or fail as brittle material. Consequently to extend the investigation of the influence of roof bolting on the distribution of pressure around a roadway, the development of the fractures, and the function of the bolts after failure of the roof strata had taken place, plaster models were made and loaded to destruction.

The plaster model technique has been used by many investigators (D1, D2, D3, etc.) in the study of stress distributions across critical sections of irregular structural models. Various model methods of stress analysis have been used also by workers in the field of rock pressure; a review of the several techniques adopted is given by Spakeler (D4) and more recently Middendorf and Jacobi (D5) used plaster models in their studies of roof bolting in rectangular galleries.

In the tests here described no attempts were made to measure strains or deflections of the models but calibration test pieces were used to illustrate the relative strengths of the various strata. The main value of the experiments lie in demonstrating general tendencies rather than the development of a method of precise analysis.

Construction of the Models

Plaster of Paris is the material usually used for brittle model analysis but due to the very short setting time difficulty arises in casting the relatively large models required for this investigation. Several different types of plaster, including moulding plaster, stucco, hardwall plaster, Keene's cement, and board finish plaster were tested for setting time and strength. The latter - one of the retarded hemi-hydrate plasters (B.S.S. 1191) - allowed a "working" time of 25 - 30 minutes with a tensile strength of 250 - 350 pounds per square inch after twenty-one days (plaster : water ratio 10 : 8) proved to be the most suitable.

The scale of the models was 1 : 48, the leading dimensions being 10 inches by 6 inches by 7 inches. They were made up of strata of various thicknesses, each stratum being cast over the previous one to ensure a uniform bearing surface. The layers were prevented from binding together by coating the surface with modelling clay. Coloured pigments were added to the plaster to distinguish between the beds in the photographs taken during the loading of the models. The base of the models was a single stratum.

The bolting pattern used throughout the investigation was the "3-bolt" pattern, with 4 feet 6 inches between each set of bolts (i.e. the same pattern studied in the photo-elastic tests and the one used underground at Northfield.) The bolts were made from the same

material as those used for the photo-elastic models. Anchorage of the bolts was obtained by rivetting the head of the bolts and inserting them downwards. The bolt holes were drilled after the models were cast. The initial tension on all the bolts was made equal to prevent localised stress concentrations (vide ante).

Loading Arrangements

Models A and B: These models were loaded with a uniform vertical compressive force in a hydraulic testing machine, without any lateral constraint. It was intended that these loading conditions would simulate, to some extent, the pressures around the main gate of a longwall face with total caving of the wastes on each side of the roadside packs.

Models C and D: The loading arrangements for these models consisted of a vertical compressive load, as before, but in this case the strata above the level of the roadway excavation were constrained laterally by means of side plates and horizontal tension bars. This constraint was to provide the conditions sometimes found in a longwall working where roof caving has only extended for approximately twice the seam height and above that horizon the strata are not completely relieved of constraint.

EXPERIMENTAL RESULTS

Models A and B: The relative tensile strengths of the various strata are shown in Table No. 1D. Each bed in model A was made from the same mix as the corresponding one in model B to provide an accurate comparison of the bolted and unbolted conditions.

TABLE No. 1D

Stratum	Tensile Strength (lb./in. ²)	Thickness (in.)	Remarks
10	304	1	Top layer
9	300	.375	
8	244	.375	Bolt anchorage horizon
7	300	.375	
6	258	.375	
5	316	.375	Immediate roof of roadway
4	248	.375	
3	288	.375	Roadside packs
2	260	.375	
1	254	.375	

The average compressive strength was found to be 2050 lb./in.² which gives the ratio tensile strength : compressive strength of the plaster as 1 : 7 approximately.

A photographic record of the models was not obtained during the loading but Tables No. 2D and 3D outline the salient effects noted as the applied load was increased.

TABLE No.2D

Model A: Roadway unsupported

<u>Load</u> <u>(lb./in.²)</u>	<u>Effects Noted</u>
123	Fracture developed in the immediate roof of the roadway, (stratum No.5) along its entire length.
From 123 to 300	Fractures developed in the strata above the roadway in a "stepped" fashion, up to stratum No.8.
310	The floor of the roadway cracked along the centre.
370	The sides of the roadway began to spill over and well-defined fractures developed approximately $\frac{1}{2}$ inch in from the roadsides. Similar breaks also appeared in the floor.
450	The roadside fractures progressed to stratum No.10 converging to form the typical arched shape "relaxed" zone over the roadway. Heaving of the floor became more pronounced.
650	The sides of the roadway failed completely and spalled over into the excavation. Bed separation developed above the roadway. The condition of the model is shown in Plate I D.

TABLE No. 3D

Model B: Strata bolted

<u>Load</u> <u>(lb./in.²)</u>	<u>Effects Noted</u>
120	Fracture developed along the length of the roadway in stratum No.5 only.
220	Roof strata up to No.8 fractured above the roadway but no separation between beds was visible.
550	Floor failed along the roadsides.
930	Roadway sides crushing markedly.
1000	Roadside packs failed violently - the shattering extended some distance up into the model but the roof of the roadway did not collapse. Bed separation above the roadway negligible. The condition of the model under this applied load is shown in Plate II D.

MODEL A

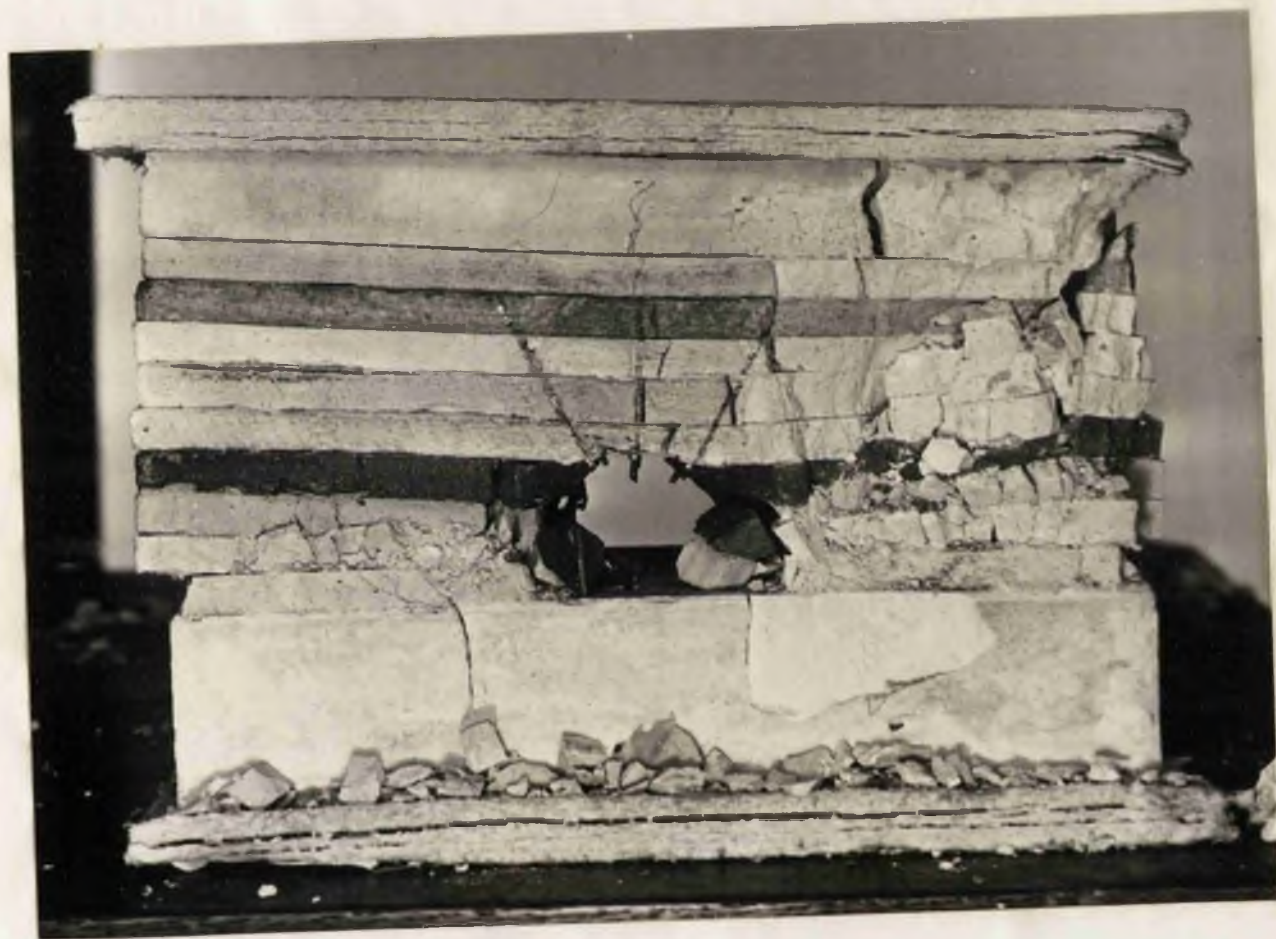
PLATE I D



Load 650 lb./in.²

MODEL B

PLATE II D



Load 1,000 lb./in.²

Models C and D: The relative strengths of the various strata, etc. are shown in Table No. 4D.

TABLE No. 4D

Stratum	Tensile Strength (lb./in. ²)	Thickness (in.)	Remarks
8	264	1	Top Layer
7	304	.375	
6	284	.375	Anchorage horizon
5	272	.375	
4	238	.375	
3	304	.875	Immediate roof of roadway
2	251	.500	
1	288	1.000	Roadside packs

The average compressive stress was found to be 2,120 lb./in.² which gives the ratio of tensile strength : compressive strength of plaster as approximately 1 : 7.

During the loading of both models C and D photographs were obtained to illustrate the major deformations taking place. Considering each model separately:-

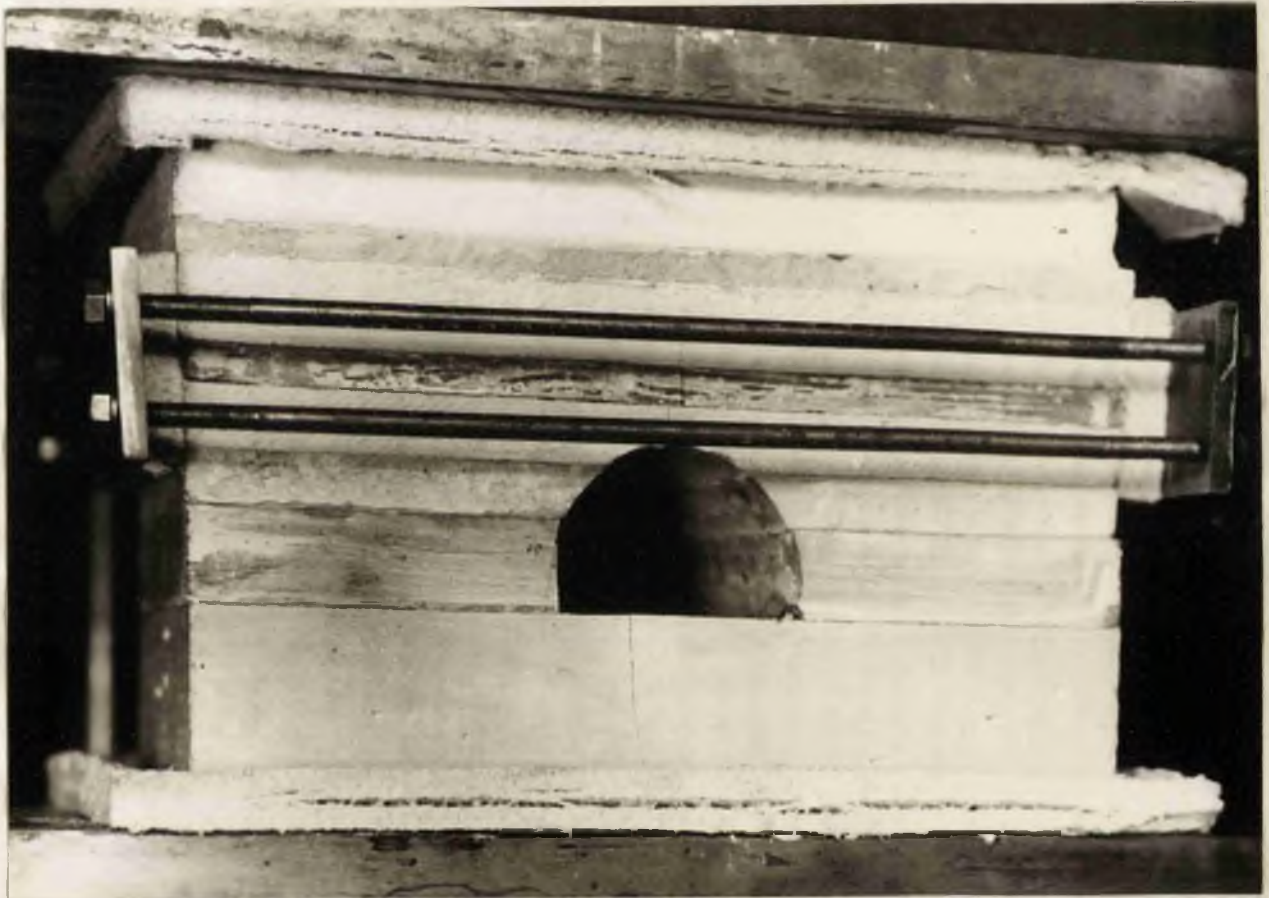
MODEL C - strata not bolted.

PLATE III D



The model fitted with the horizontal retaining frame prior to applying the vertical load. The various thicknesses of strata are clearly seen as well as the fibre boarding between the model and the machine platens to prevent localised regions of high stress.

PLATE IV D



Applied load 300 lb./in.². The immediate roof bed failed along the centre of the roadway at a load of 56 lb./in.² and extended to stratum No.4 when the applied load was 185 lb./in.². The floor failed along the roadway at 280 lb./in.² and fractures developed in the floor approximately $\frac{3}{4}$ inch from the roadsides.

PLATE V D



Applied load 425 lb./in.². Note particularly the marked deterioration of the roadsides and the position of the major fractures, $\frac{1}{2}$ inch from the sides of the excavation, forming the familiar arched-shaped zone over the roadway. The pavement heave has also become more pronounced.

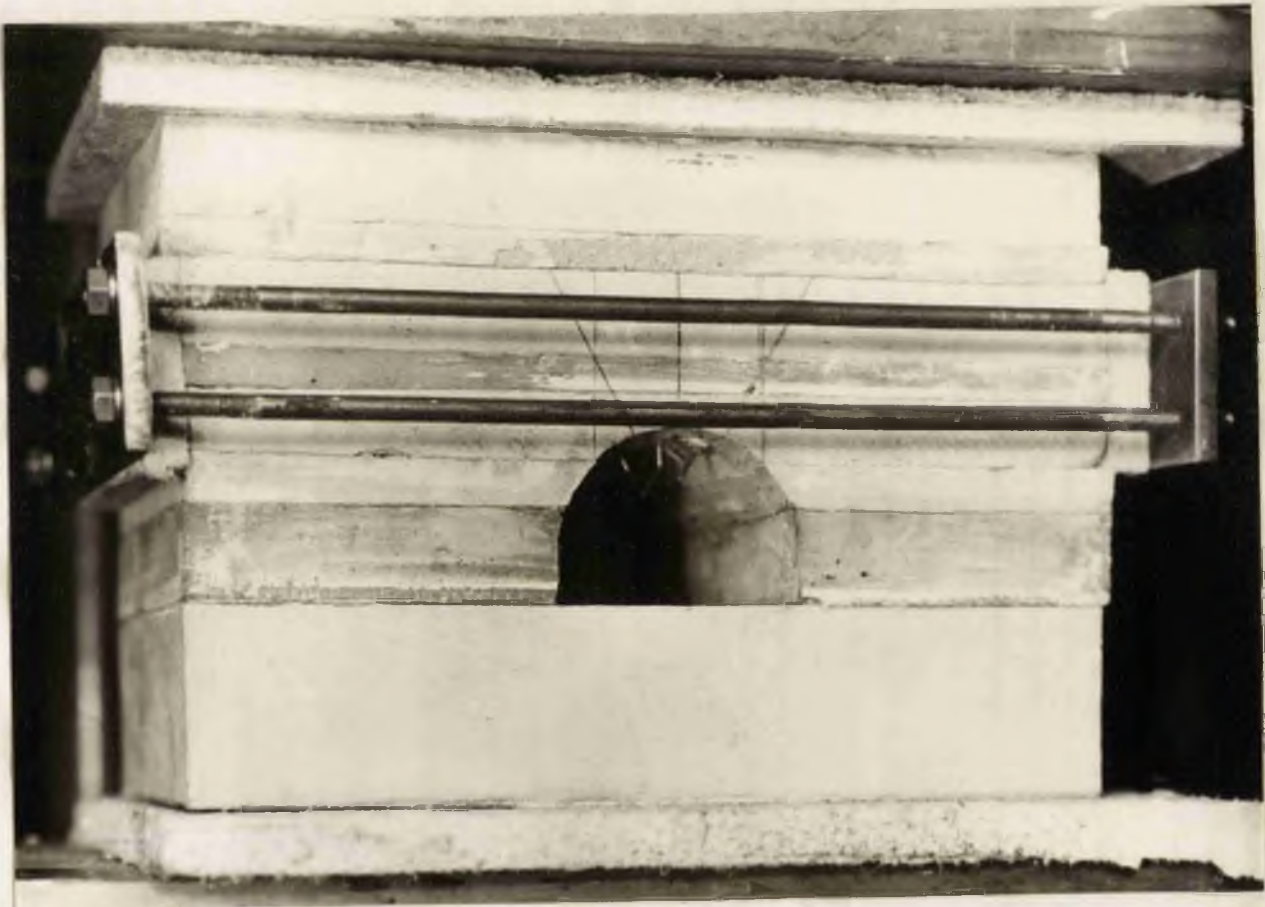
PLATE VI D



Applied load 485 lb./in.². The roadsides have now failed completely and deformation of the model continued without further increase in the applied load.

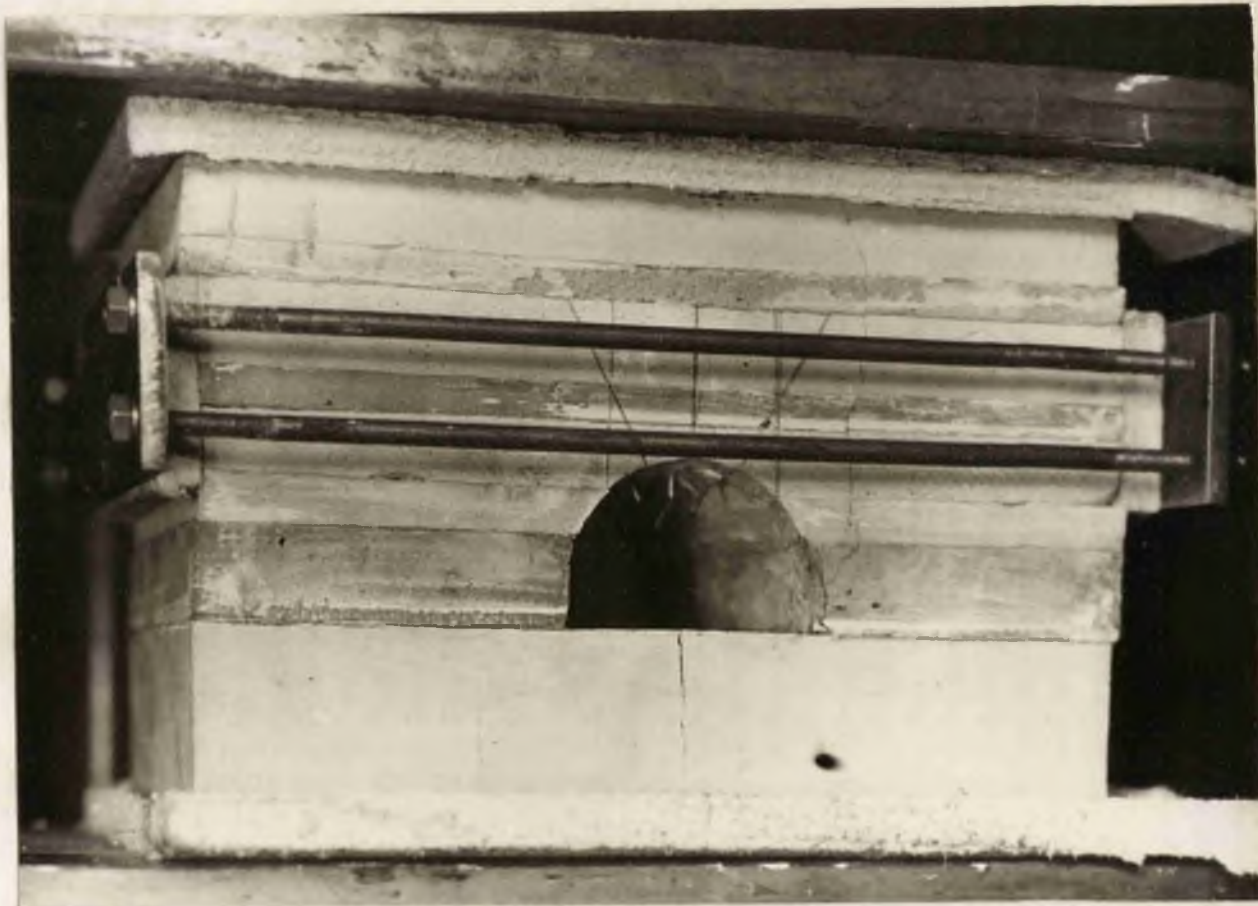
MODEL D - strata bolted

PLATE VII D



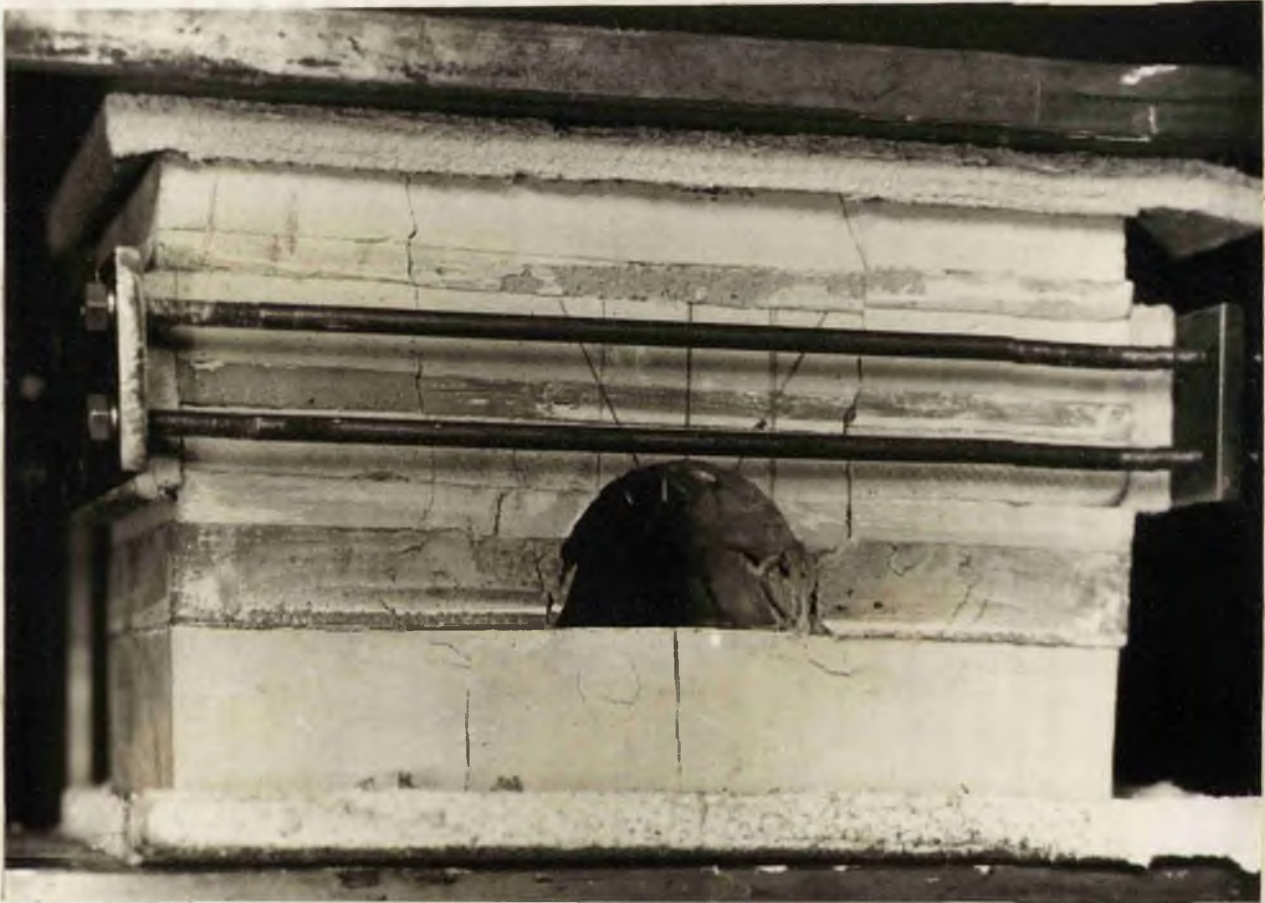
The position of the bolts is shown by pencil lines on the front of the model. The roof strata are constrained in exactly the same manner as for model C.

PLATE VIII D



Applied load 185 lb./in.². Fractures developed in the floor at 40 lb./in.² and the immediate roof bed failed, at the ends of the roadway only, when the load reached 70 lb./in.².

PLATE IX D



Applied load 300 lb./in.². Cracks developed remote from the roadsides (about $1\frac{1}{2}$ inches) and extended almost vertically to the top of the model without showing any tendency to form an arch. The failure of the roadside packs extended further in from the roadsides.

PLATE X D



Applied load 425 lb./in.². The roadside packs disintegrated completely but no bed separation or collapse of the bolted strata became visible.

ANALYSIS OF RESULTSModels A and B - (no lateral constraint)

(a) From Table No. 1D it is apparent that even with accurately controlled amounts of plaster and water the variation in tensile strength of the individual beds ranges $\pm 10\%$ from the mean. Probably this "scatter" could be reduced by closer control of the mixing time, but the variation of the strength and tensile : compressive strength ratio are quite suitable for models illustrating the trends in the development of deformations around underground excavations.

(b) In both cases, the initial failure of the roof bed occurs with approximately the same applied load, but the extent of the fracture is limited when the strata are bolted. Furthermore, bed separation in the bolted case does not develop to the same extent.

(c) In the unsupported roadway fractures develop approximately 2 feet (by scale) in from the roadsides and converge above the excavation forming an arch of loose material. However in the bolted roadway the fractures develop much further from the roadsides.

(d) The "pack area" is more severely crushed in the bolted roadway. This is probably due to the formation of a composite beam above the excavation and consequent distribution of higher loads to the abutment zones. This is in agreement with the observations of Middendorf and Jacobi (D5) both underground and in laboratory experiments.

(e) The bolts serve to form a consolidated "keystone" above the

roadway which, even when the roadsides are shattered, does not collapse into the excavation. The "keystone" if retained in position will prevent lateral movement of the strata into the excavation and reduce side thrusts on the normal supports (compare with the results of the measuring stations at Northfield).

(f) The increased loading over the pack area in the bolted roadway induces shear fractures in the floor along the roadsides.

Models C and D - (with lateral constraint)

(a) Similarly to the unconstrained conditions, the major breaks develop much further from the roadsides in the bolted section than in the unsupported one - approximately 5 feet as compared with 2 feet.

(b) The increased loading over the pack area in the bolted roadway is much more defined than in the same conditions without lateral constraint. Actually on removing the models from the testing machine, the base block under the packs in the bolted model disintegrated completely.

(c) The roadsides fractures develop at lower values of applied load when the roof beds are constrained.

(d) The formation of a "keystone" is again demonstrated. When the constraining frame was removed from the unbolted model the strata collapsed into the excavation, but in the bolted model the strata did not separate when the constraint was released.

NOTE:- Since the stratification of models A and B differs from that in models C and D further comparisons between the unconstrained and constrained models are not warranted.

C O N C L U S I O N S

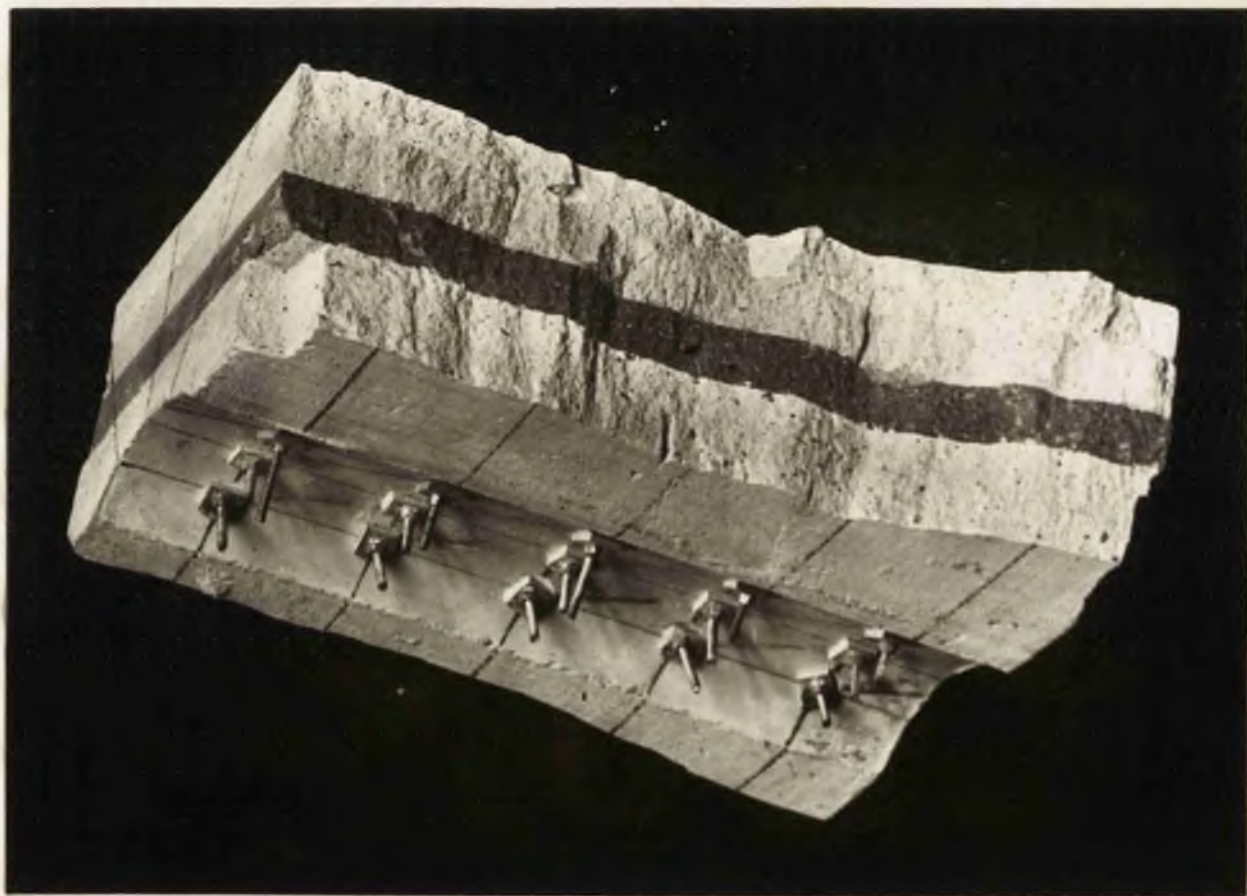
It is not possible to draw definite conclusions, generally applicable to underground conditions, from the model tests because true structural similitude (& dynamic similarity) could not be obtained throughout due to the difficulty in reproducing the loading conditions encountered underground. However, the following points emerge:-

- (1) No arched-shaped relaxed zone is formed above the roadway when bolts are used: the breaks extend almost vertically instead of converging.
- (2) Roof bolts installed in the "tension zone" over an arched excavation form a "keystone" which rests on the side abutments and does not collapse into the excavation with the failure of the surrounding strata.
- (3) The introduction of the bolts seems to re-distribute the forces acting around the excavation, causing an increased loading over the pack area and moves the major fractures away from the roadsides.
- (4) The fact that the roadside breaks are further removed from the sides when the strata is bolted indicates that side movements should be less. This agrees with the measurements of roof and side convergence recorded in the bolted roadway at Northfield (vide ante).
- (5) The development of the shear fractures at the roadsides is more pronounced when the roof beds are constrained, indicating that the driving of "stress-relief" roadways, or the adoption of the "double-

packing" system to reduce constraint in the vicinity of the roadway would improve conditions where roof bolting was being used in the supporting system.

(6) The improvement of the roof conditions due to bolting, and the formation of the "keystone" indicates that the system would be a useful adjunct to normal arched girders for the support of longwall gate-roads at depth, where horizontal pressures necessitate the use of roadside supports. It is thought that the bolting would reduce the lateral pressures because it reduces bed separation and transfers the load to the pack areas.

PLATE XI D



"Keystone" formed by bolting.

B I B L I O G R A P H Y

- (A1) OEBERT, WINDES & DUVALL Standardised Tests for Determining Physical Properties of Mine Rock. U.S. Bur. of Mines, R.I. 3891.
- (A2) TINCELIN Research on rock pressure in the iron-mines of Lorraine. Int. Conf. Rock Press, Liege 1951, p.158.
- (A3) MULLER Untersuchungen an Carbongesteinen zur Klärung von Gebirgsdruckfragen. Gluckauf, 1930.
- (A4) WOHLBIER Untersuchung von Gesteiner der Zechstein formation zur Klärung von Gebirgsdruckfragen. Diss. Breslau 1931 u. Kali 1931.
- (A5) WEISS Possibilities of Geophysical Methods of Predicting Rock Bursts. Journ. Chem. Met. & Min. Society of South Africa, Vol. 38, p.273.
- (A6) WEISS Experiments on the Fracturing of Witwatersrand Quartzites under Direct Pressure. Ibid. Vol. 41, p.235.
- (A7) JEPPE Review of the Rock Pressure Problem. Ibid. Vol. 44, p.3.
- (A8) HOLLAND Physical Properties of Coal and Associated Rocks as Related to Causes of Bumps in Coal Mines. Trans. Am. Inst. Min. & Met. Eng. (Coal Division) Vol. 149, 1942, p.75.
- (A9) PHILLIPS & DAVIES The Physical Properties of Coal Measures Rocks. S.M.R.E. Pub., Vol XI, 1936.
- (A10) PHILLIPS Tectonics of Mining. Coll. Eng. June - Oct. 1948.
- (A11) PHILLIPS The Nature & Physical Properties of Some Coal Measures Strata. T.I.M.E. vol. 80.

- (A12) TUKERMAN Proc. Am. Soc. Test. Mat.
Vol. 23 (II), p.602.
- (A13) PETERS & JOHNSON Ibid. Vol. 23, p.892.
- (A14) PETERS Ibid. Vol. 27, p. 522.
- (A15) BENNET, RICHARDS & VOSS Electronics applied to the Measurement
of Physical Quantities.
R.A.E. Report Inst. No.1.
- (A16) JOHNSTON & HOBBS Electronics in Strain Measurement.
Inst. Practice 7 (3) p.191.
- (A17) JONES & MASLEN The Physical Characteristics of Wire
Resistance Strain Gauges.
Aer. Res. Council Report & Me.
2661/ARC.
- (A18) YARNELL Electrical Resist. Strain Gauges.
Pubr. Elec. Eng., Essex Street, London.
- (A19) MILNER Sedimentary Petrography.
- (A20) HUDSPETH & PHILLIPS Coal Measure Rocks Pt.1 - Classific-
ation, Nomenclature, & Relative
Strengths.
S.M.R.B. Paper No.98.
- (A21) HARLEY Proposed Ground Classification for
Mining Purposes.
Eng. & Min. Jour. Vol. 122, p.368.
- (A22) LAIDLAW Private correspondence regarding the
fixing of bakelite gauges.
(Chief Vibration Test. Engineer,
De Havilland Propellers Ltd.)
- (A23) GLANVILLE Tech. Paper No.12, D.S.I.R.
- (A24) EVANS Elasticity & Plasticity of Rocks &
Artificial Stone.
Proc. Leeds Phil. & Litt. Soc. Vol.3,
1936.
- (A25) CORTEN, CLARK & SIDEBOTTOM Peculiar Behaviour of Steel Beams under
Dead Loads that produce Inelastic
Strains.
Trans. A.S.M.E. April, 1952, p.349.

- (A26) PAO and MARIN Prediction of Creep Curves from Stress-Strain Data. Proc. Am. Soc. Test. Mater. Vol. 52, p. 951.
- (A27) HOLLAND Some Aspects of Pillar Stresses & their Control in Mines. Trans. Can. Inst. of Min. & Met. Vol. 57, p.248.
- (A28) NADAI Theory of Flow and Fracture of Solids. McGraw Hill Ltd., (N.Y.) 1950.
- (B1) Proc. Int. Rock Press. Conf., Liege, 1951.
- (B2) COKER & FILON A Treatise on Photo-elasticity. Cambridge University Press (1931).
- (B3) FROCHT Photo-elasticity. John Wiley & Sons, New York (1941).
- (B4) HETENYI Handbook of Experimental Stress Analysis. Chapman & Hall Ltd., 1950.
- (B5) BUCKY & SINCLAIR Photo-elasticity and its application to Mine Pillar & Tunnel Problems. Am. Inst. Min. & Met. Eng. Tech. Pub. 1140, p.1 - 29. 1940.
- (B6) MINDLIN Stress Distribution around a Tunnel. Proc. A.S.C.E., p.619, 1939.
- (B7) DUVALL Stress Analysis applied to Underground Mining Problems. Pt. I. U.S. Bur. Mines R.I. 4192.
- (B8) DUVALL do. Pt. II. U.S. Bur. of Mines R.I. 4387.
- (B9 & C18) TINCELIN Results of Measurements made Concerning Rock Pressure in the Lorraine Iron Mines. Leeds Un. Min. Soc; Journal, Vol. 30, 1954.

- (B10) GUINARD
Choice of Gallery Forms and Widths of Pillars in Rocks assimilable to Elastic Solids.
Proc. Liege Conf. on Rock Press. (1951), p.98.
- (B11) PIRARD
Principles of Photo-elastic Methods: Signification of Tests in Field of Rock Pressure.
Proc. Liege Conf. on Rock Press., p. 121.
- (B12) HUDSPETH & PHILLIPS
The Forces induced by the Extraction of Coal and some of their Effects on Coal Measure Strata.
T.I.M.E., Vol, 85, p.42.
- (B13) POTTS, ALDER & WALKER
Research on Strata Control in the Northern Coalfield of Gt. Britain.
Proc. Liege Conf. Rock Press. (1951), p. 106.
- (B14) POTTS & BOURNE
Pit Bottom Disturbances at Bradford Colliery, Manchester.
Kings Coll. Res. Pub., Vol. I, 1953.
- (B15) POTTS
Stress Distribution and Underground Excavations.
Journal Camb. Univ. Eng. Soc., Vol. 23, 1953.
- (B16) POTTS
Stress Distribution Rock Pressure & Support Loads.
Univ. Leeds Min. Soc., Vol. 30, 1954.
- (B17) POTTS
Research on Rock Pressure: Stress Distribution around Underground Mining Excavations.
Iron & Coal Trades Rev. Vol. 169, p.449.
- (B18) DIXON
Stress Distribution in Auger Mining and when Working Seams in Close Proximity.
Kings Coll. Res. Pub. Vol. 2, 1954, p.40.

- (B19) BIRON
Photo-Elastic Analysis of Stress
Distribution in Coal Pillars.
Ibid., p.48.
- (B20) JENKINS
(Reader, King's College)
Private correspondence regarding
the preparation of photo-elastic
models.
- (B21 &
C1) BUCKY
Roof Bolting.
Coal Mine Modernisation 1950
Handbook, p.13.
- (B22 &
C8) WUERKER
Testing of Roof-Bolting Systems
Installed in Concrete Beams.
Mining Engineering, June, 1953, p.606
- (B23) BEYER and SOLAKIAN
Photo-elastic Analysis of Stresses
in Composite Materials.
Proc. Amer. Soc. C.E., Vol. LIX,
p.1120.
- (B24) JENKINS
Mechanics of Floor Penetration in
Mines.
Iron & Coal Trades Rev. Vol. CLXXI,
p.541
- (C1) See (B21)
- (C2) STEVENS
Successful Roof Bolting in Alabama.
Ibid., p. 31 - 39.
- (C3) WEIGEL
Channel Irons for Roof Control.
Eng. & Min. Journal, Vol. 144, p.70.
- (C4) MACDONALD AND WRIGHT
Report on Roof Bolting in U.S.A.
N.C.B. Production Dept. Report.
- (C5) PLATT
Roof Bolting in the Delaware
Aqueduct.
U.S. Bur. of Mines Inf. Circ. 7652.
- (C6) THOMAS
Suspension Roof Support.
Coal Age, July. 1948, 53, p.87.
- (C7) BROWN
Roof Bolting in Canadian Coal Mines.
Trans. Can. Inst. of Min. & Met.,
Vol. LVI (1953), p.400.
- (C8) See (B22)

- (C9) HODKIN AND LAWRENCE Some Factors Influencing the Behaviour of Roof Bolts in Mines. T.I.M.E. Vol.114, p.834.
- (C10) BARRY, PANEK & McCORMICK Use of Torque Wrench to determine Load in Roof Bolts - Pt. 2, Expansion-type $\frac{3}{4}$ inch bolts. U.S. Bur. Mines R.I. 5080.
- (C11) RABCEWICZ Bolted Support for Tunnels. Min. & Quarry Eng. Vol. 21, 1955, p.111.
- (C12) LANIER Pinning Roof with Wood. Coal Age (1950) 55, No.6, p.78.
- (C13) LANIER Wooden Pins for Mine Roof Control. Coal Mine Modernisation Year Book 1950, p.31.
- (C14) KELLY Successful use of Wooden Roof Bolts in Stony Point Mine. U.S. Bur. Mines Inf. Circ. 7636.
- (C15) MCKENSEY Roof Bolting in Bord & Pillar Workings, Elrington and Hebburn Collieries. Pre-print of paper read before Australasian Inst. of Min. & Met.
- (C16 & D5) MIDDENDORF AND JACOBI Anker Ausbau in Abbaustrecken from Gluckauf, June, 1952.
- (C17) VERDE T. & TREMBLAY Versuche zur Verbesserung des Ausbaus in den Abbaun und Strecken im Bassin Nord und Pas-de-Calais. from Grubensicherheit u. Grubenausbau, Lesben, 1952.
- (C18) See (B9)
- (C19) JENKINS AND ROWELL Strata Control in Longwall Workings: The Measurement of Prop Loads. King's Coll. Min. Soc. Journal, 1952.

- (C20) BARRY, PANEK & McCORMICK Use of Torque Wrench to determine Load in Roof Bolts: Pt. 1 Slotted-type Bolts.
U.S. Bur. Mines R.I. 4967.
- (C21) PHILIPS INDUS. TECH. LIBRARY Strain Gauges: Theory and Application
- (C22) WRIGHT American Developments No.3: Roof Bolting.
T.I.M.E. Vol. 113, p.865.
- (C23) BARRY, PANEK & McCORMICK Anchorage Testing of Mine Roof Bolts, Pt.1 Slotted-type Bolts.
U.S. Bur. Mines R.I. 5040.
- (C24) WINSTANLEY Strata Control in Mechanised Working of Coal Seams.
Proc. Liege Conf. on Rock Press. (1951), p.203.
- (C25) COWAN AND SHARPE Some Experiments on Roof & Floor Bolting.
T.I.M.E. Vol.113.
- (C26) MIDLAND INSTITUTE COMMITTEE ON SHOT FIRING An Optical Viewer for the Examination of Shotholes.
T.I.M.E. Vol.107, p.7.
- (C27) GRICE AND RUSSELL Still Photography in Coal Mines.
S.M.R.E. Research Report No.53.
- (C28) MIDDENDORF AND JANSSEN Erfahrungen mit dem Anker Ausbau from Gluckauf 33/34, 1953.
- (C29) NOLTINGK Private correspondence on Tincelin's Research in French Iron Ore Mines (N.C.B. C.R.E.II, I.R.6).
- (C30) Unpublished N.C.B. Report
- (D1) SEELY AND JAMES The Plaster-model Method of determining Stresses applied to Curved Beams.
Univ. of Illinois Bull. No.195, Aug. 1929.

- (D2) SEELY AND DOLAN
Stress Concentration at Fillets,
Holes and Keyways as found by the
Plaster-model Method.
Ibid., Bull. No.276, Jun, 1935.
- (D3) NEWMARK AND IEPPEER
Tests of Plaster-model Slabs
Subjected to Concentrated Loads.
Ibid., Bull.No.313, June, 1939.
- (D4) SPAKELER
Methods of Research on Rock Pressure.
Proc. Inter. Conf. about Rock Press.
& Support in the Workings.
Liege, 1951. p.176.
- (D5) See (C16)

ILLUSTRATIONS

PLATES

SECTION A

	<u>No.</u>
De Havilland Bridge and Bending Apparatus	IA
Phillips Bridge and Bending Apparatus	IIA
Tensile Testing Clamps	IIIA
Rock Dressing Apparatus	IVA
Representative Group of Rock Specimens	VA
Specimens fitted with Strain Gauges	VIA
Specimens after Testing	VIIA

SECTION B

Photo-elastic Bench and Models	IB
Machining Stresses around Drill Hole in C.R.39	IIIB
Elimination of Machining Stresses with Modified Technique	IIIB
Suspension Support:	
Bolt Tension Zero	IVB
Equal Bolt Tensions (Load 227 lb./in. ²)	VB
Equal Bolt Tensions (Load 328 lb./in. ²)	VIB
Bolt Load Alone	VIIIB
Unequal Bolt Tensions	VIIIIB
Bolts with Roof Bar	IXB
Compound Beam:	
Without Bolts	XB
4-Bolts with Equal Tensions	XIB
Effect of Rubber 'Washer'	XIIB
Arched Roadway:	
Without Bolts	XIIIIB
3-Bolts without Tension	XIVB
3-Bolts Equal Tension	XVB
3-Bolts Centre Tensioned	XVIB

SECTION C

Control Bolt to Check Drift of Strain Gauges	IC
Shell Bolt and Gauge Protection	IIC
Strain Bridge in use Underground	IIIC
Stratascope	IVC
Crack in Sandstone Specimen (Stratascope)	VC
Infra-Red Drying Lamp	VIC

	<u>No.</u>
Strain Gauges on Roof of Roadway	VIIC
Ripping Lip - showing variation in Strata Conditions	VIIIC
Looking Outbye into Unbolted Roadway	IXC
Looking Inbye from Unbolted Roadway	XC
Distortion of Girders in Unbolted Roadway	XIC
Wedge-bolted Roadway	XIIC
Shell-bolted Roadway	XIIIC
Wedge Bolts No.73 - 75 (December, 1954)	XIVC
Wedge Bolts No.73 - 75 (May, 1955)	XVC
Wooden Bolts after Installation	XVIC
Wooden Bolts three months Later	XVIIIC

SECTION D

Unbolted Model (without constraint) - Load 650 lb./in. ²	ID
Bolted Model (without constraint) - Load 1,000 lb./in. ²	IID
Unbolted Model (with constraint) - Load Zero	IIID
" " " " - Load 300 lb./in. ²	IVD
" " " " - Load 425 lb./in. ²	VD
" " " " - Load 485 lb./in. ²	VID
Bolted Model (with constraint) - Load Zero	VIID
" " " " - Load 185 lb./in. ²	VIIID
" " " " - Load 300 lb./in. ²	IXD
" " " " - Load 425 lb./in. ²	XD
"Keystones" formed by Bolting	XID

DIAGRAMS

SECTION A

	<u>No.</u>
Circuit Diagram De Havilland Bridge (D.C.)	1A
Circuit Diagram Phillips Bridge (A.C.)	2A
Stress ν Strain for Various Strain Rates	3A
Stress ν Total Elapsed Time	4A
Reciprocal of Time Rate ν Time Strain	5A
Stress ν Strain (Compression) for CM.1	6A
E_T and E_S ν Stress for CM.1	7A
G_T and G_S ν Stress for CM.1	8A
Strain Energy ^S per Unit Volume ν Stress for CM.1	9A
Stress ν Strain (Compression) for CM.5	10A
E ν Stress (Compression) for CM.2, 3, 5	11A
E ν Stress (Compression) for DH.1, 2, 4, 5, 6	12A
E ν Stress (Compression) for DH.3, 7	13A
G ν Stress (Compression) for DH.6, 5 4 2 and CM.2, 3, 5	14A
Strain Energy per Unit Volume ν Stress	15A
Stress ν Strain (Tension) for DH.2	16A
E ν Stress (Tension) for DH.2	17A
E ν Stress (Tension) for Remaining Specimens	18A
Load ν Strain (Bending) Simply Supported for DH.2	19A
Load ν Strain (Bending) Fixed End for DH.2	20A
Load ν Strain (Bending) for CM.1	21A
Time Strain (Tension) for DH.2	22A
Time Strain (Bending) for DH.2	23A
Stress ν Strain for Various Strain Rates (Bending) for CM.1	24A
Stress ν Total Elapsed Time for CM.1	25A
Reciprocal Time Rate ν Time Strain for CM.1	26A
Calculated and Experimental Time Strain ν Time (Bending) for CM.1	27A
Stress ν Strain for Various Strain Rates (Tension) for CM.5	28A
Calculated and Experimental Time Strain ν Time (Tension) for CM.5	29A

SECTION B

Details of Model Loading Arrangements	1B
Calibration of C.R.39 in Pure Bending	2B
Calibration of Loading Tubes	3B

Unbolted Span - Isoclinics and Trajectories	4B
Bolted Span - Isoclinics and Trajectories	5B
Boundary Stresses - Suspension Support	6B
Keystone Stresses - Arched Roadway Support	7B

SECTION C

South District Plan - Northfield Colliery	1C
Details of Wooden Bolts	2C
Fixing of Gauges to Wedge Bolts	3C
Fixing of Gauges to Shell Bolts	4C
Construction of Stratascope	5C
Measuring Station	6C
Supervisor's Chart	7C
Calibration Curve - Wedge Bolt No.3	8C
Calibration Curve - Wedge Bolt No.6	9C
Torque v Tension Relationship - Wedge Bolts	10C
Tension v Time Curves for Wedge Bolts No. 19 and 20	11C
Tension v Time Curves for Wedge Bolts No. 89, 101 and 110	12C
Calibration Curve - Shell Bolt A	13C
Calibration Curve - Shell Bolt E	14C
Tension v Time Curves for Shell Bolts A and E	15C
Tension v Time Curves for Shell Bolts B and D	16C
Convergence Records for Wedge-bolted Zone	17C and 18C
Location Plan for Measuring Stations	19C
Measuring Station Results	20C, 21C and 22C
Rock Strain v Time Relationship	23C
Bolt Tension v Time (after Tincelin)	24C
Bolt Tension v Time (after Middendorf and Jacobi)	25C
Bolt Torque v Time (Cossall Colliery)	26C

SECTION D

No Diagrams

A P P E N D I X

Specimen DH1

Location: Cardowan Colliery, Lanarkshire.
6 feet above Meiklehill Wee Coal Seam

Mineral Content: Quartz, limonite and mica. The limonite and mica occur in streaks through the main matrix of quartz.

Cementing Medium: Siliceous

Particle Size: Overage 0.094 mm.

Specific Gravity: 2.64

Rock type: Fine grained sandstone

Specimen DH2

Location: Kingshill No.1 Colliery, Allanton.
Immediate roof of Allanton Upper Seam
(Limestone Coal Group)

Mineral Content: Mainly quartz with streaks of carbonaceous matter

Cementing Medium: Siliceous

Particle Size: Average 0.136 mm.

Specific Gravity: 2.42

Rock Type: Medium grained sandstone

Specimen DH3

Location: Cardowan Colliery. Immediate roof of Meiklehill Main Coal

Mineral Contents: Mica, quartz and an abundance of feldspars

Cementing Medium: Indefinite - probably decomposed feldspar

Particle Size: Average 0.023 mm.

Specific Gravity: 2.48

Rock Type: Micaceous siltstone

Specimen DH4

Location: Cardowan Colliery, above Meiklehill Wee Coal, between roof shale and sandstone DH1

Mineral Contents: Quartz, feldspar and some mica. The rock had a streaky appearance both in the hand specimen and under the microscope

Particle Size: Average 0.036 mm.

Specific Gravity: 2.64

Rock Type: Siltstone (or Fakes)

Specimen DH5

Location: Garscube Mine, Glasgow, about 2 feet below
the Possil Main Coal

Mineral Content: Quartz, iron, calcite, mica and felspar

Cementing Medium: Calcite

Particle Size: Average 0.089 mm.

Specific Gravity: 2.58

Rock Type: Fine Grained sandstone

Specimen DH6

Location: Cardowan Colliery. Approximately 10 feet
above Meiklehill Main Coal Seam

Mineral Content: Quartz

Cementing Medium: Mainly siliceous

Particle Size: 0.620 mm.

Specific Gravity: 2.45

Rock Type: Coarse grained sandstone

Specimen DH7

Location: Cardowan Colliery, immediate roof of
Kilsyth Coking Coal Seam

Mineral Content: Felspars, quartz with some iron

Particle Size: Average 0.020 mm.

Specific Gravity: 3.20

Rock Type: Clay siltstone (ironstone)

Specimen CMI

Location: Easton Colliery, immediate roof of Main
Coal Seam

Mineral Content: Quartz and orthoclase with some iron

Cementing Medium: Siliceous

Particle Size: Average 0.45 mm.

Specific Gravity: 2.50

Rock Type: Medium grained sandstone

Specimen CM2

Location: Bogton Colliery, Ayrshire. Approximately
15 feet above the Lodgement Coal

Mineral Contents: Quartz and iron

Particle Size: Quartz - 0.077 mm; Iron - 0.144 mm.

Specific Gravity: 2.82

Rock Type: Fine grained sandy ironstone

Specimen CM3

Location: Dalquharrn Colliery, Ayrshire - Calciferous
Sandstone Series

Mineral Contents: Quartz, calcite and some clayey material

Cementing Medium: Calcareous

Particle Size: From 0.13 mm. to 0.37 mm.

Specific Gravity: 2.60

Rock Type: Medium grained calcareous sandstone

Specimen CM4

Location: Dalquharrn Colliery, Ayrshire. Calciferous Sandstone Series

Mineral Content: Quartz, iron and calcite

Cementing Medium: Ferruginous

Particle Size: 0.12 mm.

Specific Gravity: 2.64

Rock Type: Medium grained ferruginous sandstone

Specimen CM5

Location: Cardowan Colliery, Stepps. 6 feet above the Meiklehill Wee Coal Seam (approximately same position as specimen DH1 - sampled one year later)

Mineral Content: Quartz, orthoclase and muscovite

Cementing Medium: Siliceous

Particle Size: 0.193 mm.

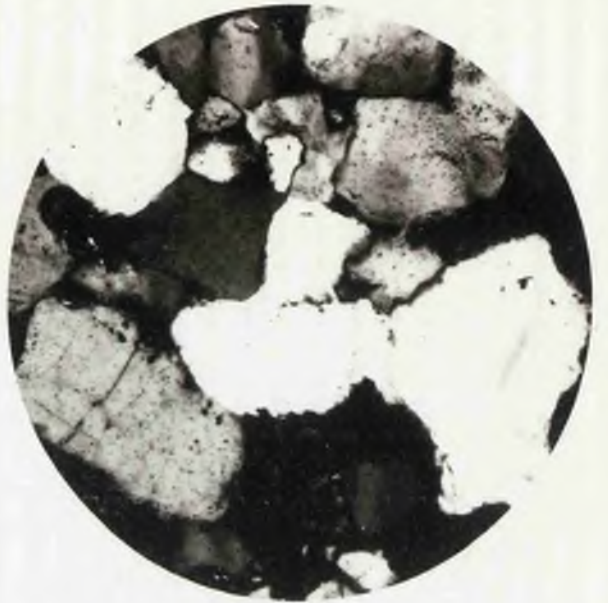
Specific Gravity: 2.64

Rock Type: Medium grained siliceous sandstone

Micro-photographs of each of the specimens are given below. All are taken with a magnification of 100 under crossed nicols, except specimen CM2 which is under plane polarised light.



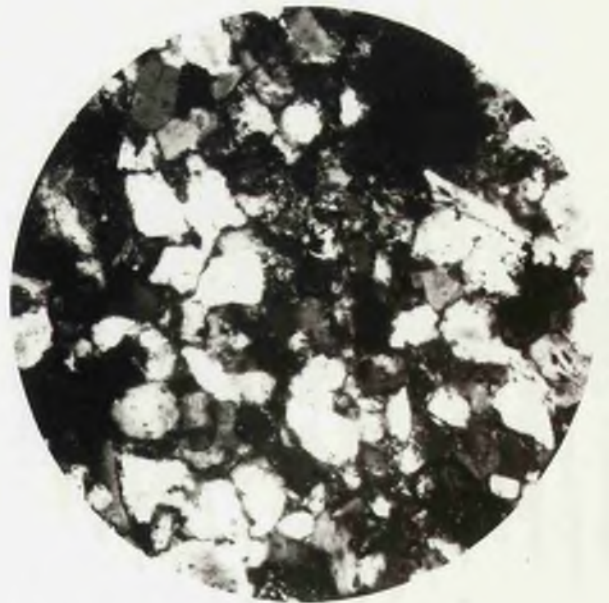
D.H.1.



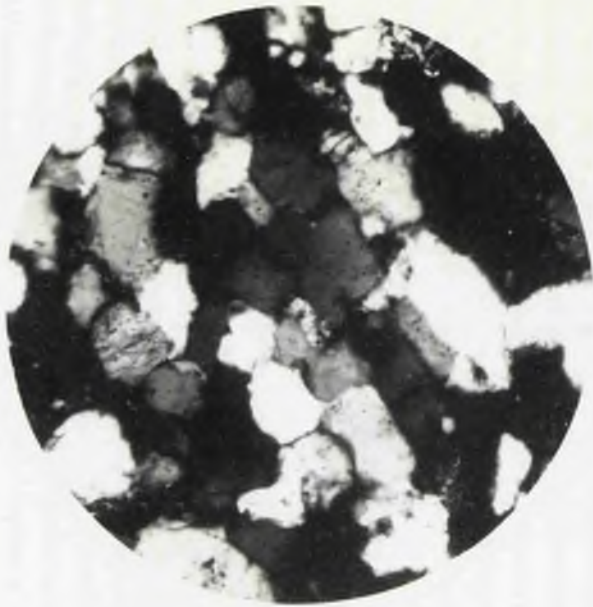
D.H.2.



D.H.3.



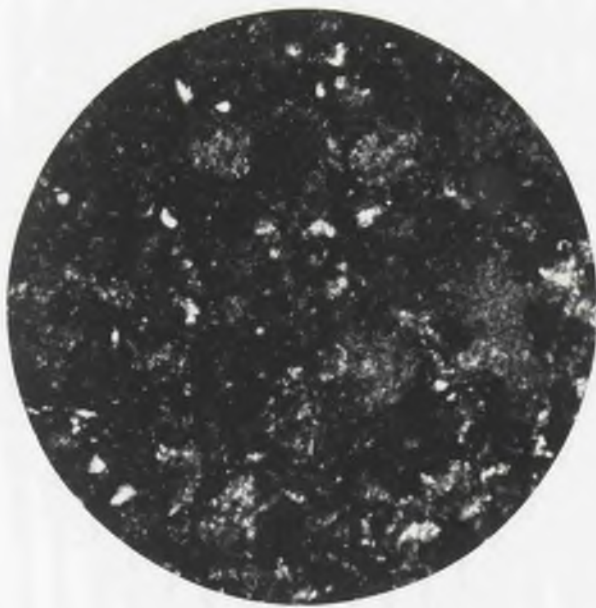
D.H.4.



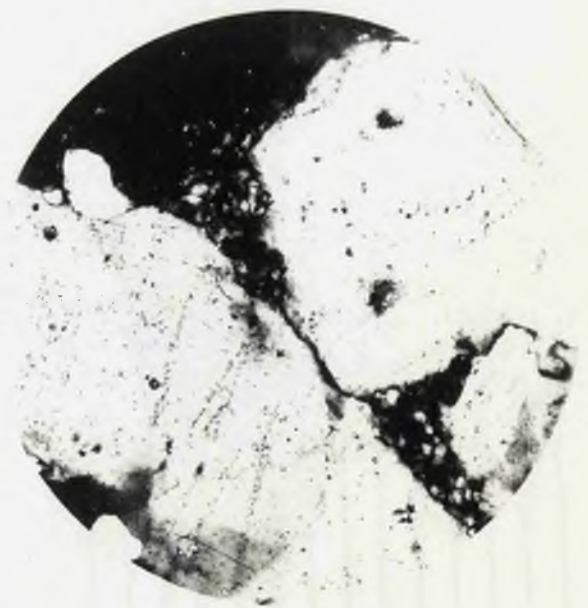
D.H.5.



D.H.6.



D.H.7.



CM.1.



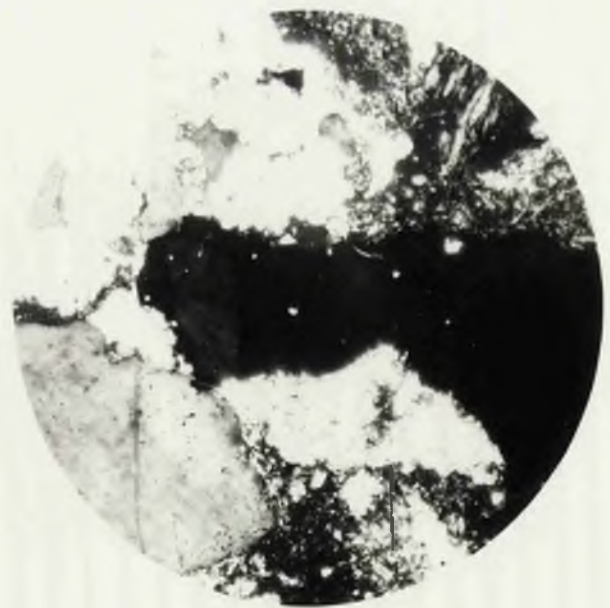
C.M.2.



C.M.3.



C.M.4.



C.M.5.

A C K N O W L E D G M E N T S

The author wishes to express his thanks to:-

Professor G. Hibberd, Ph.D., A.R.T.C., M.I.Min.E., F.R.S.E.,
Mining Department, The Royal Technical College, supervisor of
the research, for the opportunity to carry out the investigation
and for his encouragement and many helpful suggestions.

W.C. Parker, Esq., Area General Manager, Central East Area,
National Coal Board, for the facilities granted during the under-
ground investigations, and also the management and workmen of
Northfield Colliery.

The Staff of the Mining Department, The Royal Technical College,
for their help during the experimental work.

Mr. A. Chattell, Laboratory Technician, Mining Department, for his
help in the construction of the apparatus.

The D.S.I.R. for grant of funds which made the investigation
possible.